5-2014

Light-Ion Production From Intermediate-Energy Heavy-Ion Interactions

Matthew Randall Beach
University of Tennessee - Knoxville, mbeach1@utk.edu

To the Graduate Council:

I am submitting herewith a dissertation written by Matthew Randall Beach entitled "Light-Ion Production From Intermediate-Energy Heavy-Ion Interactions." I have examined the final electronic copy of this dissertation for form and content and recommend that it be accepted in partial fulfillment of the requirements for the degree of Doctor of Philosophy, with a major in Nuclear Engineering.

Lawrence H. Heilbronn, Major Professor

We have read this dissertation and recommend its acceptance:

Lawrence W. Townsend, Laurence F. Miller, Robert Grzywacz

Accepted for the Council:

Carolyn R. Hodges

Vice Provost and Dean of the Graduate School

(Original signatures are on file with official student records.)

Light-Ion Production from Intermediate-Energy Heavy-Ion Interactions

A Dissertation Presented for the
Doctor of Philosophy
Degree
The University of Tennessee, Knoxville

Matthew Randall Beach
May 2014

ACKNOWLEDGMENTS

I would like to thank Dr. Lawrence Heilbronn for advising me all these years during my graduate education. Being the first one in my family to pursue a PhD, it felt like quite a daunting task, but Dr. Heilbronn's guidance helped curb any of my doubts. His dedication to helping me, as well as any other student seeking him out, seemed to go above and beyond what one would expect. You couldn't ask for a more helpful and personable advisor. I can only hope that I, being his first PhD student, made the journey as painless for him as he did for me.

ABSTRACT

As missions in space become longer, the dangers posed to astronauts become increasingly prevalent. One of the many dangers is an increasing radiation dose caused by the unique radiation present in space called Galactic Cosmic Radiation (GCR). The complexity of GCR usually requires the use of transport codes when testing new materials for use in space. Some of these codes use the coalescence model to provide fragmentation light-ion production cross section data when no tabulated data is available. The accuracy of this model depends on the availability of experimental proton, neutron, and light-ion production cross section data. Since there is little experimental data that is applicable to the coalescence model, the validity of the model over the wide range of energies and interactions that are present in GCR is uncertain.

Described in this thesis is an experiment that provides the means of measuring double differential cross section data for protons, deuterons, and tritons for 39 different projectile/target systems with projectile energies ranging from 250 to 600 AMeV. Eight of these systems also provide cross section data for ^{3}He and ^{4}He. The cross sections were provided at energies ranging between 50 and 300 AMeV at the angles of 5, 10, 20, 30, 40, 60, and 80 degrees off the beam axis. As of this paper, no other reports or articles have included such an extensive set of both neutron and proton, as well as light-ion cross sections.

The cross sections obtained from this experiment were used to calculate coalescence radii for each measured angle for each system. Coalescence radii were also determined over all angles to provide system-wide radii. The calculated radii varied from system to system, and ranged from 60 to 200 MeV/c. The radii tended to be larger with lower mass systems (either the projectile or target), and fell as the mass of the systems increased.

TABLE OF CONTENTS

LIST OF TABLES

LIST OF FIGURES

CHAPTER I
INTRODUCTION AND GENERAL INFORMATION

The unique radiation present in space is comprised of a wide variety of charged and neutral particles at an extremely wide range of energies. It is difficult to reproduce experimentally in ground-based experiments, usually requiring the use of accelerators that focus on a specific isotope at a specific energy. Since accelerators can only reproduce a small subset of the galactic cosmic radiation (GCR) spectrum at a time, this makes testing radiation transport in materials for space applications difficult. It is very impractical to test every component of the GCR spectrum; therefore, computer codes are often employed in order to provide simulated results for new systems. However, the accuracy of these codes depends on the accuracy of the models used and the availability of cross section data used to verify that accuracy.

1.1 Background Information

1.1.1 Galactic Cosmic Radiation

The galactic cosmic radiation (GCR) spectrum is comprised of a wide variety of charged and neutral particles over a large range of energies. GCR is a continuous flux of radiation that originates from sources outside the solar system. Of the charged particles, protons are the most prominent, composing 87% of the GCR spectrum [1]. Shown below, in Figure 1, are the relative abundances of charged particles in the GCR spectrum as well as their relative dose contributions (which are a function of Z^2 of the particles).

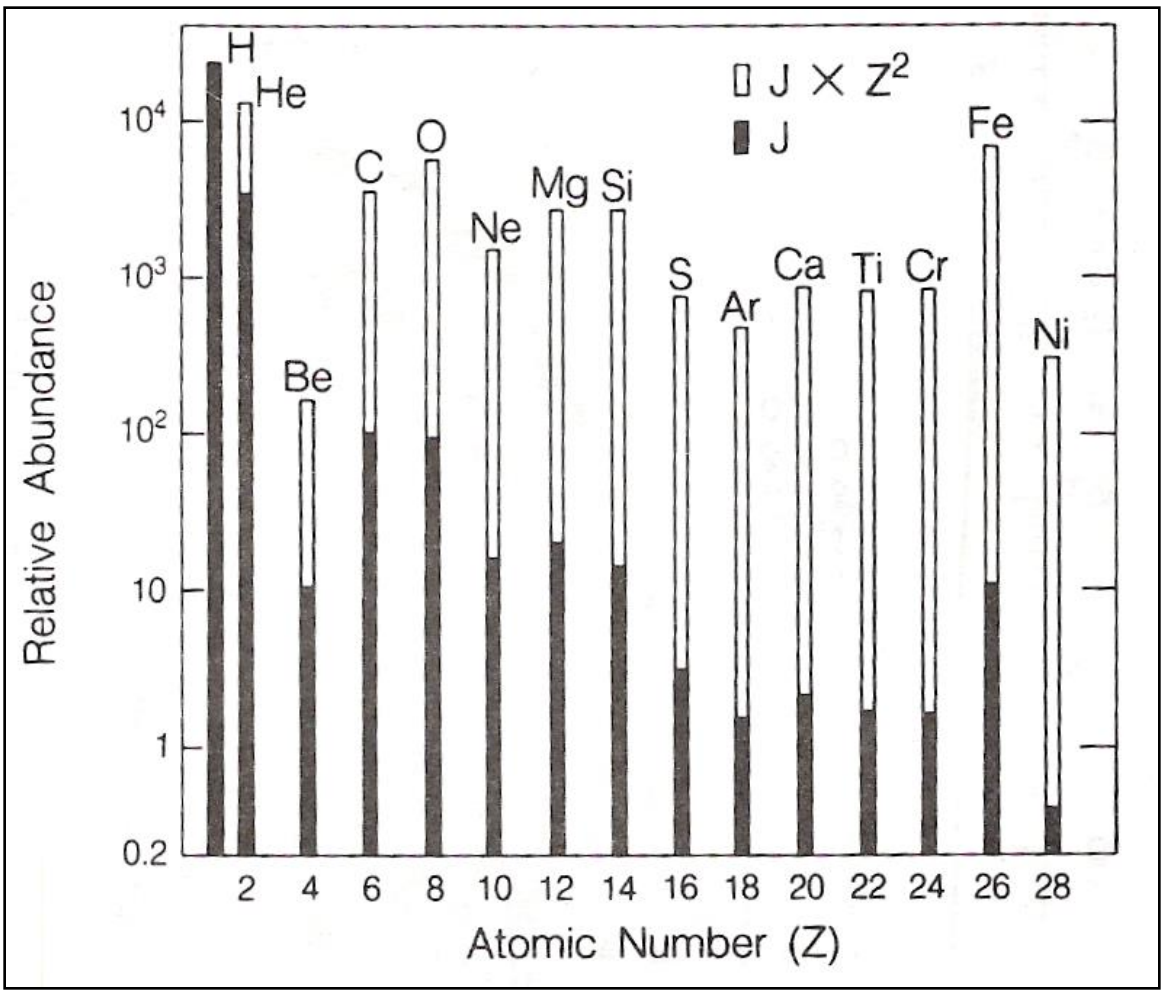

Figure 1. Histogram of the relative abundance (black bars) and dose contribution (white bars) of ions in GCR [2].

1.1.2 Particle Accelerators

The GCR spectrum covers a wide range of energies, which peaks at around 600-1000 AMeV. The high energies of the particles that make up the GCR spectrum require the use of particle accelerators for experiments that focus on GCR applications. Unfortunately, the limitations of these accelerators generally allow for the production of an incident radiation beam of only one ion at a specific energy. Because of this, the results of various experiments at accelerators apply to a very specific set of parameters related to the radiation field.

In addition to the limitations imposed by the accelerators, heavy ions in the GCR energy regime can undergo a multitude of interactions, which can produce

a complex secondary radiation field. A single high energy projectile has the possibility of producing many secondary radiation particles at a wide range of energies. Firstly, the projectile can break up into lighter ion fragments. The projectile also has a chance of breaking up the target into smaller fragments. Additionally, these fragments may be produced in an excited state and will undergo de-excitation by emitting a cascade of gammas or nucleons.

1.1.3 Transport Models

Transport codes such as PHITS and FLUKA can be utilized to simulate experiments focusing on GCR issues. They are useful tools due to the complexity and limitations of real experiments. For space applications, the primary function of transport codes is to predict the fluence of particles that contribute dose to astronauts and electronics. As such, the codes need to accurately predict inclusive particle spectra over a wide range of GCR energies and species. Once the spectra are predicted, one can calculate dose and dose equivalent by applying the appropriate biological weighting factors.

Each of the steps that are required to calculate dose equivalent have uncertainties associated with them. Errors that arise in the first step (predicting the particle spectra) will only be carried through to the final step. Therefore, it is important to have accurate predictions of particle fluences, which can be difficult due to the large amount of possible GCR interactions.

These codes rely on experimental neutron data in order to provide accurate results. Shown below in Figure 2 are some experimental data compared to FLUKA calculations [3]. The figure shows that in some areas, there is agreement between the data and calculations, but the agreement falls off in certain areas. At forward angles, below the peaks that are near neutron energies corresponding to velocities equal to beam velocity, the difference is as large as an order of magnitude. The cause of the discrepancies between the model and data could be a variety of reasons related to the physics models used in the transport calculations. Building a large cross section database can help validate the models used in these codes and further improve the accuracy of the codes by allowing code developers to test and modify the physics models they use.

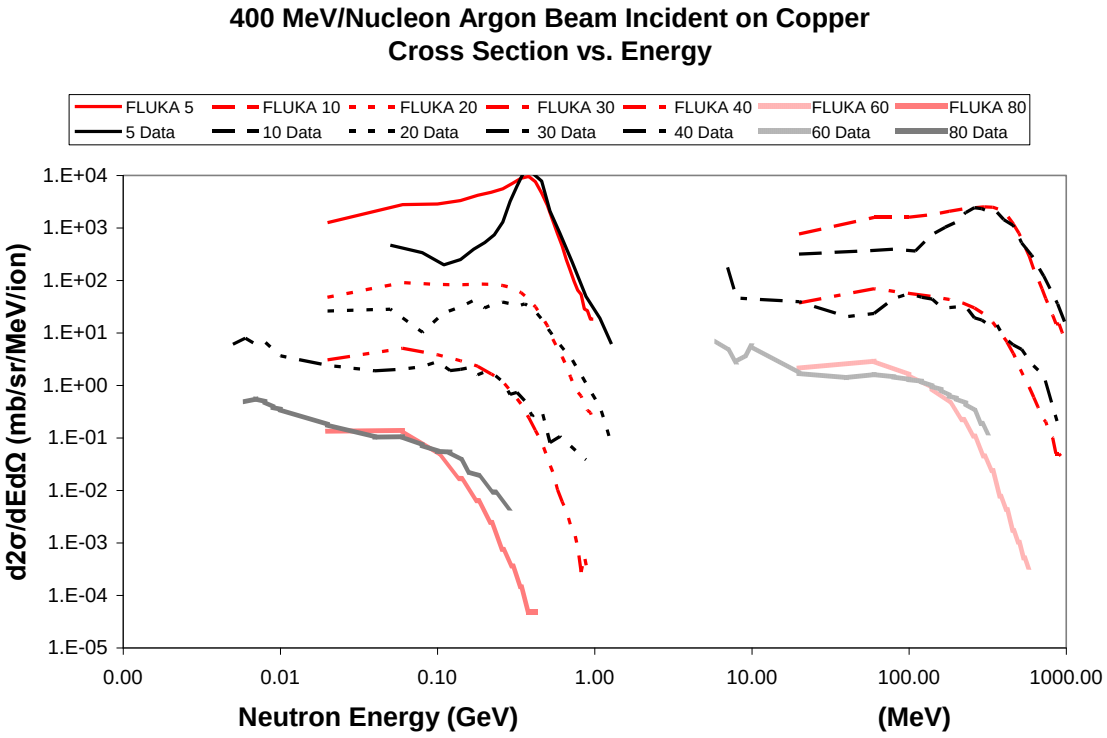

Figure 2. Graph showing comparisons between experimental cross section data and cross sections calculated from FLUKA. Red lines show FLUKA results and black lines show experimental data. This particular scenario shows good agreement at larger angles, but the agreement falters at forward angles [3].

Since many transport codes often use different physics models for propagating particles through matter, discrepancies may arise from one code to another. Figure 3 below shows a comparison between three different transport codes that model the same setup. In this particular example, the results can also differ by an order of magnitude.

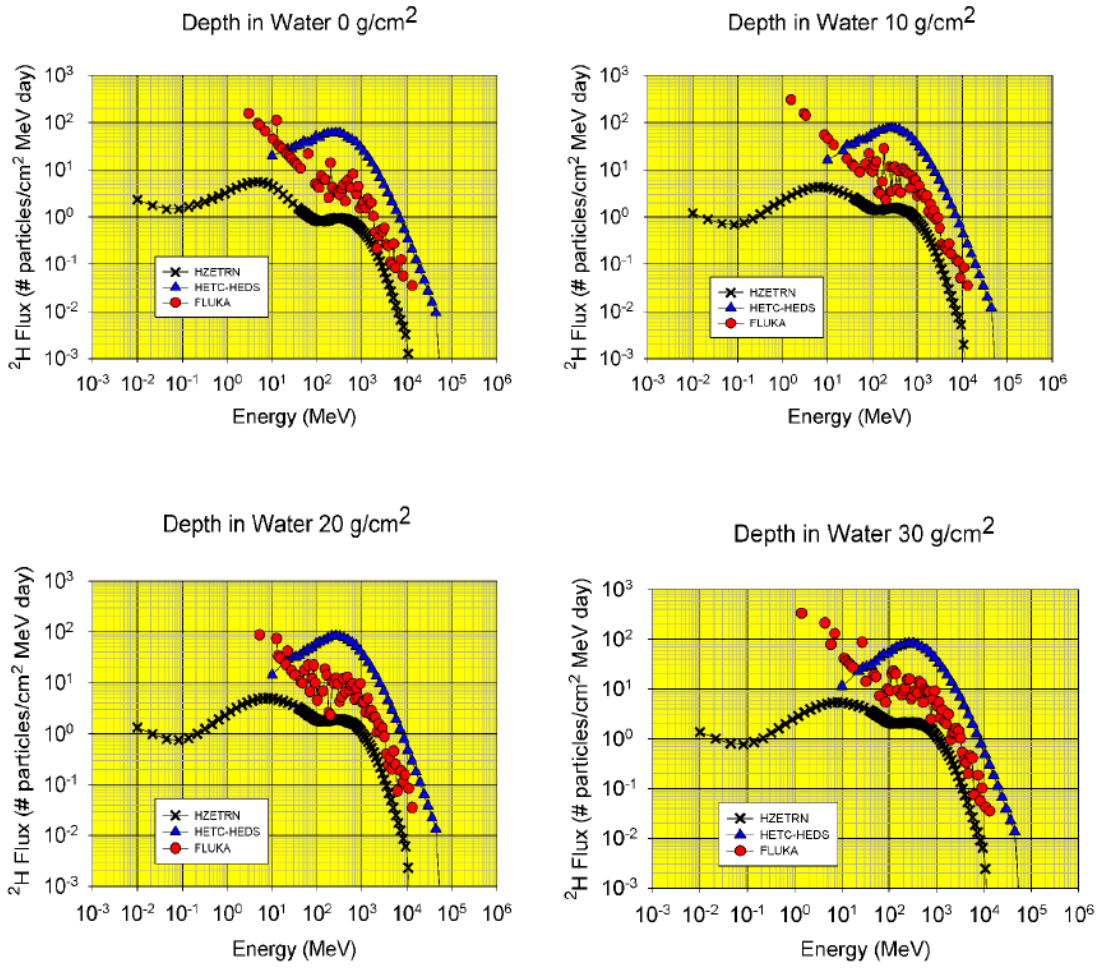

Figure 3. Forward deuteron flux for helium on an aluminum shield. The black, blue, and red data points correspond to HZETRN, HETC-HEDS, and FLUKA respectively [4].

These transport codes are the only calculational methods available for predicting inclusive particle spectra over the entire range of GCR species and energies and over the entire range of the secondary particle species. Light-ion spectra are particularly important for space applications since they contribute a significant portion of the dose received by astronauts, especially behind thick shielding (whereas most heavy ions range out in the material). However, as shown in the figures above, the accuracy and consistency between the codes can falter. This can partly be explained by the lack of light-ion inclusive data that is available to test and validate the codes.

1.1.4 Coalescence Model

The coalescence model has been used to model light ion (deuterons, tritons, ^{3}He, and ^{4}He) production in heavy ion interactions [5, 6, 7, 8, 9, 10, 11, 12, 13, 14]. With this model, protons and neutrons produced by a heavy ion interaction can join together, or "coalesce," to form light ions when they are close enough to each in phase. Generally, it is thought that the coalescence occurs soon after the initial interaction, when the ejected protons and neutrons are still close to each other. In order to properly test the model, proton and neutron spectra are needed as well as the spectra of the light ions one intends to produce.

There is still some uncertainty concerning the coalescence model as there is a lack of data on the subject, especially at the beam energies studied here. Research has gone into model development but with little experimental data with which to compare the model to [11]. Essentially, improvements to the model have been hindered until more experimental data is available.

1.1.5 Cross Section Databases

There have been many experiments that generated light-ion production cross section data for several systems but, so far, there hasn't been a set that encompasses neutrons, protons, and lighter ions for each system [15]. The experiments described in this paper have previously been analyzed to produce neutron cross section data. This information will be referenced, but not detailed, in this paper. Data from the same experiments that produced the neutron data have been analyzed here to produce proton, deuteron, and triton cross section data on the same systems.

1.2 Justification and Originality

For applications involving protection from space radiation, it is important that nuclear interaction cross sections for particles that compose the GCR spectrum are accurately known. The GCR spectrum is comprised of a wide variety of charged and neutral particles with a large range of energies, with the peak energy being 600-1000 AMeV. The most prominent charged particles in the spectrum range from protons to iron particles.

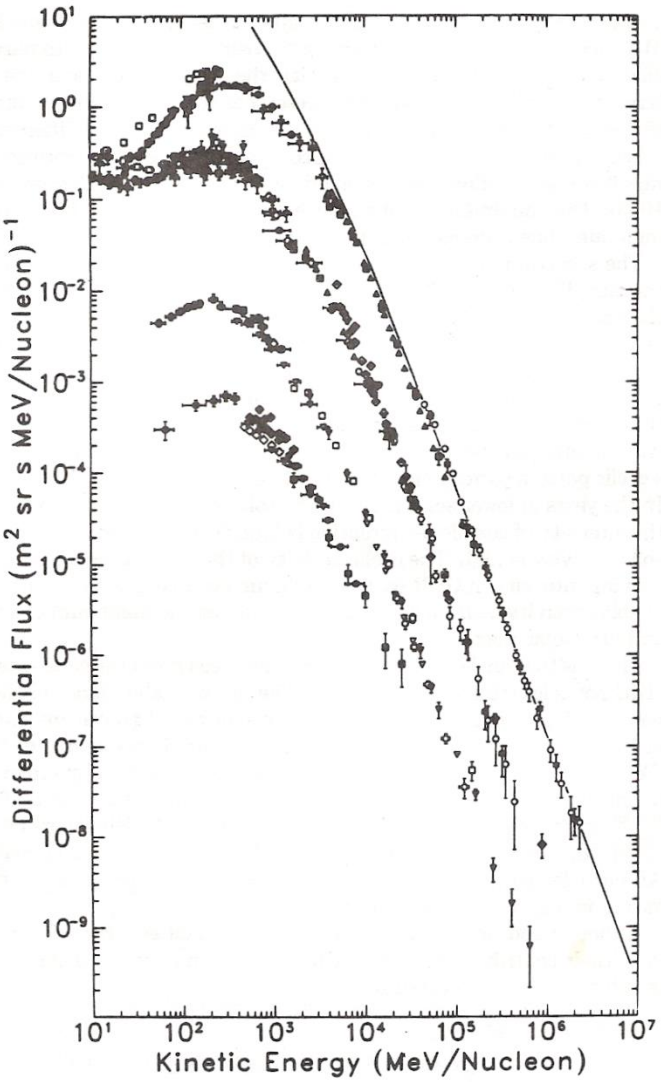

Figure 4. Energy dependent GCR flux distributions of (from top to bottom) galactic protons, helium ions, carbon ions, and iron ions [16].

What makes shielding people or equipment from incident GCR difficult is that the heavier ions can fragment when interacting with the shielding as well as the human body. These fragments tend to retain the velocity of the original projectile and can travel much further in the shield due to having a smaller stopping power. Equation (1) below is an describes this phenomenon and applies to particles of the same energy per nucleon:

$$R_A = R_P \left(\frac{M_A}{{Z_A}^2}\right) \quad (1)$$

where R_A is the range of the ion A, R_P is the range of a proton, and M_A and Z_A are the mass and charge numbers of the ion. As an example, the range of a 300 MeV proton is three times the range of a 300 MeV/nucleon ^{12}C ion. With such occurrences, it is possible to increase the dose a person would receive by shielding heavy ions (as seen below in Figure 5). This can heavily complicate transport calculations, which is why an extensive database of cross sections is important. Unfortunately, there is a lack of experimental data for these heavy ions at the required energy ranges and, as such, secondary particle production cross section data relies heavily on models to predict their values over an extensive range of GCR ions, energies, and shielding materials.

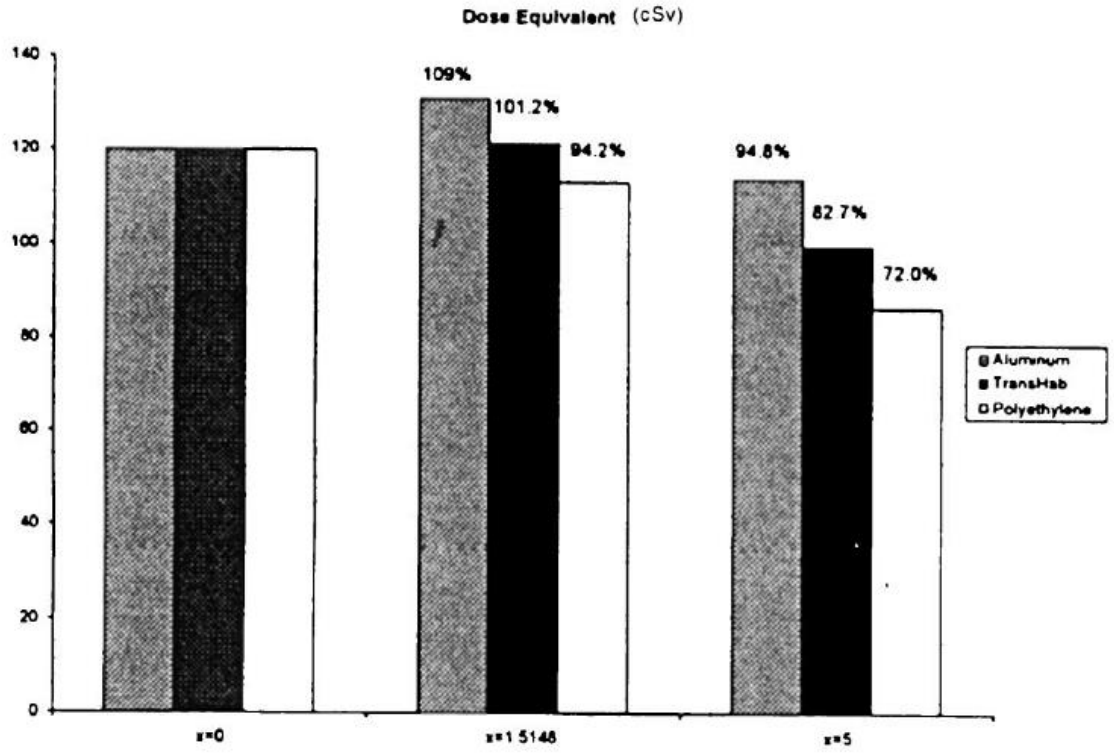

Figure 5. Plots of dose equivalent behind various thicknesses of shielding [17].

One such model is the coalescence model. This model works under the presumption that when a particle fragments, it can fragment into a smaller ion and a participant region containing all the constituent neutrons and protons that were sheared off of the projectile and target nuclei during the interaction.

Nucleons within this region that are close enough in space and momentum may then coalesce into larger ions such as deuterons, tritons, or helium particles. Once the nucleons exceed the boundaries of the region, coalescence ceases and the nucleons become free particles. This space and momentum range is known as the coalescence radius.

Once one knows the production cross sections for neutrons or protons and other light ions for projectile/target systems, one can calculate the coalescence radii. Conversely, knowing the coalescence radii will allow one to derive production cross sections. This is the basis for the coalescence model, the accuracy of which depends greatly on the formulated coalescence radii. Coalescence radii can be calculated for systems that have reliable neutron and light ion cross sections, but with the very limited supply of experimental data that provides this information, the accuracy of these radii is questionable. Expanding the neutron and light ion production cross section databases will help improve the accuracy of the coalescence radii, which will, in turn, improve the accuracy of the model as a whole.

The experiment described in this paper provides double differential cross production cross section data for neutrons and light ions for 39 systems (where a system is defined as a specific projectile ion at a specific energy incident on a specific target). As of the writing of this thesis, no previous data set has been quite this extensive. The cross section data produced from the analysis should provide a large amount of data for coalescence radii calculations, which can then be used to verify the accuracy of existing, analytically calculated coalescence radii. With a large range of systems, the systematics of the derived coalescence radii on projectile mass, projectile energy, and target mass can be explored.

1.3 Goal of Dissertation

The goals of this dissertation are the following, with some further discussion added below:

1. Produce never before measured light-ion (p, d, t, ^{3}He, ^{4}He) double differential inclusive spectra over a wide range of heavy ion species, energies, and target materials that are relevant to space radiation protection.
2. Apply the data produced here to coalescence model calculations over a wide range of systems, providing a comprehensive, systematic test of the coalescence model that has never been done before.
3. Using the results from coalescence model calculations, determine the systematic dependencies (if any) of the coalescence model on beam + target mass, beam energy, and secondary light ion species.

The experiment described in this paper was one that was originally analyzed for double differential neutron production cross section data. It was later determined that the same data that was collected could be used to produce light ion cross section data as well. The addition of this analysis would provide a large set of both neutron and light-ion production cross section data for a large amount of projectile/target systems.

One aspect of the usefulness of this large semi-inclusive set of data is its application to the coalescence model. The coalescence model is a model that calculates light-ion (deuterons, tritons, ^{3}He, and ^{4}He) production cross sections based on parameters known as coalescence radii, which vary from system to system. For systems that already have these cross sections, one can easily calculate the coalescence radius, but for systems that do not have this information, the radii need to be inferred from measured systems that are similar to the system of interest. This proves to be a difficult task given the lack of data on inclusive light-ion cross sections from medium energy heavy-ion interactions. However, the large data set that this experiment provides would be a significant addition to the cross section databases used in providing more accurate coalescence radii.

1.4 Outline

This paper is organized, by chapter, in the following manner:

Chapter I is a basic introduction of the concepts covered in the paper.

Chapter II is an in-depth review of the literature on the coalescence model.

Chapter III contains descriptions of the experimental setup as well as methods used for analyzing the data. This chapter goes into detail about calculating cross sections from the data and applying the results to the coalescence model.

Chapter IV contains the results and a discussion of their significance. The results include cross section and coalescence radii calculations.

Chapter V states the conclusions drawn from the analyzed data and recommendations for future work.

CHAPTER II
LITERATURE REVIEW

The coalescence model was originally proposed to account the production of deuterons in proton-induced reactions at energies of 25-30 AMeV [5]. The model was later adjusted to apply to high-energy heavy-ion interactions [6, 9, 14, 7, 8] and then, more recently, to lower-energy heavy-ion interactions [18, 13, 12]. Explained in this section is the coalescence model as it applies to higher-energy heavy-ion interactions as that is the scope of the data analyzed in this experiment [15].

2.1 Coalescence Model

2.1.2 General Information about the Coalescence Model

The intent of the coalescence model is to relate light-ion (deuterons, tritons, ^{3}He, and ^{4}He) production cross sections with nucleon production cross sections through a parameter called the coalescence radius. During a fragmentation event, a projectile interacts with a target causing breakup of the projectile and target. During the interaction, there is a region where the projectile and target overlap and nucleons within this region are sheared off (see Figure 6 below). The resulting cluster of nucleons is unstable and begins evaporating until a stable ground state is reached. The projectile and target fragments may also evaporate nucleons to reach a ground state if needed. It is with these ejected nucleons that coalescence can take place.

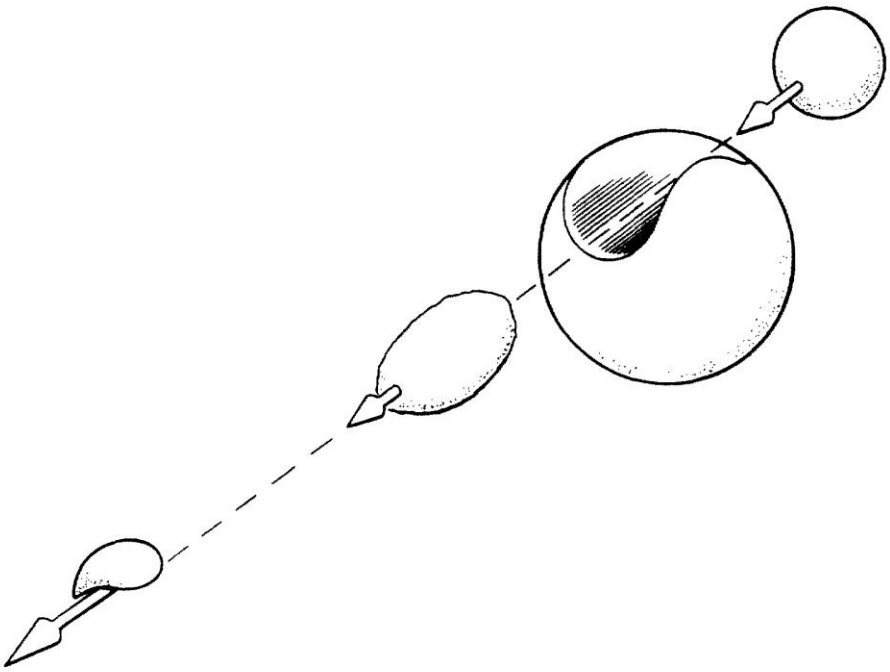

Figure 6. Depiction of particle fragmentation known as the fireball model. In this model, the target and projectile make clear cylindrical cuts through each other leaving a target spectator, and if the impact parameter is large enough, a projectile spectator [19].

The types of ions that are produced by coalescence depend on the types and numbers of nucleons within the coalescence sphere. If the sphere contains a single proton and two neutrons, then a triton may be produced. If the sphere contains two neutrons and two protons, then an alpha particle may be produced. The formulation of the coalescence model begins by determining the probabilities of finding a specific number of each nucleon within the sphere. These probabilities are related to a measureable quantity: nucleon production cross sections. The higher the production cross section, the more likely a nucleon will be found within the coalescence sphere.

2.1.2 Formulation of the Power Law Formula

The parameter that defines the critical point at which coalescence ceases is the coalescence radius P_0, which can be used to define a coalescence sphere. The probability of finding a single nucleon within the sphere, centered around momentum $\overline{p}$ is defined by Awes [18] and shown below:

$$P = \frac{4\pi}{3} P_0^3 \frac{\gamma}{\overline{m}} \frac{d^3N(\overline{p})}{dp^3} \quad (2)$$

where $(d^3N(\overline{p}))/(dp^3)$ represents the differential nucleon multiplicity and $\overline{m}$ represents the average nucleon multiplicity.

In order to produce a complex ion with N neutrons and Z protons, there must be N neutrons and Z protons within the coalescence sphere. The average probability of finding N neutrons and Z protons within the sphere is defined below:

$$\langle P(N,Z) \rangle = \frac{(\overline{m}_Z P_Z)^Z}{Z!} \frac{(\overline{m}_N P_N)^N}{N!} \quad (3)$$

where P_Z and P_N are defined in Equation (2).

The coalescence model also assumes that the proton and neutron distributions have the same shape and are related to one another by the ratio of protons to neutrons in the projectile/target system:

$$\left(\frac{d^3N(\overline{n})}{dp^3}\right) = \left(\frac{N_T+N_P}{Z_T+Z_P}\right)\left(\frac{d^3N(\overline{p})}{dp^3}\right) \quad (4)$$

where N_T, N_P Z_T and Z_P are the number of neutrons and protons in the target and projectile respectively. Essentially, the more neutrons in the system, the more unbound neutrons that can be produced, and the same applies to protons.

Substituting Equation (2) and Equation (4) into Equation (3) gives the following:

$$\left(\frac{d^3N}{dp^3}\right)_A = \frac{A^{-3}}{N!Z!}\left(\frac{N_T+N_P}{Z_T+Z_P}\right)^N \left(\frac{4\pi\gamma P_0^3}{3}\right)^{A-1} \left(\frac{d^3N}{dp^3}\right)^A_{proton} \quad (5)$$

where A is the mass number of the coalesced light-ion. In order to be applicable to the experimental data, the nucleon multiplicity needs to be related to the measured double differential cross sections. This can be accomplish by first normalizing the multiplicity to the total reaction cross section σ_{tot} of the projectile/target system.

$$\frac{d^3N}{dp^3} = \frac{1}{\sigma_{tot}} \frac{d^3\sigma}{dp^3} \quad (6)$$

The Lorentz invariant differential cross section can then be related to the double differential cross section:

$$E\frac{d^3\sigma}{dp^3} = \frac{1}{p}\frac{d^2\sigma}{dEd\Omega} \quad (7)$$

where E and p are the total energy and momentum of the particle. Substituting Equation (6) and Equation (7) into Equation (5) then gives:

$$\frac{1}{\sigma_{tot}}\frac{1}{E_A p_A}\left(\frac{d^2\sigma}{dE_A d\Omega}\right)_A = \frac{A^{-3}}{N!Z!}\left(\frac{N_T+N_P}{Z_T+Z_P}\right)^N\left(\frac{4\pi\gamma P_0^3}{3}\right)^{A-1}\left(\frac{1}{\sigma_{tot}}\frac{1}{E_p p_p}\frac{d^2\sigma}{dE_p d\Omega}\right)^A_{proton} \quad (8)$$

It's important to note that the double differential cross sections are evaluated at the same energy per nucleon. Therefore the velocities of the protons and light ions are the same. Using this information, the following substitutions can be applied:

$$\begin{aligned} E_A &= AE_p \\ p_A &= Ap_p \\ m_A &= Am_p \end{aligned} \quad (9)$$

The following equation shows what is known as the power law formula which connects the complex ion *A* production cross section with the *A*th power of nucleon production cross section [6, 9, 10]:

$$\left(\frac{d^2\sigma}{dE_p d\Omega}\right)_A = \frac{1}{N!Z!}\left(\frac{N_T+N_P}{Z_T+Z_P}\right)^N\left(\frac{4\pi\gamma P_0^3}{3E_p p_p\sigma_{tot}}\right)^{A-1}\left(\frac{d^2\sigma}{dE_p d\Omega}\right)^A_{proton} \quad (10)$$

where N and Z are the neutron and proton number of the ejected ion, σ_{tot} is the total reaction cross section for the projectile/target system, and P_0 is the coalescence radius.

While there is a lack of data applicable to the coalescence model, some calculations have been made in the past. Gutbrod, et al. calculated radii ranging from 106 to 147 MeV/c for deuteron, triton, ^{3}He, and ^{4}He production for intermediate to high energy neon on uranium [6]. Lemaire, et al has much larger set of systems at intermediate to high energies with radii ranging from 170 to 300 MeV/c for deuterons, tritons, and ^{3}He [9]. Finally, Datta, et al shows a slight variation in the model as it applies to lower energy systems. Not only does the paper provide system-wide coalescence radii, it also provides angular dependent radii for angles of 10, 30, 50, and 70 degrees. The projectile energies in the paper range from 15 to 25 AMeV and calculated coalescence radii range from about 50 to slightly over 100 MeV/c [12].

2.1.3 Formulation of the Thermodynamic Formula

The thermodynamic coalescence model [10] does not require nucleon and light-ion production cross sections in order to calculate coalescence radii. Instead, this model uses a parameter called the source emission radius, which is inversely proportional to the coalescence radius. The model treats the participant region created after a projectile/target collision as a thermodynamic system in equilibrium. While this equilibrium is maintained, coalescence may still occur. The source emission radius is the average radius at which thermal equilibrium is maintained.

The thermodynamic model can be derived using adjusting power law formula shown in Equation (5).

$$\left(\frac{d^3N}{dp^3}\right)_A = \frac{\mathbf{1}}{N!Z!}\left(\frac{N_T+N_P}{Z_T+Z_P}\right)^N \frac{\mathbf{2}\boldsymbol{s}\mathbf{+1}}{\mathbf{2}^{\boldsymbol{A}}}\left(\frac{4\pi\gamma\tilde{P}_0^3}{3}\right)^{A-1}\left(\frac{d^3N}{dp^3}\right)^A_{proton} \quad (11)$$

where s is the spin of the light-ion. Equation (11) separates the spin alignment from P_0 which introduces a new term $\tilde{P}_0^3$. This term is related to the source emission radius as follows:

$$\left(\frac{4\pi\gamma\tilde{P}_0^3}{3}\right)^{A-1} = \left(\frac{\gamma(hc)^3}{\frac{4}{3}\pi R^3}\right)^{A-1} e^{\frac{BE_A}{\theta_{avg}}} N!\,Z! \quad (12)$$

where BE_A is the binding energy of the light-ion, θ_{avg} is the average emitting source temperature, h is Plank's constant, c is the speed of light, and R is the source radius. Substituting Equation (12) into Equation (11) and then setting equal to (5) will allow for the calculation of the coalescence radius using the source radius as an input.

$$P_0 = \left(A^3\left(\frac{2s+1}{2^A}\right)\left(e^{\frac{BE_A}{\theta_{avg}}}N!\,Z!\right)\right)^{\frac{1}{3(A-1)}}\left(\frac{9\gamma}{2\pi^2}\right)^{\frac{1}{3}}\frac{hc}{2R} \quad (13)$$

CHAPTER III
MATERIALS AND METHODS

3.1 Experimental Setup

3.1.1 Run Descriptions

The experiment was set up at the Heavy-Ion Medical Accelerator in Chiba (HIMAC) facility in Japan. Several systems were run where each system is composed of a specific ion that is accelerated to a specific energy. Multiple targets were used for each system. The targets included Al, Cu, Li, C, and Pb. The ions used in the experiment ranged from He to Xe at energies between 230 and 600 MeV/nucleon. A full description of the systems and targets can be seen below in Table 1.

Table 1. List of beam types and energies and the targets used with them.Most of the targets are square with dimensions of 10 cm by 10 cm. The lithium targets are circular with a 5.7 cm diameter.

Date (Month-Year)	***Beam ion and energy (MeV/u)***	***Target type, thickness (cm) and areal density [(g/cm^2)]***				
		Al	***Pb***	***Cu***	***C***	***Li***
Apr 00	C (290)	-	0.2 [2.27]	0.5 [4.48]	1.0 [1.784]	-
Apr 00	Ne (600)	-	0.4 [4.54]	0.5 [4.48]	2.0 [3.568]	-
Apr 00	Ne (400)	-	0.2 [2.27]	0.5 [4.48]	1.0 [1.784]	-
Apr 01	C (290)	-	0.2 [2.27]	-	1.0 [1.8]	-
May 01	Si (600)	-	0.4 [4.54]	0.4 [3.584]	1.0 [1.784]	-
May 01	Ne (600)	1.2 [3.24]	-	-	-	5.28 [2.7984]
May 01	Xe (400)	0.095 [0.2565]	-	-	-	0.9 [0.477]
Jan 02	Fe (500)	0.476 [1.2852]	-	-	-	1.7 [0.901]
Jan 02	Kr (400)	0.2 [0.54]	0.09 [1.0215]	0.1 [0.896]	0.3 [0.549]	0.885 [0.46905]
June 02	He (230)	2 [5.4]	-	0.6 [5.376]	-	-
June 02	Xe (400)	0.095 [0.2565]	0.05 [0.5675]	0.05 [0.448]	0.15 [0.2676]	0.9 [0.477]
June 02	N (400)	-	-	0.3 [2.688]	1.0 [1.784]	-
Nov 02	C (400)	1.476 [3.9852]	0.4 [4.54]	0.5 [4.48]	2.0 [3.568]	5.6 [2.968]
Nov 02	Ne (400)	1.476 [3.9852]	-	-	-	5.6 [2.968]

3.1.2 Detector Setup

The experimental setup used 15 organic scintillators. One detector, the "trigger" detector, was placed at the beam exit window. The rest of the detectors were grouped into seven sets of two. Each detector set consisted of one 5" by 5" square, ¼" (6 mm) thick plastic scintillator directly in front of a 5" liquid scintillator. The plastic scintillators in each detector set are "veto" detectors. The trigger detector was a plastic 2" by 2" square scintillator that ranged in thickness from 0.1 to 0.5 mm depending on the beam type. The detector s can be seen below in Figure 7 and Figure 8 and a schematic of the detector setup can be seen below in Figure 9.

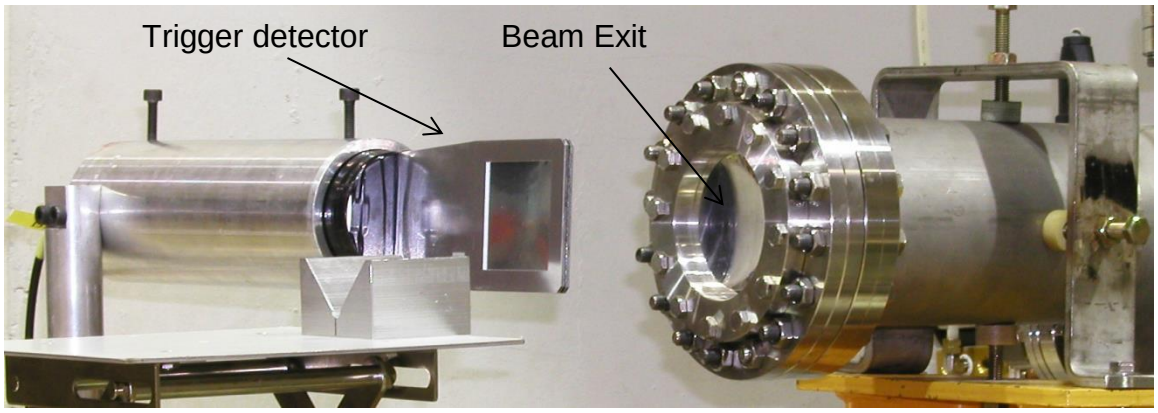

Figure 7. The beam detecting scintillator ("trigger plastic") located approximately 5 cm downstream from the beam exit. The beam travels from right to left in the picture. The target materials were placed on the stand directly downstream from the beam scintillator.

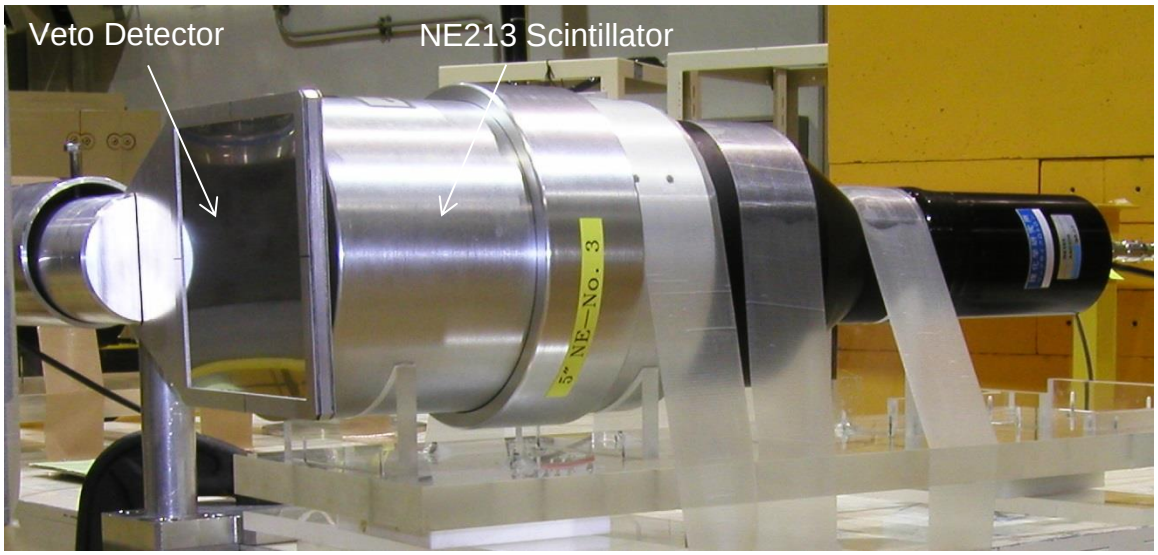

Figure 8. A view of a thin plastic “veto” detector followed by a 5” liquid scintillator.

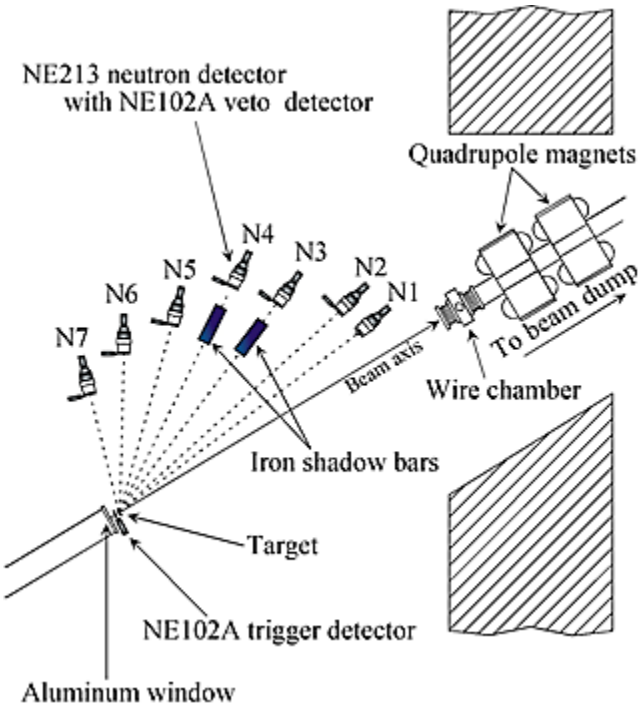

Figure 9. Schematic of the experimental setup.

The trigger detector was placed 5 cm downstream from the beam exit window followed by the targets, which were placed 19 cm downstream from the beam exit window. For some runs, a 4 meter long, 30 cm diameter He-filled tube was also placed along the beam axis, downstream from the beam exit window (not shown in Figure 9). Finally, the beam dump was located 7 meters downstream.

The neutron and veto detector sets were arranged at various angles ranging from 5 to 80 degrees off of the beam axis. The centers of the scintillator cells were positioned between 306 cm and 506 cm from the center of the target (distances to the front faces of the detectors are 6 cm shorter, ranging from 300 to 500 cm), depending on the laboratory angle at which the detectors were placed. More detailed information about the detector setup can be seen below in Table 2.

Table 2. Description of the seven detector set positions.

Detector Set	***Flight Path Length (cm)***	***Lab Angle (deg)***	***Solid Angle (mSr)***
N1	506	5	0.494 ± 5.0%
N2	506	10	0.494 ± 5.0%
N3	456	20	0.608 ± 5.6%
N4	456	30	0.608 ± 5.6%
N5	406	40	0.767 ± 6.2%
N6	356	60	0.989 ± 7.1%
N7	306	80	1.35 ± 8.3%

3.1.3 Shadow Bar Setup

For background spectra, 1 to 3 shadow bars were included in the setup (depending on the system and run number). One shadow bar was composed of two solid iron blocks that were 15 cm by 15 cm square and 50 cm long. The other shadow bars were made by stacking 5 cm by 5 cm long iron bars together. The shadow bars are and were placed in front of the certain detectors to prevent ions originating from the direction of the target from interacting with the detectors directly behind the shadow bars. A picture of two shadow bars can be seen below in Figure 10.

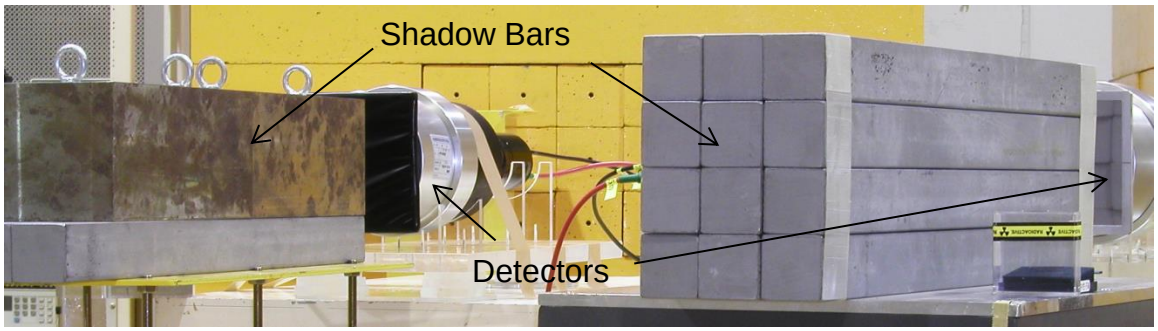

Figure 10. A view of two shadow bars.

3.1.4 Beam Setup

The beam was delivered to the target in pulses every 3.3 seconds. The duration of each pulse lasted between 0.5 and 1 second depending on the beam type. The average intensity of each pulse varied between 10^4 and 10^5 particles per pulse. The beam spot size on the target was a few millimeters in diameter and the beam spread was negligible compared to the divergence caused by coulomb scattering in the target and surrounding air.

3.2 Data Acquisition

This section describes the processes by which the particles are detected and the data is collected. Descriptions include how events are triggered and stopped, and how background spectra are created.

3.2.1 Triggering Events

When a beam particle exits the beam window, it first interacts with the trigger detector. The trigger detector sends out a delayed signal, which triggers the end of an event (rather than the start of one). The beam particle then enters the target and has a chance to interact in a multitude of ways including fragmentation. Beam particles that undergo nuclear interactions expel fragments in all directions with many of them heading toward one of the seven detector sets. Heavier fragments come from projectile breakup and are focused more toward the forward angles, whereas lighter ions, which come from target breakup and the decay of the overlap region, have less forward momentum than the projectile fragments and can be seen at broader angles. When one of the fragments interacts with a liquid scintillator, it signals the start of the event.

Charge deposition and timing information are recorded for all detectors until the delayed timing signal from the trigger detector arrives to end the event.

The purpose for having the trigger detector signal the end of the event is to eliminate a multitude of events that register a beam particle in the trigger detector but no events in the downstream detectors. Relatively few of the beam particles create fragments that interact with one of the detector sets. It also helps prevent pileup issues involved with having large timing windows looking for a stop signal when none will actually show up.

3.2.2 Background Spectra

In order to measure background information, shadow bars were used in the setup. The shadow bars are placed in front of a specific detector set in order to block all fragments that originate from the target and travel directly to the detector. Therefore, events that are triggered by the detectors behind the shadow bars are treated as background events that must be removed from the non-shadow bar data.

For many of the target and beam combinations, there were four separate runs. Each run used a different shadow bar configuration in order to produce background spectra for every detector set. Most of the systems used the following configurations: (1) shadow bars in front of N1 and N2, (2) shadow bars in front of N3 and N4, (3) shadow bars in front of N5 and N6, and (4) shadow bars in front of N7. The Xe and Ne beam systems from May 2001 utilized only 5 of the 7 detector sets (omitting detector sets N4 and N6). The shadow bar configurations for these systems were the following: (1) shadow bars in front of N1 and N2, (2) shadow bars in front of N3 and N5, and (3) shadow bars in front of N7. The C beam system from April 2001 did not include the N7 detector set. The shadow bar configuration for this system was as follows: (1) shadow bars in front of N1 and N2, (2) shadow bars in front of N3 and N4, and (3) shadow bars in front of N5 and N6. The systems from November 2002 included all 7 detector sets, but used 3 different configurations instead of 4: (1) shadow bars in front of N1, N2, and N7, (2) shadow bars in front of N3 and N4, and (3) shadow bars in front of N5 and N6. Additional details for these runs can be seen above in Table 1.

For each system, a set of “blank target” runs were included using the same shadow bar configurations described above. This allows for the elimination of background caused by beam interactions in materials near the target region other than the target (such as the trigger detector, beam exit window, and air), since the shadow bars can’t distinguish between these particles and those actually created in the target.

3.3 Cross Section Calculations

3.3.1 Charged and Neutral Particle Discrimination

Events are triggered when particles interact in one of the seven liquid scintillators. Events can be triggered by both charged and neutral particles. Discriminating between the two can be accomplished by observing the signals produced by the veto detectors (the plastic scintillators located directly in front of the liquid scintillators). Charged particles deposit a small fraction of their energy in these plastic scintillators whereas neutral particles generally pass through unimpeded. Since the scope of the analysis includes charged particles, but not neutral particles, events that contain veto detector signals above a certain threshold are kept and all others are ignored. A histogram of a typical veto detector output can be seen below in Figure 11.

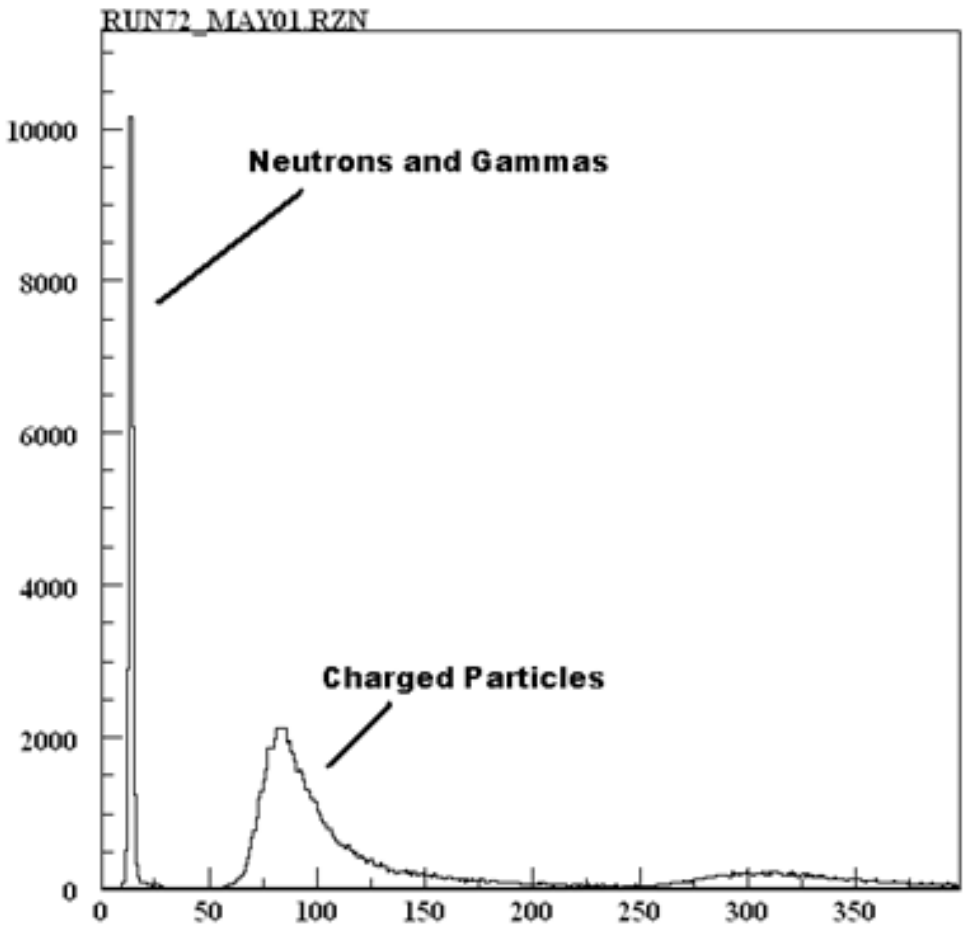

Figure 11. Histogram of energy deposition in a veto detector. The x axis corresponds to charge collection in the veto detector during the event. This histogram was extracted from detector set N4 (30 degrees).

3.3.2 Ion Identification

After discarding events that were triggered by neutral particles, the events that remain are those triggered by charged particles. Since the goal of the analysis is to calculate light ion production cross sections, it is necessary to identify the specific ions that triggered each event. The projectile and target may fragment into a variety of charged particles with different masses and kinetic energies, but given the experimental setup, only the lighter, more energetic ions will be able to reach the detectors before being absorbed in air. This can be accomplished by analyzing the measured time-of-flight of the particle and its associated energy deposition in a liquid scintillator. By producing two-dimensional pdt (proton-deutron-triton) plots of energy deposition vs time-of-

flight, the different isotopes can be identified and separated. This can be observed in Figure 12 below.

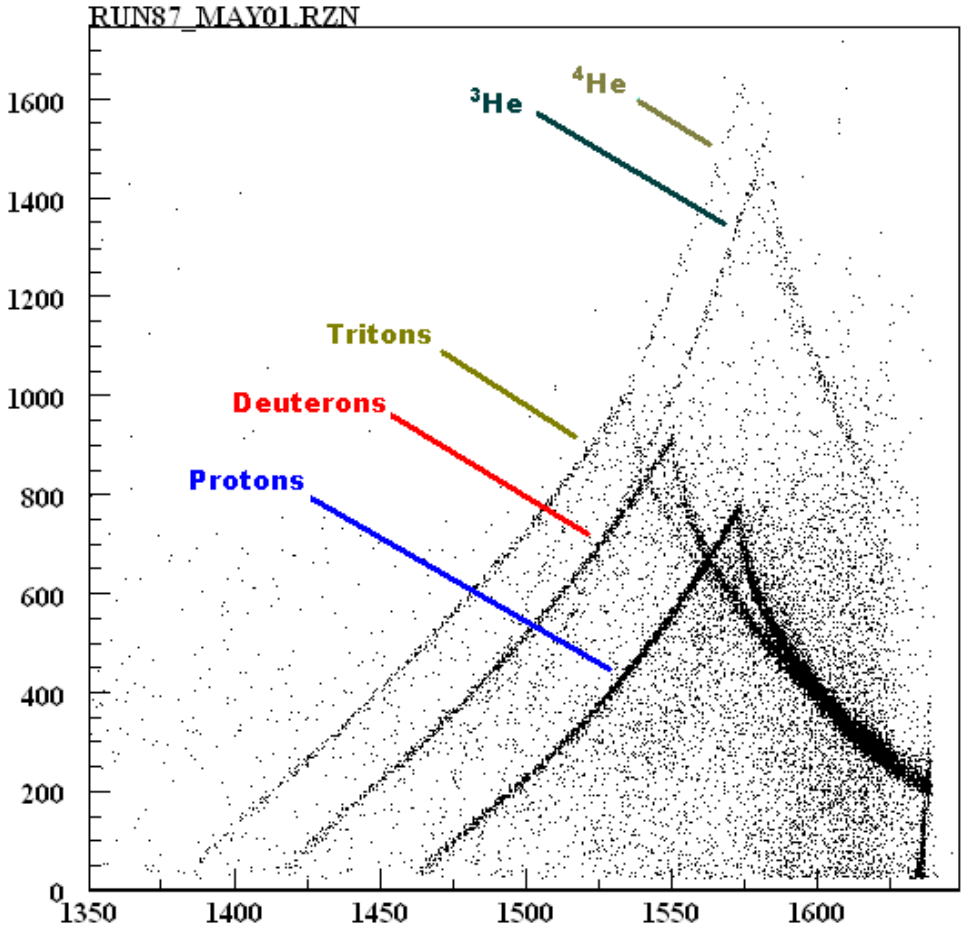

Figure 12. 2D plot of pulse height vs time-of-flight. The x axis corresponds to channel numbers, each of which represents 0.25 ns (note that time-of-flight decreases from left to right). The y axis corresponds to charge collection in the liquid scintillator during the event. This plot was extracted from the detector set N4 (30 degrees).

The interesting peaked lines can be explained by a few different phenomena. Different isotopes with similar time-of-flights will have similar velocities (with small deviations due to differing energy losses in air); however, the heavier ions will have higher energies and will deposit more energy in a detector. As time-of-flight decreases, the particle's energy also increases,

allowing for the deposition of more energy, assuming that the particle stops in the detector. This produces the upward sloping lines in the pdt plots. Since the detectors have a finite depth, this trend continues until a point where the particles are energetic enough to punch straight through the detector. At this point (the punch through point), a peak appears in the pdt plot, and the lines begin a downward sloping trend. This trend signifies a decrease in the energy deposition with decreased time-of-flights. In the energy regime that is detected in this experiment, higher energy particles have a lower linear-energy-transfer (LET) meaning they deposit less energy over a given distance. At energies past the punch through point, particles will pass through the same 5" of detector, but deposit less energy while doing so.

3.3.3 Particle Identification

The specific ions that produce each of the peaked lines in the pdt plots can be verified by comparing the measured punch through points to tabulated data. As described earlier, the punch through points occur when the ions are energetic enough completely range out in the 5" liquid scintillators. Energy dependent range values for protons incident on various target materials (including scintillating materials) are well known. Agreement between this tabulated data and the data in this experiment will verify the ions that were identified in the pdt plots.

The tabulated data provided by Janni [20] contains range-energy data for protons only. However, this information can be used to estimate deuteron and triton energies, where they range-out, by using the following formula:

$$R_A = R_P \left(\frac{M_A}{{Z_A}^2}\right) \qquad (14)$$

Where R_A is the range of particle with atomic number A, R_P is the range of a proton, Z is the charge, and M_A is the mass of the particle with atomic number A. Equation (14) can be applied to ions with the same energy per nucleon. Since the goal is to find the energy at which deuterons and tritons stop at the edge of the liquid scintillators, R_A has a value of 5" allowing one to calculate R_P. The calculated R_P value is cross-referenced in the lookup tables to find the energy at which protons travel the full range of R_P. The listed energy is, therefore, the energy per nucleon at which the ion in question stops completely after travelling through 5" of liquid scintillating material.

3.3.4 TOF Calculations

In order to compare the experimental data with the tabulated data, the time-of-flight measurements need to be calibrated and converted into energy.

The raw time-of-flight measurements are binned into histograms with channels widths of 0.25 ns (the time-to-digital converter (TDC) spectra were calibrated with an ORTEC Time Calibrator before and after the experiments). The time-of flight values associated with each channel number can be calculated by identifying the channel at which the prompt gamma rays pile up (prompt gammas refer to gamma rays produced by beam interactions in the target). All prompt gammas travel at the speed of light and will, therefore, have the same time-of-flight. Since gamma rays are neutral particles, calculating their time-of-flight is a straightforward process:

$$TOF = \frac{d}{v} \quad (15)$$

Where d is the flight distance and v is the particle velocity.

After the gamma peak and associated time-of-flight have been identified, the time-of-flight can be calculated with the following formula:

$$TOF(CH) = \left(CH_\gamma - CH\right) * 0.25 + TOF_\gamma \quad (16)$$

where CH_γ is the channel number of the gamma peak, TOF_γ is the time-of-flight for gammas, and CH is the channel number in question. The result is a time-of-flight for the chosen channel number. An example time-of-flight histogram is shown below in Figure 13:

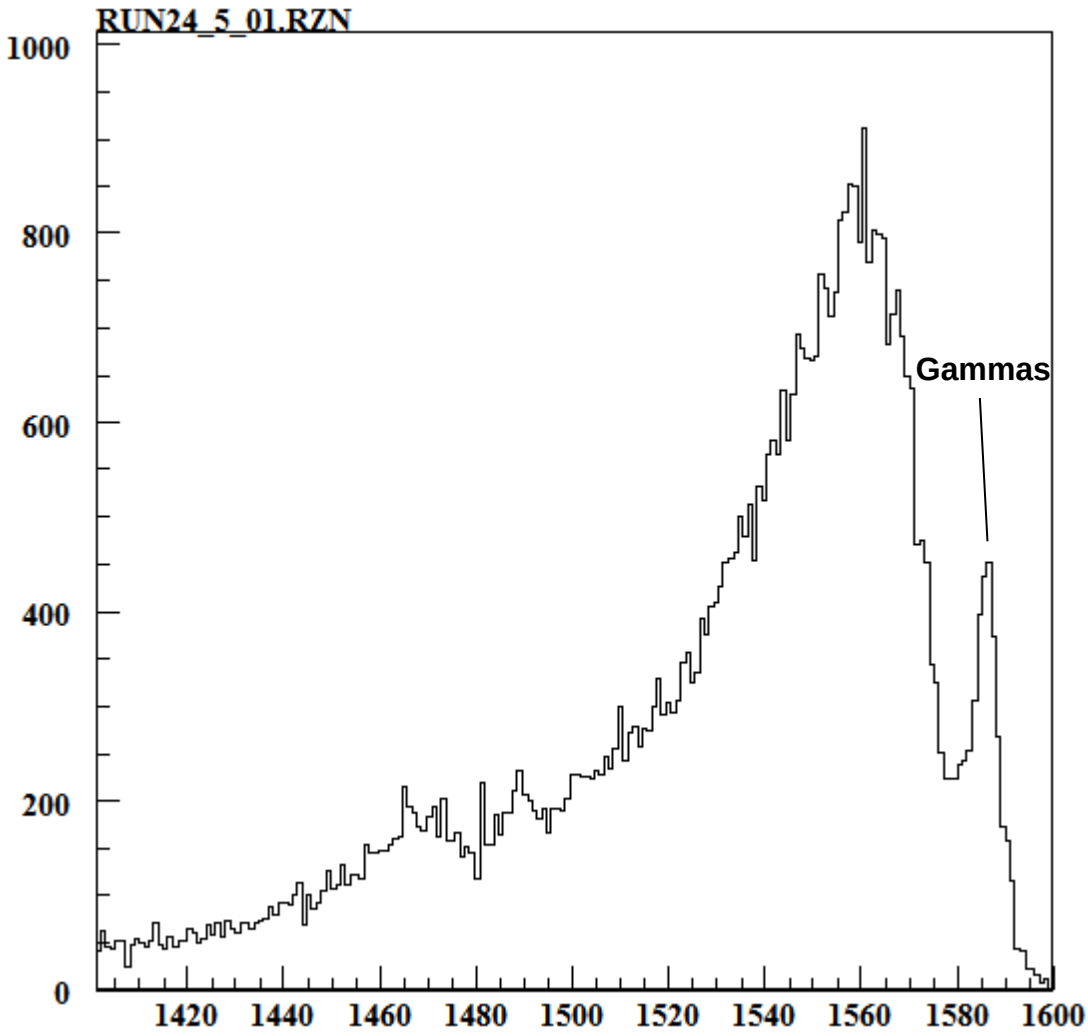

Figure 13. Histogram of time-of-flight values measured in one of the detector sets.The x axis corresponds to channel numbers, each of which represents 0.25 ns (note that time-of-flight decreases from left to right). This histogram was extracted from detector set N5 (40 degrees).

3.3.5 TOF to Energy Conversion

In order to generate double differential cross section data, the time-of-flight measurements need to be converted into energies at the point of particle production. Although interactions occur all along the path of the beam in the target, the point of production is assumed to be at the halfway point through the target. This conversion is complicated with charged particles due to the slowing down mechanism they experience as they lose energy while traveling through a

medium (referred to as stopping power). The stopping power depends on several factors including particle type, medium composition, and particle energy. The energy dependence of the stopping power typically necessitates the use of computer codes to help with calculations that involve charged particle transport through a significant amount of material. The code developed for this particular part of the analysis tracks particles from the point of production in the target to the point where the particles interact in the detectors. The code uses an iterative process that tracks changes in energy and time between several points from the target to the detector. The changes in energy are calculated using stopping power values obtained from NIST [21]. The result of the calculation gives both an energy at the point of production and a final energy (energy of the particle when it reaches the detector) for every time-of-flight channel. This code can be seen in Appendix B.4 TOF and Energy Calculations.

Double differential cross sections for particle production can be calculated once the particle energy, angle, and intensity are known. Double differential cross sections are in units of b/(MeV-Sr) and integrating over all energies and angles will provide a total production cross section of that particle.

Secondary particles are produced at a continuum of energies, but the nature of the data acquisition system (DAQ) discretizes the information into energy bins (or more precisely, time-of-flight bins which are later converted into energy bins). The data in these experiments are binned into channels with a 0.25 nanosecond window. The angular distribution is also a continuum, but detectors are discrete sizes with an angular resolution of that of detector itself. The experiment described in this paper uses seven detectors in most setups, which means the double differential cross section is only measured at seven different angles in most cases, spanning an angular range between 5 and 80 degrees relative to the beam axis.

Increasing the size of the energy bins (and, even though this does not occur in this analysis, the angular bins) will worsen the resolution of the measurements, but the statistics will improve due to the increased count rate in each bin. Most of the measurements taken in these experiments were re-binned at lower energies in order to take advantage of this concept to increase statistical accuracy.

3.4 Cross Section Corrections

Once the cross sections are calculated, they need to be corrected for various effects present in the experiment and in the analysis. These corrections include overlap adjustments, reaction cross section adjustments, and scattering adjustments. Each of these will be explained in more detail in the following sections.

3.4.1 PDT Overlap Corrections

As shown below in Figure 14, each of the isotope lines in the pdt plots overlap with a neighboring line at some point. When calculating a specific particle intensity, the count rates will be inflated at these overlap points due to the presence of counts from at least two different particles. In order to adjust the data, two assumptions were made. First, the data from each ion is assumed to be continuous with no abrupt changes in magnitude throughout this energy regime. Second, the count rates at the overlap points consist solely of the particles in that overlap. This means that if half the particles in the p-d overlap are protons, then the other half will be deuterons.

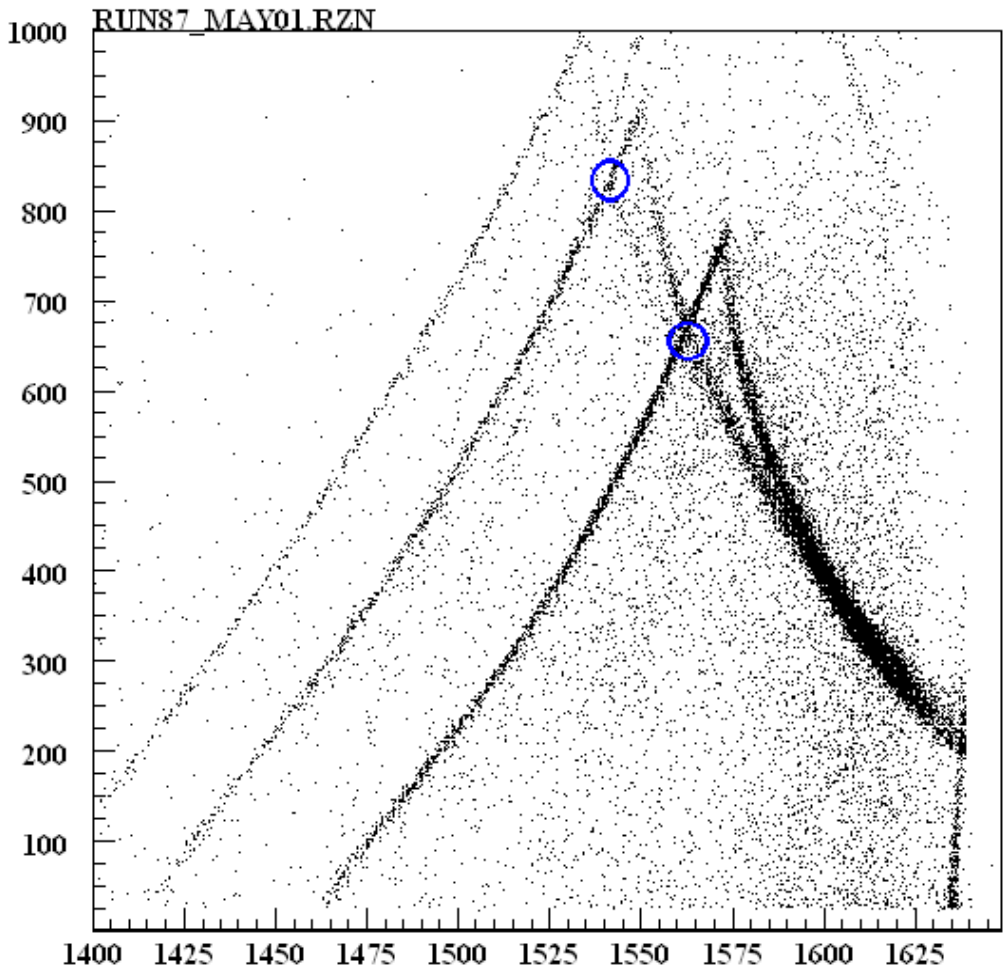

Figure 14. A pdt plot showing overlap points. The x axis corresponds to channel numbers, each of which represents 0.25 ns (note that time-of-flight decreases from left to right). The y axis corresponds to charge collection in the liquid scintillator during the event. This plot was extracted from the detector set N4 (30 degrees).

The overlap corrections are not calculated, but, rather, determined by graphical observations. The applied corrections attempt to deflate the data so that the resulting cross section plot looks continuous while also ensuring the second assumption is maintained, e.g., if 30% of the counts are removed from protons in the p-t overlap, then 70% are removed from the tritons in the p-t overlap, ensuring a conservation of the total number of counts in the overlap region. An example correction can be seen below in Figure 15.

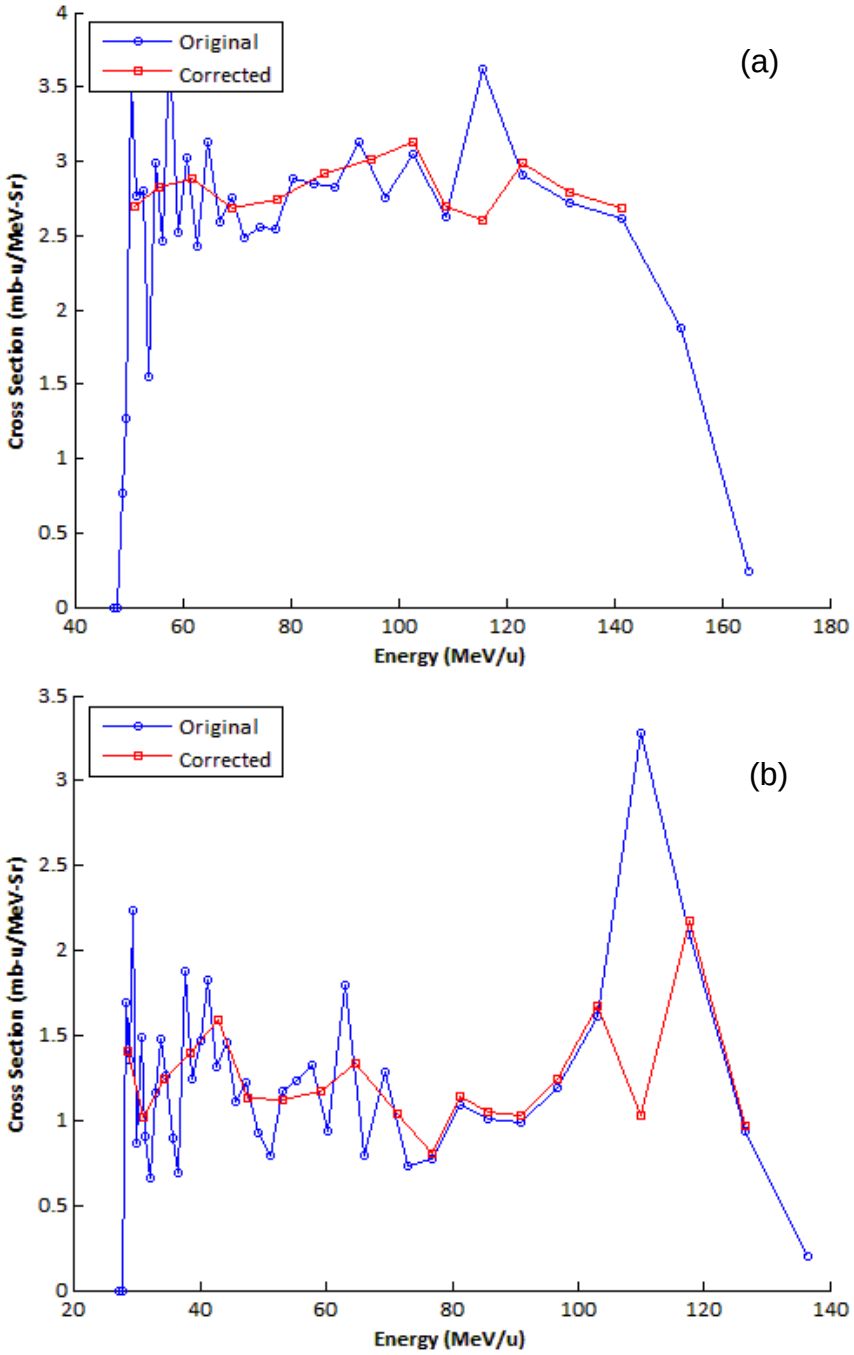

Figure 15. Plots showing data corrected for the pdt overlap compared to the original data. (a) shows protons and (b) shows deuterons. This data is taken from the 30 degree detector in the 290 AMeV carbon on carbon system.

3.4.2 Reaction Cross Section Corrections

When the light ions travel toward a detector set, there is a chance that some will be absorbed in the target or surrounding air. The result is that some of the particles that should have made it to the detectors were lost. This effectively lowers the measured cross sections, and the loss of counts should be corrected.

In order to correct for the particle loss due to absorption, one can apply the following equation:

$$I = I_0 e^{(-N\sigma_r t)} \qquad (17)$$

where I is the intensity of particles at the end of the flight path, I_0 is the original intensity, N is the atomic density of the medium that the particles are traveling through, σ_r is the reaction cross section, and t is the length of the flight path. Assuming an initial intensity of 1, the result is the ratio of particles that actually survive after travelling through path length t.

There is not an abundance of cross section data at the energy regimes for this experiment, so reaction cross section models must be employed in order to use this equation. The model used for this analysis is described in full in Tripathi [22, 23, 24].

The difficulty with Equation (17) lies in the fact that the charged particles slow down when travelling through a medium and that the reaction cross sections are dependent on the energy of the particles. This problem is overcome by tracking particles over very short segments of the total path length so that the energy loss is very small. The equation is applied several times until the entire path length is compensated for. The code used for this process can be seen in B.4 TOF and Energy Calculations.

3.5 Limitations in Data

Throughout many of the runs in this experiment, some phenomena arise that limit the scope of the data. The three phenomena described in this section are PDT convergence, QDC (charge to digital converter) saturation, and superfluous PDT lines. The first two limit the useable energy range when calculating cross sections. The third one, while not necessarily limiting the scope of the data, poses an interesting question as to the cause of the extra lines.

3.5.1 High-Energy PDT Plot Convergence

With every data set comes a phenomenon that limits the useable energy window for the cross section calculations. Each of the peaked lines in the pdt plots begin to merge together at lower time-of-flights, effectively preventing the discrimination between the different ions. This phenomenon can be seen in Figure 16 with the red region (merged deuteron and triton lines) and the blue region (merged proton, deuteron, and triton lines). Corrections at this point are impractical as the trend in the data beyond the merging point is uncertain. Combining the information for each ion beyond the merging point into one set is possible, but the resulting cross section calculations would need to be in terms of flight time, as the energies would be different for each ion. However, double differential time-of-flight spectra have limited utility and are not considered here.

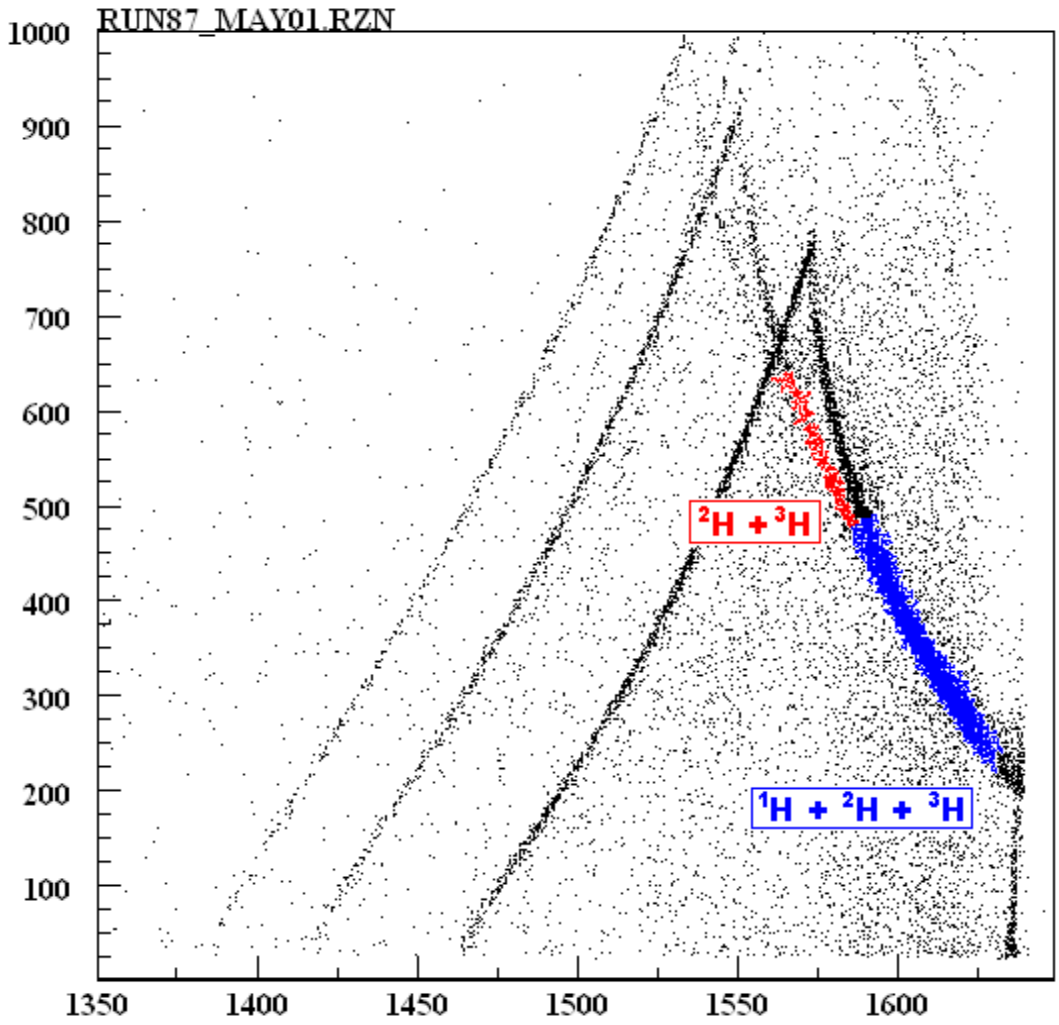

Figure 16. Histogram of time-of-flight values measured in one of the detector sets.The x axis corresponds to channel numbers, each of which represents 0.25 ns (note that time-of-flight decreases from left to right). The y axis corresponds to charge collection in the liquid scintillator during the event. This plot was extracted from the detector set N4 (30 degrees).

3.5.2 QDC Saturation

QDC (charge to digital converter) saturation issues arise in some of the earlier measured systems for this experiment. Since the original focus of the experiments was to observe neutron production, the detector gain settings weren't optimal for charged particle analysis. As such, some charged light ion pulses saturated the QDC and had recorded QDC values at the maximum channel number, 2047. Some runs include two-dimenstional QDC vs TDC p-d-t plots where the peaked lines saturated at the top of the graph. This can be seen

in Figure 17 below by the horizontal line at a QDC value above channel 2000, extending across the entire range of TDC channel numbers. This limits the dynamic range of useable data because particle identification is not possible in the region of saturation.

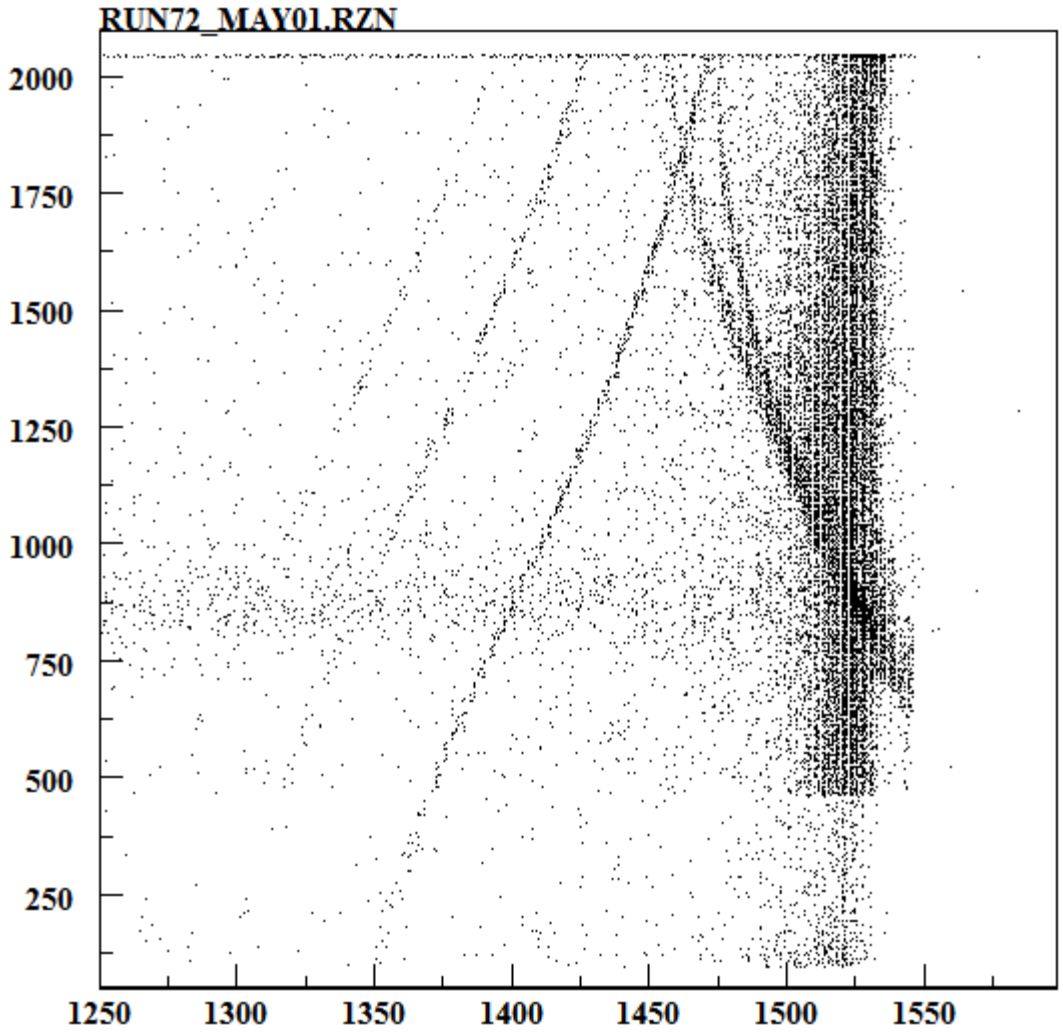

Figure 17. An example pdt plot showing line saturation.The x axis corresponds to channel numbers, each of which represents 0.25 ns (note that time-of-flight decreases from left to right). The y axis corresponds to charge collection in the liquid scintillator during the event. This plot was extracted from the detector set N1 (5 degrees).

3.5.3 Superfluous PDT Lines

Some of the later-run sets have extra particle lines that appear in the pdt plots. These lines behave much in the same way as the pdt lines and they can be easily subtracted using the background runs. An example of this phenomenon can be seen below in Figure 18.

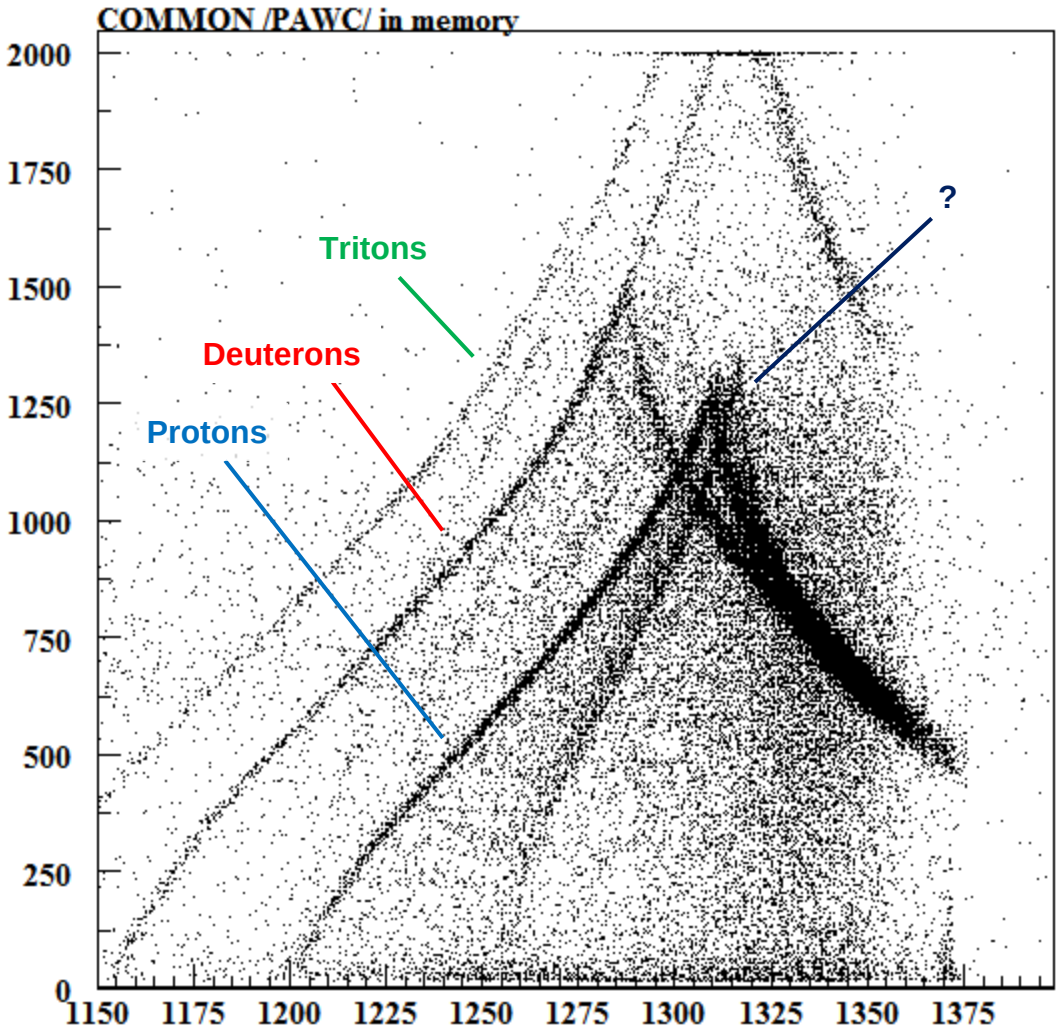

Figure 18. An example pdt plot showing an extraneous peaked line. The x axis corresponds to channel numbers, each of which represents 0.25 ns (note that time-of-flight decreases from left to right). The y axis corresponds to charge collection in the liquid scintillator during the event. This plot was extracted from the detector set N4 (30 degrees).

3.6 Coalescence Model Application

After the cross sections have been corrected, coalescence radii can finally be calculated. These radii can be calculated using only nucleon and light-ion production cross-sections, explained in further detail below.

3.6.1 Calculating Coalescence Radii

Using the cross sections calculated in this experiment, coalescence radii can be calculated for a wide range of energy and angles for many systems. Normally, the coalescence model uses nucleon cross section data alongside coalescence radii in order to calculate light-ion cross sections. The equation below is the power law formula and its derivation was described in Section 2.1.2 Formulation of the Power Law Formula:

$$\left(\frac{d^2\sigma}{dE_p d\Omega}\right)_A = \frac{1}{N!Z!}\left(\frac{N_T+N_P}{Z_T+Z_P}\right)^N \left(\frac{4\pi\gamma P_0^3}{3E_p p_p \sigma_{tot}}\right)^{A-1} \left(\frac{d^2\sigma}{dE_p d\Omega}\right)^A_{proton} \quad (18)$$

where N, N_P, N_T and N, Z_P, Z_T are the neutron and proton numbers of the light ion, projectile, and target, respectively. A is the mass number of the light ion, σ_{tot} is the total reaction cross section of the projectile/target system, $E_p$is the total energy of the protons, p_p is the momentum of the protons, γ is the Lorentz factor, and $P_0$is the coalescence radius in momentum space. The cross sections are in units of mb/Sr-MeV and the coalescence radius is in units of MeV/c. Note that the result of Equation (18) is a double differential cross section at the same energy per nucleon and projection angle as the provided proton cross section. This means that:

$$E_A = AE_p \quad (19)$$

The experiment described in this paper provides proton, neutron, and light-ion cross sections for many systems. As such, one goal was to provide coalescence radii for these systems. Equation (18) can be rearranged to provide coalescence radii as shown below:

$$P_0 = \left(\left(\frac{\left(\frac{d^2\sigma}{dE_p d\Omega}\right)_A}{\left(\frac{d^2\sigma}{dE_p d\Omega}\right)^A_{proton}} \frac{N!Z!}{\left(\frac{N_T+N_P}{Z_T+Z_P}\right)^N} \right)^{\left(\frac{1}{A-1}\right)} \left(\frac{3E_p p_p \sigma_{tot}}{4\pi\gamma}\right) \right)^{1/3} \quad (20)$$

By assuming the proton and neutron distributions have a similar shape, the proton and neutron multiplicities can be related to one another by using the ratio of neutrons to protons in the projectile/target system:

$$\left(\frac{d^2\sigma}{dE_n d\Omega}\right) = \left(\frac{N_T+N_P}{Z_T+Z_P}\right)\left(\frac{d^2\sigma}{dE_p d\Omega}\right) \quad (21)$$

Even though the experiment provides proton, neutron, and light ion cross sections for many energies, angles, and systems, many of these cross sections do not overlap with one another. By substituting (21) into (18), neutron cross sections can be used in lieu of proton cross sections. Utilizing both version helps provide both a broader range of coalescence radii.

CHAPTER IV
RESULTS AND DISCUSSION

This section will provide some of the results of the analysis of the experimental data. The results include double differential cross section calculations for proton, deuteron, and triton production as well as coalescence radii calculations. Due to the sheer volume of data, only some sample results will be presented in this section. The remainder of the data will be presented in Appendix A.

4.1 Cross Sections

The first step in calculating coalescence radii involves calculating the light-ion production cross sections from the experimental data. The coalescence radius calculation requires a comparison between neutron or proton cross sections and composite particle (such as a deuteron or triton) cross sections. The following figures show measured double differential cross sections for a particular system that was analyzed for this experiment. The x axes are all in units of AMeV and the y axes are all in units of mb/(AMeV*Sr). Although only one system is shown here, the entire data set from all 39 systems can be seen in A.1.

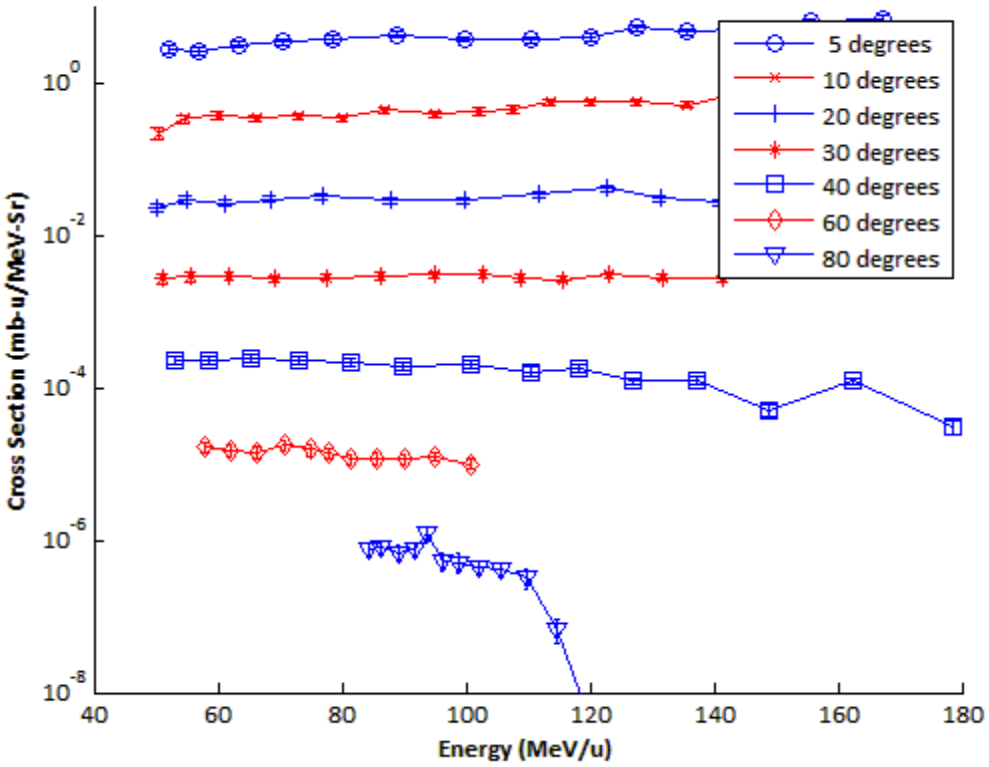

Figure 19. Proton production cross sections for 290 MeV/u carbon on carbon.The cross sections at each successive angle beyond 5 degrees are offset by successive factors of 10. For example, the values plotted for 10 degrees need to be multiplied by 10 to achieve their true values, the values for 20 degrees need to be multiplied by 100, and so on. Displayed statistical uncertainties may be smaller than the graphing symbols.

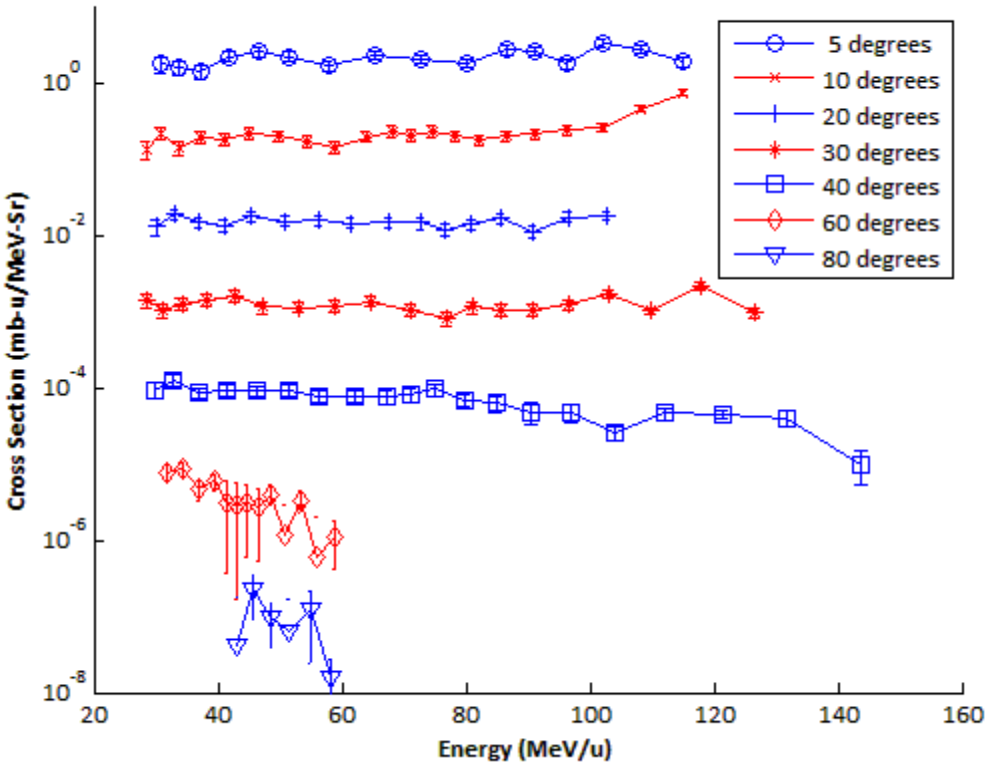

Figure 20. Deuteron production cross sections for 290 MeV/u carbon on carbon.The cross sections at each successive angle beyond 5 degrees are offset by successive factors of 10. For example, the values plotted for 10 degrees need to be multiplied by 10 to achieve their true values, the values for 20 degrees need to be multiplied by 100, and so on. Displayed statistical uncertainties may be smaller than the graphing symbols.

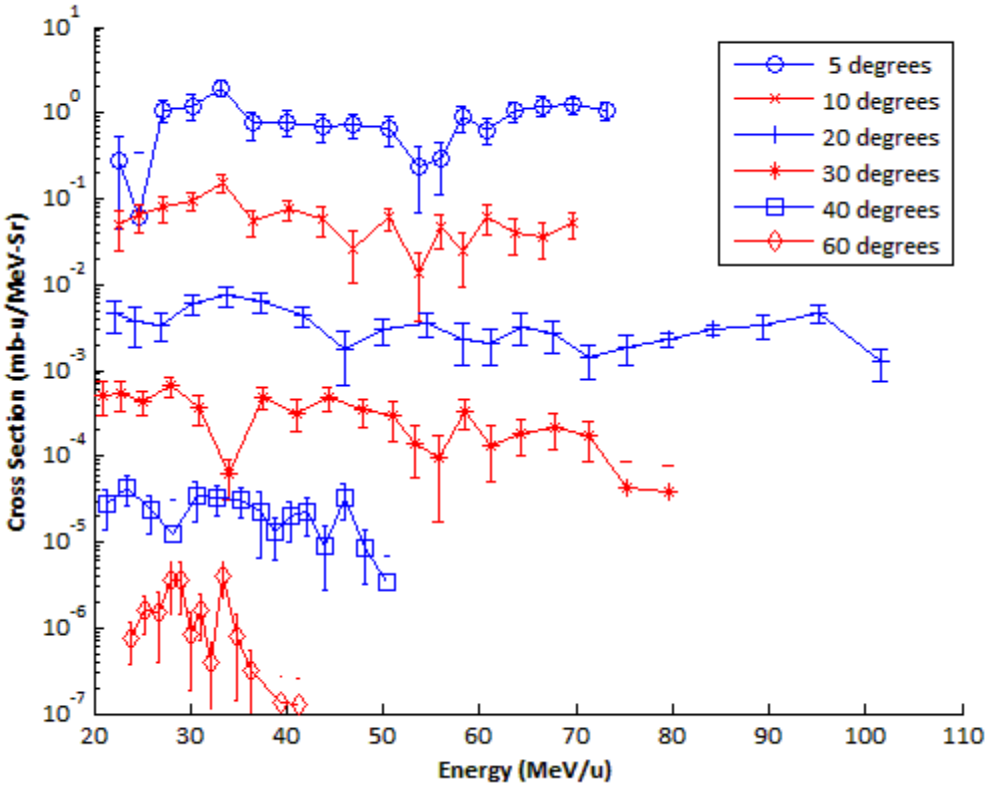

Figure 21. Triton production cross sections for 290 MeV/u carbon on carbon.The cross sections at each successive angle beyond 5 degrees are offset by successive factors of 10. For example, the values plotted for 10 degrees need to be multiplied by 10 to achieve their true values, the values for 20 degrees need to be multiplied by 100, and so on. Displayed statistical uncertainties may be smaller than the graphing symbols.

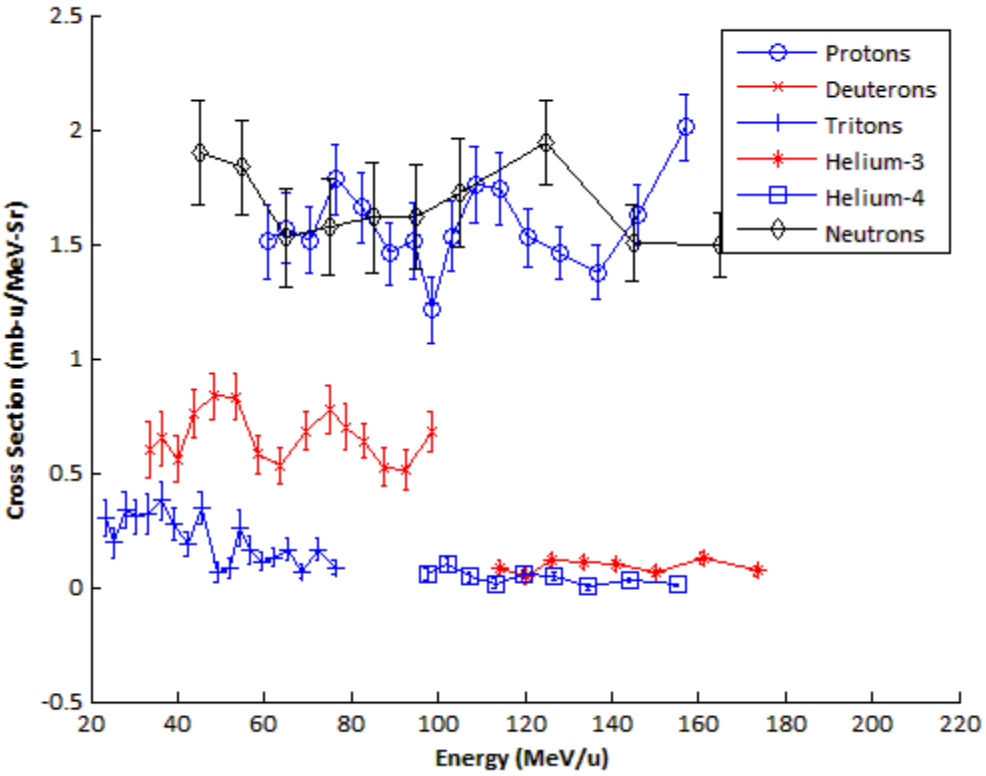

Figure 22. All measured cross sections for particles produced at 30 degrees from the 400 AMeV carbon on carbon system. This plot also includes neutron cross section data.

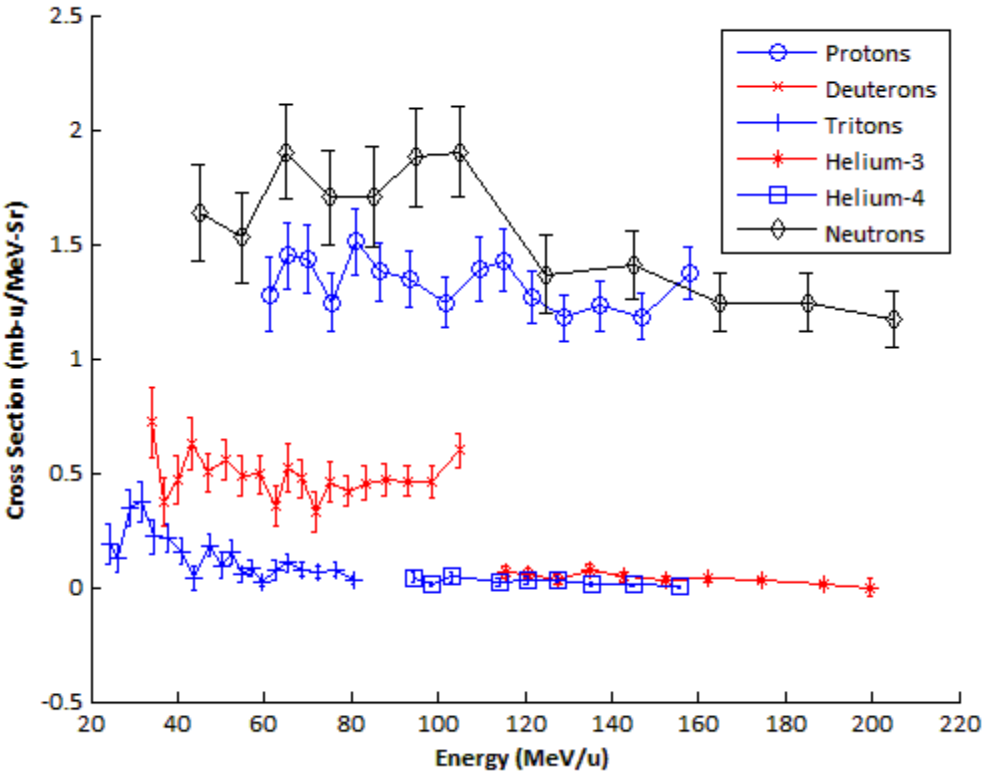

Figure 23. All measured cross sections for particles produced at 30 degrees from the 400 AMeV carbon on carbon system. This plot also includes neutron cross section data.

Given that light ion measurements were not a priority for data collection, some of the information isn't available for all 39 systems (the 39 systems are described in Table 1 in section 3.1.1 Run Descriptions). For example, the point at which the pdt plot lines merge severely limits the upper energy ranges for the cross section calculations. Another common occurrence in the measurements is pdt line saturation which has the potential to limit the energy range even further. The lower energy ranges are limited by the long flight paths from the point of production in the target to the detectors. Lower energy ions cannot be measured since they slow down and are absorbed in the air.

In addition to the limited energy ranges, not all angles were available for each of the 39 data sets. The seven measurement angles were 5, 10, 20, 30, 40, 60, and 80 degrees off the beam axis, however, some systems excluded angles 30 and 60, and a few others excluded angle 80. Proton, deuteron and triton data are available for most of the data sets. Some of the steeper angles have too few

triton counts to provide any cross section data, and helium data is available for only a select few angles and systems. A full description of the available light ion fragments and trajectories are listed below in Table 3.

Table 3. List of light-ion fragments measured for each angle and system.

Date (Month-Year)	***Beam ion and energy (MeV/u)***	***Available Targets***	***Available Ions for Each Angle***						
			5	***10***	***20***	***30***	***40***	***60***	***80***
Apr 00	C (290)	Pb, Cu, C	p d t	p d t He	p d t	p d t	p d t	p d t	p d
Apr 00	Ne (600)	Pb, Cu, C	p d t	p d t He	p d t	p d t	p d t	p d t	p d t
Apr 00	Ne (400)	Pb, Cu, C	p d t	p d t He	p d t	p d t	p d t	p d t	p d t
Apr 01	C (290)	Pb, C	p d t	p d t	p d t	p d t	p d t	p d t	-
May 01	Si (600)	Pb, Cu, C	-	p d t	p d t	p d t	p d t	p d t	p d t
May 01	Ne (600)	Al, Li	p d	p d	p d t	-	p d t	-	p d
May 01	Xe (400)	Al, Li	p d	p d	p d t	-	p d t	-	p d
Jan 02	Fe (500)	Al, Li	p d t	p d t	p d t	p d t	p d t	p d t	p d t
Jan 02	Kr (400)	AL, Pb, Cu, C, Li	p d t	p d t He	p d t He	p d t He	p d t He	p d t	p d t
June 02	He (230)	Al, Cu	p d t	p d t	p d t	p d t	p d t	-	p d t
June 02	Xe (400)	AL, Pb, Cu, C, Li	p d	p d t	p d t	p d t	p d t	-	p d t
June 02	N (400)	Cu, C	p d t	p d t	p d t	p d t	p d t	-	p d t
Nov 02	C (400)	AL, Pb, Cu, C, Li	p d t	p d t He	p d t He	p d t He	p d t He	p d t	p d t
Nov 02	Ne (400)	Al, Li	p d t	p d t He	p d t He	p d t He	p d t He	p d t	p d t

4.2 Coalescence Radii

Once the double differential cross sections have been calculated, the coalescence radii can then be calculated. This is achieved by using the equations derived in section 3.6.1 Calculating Coalescence Radii. While the coalescence radii can be calculated for specific energies and angles, these numbers are usually determined by fitting the data to one parameter. Typically, one radius is determined for the entire energy range at one angle, or even the entire system. The method used to calculate the coalescence radii was a least squares fit applied over both of these approaches. The results can be seen in the tables below.

Table 4. Coalescence radii for 290 MeV/u carbon on carbon. The first column in each ion set are radii calculated with proton cross sections and the radii in the second column are calculated with neutron cross sections.

	Light-Ion Fragment							
Angle	Deuterons		Tritons		Helium-3		Helium-4	
5	218 (12.2)	179 (30.5)	247 (14.9)	188 (32.8)	N/A	N/A	N/A	N/A
10	220 (12.2)	192 (19.0)	204 (12.8)	186 (30.6)	209 (10.6)	175 (15.8)	N/A	127 (12.9)
20	215 (13.2)	261 (29.9)	211 (10.6)	247 (22.1)	N/A	N/A	N/A	N/A
30	207 (11.9)	217 (15.9)	196 (12.4)	219 (13.1)	N/A	N/A	N/A	N/A
40	202 (14.9)	286 (34.9)	N/A	311 (43.1)	N/A	N/A	N/A	N/A
60	127 (41.1)	218 (34.3)	N/A	350 (60.2)	N/A	N/A	N/A	N/A
80	N/A	340 (135.6)	N/A	N/A	N/A	N/A	N/A	N/A
All	217 (6.9)	192 (15.5)	217 (7.3)	190 (22.4)	209 (10.6)	175 (15.8)	N/A	127 (12.9)

Table 5. Coalescence radii for 290 MeV/u carbon on copper. The first column in each ion set are radii calculated with proton cross sections and the radii in the second column are calculated with neutron cross sections.

	Light-Ion Fragment							
Angle	Deuterons		Tritons		Helium-3		Helium-4	
5	174 (9.2)	137 (12.9)	183 (11.6)	148 (13.2)	N/A	N/A	N/A	N/A
10	160 (8.6)	143 (12.2)	154 (10.2)	146 (14.1)	172 (8.2)	120 (6.8)	186 (7.0)	134 (8.8)
20	169 (9.8)	193 (25.3)	164 (10.2)	179 (16.7)	N/A	N/A	N/A	N/A
30	168 (14.7)	202 (17.4)	172 (20.5)	200 (16.6)	N/A	N/A	N/A	N/A
40	172 (12.5)	218 (27.7)	N/A	203 (21.3)	N/A	N/A	N/A	N/A
60	N/A	227 (29.4)	N/A	211 (24.8)	N/A	N/A	N/A	N/A
80	N/A	246 (28.0)	N/A	N/A	N/A	N/A	N/A	N/A
All	167 (5.1)	144 (8.8)	167 (6.7)	149 (9.6)	172 (8.2)	120 (6.8)	186 (7.0)	134 (8.8)

Table 6. Coalescence radii for 290 MeV/u carbon on lead. The first column in each ion set are radii calculated with proton cross sections and the radii in the second column are calculated with neutron cross sections.

	Light-Ion Fragment							
Angle	Deuterons		Tritons		Helium-3		Helium-4	
5	137 (12.4)	107 (12.9)	141 (13.8)	127 (16.7)	N/A	N/A	N/A	N/A
10	136 (9.4)	87 (7.1)	134 (10.6)	96 (8.3)	148 (8.8)	91 (11.0)	150 (7.7)	96 (11.5)
20	140 (13.3)	140 (19.8)	143 (10.2)	140 (18.0)	N/A	N/A	N/A	N/A
30	127 (13.4)	104 (54.1)	124 (9.5)	85 (34.8)	N/A	N/A	N/A	N/A
40	131 (15.3)	138 (23.1)	N/A	133 (21.9)	N/A	N/A	N/A	N/A
60	98 (26.2)	130 (17.0)	N/A	137 (14.8)	N/A	N/A	N/A	N/A
80	N/A	124 (14.1)	N/A	N/A	N/A	N/A	N/A	N/A
All	135 (5.8)	94 (7.2)	136 (6.6)	92 (21.5)	148 (8.8)	91 (11.0)	150 (7.7)	96 (11.5)

Table 7. Coalescence radii for 400 MeV/u neon on carbon. The first column in each ion set are radii calculated with proton cross sections and the radii in the second column are calculated with neutron cross sections.

	Light-Ion Fragment							
Angle	Deuterons		Tritons		Helium-3		Helium-4	
5	201 (11.8)	N/A	216 (10.4)	N/A	N/A	N/A	N/A	N/A
10	194 (12.5)	198 (45.0)	203 (9.8)	200 (35.0)	196 (8.9)	243 (73.6)	N/A	N/A
20	180 (13.6)	288 (63.2)	191 (13.6)	268 (43.3)	N/A	N/A	N/A	N/A
30	178 (11.1)	183 (24.6)	175 (13.4)	191 (26.5)	N/A	N/A	N/A	N/A
40	183 (17.2)	N/A	N/A	N/A	N/A	N/A	N/A	N/A
60	N/A	234 (31.9)	N/A	225 (24.5)	N/A	N/A	N/A	N/A
80	N/A	N/A	N/A	N/A	N/A	N/A	N/A	N/A
All	191 (6.1)	197 (27.4)	205 (6.1)	199 (27.1)	196 (8.9)	243 (73.6)	N/A	N/A

Table 8. Coalescence radii for 400 MeV/u neon on copper. The first column in each ion set are radii calculated with proton cross sections and the radii in the second column are calculated with neutron cross sections.

	Light-Ion Fragment							
Angle	Deuterons		Tritons		Helium-3		Helium-4	
5	203 (12.2)	111 (13.8)	225 (11.9)	119 (15.6)	N/A	N/A	N/A	N/A
10	190 (11.6)	106 (13.4)	211 (10.4)	150 (18.0)	220 (8.7)	113 (5.1)	N/A	N/A
20	195 (10.4)	126 (17.4)	214 (11.8)	152 (23.9)	N/A	N/A	N/A	N/A
30	192 (12.4)	112 (11.9)	192 (11.7)	142 (14.2)	N/A	N/A	N/A	N/A
40	181 (17.8)	125 (17.1)	N/A	140 (16.1)	N/A	N/A	N/A	N/A
60	N/A	114 (9.3)	N/A	132 (7.3)	N/A	N/A	N/A	N/A
80	N/A	134 (11.6)	N/A	142 (7.8)	N/A	N/A	N/A	N/A
All	195 (5.9)	112 (7.1)	214 (6.2)	128 (12.7)	220 (8.7)	113 (5.1)	N/A	N/A

Table 9. Coalescence radii for 400 MeV/u neon on lead. The first column in each ion set are radii calculated with proton cross sections and the radii in the second column are calculated with neutron cross sections.

	Light-Ion Fragment							
Angle	Deuterons		Tritons		Helium-3		Helium-4	
5	124 (8.5)	108 (14.5)	139 (8.1)	121 (28.1)	N/A	N/A	N/A	N/A
10	117 (9.7)	85 (10.5)	126 (7.7)	98 (18.4)	136 (7.1)	89 (5.3)	N/A	N/A
20	121 (8.3)	88 (15.3)	129 (6.9)	94 (21.8)	N/A	N/A	N/A	N/A
30	111 (8.3)	102 (14.5)	113 (8.5)	110 (18.8)	N/A	N/A	N/A	N/A
40	108 (9.1)	111 (14.4)	N/A	110 (14.4)	N/A	N/A	N/A	N/A
60	99 (24.8)	104 (9.8)	N/A	106 (8.8)	N/A	N/A	N/A	N/A
80	N/A	121 (11.2)	N/A	114 (6.3)	N/A	N/A	N/A	N/A
All	117 (4.1)	93 (6.8)	128 (4.2)	99 (12.4)	136 (7.1)	89 (5.3)	N/A	N/A

Table 10. Coalescence radii for 600 MeV/u neon on carbon. The first column in each ion set are radii calculated with proton cross sections and the radii in the second column are calculated with neutron cross sections.

	Light-Ion Fragment							
Angle	Deuterons		Tritons		Helium-3		Helium-4	
5	190 (10.2)	239 (26.0)	201 (9.5)	247 (409.4)	N/A	N/A	N/A	N/A
10	192 (12.8)	484 (163.7)	201 (11.4)	409 (1004.8)	208 (9.3)	398 (122.7)	N/A	N/A
20	178 (10.4)	284 (54.5)	181 (10.3)	268 (46.3)	N/A	N/A	N/A	N/A
30	174 (11.2)	279 (60.1)	170 (14.8)	272 (63.1)	N/A	N/A	N/A	N/A
40	157 (18.4)	227 (59.7)	N/A	267 (66.7)	N/A	N/A	N/A	N/A
60	N/A	238 (38.8)	N/A	297 (62.3)	N/A	N/A	N/A	N/A
80	N/A	278 (37.2)	N/A	285 (39.1)	N/A	N/A	N/A	N/A
All	184 (5.5)	257 (20.1)	195 (5.7)	255 (308.5)	208 (9.3)	398 (122.7)	N/A	N/A

Table 11. Coalescence radii for 600 MeV/u neon on copper. The first column in each ion set are radii calculated with proton cross sections and the radii in the second column are calculated with neutron cross sections.

	Light-Ion Fragment							
Angle	Deuterons		Tritons		Helium-3		Helium-4	
5	150 (8.8)	238 (74.6)	164 (8.0)	150 (14.3)	N/A	N/A	N/A	N/A
10	142 (11.3)	187 (37.9)	160 (7.9)	129 (249.9)	167 (7.9)	247 (65.1)	N/A	N/A
20	141 (9.2)	146 (11.9)	153 (7.6)	152 (10.1)	N/A	N/A	N/A	N/A
30	137 (9.4)	132 (10.3)	145 (11.3)	140 (43.0)	N/A	N/A	N/A	N/A
40	130 (15.4)	140 (13.7)	N/A	146 (10.2)	N/A	N/A	N/A	N/A
60	N/A	160 (15.1)	N/A	147 (9.7)	N/A	N/A	N/A	N/A
80	N/A	185 (20.4)	N/A	172 (13.4)	N/A	N/A	N/A	N/A
All	142 (4.7)	145 (6.9)	157 (4.3)	141 (87.8)	167 (7.9)	247 (65.1)	N/A	N/A

Table 12. Coalescence radii for 600 MeV/u neon on lead. The first column in each ion set are radii calculated with proton cross sections and the radii in the second column are calculated with neutron cross sections.

	Light-Ion Fragment							
Angle	Deuterons		Tritons		Helium-3		Helium-4	
5	127 (10.9)	93 (6.2)	139 (8.1)	107 (5.6)	N/A	N/A	N/A	N/A
10	130 (9.9)	130 (26.0)	138 (9.9)	128 (19.6)	150 (8.0)	199 (48.0)	N/A	N/A
20	121 (8.8)	102 (158.9)	127 (11.0)	113 (10.5)	N/A	N/A	N/A	N/A
30	115 (8.5)	96 (6.7)	123 (8.9)	96 (50.3)	N/A	N/A	N/A	N/A
40	117 (13.7)	96 (9.0)	N/A	102 (5.6)	N/A	N/A	N/A	N/A
60	N/A	119 (11.4)	N/A	107 (5.6)	N/A	N/A	N/A	N/A
80	N/A	119 (8.4)	N/A	124 (8.4)	N/A	N/A	N/A	N/A
All	122 (4.6)	99 (30.3)	132 (5.0)	102 (28.6)	150 (8.0)	199 (48.0)	N/A	N/A

Table 13. Coalescence radii for 290 MeV/u carbon on carbon. The first column in each ion set are radii calculated with proton cross sections and the radii in the second column are calculated with neutron cross sections.

	Light-Ion Fragment							
Angle	Deuterons		Tritons		Helium-3		Helium-4	
5	264 (18.0)	165 (22.6)	304 (37.2)	214 (35.1)	N/A	N/A	N/A	N/A
10	195 (16.8)	153 (19.8)	243 (19.7)	210 (25.7)	N/A	N/A	N/A	N/A
20	258 (21.1)	223 (27.1)	277 (25.5)	269 (34.6)	N/A	N/A	N/A	N/A
30	246 (21.9)	179 (15.1)	263 (38.0)	222 (16.6)	N/A	N/A	N/A	N/A
40	228 (20.0)	270 (52.9)	256 (29.5)	293 (44.8)	N/A	N/A	N/A	N/A
60	207 (32.3)	199 (40.9)	0 (0.0)	237 (34.7)	N/A	N/A	N/A	N/A
80	N/A	N/A	N/A	N/A	N/A	N/A	N/A	N/A
All	239 (10.3)	165 (15.1)	260 (15.5)	213 (24.7)	N/A	N/A	N/A	N/A

Table 14. Coalescence radii for 290 MeV/u carbon on lead. The first column in each ion set are radii calculated with proton cross sections and the radii in the second column are calculated with neutron cross sections.

	Light-Ion Fragment							
Angle	Deuterons		Tritons		Helium-3		Helium-4	
5	162 (14.2)	99 (12.4)	180 (24.2)	148 (27.2)	N/A	N/A	N/A	N/A
10	139 (11.7)	79 (7.3)	165 (12.1)	106 (12.0)	N/A	N/A	N/A	N/A
20	155 (20.6)	124 (16.8)	171 (24.1)	143 (16.0)	N/A	N/A	N/A	N/A
30	155 (20.0)	93 (7.6)	159 (21.1)	107 (80.2)	N/A	N/A	N/A	N/A
40	146 (15.3)	127 (18.9)	154 (17.7)	128 (23.6)	N/A	N/A	N/A	N/A
60	139 (17.7)	111 (13.2)	195 (35.8)	131 (12.5)	N/A	N/A	N/A	N/A
80	N/A	N/A	N/A	N/A	N/A	N/A	N/A	N/A
All	152 (7.4)	88 (5.7)	172 (11.2)	111 (15.6)	N/A	N/A	N/A	N/A

Table 15. Coalescence radii for 400 MeV/u krypton on aluminum. The first column in each ion set are radii calculated with proton cross sections and the radii in the second column are calculated with neutron cross sections.

	Light-Ion Fragment							
Angle	Deuterons		Tritons		Helium-3		Helium-4	
5	161 (8.4)	113 (32.2)	177 (11.1)	152 (49.7)	N/A	N/A	N/A	N/A
10	159 (9.2)	111 (28.1)	151 (10.4)	120 (43.5)	123 (7.2)	119 (27.1)	150 (13.6)	141 (25.0)
20	145 (9.9)	76 (11.4)	145 (8.2)	103 (14.3)	135 (7.1)	84 (12.2)	146 (11.0)	98 (11.4)
30	151 (8.2)	151 (42.3)	155 (10.5)	N/A	163 (11.1)	151 (34.8)	179 (10.1)	183 (50.6)
40	141 (9.0)	121 (21.7)	149 (11.9)	144 (27.9)	152 (9.3)	122 (19.0)	175 (10.5)	150 (23.4)
60	127 (12.3)	107 (61.0)	149 (12.7)	114 (63.8)	N/A	N/A	N/A	N/A
80	141 (22.9)	169 (66.1)	N/A	N/A	N/A	N/A	N/A	N/A
All	155 (4.7)	89 (10.8)	162 (5.7)	112 (15.4)	125 (6.5)	88 (11.9)	149 (10.4)	99 (11.3)

Table 16. Coalescence radii for 400 MeV/u krypton on carbon. The first column in each ion set are radii calculated with proton cross sections and the radii in the second column are calculated with neutron cross sections.

	Light-Ion Fragment							
Angle	Deuterons		Tritons		Helium-3		Helium-4	
5	179 (9.2)	175 (55.4)	199 (11.4)	N/A	N/A	N/A	N/A	N/A
10	173 (8.8)	128 (39.0)	157 (12.4)	168 (71.0)	134 (7.6)	117 (28.7)	160 (12.7)	124 (35.1)
20	174 (7.6)	91 (21.4)	157 (12.4)	91 (21.8)	146 (7.1)	135 (28.4)	161 (10.5)	139 (46.4)
30	186 (10.3)	106 (27.6)	177 (13.0)	117 (34.6)	178 (11.4)	129 (24.1)	209 (13.5)	160 (28.4)
40	163 (10.3)	144 (29.9)	158 (12.4)	162 (55.0)	172 (11.7)	141 (23.6)	191 (18.2)	171 (39.4)
60	161 (20.3)	110 (36.8)	170 (21.2)	138 (39.9)	N/A	N/A	N/A	N/A
80	166 (31.6)	132 (49.9)	N/A	N/A	N/A	N/A	N/A	N/A
All	176 (4.9)	108 (17.2)	185 (7.9)	97 (20.0)	135 (6.9)	119 (27.3)	160 (10.4)	126 (33.3)

Table 17. Coalescence radii for 400 MeV/u krypton on copper. The first column in each ion set are radii calculated with proton cross sections and the radii in the second column are calculated with neutron cross sections.

	Light-Ion Fragment							
Angle	Deuterons		Tritons		Helium-3		Helium-4	
5	138 (6.8)	96 (16.5)	148 (10.9)	142 (37.5)	N/A	N/A	N/A	N/A
10	131 (6.1)	97 (20.3)	127 (8.0)	101 (29.3)	104 (5.9)	102 (15.6)	135 (8.9)	125 (15.4)
20	127 (6.1)	66 (7.4)	125 (6.7)	74 (11.2)	118 (4.8)	77 (9.5)	137 (7.8)	96 (9.8)
30	127 (6.2)	72 (11.7)	135 (8.3)	90 (13.9)	128 (6.9)	103 (27.1)	158 (9.2)	114 (22.1)
40	122 (7.9)	78 (10.5)	130 (7.0)	103 (11.7)	131 (6.9)	88 (12.4)	154 (8.3)	108 (15.4)
60	119 (13.9)	80 (17.5)	123 (9.6)	91 (16.1)	N/A	N/A	N/A	N/A
80	113 (12.7)	94 (22.7)	N/A	N/A	N/A	N/A	N/A	N/A
All	131 (3.2)	75 (5.8)	135 (4.2)	81 (9.5)	106 (5.2)	82 (8.8)	136 (6.9)	98 (9.4)

Table 18. Coalescence radii for 400 MeV/u krypton on lithium. The first column in each ion set are radii calculated with proton cross sections and the radii in the second column are calculated with neutron cross sections.

	Light-Ion Fragment							
Angle	Deuterons		Tritons		Helium-3		Helium-4	
5	233 (14.1)	160 (28.3)	270 (18.9)	N/A	N/A	N/A	N/A	N/A
10	202 (10.0)	202 (89.7)	185 (13.8)	N/A	156 (10.0)	188 (43.3)	200 (15.8)	203 (51.0)
20	205 (12.5)	127 (20.7)	177 (12.8)	137 (30.8)	161 (12.0)	125 (19.1)	188 (17.0)	154 (18.4)
30	192 (11.4)	146 (29.6)	193 (13.4)	175 (39.6)	203 (15.6)	167 (39.8)	227 (29.1)	195 (70.7)
40	192 (14.4)	136 (28.5)	203 (17.1)	212 (65.7)	182 (14.8)	140 (22.3)	224 (26.3)	170 (38.6)
60	164 (24.5)	109 (26.9)	197 (22.1)	139 (23.4)	N/A	N/A	N/A	N/A
80	206 (34.4)	151 (91.5)	N/A	N/A	N/A	N/A	N/A	N/A
All	213 (6.5)	143 (15.6)	222 (9.2)	141 (24.7)	157 (8.9)	132 (19.0)	196 (12.0)	157 (18.1)

Table 19. Coalescence radii for 400 MeV/u krypton on lead. The first column in each ion set are radii calculated with proton cross sections and the radii in the second column are calculated with neutron cross sections.

	Light-Ion Fragment							
Angle	Deuterons		Tritons		Helium-3		Helium-4	
5	99 (5.5)	56 (9.8)	107 (6.8)	70 (12.1)	N/A	N/A	N/A	N/A
10	98 (5.5)	52 (12.2)	102 (6.8)	62 (15.8)	75 (3.6)	70 (11.2)	89 (7.5)	82 (11.0)
20	96 (5.2)	45 (9.6)	99 (6.7)	56 (8.5)	84 (4.4)	63 (8.7)	101 (7.4)	77 (11.3)
30	95 (5.7)	50 (9.1)	99 (7.3)	63 (23.7)	104 (7.0)	78 (17.7)	117 (7.2)	89 (14.4)
40	95 (6.6)	51 (19.0)	100 (8.8)	59 (21.1)	100 (6.0)	67 (9.5)	112 (7.3)	81 (9.3)
60	84 (9.5)	66 (19.4)	92 (8.7)	71 (18.2)	N/A	N/A	N/A	N/A
80	89 (8.7)	52 (10.4)	N/A	N/A	N/A	N/A	N/A	N/A
All	97 (2.6)	50 (5.5)	103 (3.3)	61 (7.6)	76 (3.3)	67 (6.8)	91 (6.9)	79 (7.9)

Table 20. Coalescence radii for 230 MeV/u helium on aluminum. The first column in each ion set are radii calculated with proton cross sections and the radii in the second column are calculated with neutron cross sections.

	Light-Ion Fragment							
Angle	Deuterons		Tritons		Helium-3		Helium-4	
5	267 (22.6)	143 (16.1)	N/A	174 (41.2)	N/A	N/A	N/A	N/A
10	264 (17.4)	168 (18.9)	279 (16.9)	187 (37.7)	N/A	N/A	N/A	N/A
20	243 (17.7)	158 (26.1)	N/A	174 (21.0)	N/A	N/A	N/A	N/A
30	N/A	237 (93.7)	225 (45.9)	158 (29.9)	N/A	N/A	N/A	N/A
40	217 (22.0)	181 (32.4)	219 (46.5)	190 (31.4)	N/A	N/A	N/A	N/A
60	N/A	N/A	N/A	N/A	N/A	N/A	N/A	N/A
80	N/A	255 (115.8)	N/A	295 (66.4)	N/A	N/A	N/A	N/A
All	260 (11.3)	163 (12.4)	278 (16.4)	176 (17.4)	N/A	N/A	N/A	N/A

Table 21. Coalescence radii for 230 MeV/u helium on copper. The first column in each ion set are radii calculated with proton cross sections and the radii in the second column are calculated with neutron cross sections.

	Light-Ion Fragment							
Angle	Deuterons		Tritons		Helium-3		Helium-4	
5	256 (24.4)	164 (32.3)	232 (47.5)	157 (136.9)	N/A	N/A	N/A	N/A
10	233 (20.0)	108 (19.7)	243 (14.3)	120 (16.5)	N/A	N/A	N/A	N/A
20	208 (16.8)	132 (23.8)	N/A	94 (24.7)	N/A	N/A	N/A	N/A
30	N/A	183 (39.2)	202 (38.1)	143 (60.6)	N/A	N/A	N/A	N/A
40	194 (23.1)	153 (24.8)	176 (33.0)	161 (59.6)	N/A	N/A	N/A	N/A
60	N/A	N/A	N/A	N/A	N/A	N/A	N/A	N/A
80	N/A	121 (21.7)	N/A	211 (39.8)	N/A	N/A	N/A	N/A
All	227 (11.5)	127 (16.9)	237 (12.5)	111 (16.2)	N/A	N/A	N/A	N/A

Table 22. Coalescence radii for 400 MeV/u nitrogen on carbon. The first column in each ion set are radii calculated with proton cross sections and the radii in the second column are calculated with neutron cross sections.

	Light-Ion Fragment							
Angle	Deuterons		Tritons		Helium-3		Helium-4	
5	293 (25.4)	173 (36.4)	295 (57.5)	236 (71.1)	N/A	N/A	N/A	N/A
10	269 (18.5)	215 (67.7)	279 (13.0)	239 (59.2)	N/A	N/A	N/A	N/A
20	237 (14.8)	178 (34.5)	251 (28.7)	214 (44.8)	N/A	N/A	N/A	N/A
30	235 (17.7)	166 (35.3)	220 (28.5)	192 (41.0)	N/A	N/A	N/A	N/A
40	237 (17.6)	186 (33.4)	220 (17.3)	204 (58.3)	N/A	N/A	N/A	N/A
60	N/A	N/A	N/A	N/A	N/A	N/A	N/A	N/A
80	161 (57.5)	199 (61.0)	N/A	240 (54.1)	N/A	N/A	N/A	N/A
All	255 (8.4)	177 (18.6)	257 (10.2)	206 (26.2)	N/A	N/A	N/A	N/A

Table 23. Coalescence radii for 400 MeV/u nitrogen on copper. The first column in each ion set are radii calculated with proton cross sections and the radii in the second column are calculated with neutron cross sections.

	Light-Ion Fragment							
Angle	Deuterons		Tritons		Helium-3		Helium-4	
5	233 (22.3)	154 (36.7)	258 (53.8)	180 (65.6)	N/A	N/A	N/A	N/A
10	210 (13.4)	118 (28.0)	207 (14.5)	127 (37.4)	N/A	N/A	N/A	N/A
20	181 (12.5)	121 (17.9)	196 (20.2)	145 (23.6)	N/A	N/A	N/A	N/A
30	188 (12.3)	104 (25.0)	202 (18.4)	128 (20.1)	N/A	N/A	N/A	N/A
40	187 (14.4)	140 (34.0)	190 (14.5)	145 (23.7)	N/A	N/A	N/A	N/A
60	N/A	N/A	N/A	N/A	N/A	N/A	N/A	N/A
80	N/A	175 (32.0)	N/A	166 (23.8)	N/A	N/A	N/A	N/A
All	196 (6.5)	116 (14.4)	201 (8.8)	131 (19.2)	N/A	N/A	N/A	N/A

Table 24. Coalescence radii for 400 MeV/u xenon on aluminum. The first column in each ion set are radii calculated with proton cross sections and the radii in the second column are calculated with neutron cross sections.

	Light-Ion Fragment							
Angle	Deuterons		Tritons		Helium-3		Helium-4	
5	173 (14.6)	62 (19.3)	N/A	N/A	N/A	N/A	N/A	N/A
10	135 (10.4)	157 (90.8)	140 (9.1)	167 (90.3)	N/A	N/A	N/A	N/A
20	147 (22.7)	97 (32.5)	192 (72.2)	134 (69.3)	N/A	N/A	N/A	N/A
30	201 (59.5)	68 (20.2)	108 (325.4)	69 (32.0)	N/A	N/A	N/A	N/A
40	116 (10.9)	N/A	130 (10.0)	N/A	N/A	N/A	N/A	N/A
60	N/A	N/A	N/A	N/A	N/A	N/A	N/A	N/A
80	109 (18.7)	122 (60.8)	N/A	162 (116.6)	N/A	N/A	N/A	N/A
All	139 (6.6)	63 (18.2)	137 (6.9)	79 (27.4)	N/A	N/A	N/A	N/A

Table 25. Coalescence radii for 400 MeV/u xenon on carbon. The first column in each ion set are radii calculated with proton cross sections and the radii in the second column are calculated with neutron cross sections.

	Light-Ion Fragment							
Angle	Deuterons		Tritons		Helium-3		Helium-4	
5	189 (14.3)	112 (28.4)	N/A	N/A	N/A	N/A	N/A	N/A
10	146 (7.8)	168 (77.6)	157 (9.7)	197 (79.0)	N/A	N/A	N/A	N/A
20	143 (9.2)	96 (21.2)	141 (13.7)	N/A	N/A	N/A	N/A	N/A
30	137 (9.6)	N/A	129 (14.8)	N/A	N/A	N/A	N/A	N/A
40	136 (11.9)	99 (33.7)	143 (10.9)	117 (31.2)	N/A	N/A	N/A	N/A
60	N/A	N/A	N/A	N/A	N/A	N/A	N/A	N/A
80	129 (18.5)	179 (189.2)	143 (39.3)	175 (113.0)	N/A	N/A	N/A	N/A
All	150 (4.9)	107 (17.3)	152 (6.9)	130 (32.6)	N/A	N/A	N/A	N/A

Table 26. Coalescence radii for 400 MeV/u xenon on copper. The first column in each ion set are radii calculated with proton cross sections and the radii in the second column are calculated with neutron cross sections.

	Light-Ion Fragment							
Angle	Deuterons		Tritons		Helium-3		Helium-4	
5	142 (9.9)	71 (14.0)	N/A	N/A	N/A	N/A	N/A	N/A
10	111 (7.3)	138 (58.4)	116 (5.9)	145 (50.9)	N/A	N/A	N/A	N/A
20	115 (7.1)	85 (26.9)	113 (8.3)	108 (41.5)	N/A	N/A	N/A	N/A
30	104 (8.6)	77 (17.0)	107 (9.1)	87 (14.8)	N/A	N/A	N/A	N/A
40	99 (7.5)	57 (12.6)	105 (7.9)	67 (13.3)	N/A	N/A	N/A	N/A
60	N/A	N/A	N/A	N/A	N/A	N/A	N/A	N/A
80	86 (13.7)	107 (47.8)	N/A	101 (37.6)	N/A	N/A	N/A	N/A
All	113 (3.8)	70 (8.5)	112 (4.0)	71 (12.4)	N/A	N/A	N/A	N/A

Table 27. Coalescence radii for 400 MeV/u xenon on lithium. The first column in each ion set are radii calculated with proton cross sections and the radii in the second column are calculated with neutron cross sections.

	Light-Ion Fragment							
Angle	Deuterons		Tritons		Helium-3		Helium-4	
5	184 (11.5)	121 (25.3)	N/A	N/A	N/A	N/A	N/A	N/A
10	150 (8.2)	128 (36.6)	155 (7.5)	144 (29.3)	N/A	N/A	N/A	N/A
20	148 (8.6)	108 (19.1)	131 (14.4)	127 (30.0)	N/A	N/A	N/A	N/A
30	135 (8.0)	103 (19.2)	143 (12.4)	121 (30.6)	N/A	N/A	N/A	N/A
40	137 (10.8)	126 (36.0)	145 (9.9)	145 (39.3)	N/A	N/A	N/A	N/A
60	N/A	N/A	N/A	N/A	N/A	N/A	N/A	N/A
80	130 (20.0)	148 (57.1)	154 (38.2)	164 (54.1)	N/A	N/A	N/A	N/A
All	155 (4.5)	116 (13.4)	151 (5.8)	130 (20.0)	N/A	N/A	N/A	N/A

Table 28. Coalescence radii for 400 MeV/u xenon on lead. The first column in each ion set are radii calculated with proton cross sections and the radii in the second column are calculated with neutron cross sections.

	Light-Ion Fragment							
Angle	Deuterons		Tritons		Helium-3		Helium-4	
5	117 (10.7)	54 (12.8)	N/A	N/A	N/A	N/A	N/A	N/A
10	85 (6.1)	59 (23.9)	92 (5.5)	67 (18.8)	N/A	N/A	N/A	N/A
20	92 (6.1)	53 (14.6)	88 (6.6)	60 (25.2)	N/A	N/A	N/A	N/A
30	81 (6.3)	47 (9.4)	82 (5.8)	57 (8.5)	N/A	N/A	N/A	N/A
40	79 (7.0)	51 (16.9)	90 (6.0)	62 (19.4)	N/A	N/A	N/A	N/A
60	N/A	N/A	N/A	N/A	N/A	N/A	N/A	N/A
80	74 (11.2)	55 (17.6)	77 (13.6)	58 (10.1)	N/A	N/A	N/A	N/A
All	88 (3.1)	52 (6.2)	88 (3.1)	60 (10.2)	N/A	N/A	N/A	N/A

Table 29. Coalescence radii for 400 MeV/u xenon on aluminum. The first column in each ion set are radii calculated with proton cross sections and the radii in the second column are calculated with neutron cross sections.

	Light-Ion Fragment							
Angle	Deuterons		Tritons		Helium-3		Helium-4	
5	116 (16.0)	86 (21.5)	N/A	N/A	N/A	N/A	N/A	N/A
10	108 (11.0)	210 (79.2)	N/A	N/A	N/A	N/A	N/A	N/A
20	109 (14.5)	98 (28.6)	122 (14.7)	128 (40.9)	N/A	N/A	N/A	N/A
30	N/A	N/A	N/A	N/A	N/A	N/A	N/A	N/A
40	107 (12.1)	98 (37.6)	137 (20.4)	N/A	N/A	N/A	N/A	N/A
60	N/A	N/A	N/A	N/A	N/A	N/A	N/A	N/A
80	111 (28.6)	102 (64.9)	N/A	N/A	N/A	N/A	N/A	N/A
All	111 (8.4)	88 (20.6)	127 (12.1)	128 (40.9)	N/A	N/A	N/A	N/A

Table 30. Coalescence radii for 400 MeV/u xenon on lithium. The first column in each ion set are radii calculated with proton cross sections and the radii in the second column are calculated with neutron cross sections.

	Light-Ion Fragment							
Angle	Deuterons		Tritons		Helium-3		Helium-4	
5	176 (21.7)	153 (31.0)	N/A	N/A	N/A	N/A	N/A	N/A
10	138 (12.6)	128 (41.9)	N/A	N/A	N/A	N/A	N/A	N/A
20	139 (12.8)	112 (17.7)	140 (15.2)	125 (26.9)	N/A	N/A	N/A	N/A
30	N/A	N/A	N/A	N/A	N/A	N/A	N/A	N/A
40	139 (12.5)	113 (25.4)	134 (22.1)	160 (49.4)	N/A	N/A	N/A	N/A
60	N/A	N/A	N/A	N/A	N/A	N/A	N/A	N/A
80	183 (52.4)	105 (110.6)	N/A	N/A	N/A	N/A	N/A	N/A
All	148 (9.9)	132 (21.3)	140 (13.9)	125 (26.6)	N/A	N/A	N/A	N/A

Table 31. Coalescence radii for 600 MeV/u neon on aluminum. The first column in each ion set are radii calculated with proton cross sections and the radii in the second column are calculated with neutron cross sections.

	Light-Ion Fragment							
Angle	Deuterons		Tritons		Helium-3		Helium-4	
5	247 (15.3)	N/A	284 (17.2)	N/A	N/A	N/A	N/A	N/A
10	207 (11.3)	N/A	227 (10.6)	N/A	N/A	N/A	N/A	N/A
20	213 (15.4)	N/A	229 (14.7)	N/A	N/A	N/A	N/A	N/A
30	N/A	N/A	N/A	N/A	N/A	N/A	N/A	N/A
40	210 (16.3)	N/A	237 (17.6)	N/A	N/A	N/A	N/A	N/A
60	N/A	N/A	N/A	N/A	N/A	N/A	N/A	N/A
80	192 (45.2)	N/A	N/A	N/A	N/A	N/A	N/A	N/A
All	218 (7.6)	N/A	251 (7.9)	N/A	N/A	N/A	N/A	N/A

Table 32. Coalescence radii for 600 MeV/u neon on lithium. The first column in each ion set are radii calculated with proton cross sections and the radii in the second column are calculated with neutron cross sections.

	Light-Ion Fragment							
Angle	Deuterons		Tritons		Helium-3		Helium-4	
5	212 (10.4)	N/A	259 (10.7)	N/A	N/A	N/A	N/A	N/A
10	172 (8.7)	N/A	179 (8.8)	N/A	N/A	N/A	N/A	N/A
20	169 (9.1)	N/A	174 (7.3)	N/A	N/A	N/A	N/A	N/A
30	N/A	N/A	N/A	N/A	N/A	N/A	N/A	N/A
40	166 (12.1)	N/A	180 (8.8)	N/A	N/A	N/A	N/A	N/A
60	N/A	N/A	N/A	N/A	N/A	N/A	N/A	N/A
80	170 (20.3)	N/A	N/A	N/A	N/A	N/A	N/A	N/A
All	186 (5.4)	N/A	215 (6.4)	N/A	N/A	N/A	N/A	N/A

Table 33. Coalescence radii for 600 MeV/u silicon on carbon. The first column in each ion set are radii calculated with proton cross sections and the radii in the second column are calculated with neutron cross sections.

	Light-Ion Fragment							
Angle	Deuterons		Tritons		Helium-3		Helium-4	
5	N/A	N/A	N/A	N/A	N/A	N/A	N/A	N/A
10	235 (13.1)	N/A	242 (12.0)	N/A	N/A	N/A	N/A	N/A
20	240 (14.2)	N/A	275 (14.7)	N/A	N/A	N/A	N/A	N/A
30	228 (14.1)	N/A	257 (13.7)	N/A	N/A	N/A	N/A	N/A
40	217 (21.2)	N/A	244 (20.0)	N/A	N/A	N/A	N/A	N/A
60	202 (18.8)	N/A	244 (18.1)	N/A	N/A	N/A	N/A	N/A
80	207 (30.6)	N/A	294 (63.6)	N/A	N/A	N/A	N/A	N/A
All	233 (7.8)	N/A	250 (8.8)	N/A	N/A	N/A	N/A	N/A

Table 34. Coalescence radii for 600 MeV/u silicon on copper. The first column in each ion set are radii calculated with proton cross sections and the radii in the second column are calculated with neutron cross sections.

	Light-Ion Fragment							
Angle	Deuterons		Tritons		Helium-3		Helium-4	
5	N/A	N/A	N/A	N/A	N/A	N/A	N/A	N/A
10	196 (12.4)	N/A	208 (8.6)	N/A	N/A	N/A	N/A	N/A
20	176 (11.1)	N/A	201 (9.5)	N/A	N/A	N/A	N/A	N/A
30	182 (11.1)	N/A	209 (9.5)	N/A	N/A	N/A	N/A	N/A
40	189 (11.8)	N/A	195 (12.0)	N/A	N/A	N/A	N/A	N/A
60	170 (13.7)	N/A	195 (13.0)	N/A	N/A	N/A	N/A	N/A
80	191 (30.1)	N/A	296 (64.2)	N/A	N/A	N/A	N/A	N/A
All	184 (6.4)	N/A	204 (5.8)	N/A	N/A	N/A	N/A	N/A

Table 35. Coalescence radii for 600 MeV/u silicon on lead. The first column in each ion set are radii calculated with proton cross sections and the radii in the second column are calculated with neutron cross sections.

	Light-Ion Fragment							
Angle	Deuterons		Tritons		Helium-3		Helium-4	
5	N/A	N/A	N/A	N/A	N/A	N/A	N/A	N/A
10	152 (10.2)	N/A	164 (8.1)	N/A	N/A	N/A	N/A	N/A
20	139 (8.0)	N/A	155 (9.1)	N/A	N/A	N/A	N/A	N/A
30	147 (10.0)	N/A	163 (10.3)	N/A	N/A	N/A	N/A	N/A
40	138 (11.4)	N/A	154 (8.1)	N/A	N/A	N/A	N/A	N/A
60	134 (10.2)	N/A	142 (10.0)	N/A	N/A	N/A	N/A	N/A
80	139 (16.8)	N/A	194 (17.8)	N/A	N/A	N/A	N/A	N/A
All	144 (4.7)	N/A	159 (5.1)	N/A	N/A	N/A	N/A	N/A

Table 36. Coalescence radii for 400 MeV/u carbon on aluminum. The first column in each ion set are radii calculated with proton cross sections and the radii in the second column are calculated with neutron cross sections.

	Light-Ion Fragment							
Angle	Deuterons		Tritons		Helium-3		Helium-4	
5	290 (30.6)	N/A	N/A	N/A	N/A	N/A	N/A	N/A
10	204 (10.4)	N/A	210 (10.3)	N/A	277 (17.4)	N/A	256 (10.8)	N/A
20	211 (11.8)	N/A	210 (11.2)	N/A	229 (12.5)	N/A	245 (13.2)	N/A
30	205 (10.8)	N/A	214 (12.2)	N/A	226 (13.0)	N/A	255 (15.8)	N/A
40	196 (10.9)	N/A	201 (13.9)	N/A	210 (15.9)	N/A	257 (16.5)	N/A
60	172 (17.0)	N/A	166 (28.5)	N/A	N/A	N/A	N/A	N/A
80	164 (34.6)	N/A	N/A	N/A	N/A	N/A	N/A	N/A
All	206 (6.2)	N/A	210 (7.4)	N/A	240 (8.4)	N/A	251 (7.8)	N/A

Table 37. Coalescence radii for 400 MeV/u carbon on carbon. The first column in each ion set are radii calculated with proton cross sections and the radii in the second column are calculated with neutron cross sections.

	Light-Ion Fragment							
Angle	Deuterons		Tritons		Helium-3		Helium-4	
5	327 (31.9)	209 (20.8)	N/A	N/A	N/A	N/A	N/A	N/A
10	233 (11.2)	322 (79.7)	256 (13.9)	274 (52.1)	273 (17.5)	820 (494.3)	298 (12.1)	535 (284.8)
20	234 (15.4)	216 (17.2)	234 (14.5)	228 (15.8)	246 (16.6)	250 (17.0)	280 (14.5)	288 (17.3)
30	228 (12.5)	209 (12.6)	232 (14.1)	217 (17.0)	254 (14.8)	255 (19.8)	290 (14.2)	264 (23.6)
40	219 (12.1)	229 (11.4)	238 (18.6)	252 (8.9)	258 (23.5)	248 (18.1)	267 (21.3)	273 (24.2)
60	187 (21.5)	227 (12.4)	234 (22.2)	250 (10.6)	N/A	N/A	N/A	N/A
80	162 (34.3)	285 (24.1)	N/A	289 (15.5)	N/A	N/A	N/A	N/A
All	231 (6.9)	221 (8.5)	247 (9.0)	232 (10.7)	262 (11.1)	251 (13.2)	292 (8.8)	277 (14.7)

Table 38. Coalescence radii for 400 MeV/u carbon on copper. The first column in each ion set are radii calculated with proton cross sections and the radii in the second column are calculated with neutron cross sections.

	Light-Ion Fragment							
Angle	Deuterons		Tritons		Helium-3		Helium-4	
5	228 (24.1)	129 (9.3)	N/A	N/A	N/A	N/A	N/A	N/A
10	183 (11.0)	204 (28.4)	193 (12.8)	202 (24.8)	212 (15.4)	265 (33.0)	228 (14.9)	287 (37.3)
20	177 (10.8)	157 (9.3)	181 (11.3)	147 (9.8)	200 (12.7)	230 (16.8)	223 (13.5)	249 (19.7)
30	175 (10.9)	150 (8.2)	184 (13.1)	154 (8.2)	207 (12.9)	210 (15.0)	220 (15.6)	219 (18.0)
40	170 (10.0)	170 (8.1)	176 (12.1)	180 (6.5)	207 (17.4)	209 (15.0)	210 (14.4)	229 (13.3)
60	159 (11.6)	170 (8.2)	168 (14.9)	169 (5.9)	N/A	N/A	N/A	N/A
80	125 (34.8)	209 (13.7)	N/A	197 (10.7)	N/A	N/A	N/A	N/A
All	178 (5.6)	155 (4.9)	186 (7.0)	155 (6.9)	207 (8.8)	229 (10.7)	224 (8.7)	236 (13.0)

Table 39. Coalescence radii for 400 MeV/u carbon on lithium. The first column in each ion set are radii calculated with proton cross sections and the radii in the second column are calculated with neutron cross sections.

	Light-Ion Fragment							
Angle	Deuterons		Tritons		Helium-3		Helium-4	
5	321 (28.4)	N/A	N/A	N/A	N/A	N/A	N/A	N/A
10	276 (15.4)	N/A	280 (15.1)	N/A	285 (16.0)	N/A	313 (16.3)	N/A
20	257 (13.7)	N/A	265 (15.2)	N/A	264 (15.0)	N/A	291 (14.2)	N/A
30	248 (14.5)	N/A	264 (17.1)	N/A	255 (15.0)	N/A	280 (20.1)	N/A
40	245 (13.1)	N/A	254 (17.2)	N/A	225 (18.0)	N/A	254 (18.6)	N/A
60	201 (16.5)	N/A	246 (21.8)	N/A	N/A	N/A	N/A	N/A
80	130 (27.3)	N/A	N/A	N/A	N/A	N/A	N/A	N/A
All	263 (7.9)	N/A	273 (9.5)	N/A	273 (9.5)	N/A	304 (10.9)	N/A

Table 40. Coalescence radii for 400 MeV/u carbon on lead. The first column in each ion set are radii calculated with proton cross sections and the radii in the second column are calculated with neutron cross sections.

	Light-Ion Fragment							
Angle	Deuterons		Tritons		Helium-3		Helium-4	
5	159 (15.3)	104 (7.2)	N/A	N/A	N/A	N/A	N/A	N/A
10	143 (8.0)	111 (9.9)	147 (10.0)	110 (8.6)	182 (15.6)	182 (18.3)	184 (12.9)	199 (30.7)
20	142 (7.2)	124 (7.7)	149 (7.4)	109 (8.4)	168 (11.1)	217 (23.0)	175 (12.9)	215 (19.7)
30	148 (8.0)	118 (6.4)	148 (9.2)	113 (7.1)	175 (13.1)	175 (10.5)	188 (14.0)	194 (15.2)
40	139 (8.4)	143 (8.5)	151 (9.8)	130 (5.7)	170 (14.6)	179 (15.5)	174 (12.0)	205 (13.0)
60	119 (10.0)	131 (6.4)	128 (12.9)	125 (3.5)	N/A	N/A	N/A	N/A
80	106 (16.8)	157 (10.7)	N/A	149 (7.1)	N/A	N/A	N/A	N/A
All	143 (4.0)	116 (4.5)	148 (5.3)	111 (5.3)	174 (8.1)	184 (12.5)	180 (8.0)	199 (16.7)

Table 41. Coalescence radii for 600 MeV/u neon on aluminum. The first column in each ion set are radii calculated with proton cross sections and the radii in the second column are calculated with neutron cross sections.

	Light-Ion Fragment							
Angle	Deuterons		Tritons		Helium-3		Helium-4	
5	269 (21.3)	N/A	N/A	N/A	N/A	N/A	N/A	N/A
10	194 (9.0)	N/A	199 (10.4)	N/A	244 (17.8)	N/A	245 (13.7)	N/A
20	200 (9.8)	N/A	202 (9.2)	N/A	231 (13.0)	N/A	238 (9.5)	N/A
30	187 (8.5)	N/A	188 (9.2)	N/A	231 (10.1)	N/A	236 (13.6)	N/A
40	185 (10.9)	N/A	193 (14.4)	N/A	412 (22.6)	N/A	410 (31.9)	N/A
60	166 (12.9)	N/A	185 (15.2)	N/A	N/A	N/A	N/A	N/A
80	142 (21.3)	N/A	N/A	N/A	N/A	N/A	N/A	N/A
All	193 (4.9)	N/A	197 (5.8)	N/A	259 (9.5)	N/A	264 (8.7)	N/A

Table 42. Coalescence radii for 600 MeV/u neon on lithium. The first column in each ion set are radii calculated with proton cross sections and the radii in the second column are calculated with neutron cross sections.

	Light-Ion Fragment							
Angle	Deuterons		Tritons		Helium-3		Helium-4	
5	643 (80.2)	N/A	N/A	N/A	N/A	N/A	N/A	N/A
10	375 (28.2)	N/A	364 (35.2)	N/A	462 (37.9)	N/A	496 (46.3)	N/A
20	249 (16.4)	N/A	227 (20.8)	N/A	257 (15.8)	N/A	301 (29.2)	N/A
30	237 (15.8)	N/A	239 (18.2)	N/A	246 (20.0)	N/A	315 (33.3)	N/A
40	220 (22.6)	N/A	206 (33.8)	N/A	N/A	N/A	N/A	N/A
60	208 (26.9)	N/A	234 (30.5)	N/A	N/A	N/A	N/A	N/A
80	271 (76.7)	N/A	N/A	N/A	N/A	N/A	N/A	N/A
All	237 (9.8)	N/A	228 (13.2)	N/A	255 (13.3)	N/A	304 (24.8)	N/A

As noted earlier, coalescence radii can be fitted to data over the entire energy range for a specific angle, or it they can be fitted to all energies and angles for a system. Table 4 through Table 42 provide coalescence radii for a particular system, first fitted for a specific angle, then fitted for the entire system. Below, Table 43 shows all of the system-specific coalescence radii (those fitted over the entire system), for ease of comparison.

Table 43. System-specific coalescence radii. The first column in each ion set are radii calculated with proton cross sections and the radii in the second column are calculated with neutron cross sections. Systems are divided by beam type. Numbers in parentheses are absolute errors.

	Light-Ion Fragment							
System	Deuterons		Tritons		Helium-3		Helium-4	
290 AMeV C on C	217 (6.9)	192 (15.5)	217 (7.3)	190 (22.4)	209 (10.6)	175 (15.8)	N/A	127 (12.9)
290 AMeV C on Cu	167 (5.1)	144 (8.8)	167 (6.7)	149 (9.6)	172 (8.2)	120 (6.8)	186 (7.0)	134 (8.8)
290 AMeV C on Pb	135 (5.8)	94 (7.2)	136 (6.6)	92 (21.5)	148 (8.8)	91 (11.0)	150 (7.7)	96 (11.5)
400 AMeV Ne on C	191 (6.1)	197 (27.4)	205 (6.1)	199 (27.1)	196 (8.9)	243 (73.6)	N/A	N/A
400 AMeV Ne on Cu	195 (5.9)	112 (7.1)	214 (6.2)	128 (12.7)	220 (8.7)	113 (5.1)	N/A	N/A
400 AMeV Ne on Pb	117 (4.1)	93 (6.8)	128 (4.2)	99 (12.4)	136 (7.1)	89 (5.3)	N/A	N/A
600 AMeV Ne on C	184 (5.5)	257 (20.1)	195 (5.7)	255 (308.5)	208 (9.3)	398 (122.7)	N/A	N/A
600 AMeV Ne on Cu	142 (4.7)	145 (6.9)	157 (4.3)	141 (87.8)	167 (7.9)	247 (65.1)	N/A	N/A
600 AMeV Ne on Pb	122 (4.6)	99 (30.3)	132 (5.0)	102 (28.6)	150 (8.0)	199 (48.0)	N/A	N/A
290 AMeV C on C	239 (10.3)	165 (15.1)	260 (15.5)	213 (24.7)	N/A	N/A	N/A	N/A
290 AMeV C on Pb	152 (7.4)	88 (5.7)	172 (11.2)	111 (15.6)	N/A	N/A	N/A	N/A
400 AMeV Kr on Al	155 (4.7)	89 (10.8)	162 (5.7)	112 (15.4)	125 (6.5)	88 (11.9)	149 (10.4)	99 (11.3)
400 AMeV Kr on C	176 (4.9)	108 (17.2)	185 (7.9)	97 (20.0)	135 (6.9)	119 (27.3)	160 (10.4)	126 (33.3)
400 AMeV Kr on Cu	131 (3.2)	75 (5.8)	135 (4.2)	81 (9.5)	106 (5.2)	82 (8.8)	136 (6.9)	98 (9.4)
400 AMeV Kr on Li	213 (6.5)	143 (15.6)	222 (9.2)	141 (24.7)	157 (8.9)	132 (19.0)	196 (12.0)	157 (18.1)
400 AMeV Kr on Pb	97 (2.6)	50 (5.5)	103 (3.3)	61 (7.6)	76 (3.3)	67 (6.8)	91 (6.9)	79 (7.9)
230 AMeV He on Al	260 (11.3)	163 (12.4)	278 (16.4)	176 (17.4)	N/A	N/A	N/A	N/A
230 AMeV He on Cu	227 (11.5)	127 (16.9)	237 (12.5)	111 (16.2)	N/A	N/A	N/A	N/A
400 AMeV N on C	255 (8.4)	177 (18.6)	257 (10.2)	206 (26.2)	N/A	N/A	N/A	N/A
400 AMeV N on Cu	196 (6.5)	116 (14.4)	201 (8.8)	131 (19.2)	N/A	N/A	N/A	N/A

Table 43 Continued.

	Light-Ion Fragment							
System	Deuterons		Tritons		Helium-3		Helium-4	
400 AMeV Xe on Al	139 (6.6)	63 (18.2)	137 (6.9)	79 (27.4)	N/A	N/A	N/A	N/A
400 AMeV Xe on C	150 (4.9)	107 (17.3)	152 (6.9)	130 (32.6)	N/A	N/A	N/A	N/A
400 AMeV Xe on Cu	113 (3.8)	70 (8.5)	112 (4.0)	71 (12.4)	N/A	N/A	N/A	N/A
400 AMeV Xe on Li	155 (4.5)	116 (13.4)	151 (5.8)	130 (20.0)	N/A	N/A	N/A	N/A
400 AMeV Xe on Pb	88 (3.1)	52 (6.2)	88 (3.1)	60 (10.2)	N/A	N/A	N/A	N/A
400 AMeV Xe on Al	111 (8.4)	88 (20.6)	127 (12.1)	128 (40.9)	N/A	N/A	N/A	N/A
400 AMeV Xe on Li	148 (9.9)	132 (21.3)	140 (13.9)	125 (26.6)	N/A	N/A	N/A	N/A
600 AMeV Ne on Al	218 (7.6)	N/A	251 (7.9)	N/A	N/A	N/A	N/A	N/A
600 AMeV Ne on Li	186 (5.4)	N/A	215 (6.4)	N/A	N/A	N/A	N/A	N/A
600 AMeV Si on C	233 (7.8)	N/A	250 (8.8)	N/A	N/A	N/A	N/A	N/A
600 AMeV Si on Cu	184 (6.4)	N/A	204 (5.8)	N/A	N/A	N/A	N/A	N/A
600 AMeV Si on Pb	144 (4.7)	N/A	159 (5.1)	N/A	N/A	N/A	N/A	N/A
400 AMeV C on Al	206 (6.2)	N/A	210 (7.4)	N/A	240 (8.4)	N/A	251 (7.8)	N/A
400 AMeV C on C	231 (6.9)	221 (8.5)	247 (9.0)	232 (10.7)	262 (11.1)	251 (13.2)	292 (8.8)	277 (14.7)
400 AMeV C on Cu	178 (5.6)	155 (4.9)	186 (7.0)	155 (6.9)	207 (8.8)	229 (10.7)	224 (8.7)	236 (13.0)
400 AMeV C on Li	263 (7.9)	N/A	273 (9.5)	N/A	273 (9.5)	N/A	304 (10.9)	N/A
400 AMeV C on Pb	143 (4.0)	116 (4.5)	148 (5.3)	111 (5.3)	174 (8.1)	184 (12.5)	180 (8.0)	199 (16.7)
600 AMeV Ne on Al	193 (4.9)	N/A	197 (5.8)	N/A	259 (9.5)	N/A	264 (8.7)	N/A
600 AMeV Ne on Li	237 (9.8)	N/A	228 (13.2)	N/A	255 (13.3)	N/A	304 (24.8)	N/A

The calculated coalescence radii shown in the tables above range 30 to 400 MeV/c. These two values are at the extremes however, and tend to be influenced by large errors induced by low count rates, especially at broader angles. The system-wide fits show a range from 50 to 230 MeV/c.

Overall, the trend in the angular-dependent coalescence radii seem to decrease as the angle increases. The radii also seem to increase as the light-ion mass increases, but this can be difficult to verify with the general lack of helium data. A good example would be the 600 AMeV Ne systems shown in Table 10 through Table 12, Table 31, and Table 32.

One of the most significant trends seems to be a decreasing coalescence radius as the combined system mass (projectile mass + target mass) increases. The can easily be observed on systems with the same projectile ion and energy, but with multiple targets, such as the 400 AMeV C systems shown in Table 36 through Table 40. This trend is illustrated below in Figure 24.

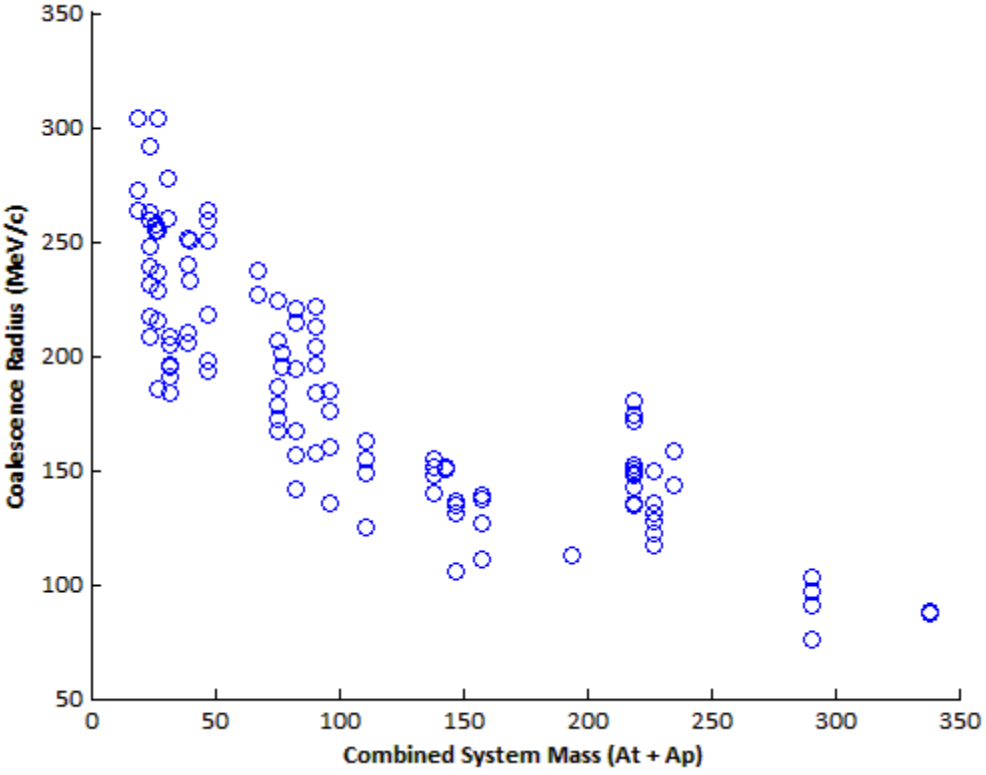

Figure 24. Plot showing the combined system mass (mass of projectile + mass of target) vs coalescence radius. This plots all of the results from using the proton cross section data.

Another significant trend is the difference between the radii calculated from proton cross sections compared to neutron cross section. The proton coalescence radii are generally higher than those calculated from the neutron cross sections. The differences in the calculations stemmed from the assumption that the proton and neutron cross sections were proportional to one another by a certain factor, the factor being the ratio of number of neutrons to the number of protons in the projectile/target system (As seen in Equation (4)). The results here indicates that the factorization used in Equation (4) overestimates the p/n cross section ratio. Table 44 below shows coalescence radii that were calculated using both proton and neutron spectra as inputs, eliminating the need for this proton/neutron ratio.

Table 44. System-specific coalescence radii using both neutron and proton spectra as inputs. Values in parentheses are absolute errors.

System	Deuterons	Tritons	Helium-3	Helium-4
290 AMeV C on C	212 (4.5)	213 (6.8)	197 (4.6)	N/A
290 AMeV C on Cu	162 (2.8)	172 (5.6)	154 (3.0)	164 (2.9)
290 AMeV C on Pb	118 (2.2)	118 (3.1)	128 (3.6)	125 (3.8)
400 AMeV Ne on C	203 (8.2)	207 (11.1)	218 (10.8)	N/A
400 AMeV Ne on Cu	149 (2.6)	173 (3.5)	177 (3.2)	N/A
400 AMeV Ne on Pb	109 (2.1)	119 (2.4)	118 (3.1)	N/A
600 AMeV Ne on C	228 (6.3)	233 (6.5)	259 (14.1)	N/A
600 AMeV Ne on Cu	157 (3.6)	165 (3.8)	191 (8.5)	N/A
600 AMeV Ne on Pb	118 (2.3)	124 (2.4)	165 (7.9)	N/A
290 AMeV C on C	203 (5.6)	214 (9.3)	N/A	N/A
290 AMeV C on Pb	122 (3.9)	135 (5.1)	N/A	N/A
400 AMeV Kr on Al	123 (3.8)	127 (6.6)	140 (4.1)	138 (3.3)
400 AMeV Kr on C	146 (4.6)	111 (7.6)	146 (5.4)	154 (6.5)
400 AMeV Kr on Cu	102 (1.9)	96 (2.9)	116 (2.3)	127 (2.4)
400 AMeV Kr on Li	176 (5.5)	149 (10.0)	167 (6.6)	191 (6.6)
400 AMeV Kr on Pb	74 (1.6)	76 (2.1)	89 (2.3)	98 (2.2)
230 AMeV He on Al	207 (6.5)	233 (8.4)	N/A	N/A
230 AMeV He on Cu	181 (5.2)	186 (7.6)	N/A	N/A
400 AMeV N on C	217 (7.8)	225 (10.7)	N/A	N/A
400 AMeV N on Cu	168 (3.8)	166 (5.6)	N/A	N/A
400 AMeV Xe on Al	109 (5.9)	102 (10.3)	N/A	N/A
400 AMeV Xe on C	132 (5.6)	149 (12.1)	N/A	N/A
400 AMeV Xe on Cu	96 (3.1)	86 (3.8)	N/A	N/A
400 AMeV Xe on Li	133 (4.1)	134 (7.5)	N/A	N/A
400 AMeV Xe on Pb	71 (2.1)	70 (2.5)	N/A	N/A
400 AMeV Xe on Al	108 (7.1)	129 (15.2)	N/A	N/A
400 AMeV Xe on Li	141 (6.0)	132 (14.4)	N/A	N/A
600 AMeV Ne on Al	N/A	N/A	N/A	N/A
600 AMeV Ne on Li	N/A	N/A	N/A	N/A
600 AMeV Si on C	N/A	N/A	N/A	N/A
600 AMeV Si on Cu	N/A	N/A	N/A	N/A
600 AMeV Si on Pb	N/A	N/A	N/A	N/A
400 AMeV C on Al	N/A	N/A	N/A	N/A
400 AMeV C on C	244 (5.8)	247 (6.7)	261 (7.0)	289 (6.2)
400 AMeV C on Cu	188 (3.2)	195 (4.5)	226 (4.6)	239 (5.1)
400 AMeV C on Li	N/A	N/A	N/A	N/A
400 AMeV C on Pb	147 (2.1)	153 (3.0)	190 (5.1)	199 (5.1)
600 AMeV Ne on Al	N/A	N/A	N/A	N/A
600 AMeV Ne on Li	N/A	N/A	N/A	N/A

Using the combined spectra coalescence radii, trends were made with respect to the combined projectile/target system mass. A trend was applied to all radii, and then to radii grouped by light-ions. The benefit of the trends is that it allows for the calculation of coalescence radii for systems that do not have applicable cross section data. The trends can be seen in the figures below:

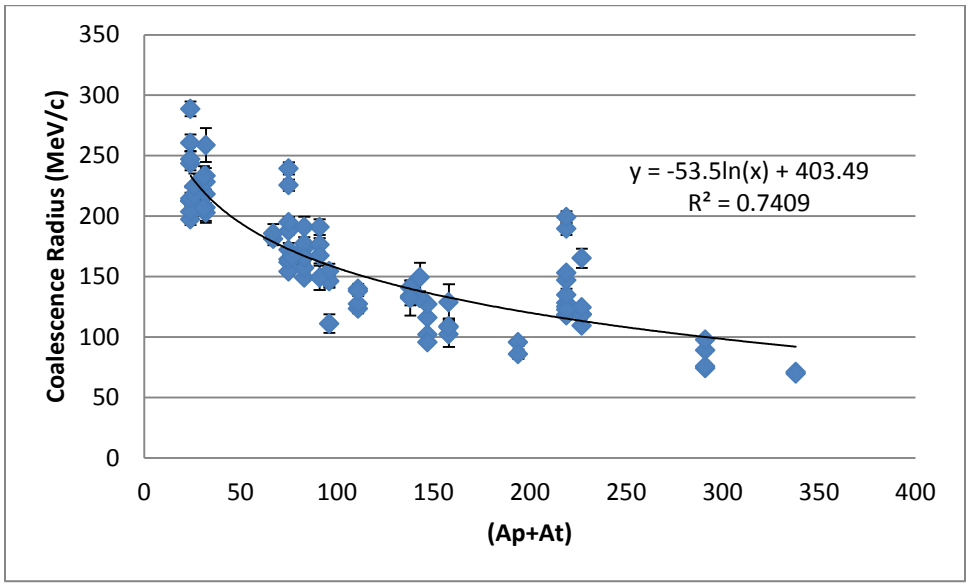

Figure 25. Plot of all calculated coalescence radii vs combined system mass.

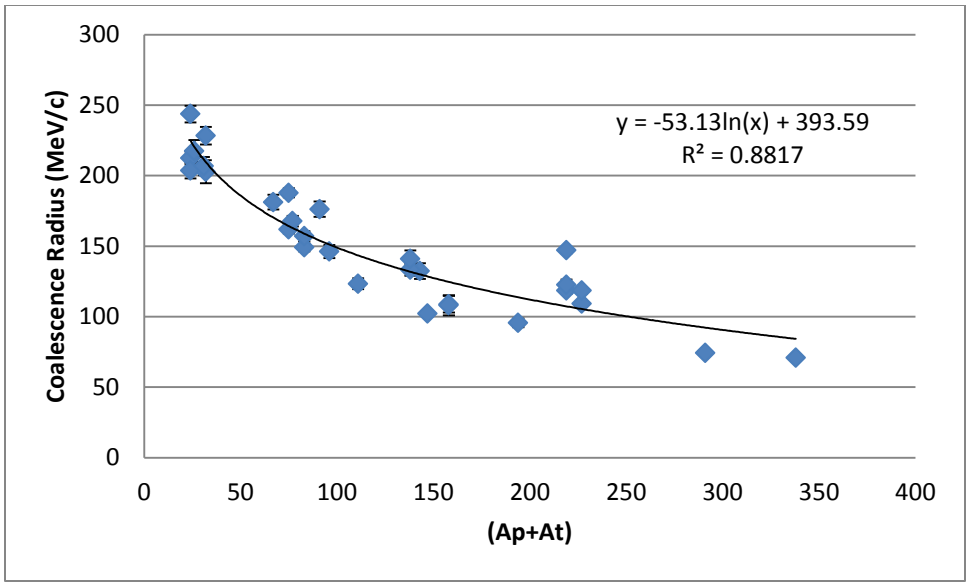

Figure 26. Plot of coalescence radii for measured deuteron spectra vs combined system mass.

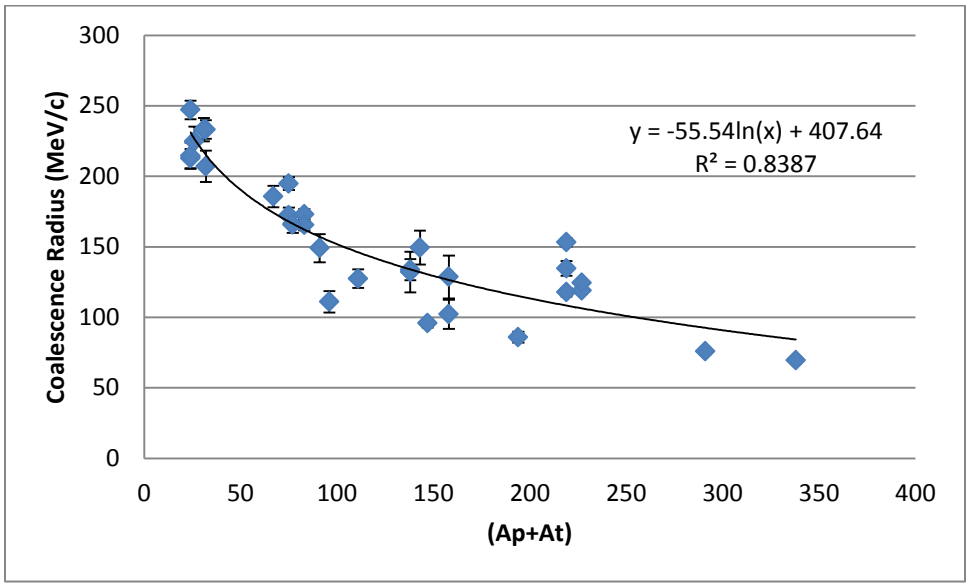

Figure 27. Plot of coalescence radii for measured triton spectra vs combined system mass.

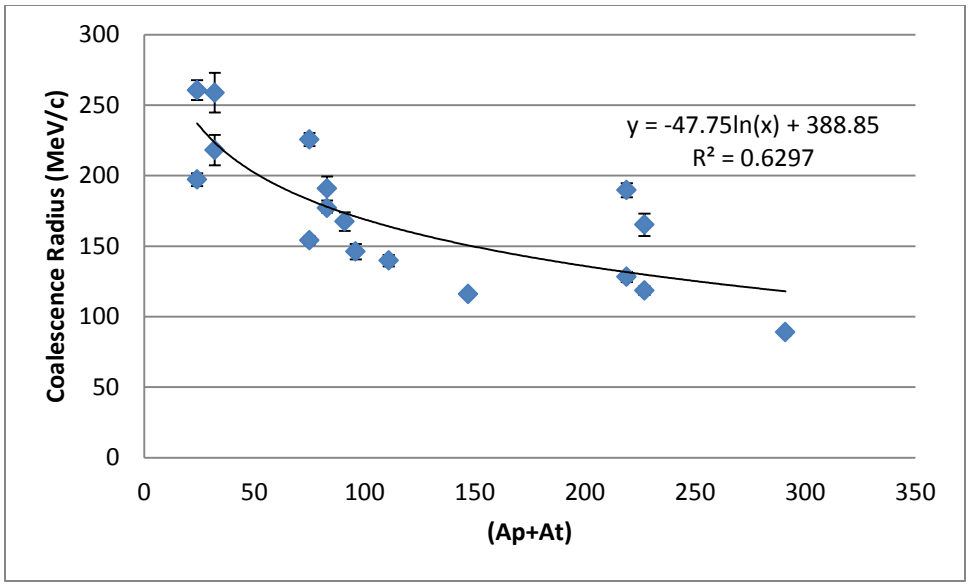

Figure 28. Plot of coalescence radii for measured helium-3 spectra vs combined system mass.

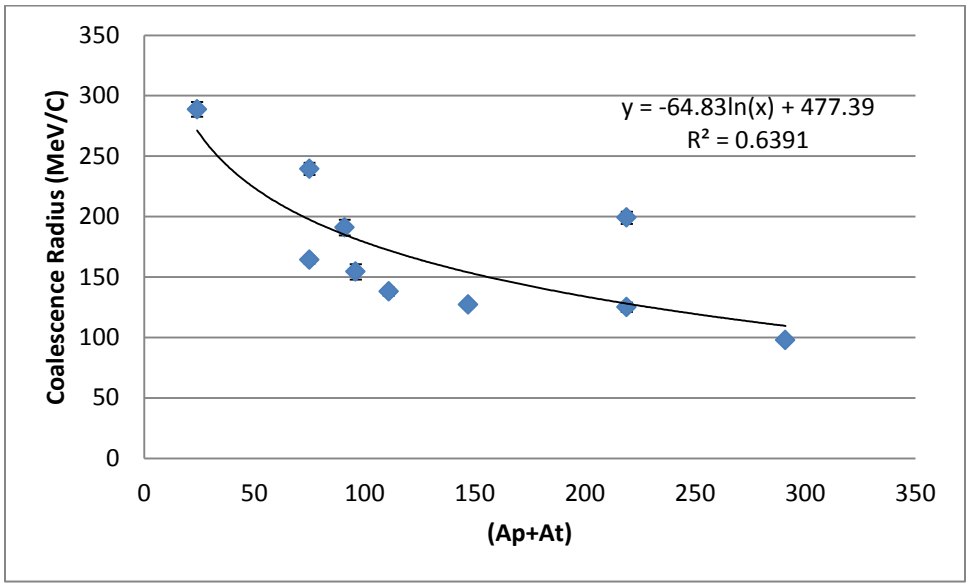

Figure 29. Plot of coalescence radii for measured helium-4 spectra vs combined system mass.

As a comparison to previous work (Gutbrod, et al [6]), shown below in Table 45 is a list of coalescence radii for systems with comparable projectile mass and energies to the systems analyzed in this paper. The results range from 106 to 147 MeV/c, which are comparable to the results for 600 AMeV Ne on Pb shown in Table 12.

Table 45. Coalescence radii calculations from Gutbrod, et al [6].The coalescence radii are in units of MeV/c.The system listed in bold font was measured using the experiments described in this paper. Numbers in parenthesis are absolute errors.

	Light-Ion Fragment			
System	deuterons	tritons	helium-3	helium-4
250 AMeV Ne on U	126	140	135	147
400 AMeV Ne on U	129	129	129	142
2100 AMeV Ne on U	106	116	106	118
400 AMeV He on U	126	127	127	132
600 AMeV Ne on Pb	**122 (4.6)**	**132 (5.0)**	**150 (8.0)**	**-**

Lemaire, et al, also lists comparable systems (shown below in Table 46), though a slightly different formulation of the coalescence model was used [9]. The values reported by Lemaire are much higher when compared to the systems that contain lead reported in this paper. A possible reason for the discrepancies could be the limited pdt energy range that was available during this experiment compared to other works.

Table 46. Coalescence radii calculations from Lemaire, et al [9]. Ions that show two different numbers are calculations from two separate runs using the same system parameters (projectile, energy, target).

	Light-Ion Fragment		
System	deuterons	tritons	helium-3
800 AMeV C on C	304	280	280
800 AMeV C on Pb	221	219	226
400 AMeV Ne on NaF	259	223	223
800 AMeV Ne on Naf	259	260	260
2100 AMeV Ne on NaF	259	212	212
400 AMeV Ne on Pb	205	207	198
800 AMeV Ne on Pb	205	199	189
2100 AMeV Ne on Pb	205 - 173	190	198
800 AMeV Ar on KCl	260 - 236	254 - 238	254 - 238
800 AMeV Ar on Pb	223 - 203	211 - 199	216 - 200

4.3 Source Emission Radii

Using the thermodynamic model explained in section 2.1.3 Formulation of the Thermodynamic Formula, emitting source radii were calculated. Typically, the model uses estimated radii in order to calculate coalescence radii, but the same formula can be applied in reverse. Table 47 below shows this experiments calculated results alongside the results provided by Mekijan, et. al. [10]. The formulas used for calculating the source radii in Mekijan, are shown below:

$$R(fm) = 0.24\left(A_P^{1/3} + A_T^{1/3}\right) + 2.0 \qquad for\ deuterons$$

$$R(fm) = 0.24\left(A_P^{1/3} + A_T^{1/3}\right) + 1.6 \qquad for\ tritons\ and\ helium-3 \quad (22)$$

$$R(fm) = 0.24\left(A_P^{1/3} + A_T^{1/3}\right) + 1.0 \qquad for\ helium-4$$

Table 47. Emitting source radii (in femtometers).The first column in each ion set are the radii calculated from the results of this experiment. The second column (in parentheses) are the absolute errors. The third column are those provided by Mekijan, et. al. for comparison [10].

System	Deuterons	Tritons	Helium-3	Helium-4
290 AMeV C on C	4.17 (0.1) | 3.10	3.52 (0.1) | 2.70	3.91 (0.1) | 2.70	N/A
290 AMeV C on Cu	5.50 (0.1) | 3.50	4.35 (0.1) | 3.10	5.02 (0.1) | 3.10	4.16 (0.1) | 2.50
290 AMeV C on Pb	7.48 (0.1) | 3.97	6.35 (0.2) | 3.57	6.02 (0.2) | 3.57	5.45 (0.2) | 2.97
400 AMeV Ne on C	4.37 (0.2) | 3.20	3.61 (0.2) | 2.80	3.53 (0.2) | 2.80	N/A
400 AMeV Ne on Cu	5.97 (0.1) | 3.61	4.33 (0.1) | 3.21	4.37 (0.1) | 3.21	N/A
400 AMeV Ne on Pb	8.09 (0.2) | 4.07	6.28 (0.1) | 3.67	6.51 (0.2) | 3.67	N/A
600 AMeV Ne on C	3.89 (0.1) | 3.20	3.21 (0.1) | 2.80	3.00 (0.2) | 2.80	N/A
600 AMeV Ne on Cu	5.66 (0.1) | 3.61	4.53 (0.1) | 3.21	4.06 (0.2) | 3.21	N/A
600 AMeV Ne on Pb	7.49 (0.1) | 4.07	6.01 (0.1) | 3.67	4.69 (0.2) | 3.67	N/A
290 AMeV C on C	4.40 (0.1) | 3.10	3.51 (0.2) | 2.70	N/A	N/A
290 AMeV C on Pb	7.33 (0.2) | 3.97	5.59 (0.2) | 3.57	N/A	N/A
400 AMeV Kr on Al	7.32 (0.2) | 3.77	5.82 (0.3) | 3.37	5.59 (0.2) | 3.37	4.93 (0.1) | 2.77
400 AMeV Kr on C	6.16 (0.2) | 3.60	6.67 (0.5) | 3.20	5.37 (0.2) | 3.20	4.41 (0.2) | 2.60
400 AMeV Kr on Cu	8.86 (0.2) | 4.01	7.75 (0.2) | 3.61	6.77 (0.1) | 3.61	5.33 (0.1) | 3.01
400 AMeV Kr on Li	5.09 (0.2) | 3.51	4.97 (0.3) | 3.11	4.69 (0.2) | 3.11	3.55 (0.1) | 2.51
400 AMeV Kr on Pb	12.13 (0.3) | 4.47	9.77 (0.3) | 4.07	8.78 (0.2) | 4.07	6.97 (0.2) | 3.47
230 AMeV He on Al	4.34 (0.1) | 3.10	3.25 (0.1) | 2.70	N/A	N/A
230 AMeV He on Cu	4.95 (0.1) | 3.34	4.08 (0.2) | 2.94	N/A	N/A
400 AMeV N on C	4.13 (0.1) | 3.13	3.35 (0.2) | 2.73	N/A	N/A
400 AMeV N on Cu	5.34 (0.1) | 3.53	4.55 (0.2) | 3.13	N/A	N/A
400 AMeV Xe on Al	8.18 (0.4) | 3.94	7.34 (0.7) | 3.54	N/A	N/A
400 AMeV Xe on C	6.74 (0.3) | 3.77	5.03 (0.4) | 3.37	N/A	N/A
400 AMeV Xe on Cu	9.32 (0.3) | 4.17	8.74 (0.4) | 3.77	N/A	N/A
400 AMeV Xe on Li	6.69 (0.2) | 3.68	5.62 (0.3) | 3.28	N/A	N/A
400 AMeV Xe on Pb	12.57 (0.4) | 4.64	10.80 (0.4) | 4.24	N/A	N/A
400 AMeV Xe on Al	8.34 (0.6) | 3.94	5.86 (0.7) | 3.54	N/A	N/A
400 AMeV Xe on Li	6.39 (0.3) | 3.68	5.71 (0.6) | 3.28	N/A	N/A
600 AMeV Ne on Al	N/A	N/A	N/A	N/A
600 AMeV Ne on Li	N/A	N/A	N/A	N/A
600 AMeV Si on C	N/A	N/A	N/A	N/A
600 AMeV Si on Cu	N/A	N/A	N/A	N/A
600 AMeV Si on Pb	N/A	N/A	N/A	N/A
400 AMeV C on Al	N/A	N/A	N/A	N/A
400 AMeV C on C	3.73 (0.1) | 3.10	3.06 (0.1) | 2.70	3.02 (0.1) | 2.70	2.35 (0.1) | 2.10
400 AMeV C on Cu	4.83 (0.1) | 3.50	3.91 (0.1) | 3.10	3.49 (0.1) | 3.10	2.87 (0.1) | 2.50
400 AMeV C on Li	N/A	N/A	N/A	N/A
400 AMeV C on Pb	6.17 (0.1) | 3.97	4.96 (0.1) | 3.57	4.15 (0.1) | 3.57	3.41 (0.1) | 2.97
600 AMeV Ne on Al	N/A	N/A	N/A	N/A
600 AMeV Ne on Li	N/A	N/A	N/A	N/A

The emission source radii shown in Table 47 show large disagreements between the values calculated from the data in this experiment and those provided by Mekijan, et. al. The differences are especially noticeable at heavy projectile/target systems. However, the trends are the same and include decreasing radii with heavier ion fragments and increasing radii with heavier systems. The discrepancies, again, may be due to the limited range of available cross section data that could be applied to the coalescence radii calculations, or even the limited amount of data available to Mekijan when calculating the source radii.

CHAPTER V
CONCLUSIONS AND RECOMMENDATIONS

Double differential production cross section data were measured for protons, deuterons, and tritons for 39 separate systems, some of which also produced cross sections for ^{3}He and ^{4}He. The use of this data, along with previously measured neutron data from the same experiment, allowed for coalescence radius calculations over a wide range of system energies and masses.

The experiments from which this data was taken were originally designed for measuring neutron cross section data. While a large quantity of data was gathered, some issues arose with the analysis of the charged light ion data that weren't present during the neutron data analysis. The long flight paths limited the lower energy range of the detected light-ion fragments, since the low energy ions would slow down completely in the air. The higher energy ranges were also limited to an extent depending on the severity of the QDC saturation. The charged particle count rates were also quite low for many systems at broader angles (and in some cases, non-existent). While there is measured cross section data at these angles, the uncertainties can be large. Because of the issues with charged particle analysis, the dynamic range of available proton, deuteron, triton, ^{3}He and ^{4}He data is limited compared with the neutron data sets.

Coalescence model calculations were performed using the model presented by Awes [18], using both the proton semi-inclusive cross sections measured here and the previously measured neutron cross sections. A comparison of the coalescence results to other measurements would be helpful, but the amount of data available to compare to is very limited. However, with the amount of data presented here, one can begin determining systematic trends for the many parameters for each system; parameters such as projectile type, projectile energy, target, fragment, and, if one wanted to be more specific, fragment trajectory angles and energies.

One trend in the coalescence radii suggested that the substituting input neutron spectra for proton spectra using a weighting factor is not entirely accurate. This substitution slightly elevates the calculated coalescence radius.

Another trend in the data suggest that the coalescence radius has a decreasing trend with increasing projectile/target system mass. Logarithmic trend lines have been included to show this trend for all coalescence radii that were calculated, as well as radii grouped by light-ion fragment. The trends show a strong correlation, especially for deuterons and tritons. With these trends, it is possible to calculate light ion cross sections without using a coalescence radius parameter, as long as a nucleon production cross section is available.

The type of extensive data presented here is needed at higher energies. The systems used in the experiments used ion beams with energies up to 600 AMeV. Higher beam energies would be useful for testing if the coalescence model can be used for high energy GCR interactions.

LIST OF REFERENCES

[1] NCRP Report No.89, "Guidance on Radiation Received in Space Activities," National Council on Radiation Protection and Measurements, 1989.

[2] J. P. Wefel, "Instrumentation for Radiation Measurement in Space," in *Proceedings of the Workshop on the Radiation Environment of the Satellite Power System (SPS)*, Springfield, VA, National Technical Information Service, 1978.

[3] I. Remec, et al, "Benchmarking of Neutron Productino of Heavy-Ion Transport Codes," *Journal of ASTM International*, vol. 9, no. 4, 2012.

[4] J. H. Heinbockel, et. al., "Comparison of Transport Codes, HZETRN, HETC and FLUKA, Using 1977 GCR Solar Minimum Spectra," *NASA Technical Papers*, no. 2009-215956, 2009.

[5] S. T. Butler and C. A. Pearson, "Deuterons from High-Engery Proton Bombardment of Matter," *Phys. Rev.*, vol. 129, no. 2, pp. 836-842, 1963.

[6] H. H. Gutbrod, et al, "Final-State Interactions in the Production of Hydrogen and Helium Isotopes by Relativistic Heavy Ions on Uranium," *Phys. Rev. Lett.*, vol. 37, no. 11, pp. 667-670, 1976.

[7] H. Sato, et al, "On the Coalescence Model for High Energy Nuclear Reactions," *Phys. Lett.*, vol. 98B, no. 3, pp. 153-157, 1981.

[8] J. I. Kapusta, "Mechanisms for Deuteron Production in Relativistic Nuclear Collisions," *Phys. Rev. C*, vol. 21, no. 4, pp. 1301-1310, 1980.

[9] M. C. Lemaire, et al, "Composite Particle Emission in Relativistic Heavy Ion Collisions," *Phys. Lett.*, vol. 85B, no. 1, pp. 38-42, 1979.

[10] A. Z. Mekjian, "Explosive Nucleosynthesis, Equilibrium Thermodynamics, and Relativistic Heavy-Ion Collisions," *Phys. Rev. C*, vol. 17, no. 3, pp. 1051-1070, 1978.

[11] M. PourArsalan, "Secondary Light Particle Data Base Development Using a Thermodynamic Coalescence Model," University of Tennessee, Knoxville, 2012.

[12] S. Datta, et al, "A Refined Coalescence Model for Intermediate-Energy Heavy-Ion Collisions. Application to Deuteron Spectra," *J. Phys. G: Nucl. Phys.*, vol. 14, pp. 937-948, 1988.

[13] S. Datta, et al, "Coalescence-Model Analysis of Alpha-Particle and Deuteron Spectra from Energetic Heavy-Ion Collisions," *Phys. Lett. B*, vol. 192, no. 3,4, pp. 302-306, 1987.

[14] T. C. Awes, et al, "Coalescence of Light Particles in the Reaction O-16 + U-238 at 315 MeV," *Phys. Rev. Lett.*, vol. 45, no. 7, pp. 513-516, 1980.

[15] John W. Norbury, et al, "Nuclear Data for Space Radiation," *Radiation Measurements*, vol. 47, pp. 315-363, 2012.

[16] J. A. Simpson, "Introduction to the Galactic Cosmic Radiation," in *Composition and*

Origin of Cosmic Rays, Dorcht, Nehterlands, Reidel Publishing, 1983, p. 1.

[17] L. C. Simonsen, et al, "Radiation Exposure for Humans Mars Exploration," *Health Physics*, vol. 79, pp. 515-525, 2000.

[18] T. C. Awes, et al, "Precompound Emission of Light Particles in the Reaction O-16 + U-238 at 20 MeV/nucleon," *Phys. Rev. C,* vol. 24, no. 1, pp. 89-110, 1981.

[19] J. Gosset, etl al, "Central Collisions of Relativistic Heavy Ions," *Phys. Rev. C,* vol. 16, no. 2, pp. 629-657, 1977.

[20] J. F. Janni, "Proton Range-Energy Tables, 1 keV-10 GeV," *Atomic Data and Nuclear Data Tables,* vol. 27, no. 2-3, 1982.

[21] M. J. Berger, et al, "Stopping-Power and Range Tables for Electrons, Protons, and Helium Ions," Nuclear Institute of Standards and Technology, August 2005. [Online]. Available: www.nist.gov/pml/data/star. [Accessed May 2012].

[22] R. K. Tripathi, et al, "Accurate Universal Parameterization of Absorption Cross Sections," *Nuclear Instruments and Methods in Physics Research B,* vol. 117, pp. 347-349, 1996.

[23] R. K. Tripathi, et al, "Accurate Universal Parameterization of Absortption Cross Sections II - Neutron Absorption Cross Sections," *Nuclear Instruments and Methods in Physics Research B,* vol. 129, pp. 11-15, 1997.

[24] R. K. Tripathi, et al, "Accurate Universal Parameterization of Absorption Cross Sections III - Light Systems," *Nuclear Instruments and Methods in Physics Research B,* vol. 155, pp. 349-356, 1999.

[25] CERN, "PAW - Physics Analysis Workstation," 6 February 2013. [Online]. Available: http://paw.web.cern.ch/paw/. [Accessed 15 November 2013].

[26] S. D. Gupta, et. al, "The Thermodynamic Model for Relativistic Heavy-Ion Collisions," *Phys. Rev. Letters,* pp. 133-183, 1981.

APPENDIX

Appendix A
Additional Results

Appendix A contains all of the results from the experiment described in this paper.

A.1 Cross Section Tables

This portion of Appendix A contains tables of the cross section measurements acquired during the experiment. Each table contains all of the measured cross sections for all available angles (in degrees) for a particular ion fragment for a projectile/target system. Each angle has three columns contained within. The first column lists to energy in MeV/nucleon. The second column presents the cross section in mb/AMeV/Sr. The third column (in parentheses) presents the absolute error. The errors provided are purely statistical.

Table 48. Proton production cross sections for 290 MeV/u carbon on carbon.

5	10	20	30	40	60	80
52 | 2.75 (0.39)	50 | 2.16 (0.35)	50 | 2.31 (0.31)	51 | 2.69 (0.39)	53 | 2.30 (0.27)	58 | 1.68 (0.27)	84 | 0.76 (0.17)
57 | 2.55 (0.34)	55 | 3.37 (0.42)	55 | 2.91 (0.32)	56 | 2.82 (0.35)	59 | 2.25 (0.26)	62 | 1.49 (0.25)	86 | 0.81 (0.17)
63 | 3.16 (0.33)	60 | 3.68 (0.37)	61 | 2.63 (0.28)	62 | 2.88 (0.29)	65 | 2.43 (0.28)	66 | 1.42 (0.25)	89 | 0.68 (0.15)
71 | 3.38 (0.35)	66 | 3.36 (0.36)	68 | 2.94 (0.29)	69 | 2.68 (0.27)	73 | 2.26 (0.24)	71 | 1.77 (0.24)	92 | 0.74 (0.15)
79 | 3.69 (0.35)	73 | 3.59 (0.34)	77 | 3.24 (0.29)	77 | 2.74 (0.26)	81 | 2.14 (0.22)	75 | 1.54 (0.28)	94 | 1.22 (0.23)
89 | 4.27 (0.34)	80 | 3.41 (0.36)	88 | 2.87 (0.25)	86 | 2.92 (0.29)	90 | 1.93 (0.21)	78 | 1.40 (0.22)	96 | 0.54 (0.14)
100 | 3.70 (0.33)	87 | 4.39 (0.40)	100 | 2.86 (0.29)	95 | 3.02 (0.27)	101 | 1.98 (0.22)	82 | 1.15 (0.20)	99 | 0.51 (0.15)
111 | 3.66 (0.31)	95 | 3.92 (0.36)	112 | 3.36 (0.27)	103 | 3.13 (0.33)	111 | 1.62 (0.23)	86 | 1.17 (0.19)	102 | 0.44 (0.10)
120 | 3.93 (0.39)	102 | 4.14 (0.44)	123 | 4.09 (0.36)	109 | 2.69 (0.30)	118 | 1.81 (0.20)	90 | 1.13 (0.17)	106 | 0.41 (0.10)
128 | 5.19 (0.46)	108 | 4.40 (0.44)	131 | 3.06 (0.28)	116 | 2.61 (0.24)	127 | 1.21 (0.14)	95 | 1.23 (0.16)	110 | 0.32 (0.10)
136 | 4.62 (0.40)	114 | 5.47 (0.48)	141 | 2.65 (0.27)	123 | 2.99 (0.33)	137 | 1.26 (0.15)	101 | 0.99 (0.14)	115 | 0.07 (0.02)
145 | 5.07 (0.41)	120 | 5.52 (0.46)	152 | 3.77 (0.34)	132 | 2.79 (0.27)	149 | 0.51 (0.09)		121 | 0.00 (0.00)
156 | 6.44 (0.47)	128 | 5.52 (0.45)	165 | 2.89 (0.27)	141 | 2.69 (0.27)	163 | 1.21 (0.13)		
167 | 6.93 (0.49)	136 | 5.07 (0.43)			179 | 0.30 (0.06)		
	145 | 7.51 (0.54)					
	156 | 6.79 (0.49)					

Table 49. Deuteron production cross sections for 290 MeV/u carbon on carbon.

5	10	20	30	40	60	80
31 | 1.77 (0.43)	28 | 1.33 (0.36)	30 | 1.28 (0.29)	28 | 1.40 (0.32)	30 | 0.94 (0.21)	32 | 0.78 (0.18)	43 | 0.04 (0.13)
34 | 1.58 (0.31)	31 | 2.18 (0.43)	33 | 1.84 (0.30)	31 | 1.02 (0.22)	33 | 1.25 (0.21)	34 | 0.85 (0.17)	46 | 0.22 (0.13)
37 | 1.38 (0.27)	34 | 1.39 (0.28)	37 | 1.48 (0.23)	34 | 1.24 (0.24)	37 | 0.85 (0.14)	37 | 0.47 (0.14)	49 | 0.09 (0.06)
42 | 2.19 (0.31)	37 | 1.95 (0.33)	41 | 1.34 (0.23)	38 | 1.40 (0.22)	41 | 0.92 (0.16)	39 | 0.59 (0.15)	51 | 0.06 (0.10)
47 | 2.53 (0.36)	41 | 1.76 (0.31)	45 | 1.74 (0.25)	43 | 1.59 (0.26)	46 | 0.91 (0.15)	42 | 0.31 (0.27)	55 | 0.12 (0.10)
52 | 2.18 (0.31)	45 | 2.16 (0.34)	51 | 1.53 (0.21)	47 | 1.13 (0.19)	51 | 0.93 (0.16)	43 | 0.28 (0.27)	58 | 0.02 (0.01)
58 | 1.66 (0.24)	50 | 1.98 (0.29)	56 | 1.59 (0.24)	53 | 1.12 (0.17)	56 | 0.75 (0.13)	45 | 0.30 (0.24)	
65 | 2.31 (0.27)	54 | 1.71 (0.31)	62 | 1.41 (0.21)	59 | 1.17 (0.20)	62 | 0.76 (0.13)	47 | 0.27 (0.21)	
73 | 2.03 (0.28)	59 | 1.42 (0.24)	68 | 1.46 (0.20)	65 | 1.33 (0.20)	67 | 0.76 (0.16)	49 | 0.40 (0.12)	
80 | 1.81 (0.24)	64 | 1.95 (0.28)	73 | 1.44 (0.26)	71 | 1.04 (0.16)	71 | 0.81 (0.16)	51 | 0.12 (0.18)	
87 | 2.65 (0.38)	68 | 2.29 (0.42)	77 | 1.17 (0.21)	77 | 0.81 (0.17)	75 | 0.94 (0.17)	53 | 0.33 (0.10)	
91 | 2.57 (0.34)	71 | 2.06 (0.38)	81 | 1.38 (0.22)	81 | 1.14 (0.20)	80 | 0.69 (0.13)	56 | 0.06 (0.14)	
96 | 1.75 (0.26)	75 | 2.27 (0.37)	86 | 1.65 (0.24)	86 | 1.05 (0.19)	85 | 0.62 (0.15)	59 | 0.11 (0.07)	
102 | 3.27 (0.37)	78 | 1.99 (0.34)	91 | 1.13 (0.19)	91 | 1.03 (0.18)	91 | 0.48 (0.15)		
108 | 2.73 (0.32)	82 | 1.75 (0.29)	97 | 1.71 (0.24)	97 | 1.24 (0.19)	97 | 0.46 (0.12)		
115 | 1.86 (0.25)	87 | 1.96 (0.30)	103 | 1.80 (0.24)	103 | 1.68 (0.21)	104 | 0.26 (0.06)		
	91 | 2.07 (0.30)		110 | 1.02 (0.10)	112 | 0.46 (0.08)		
	96 | 2.38 (0.32)		118 | 2.18 (0.30)	121 | 0.44 (0.05)		
	102 | 2.61 (0.33)		127 | 0.97 (0.14)	132 | 0.40 (0.09)		
	108 | 4.50 (0.43)			144 | 0.10 (0.05)		
	115 | 7.29 (0.57)					

Table 50. Triton production cross sections for 290 MeV/u carbon on carbon.

5	10	20	30	40	60	80
23 | 0.28 (0.24)	23 | 0.49 (0.24)	22 | 0.46 (0.19)	21 | 0.51 (0.22)	21 | 0.27 (0.13)	24 | 0.08 (0.04)	
25 | 0.06 (0.28)	25 | 0.64 (0.23)	24 | 0.36 (0.18)	23 | 0.53 (0.20)	24 | 0.43 (0.17)	25 | 0.16 (0.07)	
27 | 1.07 (0.29)	27 | 0.80 (0.29)	27 | 0.34 (0.12)	25 | 0.44 (0.14)	26 | 0.24 (0.11)	27 | 0.15 (0.11)	
30 | 1.22 (0.39)	30 | 0.95 (0.23)	30 | 0.60 (0.16)	28 | 0.65 (0.18)	28 | 0.12 (0.19)	28 | 0.36 (0.21)	
33 | 1.94 (0.41)	33 | 1.51 (0.35)	34 | 0.73 (0.19)	31 | 0.37 (0.14)	31 | 0.34 (0.16)	29 | 0.36 (0.22)	
36 | 0.76 (0.28)	36 | 0.54 (0.18)	37 | 0.63 (0.16)	34 | 0.06 (0.03)	33 | 0.33 (0.12)	30 | 0.09 (0.07)	
40 | 0.79 (0.26)	40 | 0.76 (0.21)	42 | 0.43 (0.12)	38 | 0.48 (0.13)	35 | 0.30 (0.12)	31 | 0.16 (0.09)	
44 | 0.69 (0.25)	44 | 0.57 (0.22)	46 | 0.18 (0.11)	41 | 0.32 (0.13)	37 | 0.23 (0.16)	32 | 0.04 (0.03)	
47 | 0.74 (0.23)	47 | 0.27 (0.16)	50 | 0.30 (0.10)	44 | 0.49 (0.15)	39 | 0.13 (0.06)	33 | 0.41 (0.19)	
51 | 0.67 (0.26)	51 | 0.60 (0.18)	54 | 0.36 (0.11)	48 | 0.34 (0.12)	40 | 0.20 (0.10)	35 | 0.08 (0.06)	
54 | 0.24 (0.17)	54 | 0.14 (0.10)	58 | 0.23 (0.12)	51 | 0.29 (0.15)	42 | 0.22 (0.10)	36 | 0.03 (0.02)	
56 | 0.29 (0.17)	56 | 0.46 (0.21)	61 | 0.21 (0.10)	53 | 0.14 (0.09)	44 | 0.09 (0.06)	39 | 0.01 (0.01)	
58 | 0.91 (0.31)	58 | 0.25 (0.16)	64 | 0.32 (0.13)	56 | 0.10 (0.08)	46 | 0.32 (0.14)	41 | 0.01 (0.01)	
61 | 0.63 (0.21)	61 | 0.60 (0.23)	68 | 0.27 (0.11)	58 | 0.33 (0.13)	48 | 0.09 (0.05)		
64 | 1.05 (0.27)	64 | 0.40 (0.17)	71 | 0.14 (0.06)	61 | 0.14 (0.09)	50 | 0.03 (0.03)		
67 | 1.21 (0.32)	67 | 0.36 (0.16)	75 | 0.18 (0.07)	64 | 0.19 (0.09)	53 | 0.00 (0.00)		
70 | 1.23 (0.28)	70 | 0.51 (0.17)	80 | 0.23 (0.04)	68 | 0.22 (0.10)			
73 | 1.08 (0.26)		84 | 0.30 (0.05)	71 | 0.17 (0.09)			
		89 | 0.33 (0.10)	75 | 0.04 (0.04)			
		95 | 0.47 (0.11)	80 | 0.04 (0.04)			
		102 | 0.12 (0.05)				

Table 51. ^{3}He production cross sections for 290 MeV/u carbon on carbon.

5	10	20	30	40	60	80
	97 | 0.87 (0.21)					
	101 | 0.79 (0.19)					
	106 | 0.77 (0.17)					
	111 | 0.70 (0.16)					
	117 | 0.69 (0.16)					
	123 | 0.74 (0.15)					
	130 | 0.83 (0.15)					

Table 52. ^{4}He production cross sections for 290 MeV/u carbon on carbon.

5	10	20	30	40	60	80
	166 | 0.02 (0.02) 175 | 0.17 (0.10)					

Table 53. Proton production cross sections for 290 MeV/u carbon on copper.

5	10	20	30	40	60	80
60 | 12.90 (1.41)	60 | 12.74 (1.36)	58 | 8.53 (0.96)	60 | 8.65 (1.02)	62 | 7.60 (0.83)	72 | 4.58 (0.68)	112 | 2.14 (0.39)
64 | 11.17 (1.15)	64 | 13.79 (1.29)	62 | 9.54 (0.97)	64 | 8.95 (0.92)	67 | 6.75 (0.69)	76 | 5.12 (0.68)	114 | 2.17 (0.42)
70 | 10.60 (0.99)	70 | 12.59 (1.11)	68 | 10.71 (0.90)	70 | 8.81 (0.83)	75 | 7.78 (0.67)	82 | 4.05 (0.60)	116 | 2.80 (0.45)
77 | 10.65 (1.00)	77 | 12.47 (1.09)	75 | 9.09 (0.87)	76 | 9.66 (0.84)	84 | 6.45 (0.60)	88 | 4.54 (0.51)	119 | 1.93 (0.44)
84 | 11.10 (0.94)	84 | 13.33 (1.06)	83 | 9.55 (0.81)	84 | 8.94 (0.75)	95 | 6.19 (0.54)	94 | 4.58 (0.48)	120 | 2.00 (0.43)
94 | 12.77 (0.95)	92 | 12.90 (1.09)	91 | 8.33 (0.74)	92 | 9.61 (0.83)	107 | 5.70 (0.53)	100 | 3.65 (0.55)	122 | 2.05 (0.40)
105 | 12.59 (1.00)	100 | 13.10 (1.04)	100 | 9.69 (0.79)	101 | 8.78 (0.72)	120 | 5.16 (0.45)	105 | 3.45 (0.45)	125 | 1.85 (0.43)
115 | 11.75 (0.89)	110 | 12.13 (0.93)	110 | 8.01 (0.64)	108 | 8.12 (0.81)	132 | 4.23 (0.39)	110 | 2.81 (0.38)	127 | 1.44 (0.29)
125 | 12.69 (1.11)	118 | 12.99 (1.03)	120 | 10.16 (0.91)	114 | 8.00 (0.73)	142 | 3.48 (0.39)	117 | 1.55 (0.24)	130 | 1.36 (0.26)
132 | 16.46 (1.28)	125 | 16.32 (1.18)	127 | 11.05 (0.91)	121 | 8.01 (0.67)	154 | 1.21 (0.21)		134 | 1.11 (0.26)
140 | 13.67 (1.08)	132 | 12.93 (1.07)	136 | 9.09 (0.75)	128 | 7.66 (0.75)	167 | 3.41 (0.35)		139 | 0.65 (0.16)
149 | 14.76 (1.11)	140 | 13.57 (1.07)	145 | 8.01 (0.71)	136 | 7.08 (0.68)	183 | 1.16 (0.15)		
159 | 19.62 (1.34)	149 | 19.56 (1.36)	156 | 11.26 (0.91)	146 | 8.82 (0.73)			
171 | 21.26 (1.41)	159 | 18.34 (1.26)	168 | 6.27 (0.60)				

Table 54. Deuteron production cross sections for 290 MeV/u carbon on copper.

5	10	20	30	40	60	80
32 | 6.42 (1.23)	32 | 6.99 (1.22)	31 | 3.35 (0.70)	32 | 4.50 (0.83)	34 | 3.05 (0.75)	38 | 3.36 (0.53)	55 | 0.42 (0.37)
35 | 8.36 (1.27)	35 | 7.32 (1.16)	34 | 4.38 (0.74)	35 | 6.70 (0.92)	37 | 5.06 (0.68)	40 | 2.15 (0.56)	57 | 1.17 (0.34)
38 | 6.17 (0.98)	38 | 8.07 (1.09)	37 | 5.76 (0.79)	38 | 6.46 (0.82)	41 | 3.99 (0.51)	43 | 2.00 (0.40)	58 | 0.97 (0.27)
41 | 6.67 (1.03)	42 | 7.19 (0.93)	40 | 6.67 (0.90)	42 | 5.52 (0.76)	46 | 4.35 (0.54)	47 | 1.80 (0.45)	60 | 0.40 (0.21)
45 | 7.96 (1.08)	46 | 9.19 (1.11)	43 | 6.15 (0.77)	45 | 4.54 (0.61)	51 | 3.94 (0.50)	50 | 1.54 (0.30)	61 | 0.74 (0.30)
49 | 7.47 (0.97)	50 | 9.82 (1.07)	48 | 6.22 (0.71)	50 | 4.61 (0.57)	56 | 2.83 (0.41)	53 | 1.51 (0.39)	63 | 0.44 (0.22)
53 | 7.60 (1.07)	55 | 8.16 (0.89)	53 | 5.86 (0.63)	54 | 4.89 (0.66)	61 | 2.45 (0.34)	55 | 1.58 (0.38)	64 | 0.26 (0.13)
56 | 7.42 (1.00)	61 | 7.63 (0.93)	58 | 4.39 (0.58)	59 | 4.38 (0.58)	68 | 2.29 (0.31)	57 | 1.37 (0.32)	66 | 0.63 (0.24)
60 | 8.95 (1.47)	66 | 7.85 (0.91)	63 | 4.08 (0.52)	64 | 4.51 (0.56)	73 | 3.30 (0.55)	60 | 0.82 (0.25)	68 | 0.09 (0.09)
67 | 6.51 (1.09)	71 | 7.71 (0.83)	69 | 5.79 (0.60)	68 | 4.07 (0.66)	77 | 3.16 (0.50)		
70 | 8.81 (1.23)	76 | 8.19 (1.10)	74 | 4.60 (0.66)	71 | 6.38 (0.85)	82 | 2.55 (0.43)		
73 | 8.00 (1.13)	80 | 7.46 (1.02)	78 | 4.71 (0.65)	75 | 5.24 (0.72)	87 | 2.68 (0.37)		
76 | 8.11 (1.12)	84 | 8.30 (1.03)	83 | 5.78 (0.71)	79 | 5.41 (0.71)	92 | 2.18 (0.32)		
80 | 7.58 (1.02)	88 | 6.20 (0.84)	87 | 5.22 (0.64)	83 | 3.59 (0.60)	99 | 2.84 (0.36)		
84 | 7.56 (0.97)	93 | 5.38 (0.74)	92 | 3.37 (0.47)	87 | 2.89 (0.45)	106 | 1.13 (0.19)		
88 | 8.72 (1.02)	98 | 9.38 (0.99)	98 | 5.09 (0.62)	93 | 3.85 (0.52)			
93 | 7.27 (0.89)	103 | 8.80 (0.93)	104 | 5.02 (0.58)	98 | 3.81 (0.53)			
98 | 6.52 (0.80)						
103 | 8.69 (0.92)						
109 | 7.35 (0.81)						
116 | 5.93 (0.68)						

Table 55. Triton production cross sections for 290 MeV/u carbon on copper.

5	10	20	30	40	60	80
26 | 3.15 (0.91)	24 | 2.70 (0.82)	23 | 2.82 (0.77)	24 | 3.16 (0.75)	24 | 1.31 (0.38)	28 | 0.58 (0.22)	
28 | 2.77 (0.82)	26 | 3.04 (0.80)	25 | 2.21 (0.56)	26 | 2.79 (0.63)	27 | 1.61 (0.40)	31 | 0.70 (0.22)	
31 | 5.51 (1.02)	29 | 3.73 (0.82)	27 | 1.94 (0.52)	29 | 1.15 (0.53)	29 | 1.41 (0.39)	33 | 0.49 (0.17)	
33 | 4.78 (1.01)	31 | 4.62 (0.84)	30 | 2.38 (0.48)	32 | 1.92 (0.42)	32 | 1.61 (0.38)	36 | 0.25 (0.33)	
36 | 2.40 (0.87)	34 | 3.14 (0.72)	33 | 2.42 (0.49)	35 | 2.21 (0.48)	35 | 0.95 (0.25)	39 | 0.49 (0.20)	
40 | 3.48 (0.75)	38 | 3.06 (0.68)	36 | 1.80 (0.53)	39 | 2.11 (0.42)	38 | 0.85 (0.27)	41 | 0.19 (0.15)	
43 | 1.47 (0.66)	41 | 3.23 (0.62)	40 | 1.76 (0.36)	43 | 2.35 (0.42)	41 | 1.56 (0.37)	43 | 0.12 (0.12)	
46 | 2.44 (0.68)	45 | 3.74 (0.77)	44 | 1.81 (0.35)	47 | 1.32 (0.33)	43 | 0.85 (0.34)		
50 | 1.95 (0.52)	48 | 2.69 (0.60)	49 | 2.03 (0.42)	51 | 1.17 (0.31)	45 | 0.94 (0.36)		
52 | 1.43 (0.77)	52 | 2.78 (0.60)	53 | 1.56 (0.32)	55 | 1.45 (0.32)	47 | 0.31 (0.16)		
55 | 2.27 (0.78)	55 | 1.68 (0.60)	58 | 1.27 (0.29)	59 | 0.95 (0.32)	49 | 0.79 (0.30)		
57 | 2.23 (0.68)	57 | 2.59 (0.73)	62 | 0.41 (0.20)	62 | 1.19 (0.36)	52 | 1.02 (0.34)		
59 | 1.97 (0.60)	59 | 1.59 (0.54)	65 | 0.75 (0.25)	65 | 1.29 (0.35)			
62 | 1.54 (0.52)	62 | 2.03 (0.60)	68 | 1.55 (0.38)	68 | 0.82 (0.28)			
64 | 4.20 (0.84)	64 | 1.07 (0.41)	72 | 1.12 (0.30)	72 | 1.10 (0.30)			
67 | 2.68 (0.65)	67 | 1.63 (0.50)	76 | 1.69 (0.38)	76 | 0.48 (0.19)			
70 | 3.05 (0.65)	70 | 2.84 (0.64)		80 | 0.00 (0.00)			
74 | 3.90 (0.73)						
77 | 2.80 (0.59)						

Table 56. ^{3}He production cross sections for 290 MeV/u carbon on copper.

5	10	20	30	40	60	80
	105 | 1.87 (0.51) 108 | 1.67 (0.39) 114 | 2.44 (0.52) 119 | 1.77 (0.38) 124 | 2.02 (0.36) 130 | 2.98 (0.58) 135 | 2.10 (0.35) 145 | 1.83 (0.30)					

Table 57. ^{4}He production cross sections for 290 MeV/u carbon on copper.

5	10	20	30	40	60	80
	87 | 1.14 (0.41) 90 | 0.92 (0.35) 94 | 0.58 (0.26) 98 | 1.07 (0.34) 102 | 0.77 (0.28) 106 | 1.04 (0.30) 112 | 0.89 (0.27) 117 | 0.93 (0.26) 124 | 0.86 (0.24) 131 | 0.79 (0.22) 138 | 0.61 (0.18)					

Table 58. Proton production cross sections for 290 MeV/u carbon on lead.

5	10	20	30	40	60	80
48 | 27.71 (4.23)	48 | 22.02 (3.71)	46 | 15.24 (2.52)	48 | 24.15 (3.22)	52 | 19.24 (2.54)	53 | 13.59 (2.23)	71 | 8.53 (1.35)
53 | 24.52 (3.63)	53 | 25.98 (3.59)	50 | 19.18 (3.11)	54 | 24.11 (2.80)	59 | 17.96 (2.19)	58 | 12.08 (2.15)	76 | 8.25 (1.26)
59 | 26.34 (3.36)	59 | 24.49 (3.14)	56 | 19.03 (2.67)	60 | 20.26 (2.54)	67 | 17.55 (2.14)	65 | 11.00 (1.79)	81 | 7.32 (1.22)
66 | 17.52 (2.81)	66 | 20.53 (2.84)	63 | 17.20 (2.19)	66 | 21.05 (2.43)	77 | 15.18 (1.80)	72 | 13.07 (1.68)	86 | 6.23 (0.97)
73 | 18.69 (2.56)	73 | 24.66 (2.88)	71 | 18.85 (2.21)	75 | 17.00 (2.03)	87 | 16.75 (2.07)	79 | 10.91 (1.51)	91 | 7.45 (1.35)
83 | 20.69 (2.43)	83 | 21.59 (2.46)	82 | 18.26 (2.01)	84 | 16.27 (2.11)	98 | 12.39 (1.66)	86 | 10.10 (1.59)	95 | 4.78 (0.95)
93 | 16.01 (2.27)	93 | 25.20 (2.85)	92 | 16.96 (2.27)	93 | 20.47 (2.12)	112 | 12.21 (1.45)	91 | 8.89 (1.68)	99 | 4.46 (0.87)
103 | 22.91 (2.50)	103 | 25.53 (2.69)	103 | 17.63 (2.09)	104 | 15.98 (1.85)	125 | 7.59 (0.96)	97 | 8.65 (1.48)	
112 | 21.62 (3.05)	115 | 25.51 (2.32)	117 | 17.47 (1.68)	114 | 15.69 (1.67)	135 | 8.14 (1.47)		
119 | 22.51 (3.04)	126 | 14.82 (1.77)	130 | 16.88 (2.08)	121 | 12.99 (1.59)	147 | 3.13 (0.95)		
126 | 32.37 (3.49)	134 | 32.73 (3.41)	139 | 17.70 (2.26)	130 | 13.92 (2.20)	161 | 8.21 (1.00)		
134 | 27.71 (3.12)	144 | 42.71 (3.92)	150 | 26.15 (2.89)	140 | 17.78 (2.36)	177 | 1.84 (0.40)		
144 | 25.54 (2.85)	154 | 45.85 (3.89)	163 | 15.06 (2.56)	151 | 9.07 (1.62)			
154 | 41.93 (3.75)						
166 | 43.90 (3.78)						

Table 59. Deuteron production cross sections for 290 MeV/u carbon on lead.

5	10	20	30	40	60	80
29 | 25.51 (5.27)	28 | 23.29 (4.92)	28 | 16.15 (3.23)	28 | 15.48 (3.38)	30 | 9.72 (1.98)	30 | 9.94 (1.88)	38 | 5.03 (1.27)
32 | 15.74 (3.85)	30 | 15.63 (3.83)	31 | 16.60 (3.05)	30 | 14.93 (3.42)	33 | 10.98 (1.91)	33 | 7.93 (2.38)	40 | 1.93 (1.79)
35 | 12.30 (3.30)	34 | 19.85 (3.77)	35 | 13.56 (2.39)	34 | 13.84 (2.44)	38 | 12.36 (1.93)	37 | 7.14 (1.67)	43 | 1.99 (1.50)
40 | 17.14 (3.17)	37 | 23.36 (4.38)	39 | 14.99 (2.70)	38 | 9.48 (2.08)	44 | 6.57 (1.78)	41 | 5.29 (1.78)	45 | 1.77 (0.67)
44 | 21.34 (3.56)	40 | 24.18 (4.08)	43 | 9.45 (1.83)	42 | 14.83 (2.42)	49 | 8.90 (1.39)	44 | 3.87 (1.72)	48 | 2.91 (1.11)
49 | 18.54 (3.15)	44 | 16.22 (3.04)	48 | 15.74 (2.28)	46 | 12.83 (2.07)	57 | 5.43 (1.10)	47 | 2.70 (1.98)	50 | 0.83 (0.48)
55 | 12.83 (2.42)	49 | 18.37 (2.99)	54 | 12.97 (1.89)	52 | 9.39 (1.91)	65 | 7.05 (1.25)	49 | 4.20 (1.29)	52 | 0.70 (0.41)
61 | 7.32 (2.39)	54 | 16.61 (3.24)	61 | 11.71 (1.91)	58 | 7.49 (1.50)	72 | 9.77 (1.37)	52 | 2.60 (1.13)	54 | 0.87 (0.50)
66 | 18.85 (3.01)	58 | 13.12 (2.62)	67 | 10.80 (1.67)	64 | 10.94 (2.11)	82 | 5.99 (1.24)	54 | 3.04 (1.14)	
72 | 14.99 (2.48)	63 | 16.87 (2.81)	74 | 7.19 (1.09)	70 | 7.87 (1.38)	90 | 6.25 (1.23)	57 | 0.54 (0.45)	
78 | 15.15 (3.14)	69 | 15.29 (2.52)	80 | 6.43 (1.45)	78 | 8.79 (1.37)	96 | 5.09 (1.24)		
82 | 12.65 (2.78)	76 | 16.42 (2.46)	85 | 8.19 (2.08)	85 | 9.39 (1.90)	103 | 2.90 (0.72)		
86 | 14.26 (2.80)	82 | 12.84 (2.71)	90 | 7.06 (1.30)	90 | 8.04 (1.64)	111 | 3.73 (0.74)		
91 | 14.09 (2.68)	86 | 7.53 (1.99)	96 | 5.64 (1.08)	96 | 10.17 (1.77)	121 | 3.36 (0.50)		
96 | 11.01 (2.28)	91 | 6.48 (1.77)	102 | 6.61 (1.29)	102 | 8.02 (1.75)	131 | 3.01 (0.97)		
101 | 16.96 (2.82)	96 | 17.67 (2.91)		109 | 8.30 (0.94)			
108 | 18.84 (2.79)	101 | 17.77 (2.82)		117 | 4.28 (0.60)			
115 | 7.69 (1.72)	108 | 23.31 (3.11)		126 | 7.02 (1.35)			
	115 | 11.11 (1.20)					
	122 | 11.83 (1.34)					
	131 | 17.01 (2.29)					

Table 60. Triton production cross sections for 290 MeV/u carbon on lead.

5	10	20	30	40	60	80
23 | 9.29 (4.12)	23 | 11.13 (3.77)	21 | 9.26 (2.88)	21 | 7.53 (2.49)	22 | 8.51 (2.33)	24 | 3.99 (1.22)	
25 | 12.10 (3.75)	25 | 10.22 (3.29)	23 | 5.09 (3.33)	23 | 12.36 (3.11)	24 | 5.43 (2.25)	26 | 2.67 (1.06)	
28 | 7.89 (3.84)	27 | 10.57 (3.17)	25 | 8.50 (2.46)	25 | 6.22 (1.85)	27 | 6.13 (1.79)	29 | 2.85 (0.92)	
31 | 1.63 (2.88)	30 | 7.07 (2.94)	28 | 10.34 (2.38)	28 | 8.17 (2.00)	30 | 7.90 (1.91)	32 | 2.03 (0.85)	
35 | 11.62 (3.49)	33 | 12.67 (3.24)	32 | 8.84 (1.94)	31 | 3.42 (1.24)	33 | 4.33 (1.37)	35 | 3.35 (1.06)	
38 | 10.97 (3.61)	36 | 7.72 (2.27)	36 | 2.75 (2.01)	35 | 7.74 (1.94)	36 | 3.76 (1.39)	37 | 1.74 (1.11)	
43 | 10.37 (2.87)	40 | 8.57 (2.34)	40 | 5.39 (1.37)	38 | 7.33 (1.74)	39 | 4.28 (1.42)	39 | 1.48 (0.94)	
47 | 8.72 (2.83)	43 | 9.21 (2.72)	45 | 3.89 (1.99)	42 | 6.37 (1.83)	42 | 6.18 (2.30)		
50 | 5.13 (2.25)	47 | 6.07 (2.06)	51 | 3.19 (0.92)	46 | 3.95 (1.27)	44 | 2.87 (1.44)		
54 | 9.61 (2.59)	50 | 4.37 (1.56)	57 | 2.25 (0.77)	50 | 3.53 (1.14)	46 | 4.85 (1.86)		
58 | 4.51 (2.04)	53 | 2.02 (1.43)	62 | 1.63 (0.59)	54 | 1.60 (0.70)	48 | 4.04 (1.68)		
61 | 6.00 (2.29)	56 | 5.76 (2.37)	69 | 3.38 (0.91)	58 | 1.43 (0.75)			
63 | 5.71 (2.19)	58 | 3.90 (1.97)	75 | 0.68 (0.31)	61 | 1.89 (1.00)			
66 | 11.05 (2.92)	61 | 5.14 (2.12)	79 | 3.47 (0.84)	64 | 1.70 (0.99)			
69 | 3.74 (1.91)	63 | 3.94 (1.77)	84 | 3.24 (0.95)	67 | 2.95 (1.08)			
73 | 5.07 (2.00)	66 | 6.60 (2.23)	89 | 0.36 (1.98)	71 | 1.92 (0.97)			
77 | 4.63 (1.66)	69 | 5.68 (2.04)	95 | 4.12 (1.48)	75 | 0.66 (0.54)			
		101 | 1.51 (0.51)				

Table 61. ^{3}He production cross sections for 290 MeV/u carbon on lead.

5	10	20	30	40	60	80
	90 | 3.87 (1.60)					
	94 | 8.64 (2.28)					
	98 | 4.45 (1.51)					
	103 | 1.98 (1.15)					
	108 | 2.58 (1.06)					
	114 | 5.50 (1.50)					
	121 | 2.63 (0.94)					
	128 | 5.08 (1.26)					
	136 | 2.43 (0.82)					

Table 62. ^{4}He production cross sections for 290 MeV/u carbon on lead.

5	10	20	30	40	60	80
	76 | 0.69 (0.69) 79 | 0.68 (0.68) 82 | 1.32 (0.95) 86 | 1.13 (0.80) 95 | 0.57 (0.57) 100 | 1.62 (0.81) 105 | 1.55 (0.78) 111 | 0.71 (0.50) 118 | 1.62 (0.73) 125 | 0.63 (0.45) 133 | 0.57 (0.40)					

Table 63. Proton production cross sections for 400 MeV/u neon on carbon.

5	10	20	30	40	60	80
50 | 4.42 (0.64)	51 | 4.39 (0.60)	48 | 3.37 (0.45)	52 | 3.34 (0.43)	53 | 3.05 (0.36)	59 | 3.06 (0.37)	86 | 2.11 (0.30)
54 | 4.49 (0.56)	56 | 4.18 (0.52)	52 | 4.49 (0.47)	57 | 3.97 (0.47)	59 | 3.89 (0.38)	64 | 2.69 (0.33)	89 | 1.56 (0.24)
60 | 4.37 (0.49)	62 | 4.37 (0.47)	58 | 4.61 (0.46)	63 | 3.50 (0.44)	65 | 3.33 (0.35)	70 | 2.56 (0.30)	93 | 1.30 (0.20)
66 | 5.53 (0.57)	68 | 4.68 (0.50)	64 | 4.56 (0.45)	69 | 4.66 (0.45)	73 | 3.25 (0.30)	76 | 2.30 (0.27)	98 | 1.15 (0.16)
73 | 4.75 (0.47)	76 | 5.34 (0.49)	71 | 4.09 (0.41)	77 | 3.61 (0.36)	83 | 2.87 (0.26)	84 | 2.35 (0.25)	102 | 0.97 (0.18)
82 | 4.96 (0.44)	85 | 4.84 (0.42)	80 | 4.50 (0.39)	86 | 5.01 (0.44)	95 | 3.63 (0.31)	90 | 2.13 (0.30)	106 | 0.89 (0.16)
91 | 4.90 (0.47)	95 | 5.55 (0.50)	90 | 5.25 (0.44)	95 | 4.39 (0.41)	107 | 3.05 (0.27)	95 | 1.90 (0.23)	110 | 0.91 (0.15)
100 | 5.12 (0.46)	105 | 5.56 (0.47)	100 | 4.32 (0.38)	106 | 4.41 (0.35)	123 | 2.32 (0.21)	101 | 1.47 (0.19)	115 | 0.55 (0.10)
111 | 5.81 (0.46)	117 | 6.96 (0.51)	112 | 5.12 (0.38)	116 | 3.95 (0.35)	137 | 1.83 (0.20)		
120 | 6.81 (0.57)	128 | 6.69 (0.59)	123 | 5.06 (0.49)	123 | 3.86 (0.37)	149 | 1.51 (0.18)		
128 | 5.34 (0.47)	136 | 7.37 (0.61)	131 | 4.33 (0.39)	132 | 3.37 (0.39)	163 | 2.98 (0.27)		
136 | 4.94 (0.46)	145 | 8.53 (0.65)	141 | 5.55 (0.46)	141 | 4.80 (0.44)	179 | 1.76 (0.18)		
145 | 7.85 (0.62)	156 | 8.19 (0.62)	152 | 6.00 (0.52)	153 | 3.36 (0.37)			
156 | 6.90 (0.56)		165 | 4.08 (0.37)				

Table 64. Deuteron production cross sections for 400 MeV/u neon on carbon.

5	10	20	30	40	60	80
30 | 1.64 (0.43)	30 | 2.00 (0.51)	28 | 1.08 (0.27)	30 | 1.78 (0.36)	30 | 1.84 (0.31)	32 | 0.74 (0.17)	42 | 0.40 (0.14)
32 | 2.21 (0.47)	33 | 2.78 (0.51)	31 | 1.89 (0.36)	32 | 1.47 (0.38)	34 | 1.24 (0.22)	35 | 0.79 (0.23)	45 | 0.15 (0.14)
35 | 2.59 (0.49)	36 | 2.35 (0.43)	34 | 1.47 (0.34)	36 | 1.72 (0.35)	38 | 1.61 (0.27)	39 | 1.15 (0.20)	47 | 0.45 (0.14)
39 | 2.35 (0.41)	41 | 1.97 (0.35)	38 | 2.01 (0.30)	40 | 1.89 (0.31)	41 | 1.16 (0.20)	42 | 0.95 (0.20)	50 | 0.30 (0.10)
44 | 2.13 (0.40)	45 | 1.88 (0.36)	42 | 2.08 (0.31)	44 | 1.70 (0.27)	46 | 1.15 (0.18)	46 | 0.78 (0.16)	52 | 0.32 (0.14)
48 | 2.63 (0.41)	50 | 2.57 (0.41)	47 | 1.90 (0.27)	49 | 1.63 (0.32)	51 | 0.97 (0.18)	49 | 0.64 (0.17)	54 | 0.17 (0.09)
54 | 2.43 (0.36)	56 | 2.20 (0.32)	53 | 2.14 (0.27)	54 | 1.06 (0.20)	56 | 1.14 (0.18)	51 | 0.89 (0.21)	56 | 0.01 (0.15)
59 | 2.13 (0.38)	61 | 2.79 (0.41)	59 | 1.37 (0.23)	58 | 1.45 (0.24)	61 | 1.41 (0.25)	53 | 0.76 (0.19)	58 | 0.08 (0.06)
64 | 2.00 (0.34)	67 | 2.66 (0.38)	64 | 1.64 (0.22)	64 | 1.35 (0.21)	64 | 1.14 (0.23)		
70 | 2.94 (0.39)	73 | 2.92 (0.35)	71 | 2.42 (0.27)	69 | 1.65 (0.31)	67 | 1.35 (0.25)		
75 | 2.99 (0.50)	78 | 2.60 (0.43)	77 | 1.22 (0.30)	72 | 1.72 (0.29)	71 | 0.58 (0.15)		
78 | 2.80 (0.47)	82 | 2.52 (0.38)	81 | 1.51 (0.22)	76 | 1.05 (0.25)			
82 | 2.91 (0.42)	87 | 2.26 (0.39)	86 | 1.55 (0.23)	80 | 1.64 (0.26)			
87 | 2.83 (0.45)	91 | 2.05 (0.34)	91 | 1.66 (0.29)	85 | 1.70 (0.27)			
91 | 2.66 (0.40)	96 | 2.25 (0.35)	97 | 1.80 (0.31)	90 | 1.72 (0.26)			
96 | 3.79 (0.48)	102 | 2.70 (0.37)	103 | 1.33 (0.22)	95 | 1.19 (0.31)			
102 | 4.01 (0.48)			101 | 0.71 (0.19)			
108 | 1.80 (0.29)						

Table 65. Triton production cross sections for 400 MeV/u neon on carbon.

5	10	20	30	40	60	80
22 | 0.55 (0.50)	23 | 0.98 (0.37)	22 | 0.78 (0.27)	23 | 0.57 (0.43)	22 | 0.25 (0.14)	24 | 0.22 (0.08)	29 | 0.20 (0.11)
24 | 0.64 (0.41)	25 | 0.51 (0.26)	24 | 0.90 (0.27)	25 | 0.43 (0.19)	24 | 0.36 (0.15)	26 | 0.26 (0.11)	30 | 0.12 (0.10)
26 | 0.40 (0.36)	27 | 0.72 (0.28)	26 | 0.53 (0.18)	28 | 0.62 (0.19)	27 | 0.28 (0.11)	29 | 0.08 (0.05)	32 | 0.21 (0.12)
29 | 0.20 (0.34)	30 | 0.97 (0.33)	29 | 0.83 (0.24)	31 | 0.34 (0.13)	30 | 0.37 (0.12)	32 | 0.26 (0.12)	33 | 0.06 (0.06)
31 | 0.31 (0.24)	32 | 1.21 (0.35)	32 | 0.60 (0.19)	34 | 0.32 (0.11)	33 | 0.26 (0.11)	34 | 0.18 (0.08)	36 | 0.07 (0.06)
34 | 0.59 (0.33)	35 | 1.11 (0.34)	35 | 0.66 (0.19)	38 | 0.49 (0.15)	37 | 0.30 (0.13)	36 | 0.04 (0.04)	38 | 0.04 (0.05)
38 | 0.53 (0.26)	39 | 0.42 (0.21)	39 | 0.37 (0.11)	42 | 0.42 (0.16)	40 | 0.20 (0.10)	38 | 0.11 (0.09)	
41 | 0.58 (0.22)	42 | 0.10 (0.10)	42 | 0.64 (0.19)	45 | 0.24 (0.10)	43 | 0.29 (0.10)		
45 | 0.53 (0.22)	45 | 0.43 (0.19)	46 | 0.24 (0.09)	49 | 0.31 (0.12)	46 | 0.06 (0.05)		
49 | 0.29 (0.25)	49 | 0.67 (0.23)	50 | 0.32 (0.11)	53 | 0.33 (0.12)	48 | 0.27 (0.13)		
53 | 0.39 (0.16)	53 | 0.34 (0.15)	54 | 0.31 (0.11)	57 | 0.14 (0.09)	50 | 0.07 (0.07)		
57 | 0.46 (0.17)	56 | 0.13 (0.13)	58 | 0.44 (0.17)	60 | 0.11 (0.06)			
61 | 1.21 (0.36)	58 | 0.21 (0.15)	61 | 0.20 (0.09)	63 | 0.17 (0.10)			
64 | 0.95 (0.34)	61 | 0.64 (0.26)	64 | 0.28 (0.11)	66 | 0.24 (0.12)			
67 | 1.03 (0.32)	64 | 0.77 (0.28)	68 | 0.30 (0.12)	70 | 0.08 (0.06)			
70 | 0.61 (0.27)	67 | 0.51 (0.21)	71 | 0.43 (0.15)				
73 | 0.81 (0.25)	70 | 0.74 (0.25)	75 | 0.38 (0.13)				
77 | 1.32 (0.29)	73 | 0.61 (0.22)	80 | 0.64 (0.09)				
81 | 1.47 (0.20)	77 | 0.90 (0.15)	84 | 0.48 (0.10)				
85 | 1.45 (0.23)	81 | 0.92 (0.14)	89 | 0.19 (0.22)				
90 | 1.10 (0.25)	85 | 0.66 (0.21)					

Table 66. ^{3}He production cross sections for 400 MeV/u neon on carbon.

5	10	20	30	40	60	80
	89 | 0.52 (0.21) 92 | 0.82 (0.24) 97 | 0.39 (0.16) 101 | 0.37 (0.15) 106 | 0.62 (0.18) 111 | 0.84 (0.21) 117 | 0.76 (0.19) 123 | 0.69 (0.17) 130 | 0.78 (0.17)					

Table 67. Proton production cross sections for 400 MeV/u neon on copper.

5	10	20	30	40	60	80
58 | 7.21 (0.89) 62 | 7.96 (0.82) 67 | 7.10 (0.69) 73 | 6.08 (0.62) 79 | 7.38 (0.65) 87 | 7.95 (0.62) 96 | 8.08 (0.67) 105 | 7.42 (0.59) 115 | 7.83 (0.58) 125 | 8.95 (0.68) 132 | 7.96 (0.66) 140 | 7.44 (0.61) 149 | 9.21 (0.69) 159 | 9.11 (0.67)	59 | 7.33 (0.82) 63 | 7.35 (0.75) 68 | 7.66 (0.69) 75 | 6.98 (0.65) 82 | 9.31 (0.73) 91 | 7.87 (0.60) 100 | 7.46 (0.60) 110 | 7.61 (0.58) 121 | 7.63 (0.52) 132 | 7.05 (0.61) 140 | 7.32 (0.61) 149 | 10.74 (0.78) 159 | 9.21 (0.67)	59 | 8.03 (0.75) 64 | 6.91 (0.61) 70 | 6.70 (0.58) 78 | 6.86 (0.58) 86 | 6.59 (0.52) 98 | 7.03 (0.51) 110 | 5.94 (0.46) 124 | 6.65 (0.47) 136 | 5.91 (0.49) 145 | 7.52 (0.58) 156 | 6.62 (0.57)	61 | 5.97 (0.62) 65 | 6.79 (0.64) 70 | 7.25 (0.66) 76 | 5.99 (0.55) 84 | 6.43 (0.52) 95 | 6.19 (0.47) 106 | 5.84 (0.47) 117 | 5.46 (0.39) 128 | 5.19 (0.44) 136 | 5.64 (0.48) 146 | 6.63 (0.55) 157 | 4.58 (0.41)	62 | 5.33 (0.59) 67 | 5.78 (0.52) 73 | 6.04 (0.53) 81 | 5.63 (0.46) 91 | 4.98 (0.40) 101 | 4.31 (0.37) 113 | 4.28 (0.33) 128 | 3.28 (0.25) 142 | 2.20 (0.25) 154 | 2.14 (0.23) 167 | 3.69 (0.32) 183 | 2.13 (0.21)	72 | 4.98 (0.51) 76 | 4.26 (0.47) 82 | 4.19 (0.41) 88 | 4.03 (0.40) 94 | 3.67 (0.34) 100 | 3.32 (0.38) 105 | 3.37 (0.35) 110 | 2.61 (0.29)	114 | 2.79 (0.37) 116 | 2.90 (0.41) 119 | 2.17 (0.29) 123 | 1.86 (0.24) 127 | 1.92 (0.30) 130 | 1.48 (0.23) 134 | 1.36 (0.20) 139 | 0.75 (0.14)

Table 68. Deuteron production cross sections for 400 MeV/u neon on copper.

5	10	20	30	40	60	80
34 | 3.80 (0.66)	34 | 5.96 (0.84)	31 | 2.89 (0.63)	33 | 3.57 (0.61)	35 | 3.35 (0.44)	38 | 1.78 (0.34)	54 | 0.97 (0.24)
36 | 5.13 (0.76)	37 | 4.72 (0.68)	34 | 4.05 (0.57)	36 | 3.41 (0.46)	38 | 2.80 (0.34)	40 | 2.42 (0.34)	56 | 0.78 (0.20)
40 | 4.61 (0.62)	41 | 5.26 (0.65)	37 | 3.75 (0.48)	40 | 4.27 (0.50)	42 | 2.72 (0.35)	43 | 1.86 (0.30)	58 | 0.66 (0.23)
44 | 3.69 (0.50)	45 | 4.57 (0.62)	41 | 3.73 (0.43)	44 | 4.95 (0.55)	46 | 2.32 (0.29)	47 | 1.30 (0.29)	61 | 0.58 (0.15)
49 | 4.73 (0.60)	49 | 4.21 (0.54)	45 | 3.82 (0.45)	48 | 3.95 (0.43)	50 | 3.01 (0.37)	50 | 1.35 (0.21)	63 | 0.84 (0.25)
54 | 4.33 (0.51)	54 | 4.08 (0.49)	49 | 4.57 (0.48)	53 | 3.76 (0.42)	54 | 2.50 (0.30)	54 | 1.56 (0.22)	64 | 0.50 (0.17)
60 | 4.13 (0.46)	58 | 3.66 (0.51)	55 | 3.70 (0.38)	58 | 3.37 (0.41)	59 | 2.26 (0.27)	57 | 1.41 (0.27)	66 | 0.57 (0.20)
66 | 4.35 (0.52)	63 | 4.04 (0.50)	61 | 3.41 (0.39)	63 | 3.13 (0.36)	63 | 2.02 (0.33)	60 | 0.64 (0.16)	68 | 0.50 (0.16)
71 | 5.62 (0.57)	68 | 5.36 (0.57)	66 | 3.01 (0.33)	69 | 3.08 (0.33)	66 | 2.20 (0.33)		
78 | 4.04 (0.43)	75 | 3.90 (0.44)	73 | 4.35 (0.43)	74 | 3.57 (0.51)	69 | 2.30 (0.33)		
84 | 3.93 (0.55)	80 | 3.25 (0.41)	78 | 3.54 (0.47)	78 | 3.07 (0.41)	73 | 1.35 (0.22)		
88 | 3.83 (0.51)	84 | 3.65 (0.47)	83 | 3.36 (0.38)	82 | 2.55 (0.32)			
93 | 4.35 (0.53)	88 | 3.03 (0.45)	87 | 2.91 (0.35)	86 | 2.20 (0.30)			
98 | 5.14 (0.57)	93 | 4.81 (0.57)	92 | 3.26 (0.36)	91 | 2.29 (0.33)			
103 | 4.95 (0.53)	98 | 4.91 (0.55)	98 | 3.21 (0.38)	97 | 2.53 (0.38)			
109 | 3.31 (0.41)	103 | 3.12 (0.42)	104 | 2.60 (0.32)	103 | 1.33 (0.24)			

Table 69. Triton production cross sections for 400 MeV/u neon on copper.

5	10	20	30	40	60	80
24 | 1.80 (0.60)	25 | 3.00 (0.67)	23 | 1.56 (0.41)	25 | 2.11 (0.44)	25 | 1.04 (0.40)	27 | 0.53 (0.14)	36 | 0.20 (0.09)
26 | 1.81 (0.55)	27 | 1.40 (0.42)	25 | 1.75 (0.41)	27 | 1.67 (0.37)	27 | 1.16 (0.25)	29 | 0.66 (0.17)	37 | 0.22 (0.12)
28 | 1.66 (0.47)	29 | 2.60 (0.53)	28 | 1.22 (0.26)	30 | 1.41 (0.28)	30 | 1.16 (0.25)	31 | 0.72 (0.17)	39 | 0.23 (0.11)
31 | 2.23 (0.48)	32 | 3.25 (0.62)	30 | 2.09 (0.41)	33 | 1.97 (0.37)	33 | 1.18 (0.23)	34 | 0.56 (0.16)	40 | 0.42 (0.17)
33 | 1.79 (0.45)	34 | 1.33 (0.37)	33 | 2.06 (0.38)	36 | 1.33 (0.29)	35 | 1.03 (0.24)	36 | 0.50 (0.14)	42 | 0.17 (0.12)
36 | 1.97 (0.44)	38 | 2.69 (0.48)	36 | 2.14 (0.36)	39 | 1.28 (0.25)	38 | 1.00 (0.22)	38 | 0.24 (0.13)	43 | 0.10 (0.06)
40 | 1.87 (0.38)	40 | 1.84 (0.45)	40 | 1.55 (0.27)	43 | 0.72 (0.30)	41 | 0.69 (0.17)	40 | 0.82 (0.25)	44 | 0.09 (0.05)
44 | 1.35 (0.30)	43 | 1.63 (0.43)	43 | 1.52 (0.29)	46 | 1.24 (0.26)	43 | 0.94 (0.28)		
48 | 0.97 (0.31)	46 | 2.18 (0.44)	47 | 1.71 (0.32)	50 | 0.75 (0.18)	45 | 0.83 (0.23)		
51 | 2.21 (0.41)	50 | 1.88 (0.38)	51 | 1.01 (0.21)	53 | 1.00 (0.30)	47 | 0.88 (0.25)		
56 | 1.41 (0.31)	52 | 1.69 (0.48)	55 | 0.86 (0.19)	56 | 1.55 (0.38)	49 | 0.44 (0.16)		
60 | 1.61 (0.30)	55 | 0.85 (0.42)	59 | 1.21 (0.30)	58 | 1.12 (0.30)			
64 | 1.33 (0.36)	57 | 0.88 (0.32)	62 | 1.04 (0.26)	61 | 0.54 (0.20)			
67 | 2.48 (0.51)	59 | 0.77 (0.30)	65 | 0.74 (0.18)	64 | 0.69 (0.19)			
70 | 1.59 (0.37)	62 | 1.11 (0.34)	68 | 0.60 (0.16)	67 | 0.77 (0.20)			
74 | 2.28 (0.44)	64 | 1.61 (0.38)	72 | 1.46 (0.29)	70 | 0.57 (0.17)			
77 | 1.89 (0.37)	67 | 1.14 (0.33)	76 | 1.43 (0.25)	74 | 0.24 (0.11)			
81 | 2.40 (0.30)	70 | 1.86 (0.40)	80 | 1.79 (0.20)				
86 | 1.40 (0.20)	74 | 1.76 (0.37)	85 | 1.47 (0.22)				
91 | 2.07 (0.37)	78 | 1.93 (0.24)					
	81 | 1.91 (0.24)					
	86 | 1.95 (0.35)					

Table 70. ^{3}He production cross sections for 400 MeV/u neon on copper.

5	10	20	30	40	60	80
	98 | 0.95 (0.26)					
	101 | 0.87 (0.25)					
	105 | 1.38 (0.34)					
	108 | 0.73 (0.19)					
	114 | 1.25 (0.29)					
	119 | 0.88 (0.20)					
	124 | 1.35 (0.23)					
	130 | 1.27 (0.28)					
	135 | 1.06 (0.20)					
	145 | 0.82 (0.15)					

Table 71. Proton production cross sections for 400 MeV/u neon on lead.

5	10	20	30	40	60	80
47 | 37.30 (6.15)	49 | 33.81 (5.34)	46 | 24.18 (4.80)	50 | 41.42 (5.49)	49 | 32.25 (3.86)	53 | 28.48 (4.00)	73 | 18.55 (2.56)
51 | 37.87 (5.43)	54 | 41.11 (5.31)	50 | 39.91 (5.17)	55 | 40.61 (4.88)	55 | 30.51 (3.24)	58 | 26.96 (4.00)	77 | 16.60 (2.74)
57 | 38.14 (4.88)	61 | 45.62 (4.99)	56 | 34.43 (3.62)	62 | 45.89 (4.73)	62 | 37.65 (3.81)	65 | 29.15 (3.22)	81 | 17.18 (2.39)
64 | 28.54 (4.27)	68 | 38.09 (4.59)	63 | 38.33 (3.97)	69 | 31.43 (3.59)	70 | 33.15 (3.33)	72 | 22.60 (2.63)	86 | 14.46 (2.04)
71 | 32.36 (4.12)	76 | 47.93 (4.73)	71 | 34.11 (3.58)	78 | 38.75 (3.59)	81 | 26.72 (2.54)	79 | 20.08 (2.42)	91 | 12.90 (2.11)
79 | 41.24 (4.23)	85 | 30.79 (3.98)	82 | 36.36 (3.50)	88 | 35.05 (3.55)	92 | 27.21 (2.93)	86 | 25.09 (3.33)	95 | 10.35 (1.75)
89 | 39.83 (4.53)	93 | 30.92 (3.71)	92 | 32.99 (3.41)	98 | 30.20 (3.01)	105 | 20.76 (2.37)	91 | 15.58 (2.52)	99 | 8.81 (1.48)
98 | 37.12 (4.03)	103 | 38.53 (3.96)	103 | 33.90 (3.30)	110 | 31.80 (3.04)	120 | 17.32 (1.74)	97 | 16.76 (2.34)	105 | 7.96 (1.39)
109 | 35.53 (3.56)	112 | 38.89 (4.11)	117 | 35.21 (3.12)	121 | 31.15 (3.65)	135 | 15.89 (2.07)		
119 | 38.17 (3.95)	119 | 37.97 (4.30)	130 | 30.76 (3.88)	130 | 24.11 (3.34)	147 | 8.24 (1.38)		
126 | 37.65 (4.14)	126 | 34.55 (4.20)	139 | 36.49 (4.31)	140 | 31.91 (4.60)	161 | 18.38 (2.23)		
134 | 38.03 (4.31)	134 | 36.68 (4.36)	150 | 34.09 (5.03)	151 | 24.44 (3.03)	177 | 9.86 (1.48)		
144 | 44.23 (4.52)	144 | 61.86 (5.62)					
154 | 44.61 (4.48)	154 | 45.97 (4.46)					

Table 72. Deuteron production cross sections for 400 MeV/u neon on lead.

5	10	20	30	40	60	80
28 | 28.33 (6.83)	29 | 35.04 (6.86)	27 | 14.09 (3.37)	30 | 32.93 (5.18)	29 | 23.22 (4.47)	31 | 20.66 (3.50)	37 | 10.23 (2.26)
31 | 25.20 (5.41)	32 | 25.61 (5.29)	30 | 23.22 (5.14)	33 | 28.81 (4.31)	32 | 22.38 (3.34)	34 | 15.79 (3.09)	39 | 7.44 (2.91)
34 | 23.65 (5.09)	35 | 28.78 (5.15)	33 | 25.98 (3.98)	37 | 27.20 (4.36)	36 | 23.93 (3.62)	38 | 16.89 (2.49)	41 | 5.16 (2.42)
38 | 14.06 (3.75)	40 | 30.66 (4.78)	37 | 26.91 (3.81)	41 | 25.49 (3.73)	40 | 21.58 (3.13)	42 | 20.95 (3.24)	44 | 9.08 (1.95)
43 | 39.91 (6.19)	44 | 23.33 (4.37)	42 | 27.28 (3.85)	46 | 34.39 (4.09)	44 | 16.10 (2.86)	46 | 15.59 (2.49)	46 | 8.40 (2.53)
47 | 35.87 (5.45)	49 | 30.70 (4.70)	46 | 30.74 (3.81)	52 | 23.76 (3.02)	48 | 16.77 (2.75)	49 | 13.64 (2.81)	48 | 3.82 (2.70)
53 | 30.89 (4.46)	55 | 29.73 (4.18)	52 | 29.86 (3.52)	58 | 26.40 (3.53)	53 | 18.01 (2.64)	52 | 7.36 (1.81)	50 | 5.58 (1.83)
58 | 19.81 (3.89)	61 | 21.46 (4.02)	58 | 20.91 (2.95)	63 | 23.03 (3.13)	57 | 15.99 (4.75)	54 | 8.28 (2.13)	52 | 6.25 (1.71)
63 | 21.00 (3.77)	66 | 25.27 (4.03)	64 | 20.46 (2.85)	70 | 16.94 (2.74)	60 | 13.96 (2.93)		
69 | 26.48 (3.99)	72 | 25.86 (3.76)	70 | 22.21 (2.80)	75 | 24.79 (3.88)	63 | 16.33 (2.88)		
74 | 25.30 (5.05)	78 | 23.05 (3.92)	76 | 19.83 (3.18)	79 | 12.07 (2.37)	66 | 15.28 (2.79)		
78 | 25.15 (4.77)	82 | 21.25 (4.23)	80 | 16.95 (2.74)	84 | 12.81 (2.37)	70 | 11.31 (2.33)		
82 | 23.89 (4.17)	86 | 23.35 (4.30)	85 | 15.99 (2.60)	89 | 12.40 (2.81)			
86 | 16.40 (3.52)	91 | 26.00 (4.32)	90 | 16.66 (2.60)	95 | 21.76 (2.99)			
91 | 24.47 (4.21)	96 | 25.85 (4.31)	96 | 15.26 (2.84)	101 | 7.85 (1.60)			
96 | 17.47 (3.36)	101 | 13.58 (2.80)	102 | 15.19 (3.12)				
101 | 27.99 (4.30)						
108 | 18.40 (3.17)						

Table 73. Triton production cross sections for 400 MeV/u neon on lead.

5	10	20	30	40	60	80
21 | 11.81 (6.03)	22 | 32.15 (7.56)	22 | 17.26 (3.83)	22 | 21.01 (4.50)	22 | 11.56 (2.81)	23 | 8.17 (2.06)	26 | 3.29 (1.29)
23 | 23.05 (6.07)	24 | 20.20 (5.50)	24 | 18.92 (6.92)	25 | 19.85 (4.18)	25 | 12.68 (2.73)	25 | 6.59 (1.91)	28 | 5.69 (2.01)
25 | 21.36 (5.83)	27 | 19.37 (5.12)	27 | 18.35 (3.66)	28 | 20.03 (3.65)	28 | 18.07 (4.48)	28 | 8.67 (2.73)	29 | 5.74 (2.04)
28 | 19.30 (4.81)	29 | 27.43 (6.48)	29 | 10.36 (2.53)	31 | 17.29 (3.56)	31 | 10.57 (2.33)	31 | 10.21 (2.56)	31 | 3.41 (1.30)
31 | 16.62 (5.07)	32 | 20.89 (5.04)	32 | 14.94 (3.04)	34 | 15.82 (3.35)	33 | 10.73 (2.91)	33 | 4.27 (1.27)	33 | 3.89 (1.85)
34 | 10.71 (4.31)	35 | 14.15 (3.85)	36 | 13.44 (2.74)	38 | 11.34 (2.40)	36 | 12.42 (2.81)	35 | 5.48 (2.17)	34 | 1.45 (1.01)
37 | 7.61 (3.07)	38 | 19.64 (4.22)	40 | 11.67 (2.20)	41 | 13.68 (3.04)	39 | 8.14 (2.08)	37 | 4.92 (1.93)	35 | 1.45 (1.01)
41 | 10.90 (2.97)	42 | 12.64 (3.87)	44 | 8.86 (2.26)	45 | 9.94 (2.36)	42 | 6.75 (2.47)		36 | 2.46 (1.24)
45 | 16.94 (4.20)	45 | 4.00 (2.30)	47 | 9.75 (2.31)	49 | 4.49 (1.49)	44 | 8.44 (2.69)		
48 | 14.33 (3.92)	48 | 8.93 (2.86)	52 | 8.80 (2.03)	53 | 10.28 (2.23)	46 | 11.35 (3.25)		
52 | 11.70 (3.08)	52 | 9.12 (2.67)	57 | 7.25 (2.47)	57 | 3.58 (1.54)	48 | 6.41 (2.31)		
56 | 11.66 (4.47)	56 | 9.94 (3.80)	61 | 11.95 (3.11)	59 | 7.71 (2.47)			
58 | 10.37 (3.71)	58 | 18.81 (5.13)	64 | 6.31 (1.92)	62 | 4.23 (1.73)			
61 | 11.19 (3.78)	61 | 14.93 (4.38)	67 | 6.12 (1.82)	66 | 5.10 (1.81)			
63 | 9.10 (3.25)	63 | 6.72 (2.77)	71 | 7.38 (2.03)	69 | 4.14 (1.50)			
66 | 8.56 (3.06)	66 | 9.75 (3.29)	75 | 8.34 (2.04)	73 | 2.83 (1.19)			
69 | 8.83 (2.98)	69 | 8.94 (3.02)	79 | 5.37 (0.87)				
73 | 12.77 (3.48)	73 | 13.14 (3.58)	84 | 7.99 (1.76)				
77 | 17.86 (4.12)	77 | 10.02 (1.68)	89 | 5.46 (2.22)				
81 | 16.71 (2.82)	81 | 13.76 (2.65)					
85 | 18.11 (3.74)	85 | 11.52 (2.94)					
90 | 16.93 (3.43)						

Table 74. ^{3}He production cross sections for 400 MeV/u neon on lead.

5	10	20	30	40	60	80
	83 | 4.86 (2.19) 86 | 2.72 (1.58) 90 | 2.55 (1.48) 94 | 5.63 (2.15) 98 | 4.19 (1.73) 103 | 7.18 (2.20) 108 | 4.28 (1.64) 114 | 2.18 (1.10) 121 | 6.16 (1.74) 128 | 3.09 (1.18) 136 | 5.12 (1.45)					

Table 75. Proton production cross sections for 600 MeV/u neon on carbon.

5	10	20	30	40	60	80
59 | 3.33 (0.45)	60 | 3.41 (0.44)	57 | 2.83 (0.39)	62 | 3.53 (0.42)	64 | 3.48 (0.37)	74 | 2.18 (0.29)	117 | 1.40 (0.22)
63 | 4.23 (0.50)	64 | 4.48 (0.47)	61 | 3.83 (0.42)	67 | 3.57 (0.36)	69 | 3.62 (0.34)	78 | 2.47 (0.30)	119 | 1.78 (0.30)
68 | 3.82 (0.38)	70 | 4.11 (0.40)	65 | 3.80 (0.38)	72 | 3.74 (0.37)	75 | 2.59 (0.26)	84 | 2.47 (0.26)	122 | 1.23 (0.20)
74 | 4.79 (0.45)	76 | 3.69 (0.37)	70 | 4.14 (0.39)	78 | 3.67 (0.34)	82 | 2.61 (0.25)	90 | 1.86 (0.21)	126 | 1.45 (0.20)
80 | 4.05 (0.37)	83 | 3.96 (0.36)	76 | 4.16 (0.36)	85 | 3.79 (0.32)	92 | 2.54 (0.22)	96 | 1.92 (0.20)	129 | 1.16 (0.20)
88 | 4.22 (0.35)	92 | 3.55 (0.31)	84 | 3.90 (0.33)	94 | 3.41 (0.33)	103 | 2.55 (0.22)	102 | 1.78 (0.23)	132 | 1.04 (0.18)
97 | 4.29 (0.39)	101 | 4.21 (0.36)	92 | 3.50 (0.31)	102 | 3.62 (0.31)	114 | 2.09 (0.18)	107 | 2.08 (0.23)	135 | 0.76 (0.14)
106 | 3.82 (0.34)	111 | 3.65 (0.31)	101 | 3.88 (0.32)	112 | 3.48 (0.28)	129 | 1.75 (0.14)	112 | 1.36 (0.16)	139 | 0.72 (0.12)
116 | 3.93 (0.31)	122 | 3.96 (0.29)	111 | 3.85 (0.29)	122 | 3.11 (0.29)	144 | 1.30 (0.14)		
125 | 4.09 (0.37)	133 | 4.17 (0.37)	121 | 4.14 (0.37)	129 | 2.99 (0.28)	155 | 1.24 (0.13)		
133 | 4.00 (0.35)	141 | 3.78 (0.34)	128 | 3.96 (0.34)	138 | 3.06 (0.29)	168 | 2.09 (0.18)		
141 | 3.98 (0.34)	150 | 3.84 (0.34)	137 | 4.12 (0.35)	147 | 3.57 (0.32)	184 | 1.56 (0.14)		
150 | 4.68 (0.37)	160 | 4.41 (0.35)	146 | 5.04 (0.40)				
160 | 5.81 (0.41)	172 | 4.39 (0.35)	157 | 3.69 (0.32)				

Table 76. Deuteron production cross sections for 600 MeV/u neon on carbon.

5	10	20	30	40	60	80
33 | 2.09 (0.40)	35 | 1.53 (0.32)	32 | 0.88 (0.23)	33 | 1.51 (0.30)	35 | 0.75 (0.17)	38 | 0.67 (0.15)	57 | 0.45 (0.13)
36 | 1.53 (0.31)	38 | 1.51 (0.29)	34 | 1.72 (0.30)	36 | 1.51 (0.28)	38 | 0.97 (0.21)	41 | 0.86 (0.17)	58 | 0.55 (0.17)
39 | 1.62 (0.28)	41 | 1.87 (0.32)	37 | 1.57 (0.26)	39 | 1.44 (0.24)	41 | 0.95 (0.18)	44 | 0.58 (0.12)	60 | 0.34 (0.12)
43 | 1.66 (0.26)	45 | 1.05 (0.30)	40 | 2.02 (0.31)	43 | 0.97 (0.24)	45 | 1.09 (0.18)	47 | 0.72 (0.19)	63 | 0.25 (0.12)
48 | 1.45 (0.25)	49 | 1.49 (0.25)	44 | 1.52 (0.24)	47 | 0.92 (0.17)	50 | 1.15 (0.17)	51 | 0.62 (0.13)	65 | 0.27 (0.12)
52 | 1.71 (0.25)	54 | 1.57 (0.23)	48 | 1.71 (0.24)	52 | 1.35 (0.19)	55 | 1.00 (0.16)	53 | 0.72 (0.24)	66 | 0.08 (0.16)
58 | 1.23 (0.22)	59 | 1.23 (0.23)	52 | 0.96 (0.23)	57 | 1.59 (0.24)	59 | 0.97 (0.15)	56 | 0.13 (0.16)	68 | 0.23 (0.10)
63 | 1.08 (0.20)	63 | 1.77 (0.26)	56 | 1.36 (0.22)	62 | 1.13 (0.18)	63 | 0.67 (0.16)	58 | 0.25 (0.09)	70 | 0.07 (0.05)
69 | 1.88 (0.25)	69 | 1.58 (0.23)	61 | 1.48 (0.21)	67 | 1.23 (0.18)	67 | 0.61 (0.14)	60 | 0.07 (0.13)	
75 | 1.84 (0.25)	73 | 1.44 (0.28)	65 | 1.64 (0.29)	72 | 1.29 (0.23)	70 | 0.88 (0.17)		
80 | 1.54 (0.27)	77 | 2.12 (0.34)	68 | 1.37 (0.25)	75 | 1.02 (0.20)	74 | 0.45 (0.11)		
84 | 1.51 (0.26)	80 | 1.54 (0.27)	71 | 1.12 (0.21)	79 | 0.81 (0.17)			
88 | 1.60 (0.23)	84 | 1.24 (0.21)	75 | 1.31 (0.23)	83 | 1.04 (0.19)			
93 | 1.90 (0.27)	88 | 1.16 (0.21)	79 | 1.18 (0.19)	88 | 0.61 (0.13)			
98 | 1.41 (0.22)	93 | 1.53 (0.24)	83 | 1.18 (0.19)	93 | 0.77 (0.14)			
104 | 2.45 (0.29)	98 | 1.50 (0.23)	88 | 1.14 (0.18)	99 | 1.18 (0.17)			
110 | 1.99 (0.25)	104 | 1.65 (0.23)	93 | 1.27 (0.19)				
	110 | 1.43 (0.23)	98 | 1.18 (0.17)				

Table 77. Triton production cross sections for 600 MeV/u neon on carbon.

5	10	20	30	40	60	80
24 | 0.38 (0.19)	24 | 0.66 (0.25)	25 | 0.62 (0.20)	25 | 0.69 (0.21)	26 | 0.42 (0.14)	26 | 0.22 (0.10)	37 | -0.09 (0.16)
26 | 0.80 (0.35)	26 | 0.94 (0.29)	27 | 0.66 (0.27)	28 | 0.84 (0.22)	28 | 0.28 (0.10)	28 | 0.22 (0.10)	39 | 0.22 (0.09)
29 | 1.10 (0.27)	29 | 0.69 (0.21)	30 | 0.82 (0.20)	30 | 0.41 (0.13)	31 | 0.31 (0.11)	30 | 0.17 (0.08)	42 | 0.09 (0.05)
32 | 0.29 (0.27)	32 | 0.43 (0.16)	33 | 0.66 (0.18)	33 | 0.31 (0.12)	34 | 0.18 (0.07)	32 | 0.10 (0.07)	45 | 0.04 (0.04)
35 | 0.83 (0.23)	35 | 0.61 (0.20)	36 | 0.29 (0.10)	37 | 0.45 (0.14)	37 | 0.32 (0.11)	34 | 0.22 (0.09)	
38 | 0.41 (0.15)	38 | 0.34 (0.13)	40 | 0.42 (0.12)	40 | 0.03 (0.03)	40 | 0.26 (0.10)	36 | 0.14 (0.10)	
41 | 0.90 (0.20)	41 | 0.58 (0.16)	44 | 0.33 (0.12)	45 | 0.22 (0.08)	43 | 0.12 (0.06)	37 | 0.07 (0.07)	
46 | 0.40 (0.12)	46 | 0.31 (0.11)	47 | 0.28 (0.10)	49 | 0.36 (0.12)	46 | 0.12 (0.09)	39 | 0.07 (0.07)	
50 | 0.61 (0.17)	50 | 0.25 (0.11)	51 | 0.35 (0.11)	53 | 0.20 (0.08)	47 | 0.06 (0.06)	40 | 0.05 (0.05)	
54 | 1.07 (0.21)	54 | 0.37 (0.12)	54 | 0.17 (0.10)	58 | 0.13 (0.06)	50 | 0.09 (0.06)		
58 | 1.00 (0.20)	58 | 0.34 (0.12)	57 | 0.15 (0.09)	62 | 0.13 (0.08)	52 | 0.09 (0.06)		
63 | 0.47 (0.13)	63 | 0.20 (0.08)	62 | 0.18 (0.09)	66 | 0.08 (0.06)			
68 | 0.40 (0.15)	68 | 0.34 (0.14)	65 | 0.11 (0.07)	69 | 0.11 (0.06)			
71 | 0.27 (0.12)	71 | 0.11 (0.08)	69 | 0.19 (0.09)	72 | 0.11 (0.06)			
74 | 0.40 (0.14)	74 | 0.21 (0.11)	72 | 0.14 (0.07)				
78 | 0.24 (0.10)	78 | 0.31 (0.12)	76 | 0.29 (0.05)				
82 | 0.46 (0.08)	82 | 0.39 (0.07)	81 | 0.21 (0.04)				
86 | 0.55 (0.08)	86 | 0.55 (0.10)	85 | 0.24 (0.08)				
91 | 0.70 (0.16)	91 | 0.61 (0.15)	90 | 0.13 (0.05)				
96 | 0.62 (0.14)	96 | 0.41 (0.15)					
102 | 0.12 (0.06)	102 | 0.59 (0.13)					
108 | 0.12 (0.06)						

Table 78. ^{3}He production cross sections for 600 MeV/u neon on carbon.

5	10	20	30	40	60	80
	101 | 0.35 (0.13) 105 | 0.27 (0.11) 109 | 0.30 (0.11) 114 | 0.15 (0.08) 118 | 0.12 (0.06) 124 | 0.24 (0.08) 131 | 0.35 (0.09) 138 | 0.36 (0.10) 146 | 0.11 (0.05) 154 | 0.23 (0.06)					

Table 79. Proton production cross sections for 600 MeV/u neon on copper.

5	10	20	30	40	60	80
58 | 12.35 (1.73)	60 | 14.98 (1.90)	58 | 15.10 (1.72)	59 | 12.58 (1.58)	62 | 13.51 (1.60)	72 | 11.06 (1.23)	113 | 5.33 (0.83)
62 | 14.90 (1.83)	64 | 17.88 (1.94)	62 | 15.84 (1.64)	63 | 16.99 (1.78)	67 | 15.35 (1.44)	76 | 10.72 (1.34)	116 | 7.48 (0.98)
67 | 14.12 (1.56)	70 | 15.25 (1.53)	68 | 15.76 (1.48)	68 | 16.47 (1.61)	73 | 12.42 (1.22)	82 | 8.24 (0.99)	119 | 7.16 (0.93)
73 | 14.80 (1.54)	77 | 14.86 (1.47)	75 | 16.15 (1.45)	74 | 14.09 (1.43)	81 | 11.18 (1.04)	88 | 9.82 (1.06)	123 | 5.82 (0.73)
79 | 16.79 (1.54)	84 | 15.99 (1.42)	83 | 14.81 (1.25)	81 | 16.09 (1.43)	91 | 11.17 (0.97)	94 | 8.38 (0.89)	127 | 4.90 (0.76)
87 | 16.29 (1.38)	94 | 14.57 (1.25)	91 | 18.15 (1.52)	91 | 14.96 (1.23)	104 | 9.59 (0.79)	100 | 7.91 (1.00)	130 | 4.16 (0.65)
96 | 14.76 (1.44)	105 | 13.96 (1.23)	100 | 12.73 (1.12)	101 | 14.52 (1.25)	120 | 7.40 (0.64)	105 | 6.13 (0.78)	134 | 4.24 (0.62)
105 | 14.54 (1.28)	115 | 13.26 (1.13)	110 | 15.78 (1.20)	111 | 12.48 (1.01)	137 | 5.72 (0.50)	110 | 6.55 (0.80)	
115 | 14.55 (1.19)	128 | 14.34 (1.10)	120 | 16.47 (1.49)	121 | 11.55 (1.03)	154 | 4.60 (0.52)		
125 | 13.56 (1.28)	140 | 12.99 (1.24)	127 | 13.89 (1.27)	128 | 11.58 (1.11)	167 | 8.21 (0.76)		
132 | 13.70 (1.30)	149 | 13.95 (1.24)	136 | 14.76 (1.30)	136 | 13.24 (1.19)	183 | 5.70 (0.57)		
140 | 12.49 (1.20)	159 | 18.00 (1.45)	145 | 21.19 (1.61)	146 | 13.85 (1.22)			
149 | 15.58 (1.35)	171 | 14.88 (1.27)	156 | 11.82 (1.06)				
159 | 18.43 (1.48)						

Table 80. Deuteron production cross sections for 600 MeV/u neon on copper.

5	10	20	30	40	60	80
32 | 8.90 (1.78)	33 | 7.82 (1.56)	31 | 9.08 (1.62)	33 | 6.38 (1.25)	35 | 6.14 (1.07)	38 | 3.95 (0.76)	54 | 2.53 (0.65)
35 | 8.06 (1.83)	36 | 10.71 (1.71)	34 | 8.00 (1.54)	36 | 7.96 (1.41)	38 | 4.27 (0.85)	40 | 4.41 (0.82)	56 | 1.49 (0.43)
38 | 7.31 (1.64)	39 | 8.01 (1.32)	37 | 9.34 (1.34)	39 | 8.09 (1.28)	42 | 4.98 (0.84)	43 | 3.63 (0.66)	58 | 1.80 (0.49)
42 | 10.39 (1.49)	43 | 9.46 (1.32)	40 | 7.68 (1.26)	43 | 6.33 (1.03)	46 | 7.03 (0.93)	47 | 3.35 (0.68)	61 | 2.37 (0.53)
46 | 9.07 (1.34)	47 | 9.37 (1.43)	43 | 8.23 (1.36)	47 | 8.98 (1.18)	50 | 6.70 (1.00)	50 | 3.60 (0.65)	63 | 1.59 (0.55)
50 | 10.99 (1.40)	52 | 7.84 (1.18)	48 | 7.53 (1.01)	52 | 7.00 (0.92)	54 | 4.91 (0.78)	53 | 4.37 (0.94)	64 | 1.04 (0.40)
55 | 7.03 (1.07)	58 | 7.36 (1.05)	52 | 7.05 (1.07)	56 | 5.96 (0.91)	59 | 3.82 (0.62)	55 | 3.43 (0.94)	66 | 0.83 (0.35)
62 | 7.27 (0.93)	63 | 4.78 (0.87)	56 | 7.98 (1.10)	61 | 7.24 (0.97)	64 | 5.12 (0.69)	57 | 2.65 (0.66)	
68 | 7.19 (1.06)	68 | 6.60 (0.97)	61 | 5.82 (0.86)	67 | 6.38 (0.85)	69 | 4.68 (0.83)		
74 | 8.42 (1.04)	75 | 7.38 (0.97)	66 | 6.83 (0.87)	71 | 6.05 (1.03)	73 | 2.91 (0.62)		
82 | 7.29 (0.89)	80 | 7.36 (1.24)	71 | 8.08 (1.24)	75 | 5.98 (0.99)			
88 | 6.95 (1.02)	84 | 6.48 (1.06)	74 | 7.42 (1.14)	79 | 5.76 (0.84)			
93 | 4.85 (0.88)	88 | 6.30 (1.05)	78 | 7.48 (1.00)	83 | 4.86 (0.73)			
98 | 7.35 (1.06)	93 | 5.59 (0.96)	83 | 6.48 (0.89)	87 | 4.50 (0.76)			
103 | 9.10 (1.14)	98 | 7.19 (1.03)	87 | 5.54 (0.85)	93 | 6.40 (0.88)			
109 | 7.00 (0.95)	103 | 8.39 (1.14)	92 | 7.28 (0.95)	98 | 5.74 (0.86)			
		98 | 6.60 (0.87)				

Table 81. Triton production cross sections for 600 MeV/u neon on copper.

5	10	20	30	40	60	80
24 | 3.38 (1.22)	25 | 2.53 (1.45)	23 | 2.11 (0.81)	24 | 5.78 (1.29)	25 | 3.38 (0.88)	26 | 2.30 (0.62)	34 | 0.00 (0.00)
26 | 2.82 (1.36)	27 | 4.25 (1.16)	25 | 3.10 (0.85)	27 | 2.16 (0.70)	27 | 2.97 (0.73)	28 | 0.98 (0.45)	35 | 0.00 (0.00)
28 | 3.77 (1.03)	29 | 4.17 (1.07)	28 | 3.83 (0.94)	29 | 3.50 (0.82)	30 | 3.65 (0.86)	31 | 0.75 (0.31)	35 | 0.49 (0.49)
31 | 5.55 (1.35)	32 | 3.44 (0.88)	30 | 1.48 (0.57)	32 | 4.09 (0.93)	33 | 1.68 (0.50)	33 | 1.21 (0.47)	36 | 1.79 (0.91)
33 | 5.53 (1.27)	35 | 3.89 (1.00)	33 | 3.26 (0.80)	35 | 3.32 (0.78)	36 | 1.69 (0.47)	35 | 0.61 (0.28)	36 | 1.09 (0.78)
36 | 2.91 (1.05)	39 | 3.88 (0.94)	36 | 2.07 (0.57)	39 | 2.19 (0.77)	39 | 1.66 (0.52)	38 | 0.87 (0.34)	37 | 0.82 (0.59)
40 | 3.12 (0.78)	43 | 2.37 (0.65)	40 | 2.15 (0.56)	42 | 2.36 (0.68)	43 | 2.39 (0.62)	40 | 1.12 (0.52)	38 | 0.00 (0.00)
44 | 4.27 (0.85)	47 | 2.51 (0.62)	43 | 2.49 (0.67)	45 | 2.97 (0.73)	45 | 1.34 (0.56)	41 | 0.49 (0.35)	38 | 0.00 (0.00)
48 | 2.96 (0.81)	52 | 2.44 (0.66)	47 | 1.45 (0.47)	49 | 2.76 (0.66)	47 | 1.76 (0.68)		39 | 0.65 (0.47)
51 | 2.31 (0.65)	56 | 2.47 (0.65)	51 | 3.09 (0.65)	52 | 2.46 (0.80)	49 | 1.90 (0.65)		40 | 1.62 (0.68)
56 | 2.87 (0.84)	60 | 1.92 (0.52)	55 | 1.95 (0.49)	54 | 2.21 (0.72)			41 | 0.00 (0.00)
60 | 3.38 (0.71)	66 | 1.96 (0.50)	59 | 1.65 (0.57)	57 | 2.03 (0.69)			42 | -0.97 (0.97)
64 | 1.67 (0.64)	70 | 2.70 (0.76)	62 | 2.10 (0.63)	59 | 1.80 (0.58)			43 | 0.45 (0.32)
67 | 2.76 (1.06)	74 | 1.38 (0.57)	65 | 2.16 (0.62)	62 | 1.80 (0.58)			44 | 0.00 (0.00)
70 | 3.61 (0.90)	78 | 3.82 (0.88)	68 | 1.86 (0.55)	65 | 1.61 (0.52)			46 | 0.00 (0.00)
74 | 3.14 (0.83)	81 | 1.86 (0.33)	72 | 2.84 (0.64)	68 | 0.77 (0.35)			
77 | 2.68 (0.71)	86 | 2.30 (0.35)	76 | 1.73 (0.24)	72 | 1.84 (0.53)			
81 | 1.78 (0.31)	91 | 2.74 (0.65)	80 | 1.51 (0.21)				
86 | 1.89 (0.26)	96 | 2.01 (0.53)	85 | 1.92 (0.47)				
91 | 1.93 (0.53)	101 | 2.04 (0.51)	90 | 1.38 (0.38)				
96 | 1.90 (0.52)						
101 | 2.08 (0.50)						

Table 82. ^{3}He production cross sections for 600 MeV/u neon on copper.

5	10	20	30	40	60	80
	101 | 1.24 (0.48) 105 | 1.03 (0.47) 108 | 1.44 (0.46) 114 | 1.46 (0.49) 119 | 1.58 (0.45) 124 | 0.88 (0.30) 130 | 1.90 (0.58) 135 | 1.28 (0.34) 145 | 0.82 (0.24) 156 | 0.53 (0.19)					

Table 83. Proton production cross sections for 600 MeV/u neon on lead.

5	10	20	30	40	60	80
53 | 34.71 (4.92)	54 | 27.96 (4.20)	52 | 32.94 (4.82)	56 | 36.60 (4.36)	57 | 25.77 (3.51)	64 | 28.05 (3.25)	97 | 19.55 (2.75)
57 | 38.90 (4.65)	59 | 37.65 (4.75)	56 | 44.01 (4.75)	60 | 37.92 (4.10)	62 | 31.45 (3.21)	69 | 24.18 (2.97)	100 | 21.81 (3.08)
63 | 33.66 (3.96)	64 | 26.88 (3.62)	61 | 37.31 (3.80)	66 | 37.45 (4.23)	69 | 33.10 (3.28)	74 | 24.84 (3.11)	103 | 18.53 (2.69)
69 | 36.63 (4.05)	71 | 35.44 (3.86)	67 | 35.35 (3.72)	72 | 34.32 (3.43)	76 | 26.17 (2.61)	78 | 24.87 (2.90)	107 | 13.89 (1.92)
76 | 33.61 (3.61)	78 | 33.29 (3.46)	74 | 37.27 (3.64)	80 | 30.15 (2.94)	87 | 25.28 (2.35)	85 | 20.33 (2.39)	110 | 20.17 (2.90)
84 | 35.72 (3.32)	88 | 25.34 (2.59)	83 | 26.51 (2.61)	89 | 32.94 (3.22)	98 | 21.44 (2.19)	90 | 18.05 (2.62)	113 | 14.22 (2.16)
93 | 32.53 (3.36)	97 | 26.76 (2.97)	92 | 32.88 (3.10)	98 | 30.56 (2.99)	110 | 21.55 (2.06)	94 | 18.52 (2.53)	117 | 14.84 (2.13)
102 | 29.40 (2.94)	107 | 30.78 (3.08)	102 | 32.82 (2.92)	108 | 29.18 (2.55)	125 | 17.35 (1.48)	99 | 15.99 (2.30)	121 | 8.56 (1.57)
113 | 26.80 (2.68)	119 | 30.07 (2.53)	114 | 29.59 (2.55)	118 | 23.40 (2.44)	139 | 11.83 (1.47)	105 | 16.44 (2.02)	
122 | 28.87 (2.89)	130 | 29.14 (3.00)	125 | 29.36 (3.06)	125 | 21.36 (2.43)	151 | 10.54 (1.28)		
129 | 27.82 (3.04)	138 | 23.01 (2.65)	133 | 32.35 (3.23)	134 | 20.71 (2.44)	164 | 16.61 (1.75)		
138 | 25.13 (2.79)	147 | 30.88 (3.15)	143 | 37.45 (3.29)	143 | 27.63 (2.80)	180 | 11.95 (1.23)		
147 | 28.70 (3.02)	157 | 36.06 (3.34)	154 | 24.31 (2.60)				
157 | 33.27 (3.09)	169 | 25.89 (2.78)					
	182 | 11.08 (1.51)					

Table 84. Deuteron production cross sections for 600 MeV/u neon on lead.

5	10	20	30	40	60	80
31 | 26.75 (4.99)	33 | 33.14 (5.27)	29 | 28.95 (5.00)	32 | 21.08 (3.83)	31 | 20.85 (3.39)	35 | 13.80 (2.67)	48 | 8.04 (1.92)
34 | 25.74 (4.49)	37 | 29.94 (4.58)	32 | 29.64 (4.51)	35 | 23.92 (4.14)	34 | 20.78 (3.06)	38 | 18.28 (2.87)	50 | 8.35 (2.79)
37 | 22.67 (3.81)	40 | 21.74 (3.70)	35 | 26.15 (3.79)	38 | 24.61 (3.46)	38 | 21.00 (3.14)	41 | 15.05 (2.48)	51 | 8.30 (1.94)
42 | 24.62 (3.60)	45 | 29.72 (4.25)	39 | 22.41 (3.59)	42 | 26.66 (3.68)	41 | 16.72 (2.56)	44 | 13.93 (2.38)	54 | 4.13 (1.20)
46 | 23.47 (3.62)	49 | 30.96 (4.04)	42 | 24.61 (3.51)	47 | 24.30 (3.23)	46 | 23.43 (2.85)	48 | 13.58 (2.20)	56 | 6.03 (1.81)
51 | 26.31 (3.57)	54 | 21.98 (3.05)	47 | 28.55 (3.55)	52 | 22.79 (2.84)	51 | 20.55 (3.09)	50 | 17.80 (3.28)	57 | 7.58 (2.06)
56 | 24.49 (3.29)	61 | 19.51 (2.74)	52 | 23.50 (2.87)	57 | 19.61 (2.82)	55 | 13.59 (2.32)	53 | 12.48 (2.54)	59 | 4.79 (1.50)
62 | 25.81 (3.58)	67 | 20.26 (2.94)	57 | 21.78 (3.02)	63 | 19.58 (2.68)	59 | 15.62 (2.91)	55 | 8.55 (1.98)	61 | 7.25 (1.82)
67 | 24.89 (3.27)	74 | 20.15 (2.72)	62 | 19.65 (2.67)	69 | 17.73 (2.37)	62 | 12.29 (2.46)	58 | 5.23 (1.46)	
74 | 25.79 (3.16)	81 | 17.22 (2.29)	68 | 20.89 (2.63)	74 | 14.95 (2.42)	65 | 16.86 (2.79)		
79 | 20.58 (3.59)	87 | 16.07 (2.77)	75 | 19.28 (2.23)	78 | 14.48 (2.22)	68 | 14.12 (2.42)		
83 | 17.78 (2.86)	92 | 11.43 (2.32)	82 | 13.92 (2.46)	82 | 12.74 (1.97)			
87 | 12.83 (2.55)	97 | 13.16 (2.39)	86 | 19.74 (2.84)	87 | 10.61 (2.01)			
92 | 13.95 (2.57)	103 | 16.27 (2.59)	91 | 24.62 (3.11)	92 | 15.45 (2.39)			
97 | 14.85 (2.56)	109 | 12.00 (2.06)	97 | 17.74 (2.63)	97 | 12.07 (1.97)			
103 | 24.16 (3.21)						
109 | 18.47 (2.64)						

Table 85. Triton production cross sections for 600 MeV/u neon on lead.

5	10	20	30	40	60	80
23 | 12.29 (5.05)	23 | 28.03 (5.90)	24 | 17.56 (3.68)	24 | 19.57 (3.96)	24 | 19.92 (3.60)	25 | 8.42 (3.09)	32 | 6.68 (1.88)
25 | 27.91 (5.37)	25 | 14.91 (3.93)	27 | 22.74 (3.93)	26 | 19.82 (3.81)	26 | 11.83 (2.49)	27 | 10.85 (2.95)	34 | 3.73 (1.23)
28 | 24.00 (5.12)	28 | 15.69 (4.30)	30 | 7.94 (2.04)	29 | 14.65 (2.91)	29 | 12.31 (2.64)	29 | 10.39 (2.71)	35 | 6.52 (1.78)
31 | 15.86 (3.34)	31 | 14.64 (3.28)	33 | 14.42 (2.91)	32 | 12.73 (2.72)	32 | 10.71 (2.22)	31 | 5.51 (1.72)	37 | 3.93 (1.29)
34 | 16.43 (4.22)	34 | 10.86 (3.59)	37 | 15.69 (2.85)	36 | 11.20 (2.43)	35 | 10.73 (2.51)	33 | 8.36 (2.02)	39 | 1.16 (0.83)
37 | 20.07 (3.75)	37 | 17.37 (3.46)	41 | 9.80 (2.01)	39 | 9.08 (2.02)	37 | 9.76 (2.23)	34 | 5.03 (2.09)	40 | 4.23 (1.64)
41 | 15.36 (3.01)	41 | 10.88 (2.50)	46 | 13.99 (2.24)	43 | 9.21 (2.25)	40 | 8.87 (1.99)	36 | 3.45 (3.11)	
45 | 12.41 (2.77)	45 | 11.40 (2.35)	50 | 9.70 (2.10)	47 | 11.38 (2.38)	43 | 12.54 (3.16)	37 | 5.73 (2.08)	
49 | 8.74 (2.30)	49 | 10.56 (2.55)	55 | 7.83 (1.74)	50 | 6.21 (1.65)	45 | 7.38 (2.29)	39 | 3.19 (1.45)	
53 | 10.40 (2.39)	53 | 6.71 (1.89)	60 | 8.87 (1.68)	54 | 6.02 (2.16)	47 | 8.44 (2.34)		
57 | 10.09 (2.21)	57 | 7.34 (1.88)	65 | 6.62 (1.89)	56 | 3.95 (1.64)			
63 | 11.50 (2.22)	63 | 10.63 (2.12)	68 | 6.76 (1.86)	59 | 11.19 (2.72)			
67 | 15.18 (3.40)	67 | 7.38 (2.37)	72 | 7.15 (1.84)	62 | 6.01 (1.86)			
70 | 11.00 (2.73)	70 | 2.57 (1.29)	76 | 8.05 (1.23)	65 | 5.37 (1.73)			
73 | 11.32 (2.73)	73 | 9.95 (2.54)	80 | 6.18 (1.14)	68 | 4.02 (1.37)			
77 | 10.23 (2.47)	77 | 9.65 (2.39)	85 | 6.11 (1.33)	72 | 3.81 (2.01)			
81 | 6.05 (1.02)	81 | 2.38 (0.51)	90 | 5.36 (1.34)				
85 | 6.22 (1.13)	85 | 4.64 (0.71)					
90 | 5.22 (1.53)	90 | 6.27 (1.71)					
95 | 4.50 (1.38)	95 | 7.59 (1.79)					
101 | 7.45 (1.67)	101 | 8.02 (1.76)					
107 | 0.33 (0.33)						

Table 86. ^{3}He production cross sections for 600 MeV/u neon on lead.

5	10	20	30	40	60	80
	100 | 5.26 (1.78) 105 | 4.01 (1.35) 110 | 3.84 (1.23) 115 | 3.43 (1.23) 121 | 0.65 (0.46) 128 | 4.38 (1.12) 135 | 2.46 (0.83) 142 | 4.45 (1.26) 150 | 2.92 (0.79)					

Table 87. Proton production cross sections for 290 MeV/u carbon on carbon.

5	10	20	30	40	60	80
53 | 2.43 (0.40)	55 | 1.10 (0.28)	51 | 0.80 (0.26)	55 | 1.44 (0.27)	53 | 1.04 (0.20)	60 | 0.73 (0.16)	
59 | 0.95 (0.25)	60 | 1.77 (0.31)	56 | 1.53 (0.26)	60 | 0.76 (0.19)	59 | 0.93 (0.17)	67 | 0.50 (0.12)	
65 | 1.11 (0.25)	66 | 2.12 (0.32)	62 | 1.37 (0.24)	67 | 1.11 (0.20)	65 | 0.91 (0.18)	75 | 0.50 (0.09)	
73 | 1.98 (0.30)	73 | 2.38 (0.30)	69 | 1.45 (0.24)	75 | 1.31 (0.20)	73 | 1.01 (0.16)	86 | 0.47 (0.08)	
82 | 1.47 (0.25)	82 | 1.72 (0.25)	77 | 1.52 (0.21)	83 | 1.36 (0.24)	81 | 1.16 (0.18)	98 | 0.52 (0.08)	
93 | 1.67 (0.23)	91 | 1.73 (0.26)	86 | 1.79 (0.24)	91 | 1.18 (0.19)	90 | 1.22 (0.16)	112 | 0.37 (0.06)	
105 | 1.84 (0.24)	100 | 1.95 (0.26)	95 | 1.50 (0.22)	100 | 1.20 (0.16)	101 | 0.93 (0.13)	130 | 0.27 (0.04)	
117 | 1.68 (0.19)	111 | 1.81 (0.23)	105 | 1.45 (0.19)	109 | 1.33 (0.21)	111 | 0.95 (0.16)	154 | 0.18 (0.03)	
132 | 1.83 (0.19)	120 | 2.13 (0.29)	115 | 1.42 (0.23)	116 | 1.05 (0.20)	118 | 1.00 (0.13)	179 | 0.14 (0.03)	
145 | 2.26 (0.33)	128 | 2.14 (0.29)	123 | 1.52 (0.21)	123 | 1.08 (0.19)	127 | 0.77 (0.12)	201 | 0.11 (0.02)	
156 | 3.17 (0.37)	136 | 2.00 (0.29)	131 | 1.29 (0.20)	132 | 1.06 (0.17)	137 | 0.64 (0.11)	227 | 0.05 (0.02)	
167 | 2.25 (0.30)	145 | 2.18 (0.33)		142 | 1.44 (0.20)	149 | 0.97 (0.12)	261 | 0.02 (0.01)	
181 | 3.28 (0.34)	156 | 2.57 (0.32)		153 | 1.19 (0.17)			

Table 88. Deuteron production cross sections for 290 MeV/u carbon on carbon.

5	10	20	30	40	60	80
30 | 1.00 (0.45)	34 | 0.91 (0.34)	30 | 0.25 (0.18)	32 | 0.60 (0.24)	30 | 0.75 (0.19)	32 | 0.16 (0.12)	
33 | 1.52 (0.40)	37 | 1.14 (0.33)	34 | 0.53 (0.24)	35 | 0.53 (0.22)	33 | 0.44 (0.15)	36 | 0.04 (0.11)	
36 | 1.66 (0.45)	41 | 1.44 (0.35)	38 | 0.68 (0.22)	39 | 0.60 (0.18)	37 | 0.71 (0.16)	40 | 0.24 (0.10)	
40 | 0.67 (0.41)	45 | 1.55 (0.32)	42 | 1.48 (0.29)	44 | 1.19 (0.22)	42 | 0.59 (0.15)	45 | 0.29 (0.09)	
44 | 1.58 (0.47)	50 | 0.96 (0.26)	47 | 0.87 (0.21)	49 | 0.44 (0.13)	47 | 0.43 (0.11)	50 | 0.17 (0.06)	
48 | 1.36 (0.37)	55 | 0.71 (0.26)	53 | 0.73 (0.16)	55 | 0.59 (0.13)	53 | 0.33 (0.09)	55 | 0.22 (0.07)	
54 | 1.19 (0.29)	59 | 1.09 (0.26)	59 | 0.80 (0.20)	62 | 0.53 (0.13)	59 | 0.29 (0.10)	61 | 0.11 (0.05)	
59 | 1.35 (0.32)	64 | 0.61 (0.22)	64 | 0.58 (0.16)	68 | 0.48 (0.13)	66 | 0.41 (0.09)	68 | 0.11 (0.04)	
64 | 1.49 (0.27)	68 | 0.45 (0.26)	71 | 0.70 (0.16)	75 | 0.47 (0.12)	73 | 0.35 (0.08)	74 | -0.02 (0.05)	
70 | 1.23 (0.23)	71 | 0.35 (0.19)	77 | 0.58 (0.18)	81 | 0.39 (0.15)	80 | 0.43 (0.11)	79 | 0.08 (0.04)	
76 | 1.52 (0.25)	75 | 0.56 (0.20)	81 | 0.48 (0.17)	86 | 0.40 (0.15)	85 | 0.23 (0.09)	85 | 0.05 (0.03)	
82 | 1.25 (0.28)	78 | 0.48 (0.16)	86 | 0.75 (0.19)	91 | 0.72 (0.18)	91 | 0.16 (0.07)	91 | 0.08 (0.04)	
87 | 1.05 (0.27)	82 | 0.65 (0.13)	91 | 0.88 (0.19)	97 | 0.32 (0.19)	97 | 0.23 (0.07)		
91 | 0.79 (0.23)	87 | 0.49 (0.16)	97 | 1.31 (0.21)	103 | 0.35 (0.13)			
96 | 0.96 (0.22)	91 | 0.60 (0.20)	103 | 0.87 (0.18)				
102 | 1.39 (0.26)						
108 | 1.60 (0.27)						
115 | 1.46 (0.24)						
123 | 1.39 (0.19)						
131 | 1.19 (0.23)						
141 | 1.59 (0.23)						

Table 89. Triton production cross sections for 290 MeV/u carbon on carbon.

5	10	20	30	40	60	80
29 | 1.74 (0.49)	29 | 1.44 (0.40)	27 | 0.77 (0.21)	26 | 0.44 (0.16)	24 | 0.18 (0.12)	25 | 0.07 (0.07)	
32 | 1.32 (0.51)	32 | 1.16 (0.40)	30 | 1.10 (0.23)	29 | 0.48 (0.17)	27 | 0.26 (0.09)	29 | 0.02 (0.05)	
35 | 1.70 (0.58)	35 | 0.58 (0.34)	34 | 0.65 (0.20)	32 | 0.37 (0.15)	31 | 0.16 (0.10)	32 | 0.15 (0.06)	
39 | 0.97 (0.49)	39 | 0.57 (0.26)	39 | 0.56 (0.16)	35 | 0.32 (0.13)	35 | 0.27 (0.10)	36 | 0.08 (0.05)	
43 | 0.70 (0.33)	43 | 0.30 (0.16)	43 | 0.31 (0.11)	39 | 0.30 (0.13)	39 | 0.29 (0.08)	41 | 0.00 (0.03)	
48 | 0.50 (0.27)	47 | 0.30 (0.21)	49 | 0.20 (0.12)	43 | 0.01 (0.07)	44 | 0.06 (0.03)	52 | 0.03 (0.03)	
53 | 0.74 (0.27)	51 | 0.14 (0.14)	54 | 0.24 (0.10)	46 | 0.19 (0.11)	51 | 0.08 (0.04)		
57 | 0.49 (0.21)	55 | 0.43 (0.15)	60 | 0.42 (0.12)	50 | 0.15 (0.12)	65 | 0.06 (0.08)		
61 | 1.02 (0.36)	58 | 0.43 (0.19)	64 | 0.25 (0.11)	53 | 0.12 (0.13)	69 | 0.12 (0.06)		
64 | 0.56 (0.26)	61 | 0.17 (0.20)	68 | 0.41 (0.15)	56 | 0.15 (0.08)			
67 | 0.29 (0.17)	64 | 0.30 (0.15)	71 | 0.16 (0.08)	58 | 0.04 (0.04)			
70 | 0.31 (0.14)	67 | 0.46 (0.18)	75 | 0.05 (0.05)	61 | 0.20 (0.09)			
	70 | 0.01 (0.11)	80 | 0.00 (0.00)	64 | 0.15 (0.09)			

Table 90. Proton production cross sections for 290 MeV/u carbon on lead.

5	10	20	30	40	60	80
49 | 18.69 (3.94)	50 | 6.06 (2.72)	48 | 13.45 (3.20)	51 | 8.66 (2.53)	49 | 10.67 (2.24)	54 | 2.39 (1.47)	
54 | 5.56 (2.96)	56 | 8.17 (2.74)	55 | 13.26 (2.44)	57 | 9.46 (2.37)	55 | 7.62 (1.82)	61 | 4.36 (1.24)	
61 | 8.30 (2.67)	63 | 6.69 (2.28)	61 | 8.50 (2.60)	64 | 8.38 (2.15)	62 | 6.83 (1.80)	70 | 6.44 (1.18)	
68 | 10.67 (2.69)	71 | 11.98 (2.47)	68 | 10.25 (2.29)	72 | 9.51 (2.05)	70 | 9.23 (1.82)	81 | 5.25 (0.95)	
76 | 13.18 (2.90)	80 | 11.03 (2.47)	76 | 6.74 (2.10)	80 | 7.23 (2.16)	78 | 8.99 (1.91)	94 | 2.67 (0.71)	
87 | 7.60 (2.16)	89 | 15.53 (2.68)	83 | 11.60 (2.20)	88 | 5.64 (1.79)	87 | 7.50 (1.63)	108 | 2.64 (0.64)	
98 | 8.44 (2.11)	98 | 8.58 (2.07)	90 | 9.88 (2.78)	98 | 7.22 (1.59)	98 | 5.16 (1.40)	126 | 1.99 (0.42)	
109 | 12.25 (2.02)	109 | 9.08 (2.23)	95 | 7.05 (2.86)	107 | 8.13 (1.66)	108 | 7.50 (1.57)	144 | 2.60 (0.55)	
122 | 11.87 (2.21)	122 | 11.32 (2.00)	100 | 5.75 (2.71)	114 | 6.04 (1.76)	116 | 5.57 (1.25)	158 | 0.95 (0.51)	
134 | 11.28 (2.50)	134 | 8.54 (2.61)	107 | 7.44 (1.83)	121 | 5.17 (2.23)	125 | 3.76 (1.14)	176 | 1.29 (0.32)	
144 | 15.52 (3.46)	144 | 8.09 (3.26)	113 | 5.76 (1.57)	130 | 10.18 (1.98)	135 | 5.90 (1.15)	198 | 1.05 (0.28)	
154 | 13.11 (3.50)	154 | 7.90 (2.94)	121 | 6.56 (1.90)	140 | 6.33 (1.94)	147 | 6.47 (1.22)	224 | 0.45 (0.20)	
166 | 8.41 (2.84)	166 | 8.42 (2.57)	130 | 6.88 (1.89)	151 | 6.72 (1.73)		258 | 0.33 (0.10)	
179 | 13.28 (3.11)		139 | 5.18 (2.71)				
		150 | 2.71 (2.17)				
		163 | 3.64 (1.23)				

Table 91. Deuteron production cross sections for 290 MeV/u carbon on lead.

5	10	20	30	40	60	80
30 | 7.19 (5.01)	33 | 8.40 (4.31)	32 | 7.06 (2.93)	31 | 7.56 (3.01)	28 | 9.26 (2.41)	31 | 3.77 (1.79)	
34 | 3.33 (5.06)	37 | 6.30 (3.37)	36 | 9.18 (3.19)	35 | 3.14 (2.15)	31 | 7.25 (2.02)	35 | 2.94 (1.26)	
37 | 4.45 (4.28)	42 | 15.42 (3.52)	41 | 5.66 (1.99)	40 | 5.52 (1.97)	36 | 6.14 (1.89)	40 | 2.52 (1.09)	
42 | 7.39 (4.42)	46 | 7.77 (2.70)	46 | 6.70 (2.26)	45 | 5.16 (1.86)	40 | 2.63 (1.41)	45 | 2.46 (1.01)	
47 | 10.74 (3.93)	51 | 10.79 (2.99)	52 | 8.24 (2.01)	50 | 5.58 (1.68)	45 | 6.19 (1.43)	51 | 3.39 (1.01)	
53 | 10.86 (3.25)	56 | 6.17 (2.39)	58 | 6.08 (2.10)	56 | 4.30 (1.83)	51 | 4.18 (1.42)	56 | 1.68 (0.76)	
59 | 13.21 (2.57)	61 | 5.92 (2.30)	64 | 4.84 (1.91)	61 | 7.58 (1.80)	55 | 5.82 (1.49)	63 | 0.74 (0.73)	
66 | 6.35 (2.48)	66 | 1.04 (2.20)	70 | 5.05 (1.49)	67 | 5.14 (1.61)	61 | 6.43 (1.34)	68 | 1.25 (0.56)	
72 | 9.12 (2.20)	71 | 5.78 (2.50)	78 | 3.95 (1.07)	74 | 3.41 (1.34)	68 | 3.85 (1.10)	73 | 2.08 (0.94)	
80 | 6.55 (1.96)	74 | 4.12 (2.12)	85 | 2.34 (1.72)	80 | 5.63 (1.93)	74 | 3.30 (1.17)	78 | 0.60 (0.35)	
88 | 2.67 (1.59)	78 | 5.18 (2.38)	90 | 5.02 (1.66)	90 | 4.25 (1.85)	79 | 3.48 (1.18)	83 | 1.06 (0.44)	
96 | 2.59 (1.99)	82 | 5.80 (1.65)	96 | 5.56 (1.93)	96 | 2.87 (2.03)	84 | 2.34 (1.08)	90 | 0.72 (0.44)	
101 | 10.16 (2.69)	86 | 3.45 (1.57)	102 | 2.69 (1.82)	102 | 1.59 (1.32)	90 | 2.90 (1.03)	97 | 0.14 (0.14)	
108 | 9.77 (2.62)	91 | 4.42 (2.08)			96 | 2.77 (0.89)		
115 | 8.71 (2.42)	96 | 1.93 (2.44)					
122 | 12.67 (3.07)	101 | 6.67 (2.50)					
131 | 7.44 (2.44)	108 | 3.00 (1.48)					
140 | 10.75 (2.25)						

Table 92. Triton production cross sections for 290 MeV/u carbon on lead.

5	10	20	30	40	60	80
31 | 19.40 (6.31)	28 | 10.44 (4.19)	27 | 13.63 (3.55)	27 | 7.34 (2.45)	23 | 2.95 (1.56)	25 | 1.94 (1.02)	
34 | 16.61 (5.69)	32 | 9.82 (3.99)	30 | 9.12 (2.93)	30 | 4.61 (1.74)	26 | 4.18 (1.35)	29 | 0.95 (0.77)	
38 | 3.69 (5.55)	40 | 3.89 (2.72)	34 | 1.18 (2.18)	34 | 5.20 (1.54)	30 | 6.86 (1.80)	33 | 2.19 (0.79)	
43 | 9.54 (4.33)	44 | 2.04 (1.94)	38 | 4.08 (1.93)	38 | 4.60 (1.76)	34 | 1.67 (1.00)	37 | 1.80 (0.74)	
47 | 0.47 (4.03)	49 | 0.11 (1.27)	43 | 3.70 (1.42)	43 | 3.36 (1.86)	38 | 2.34 (0.84)	41 | 0.83 (0.72)	
50 | 10.48 (3.49)	54 | 2.88 (1.88)	47 | 3.61 (1.53)	48 | 0.99 (0.71)	43 | 1.84 (0.83)	46 | 0.15 (0.55)	
54 | 3.84 (3.05)	59 | 1.53 (1.46)	52 | 5.57 (1.59)	52 | 1.83 (1.27)	47 | 1.57 (0.71)	49 | 0.26 (0.77)	
58 | 5.16 (3.03)	65 | 2.19 (0.99)	57 | 1.39 (0.94)	57 | 0.33 (0.33)	51 | 1.37 (0.72)	52 | 0.36 (0.36)	
61 | 5.57 (2.99)	69 | 1.35 (1.66)	62 | 3.39 (1.22)	62 | 2.55 (0.92)	61 | 1.10 (0.99)	55 | 0.69 (0.68)	
63 | 6.37 (3.09)	73 | -0.77 (1.64)	67 | 3.89 (1.76)	67 | 1.64 (0.96)	65 | 0.98 (1.03)	59 | 0.59 (0.42)	
66 | 2.86 (1.83)	77 | 1.54 (1.93)	71 | 1.74 (1.01)	71 | 0.93 (0.66)	69 | 0.67 (0.48)		
69 | 2.51 (1.26)	81 | 3.26 (0.90)					
	85 | 2.92 (1.89)					
	90 | 3.03 (2.19)					

Table 93. Proton production cross sections for 400 MeV/u krypton on aluminum.

5	10	20	30	40	60	80
46 | 7.66 (1.99)	45 | 6.13 (1.75)	41 | 9.32 (1.77)	45 | 8.89 (1.32)	43 | 6.31 (1.41)	46 | 4.99 (0.95)	54 | 4.46 (0.66)
52 | 10.76 (1.85)	50 | 10.32 (1.52)	46 | 6.44 (1.18)	51 | 7.89 (1.08)	50 | 6.82 (0.99)	54 | 4.67 (0.75)	60 | 2.44 (0.44)
59 | 10.48 (1.51)	57 | 7.26 (1.30)	52 | 5.98 (1.17)	59 | 5.57 (1.09)	57 | 6.70 (0.91)	64 | 5.25 (0.74)	68 | 2.36 (0.39)
67 | 9.33 (1.72)	65 | 12.43 (1.64)	60 | 9.03 (1.38)	68 | 7.42 (1.10)	66 | 7.71 (1.06)	76 | 4.24 (0.55)	77 | 1.88 (0.37)
77 | 11.40 (1.51)	73 | 9.39 (1.51)	68 | 12.27 (1.25)	79 | 7.96 (0.97)	75 | 6.59 (0.99)	89 | 3.16 (0.52)	87 | 1.77 (0.30)
86 | 11.28 (1.49)	84 | 8.70 (1.13)	78 | 9.93 (1.10)	90 | 8.33 (1.10)	84 | 6.54 (0.96)	103 | 3.48 (0.47)	101 | 1.25 (0.21)
95 | 11.51 (1.39)	95 | 11.03 (1.33)	90 | 11.07 (1.32)	101 | 7.25 (0.95)	95 | 7.38 (0.95)	122 | 2.70 (0.33)	119 | 1.17 (0.17)
106 | 10.10 (1.23)	106 | 11.24 (1.31)	101 | 10.97 (1.15)	115 | 7.21 (0.83)	105 | 6.90 (0.97)	140 | 2.39 (0.35)	138 | 0.99 (0.18)
120 | 12.37 (1.06)	116 | 12.98 (1.47)	115 | 10.14 (1.02)	127 | 6.63 (1.10)	113 | 6.31 (0.84)	155 | 2.49 (0.32)	154 | 0.62 (0.12)
132 | 9.35 (1.64)	124 | 10.63 (1.68)	127 | 8.95 (1.40)	137 | 6.43 (0.97)	122 | 5.64 (0.84)	173 | 2.43 (0.29)	174 | 0.69 (0.11)
142 | 8.49 (1.55)	132 | 12.40 (1.79)	137 | 13.40 (1.75)	149 | 10.17 (1.63)	132 | 4.98 (0.81)	194 | 1.87 (0.22)	199 | 0.58 (0.10)
152 | 9.04 (2.05)	142 | 15.12 (2.35)	148 | 14.08 (2.07)	161 | 7.88 (1.15)	144 | 8.49 (0.99)	221 | 1.05 (0.15)	230 | 0.35 (0.06)
164 | 5.11 (2.06)	152 | 18.42 (2.55)	161 | 13.48 (1.93)	176 | 6.22 (1.11)	158 | 5.62 (0.84)	255 | 0.85 (0.12)	272 | 0.22 (0.04)
178 | 6.14 (1.52)	164 | 24.78 (2.56)	176 | 11.37 (1.46)			298 | 0.58 (0.08)	330 | 0.05 (0.02)

Table 94. Deuteron production cross sections for 400 MeV/u krypton on aluminum.

5	10	20	30	40	60	80
28 | 8.78 (2.52)	29 | 4.49 (2.07)	28 | 2.75 (1.52)	28 | 5.32 (1.14)	26 | 4.27 (1.19)	28 | 2.94 (0.75)	33 | 1.40 (0.39)
31 | 6.44 (2.67)	32 | 6.19 (1.96)	31 | 6.03 (1.29)	31 | 3.54 (1.02)	30 | 2.60 (0.79)	32 | 1.11 (0.77)	38 | 1.35 (0.46)
35 | 5.73 (2.32)	36 | 8.28 (2.04)	36 | 8.81 (1.38)	36 | 3.98 (1.12)	34 | 2.69 (0.61)	37 | 2.04 (0.60)	44 | 0.81 (0.27)
39 | 5.66 (2.35)	40 | 10.90 (2.00)	41 | 6.89 (1.20)	40 | 5.15 (1.06)	39 | 2.83 (0.80)	43 | 2.28 (0.50)	49 | 0.46 (0.21)
43 | 8.50 (1.98)	45 | 8.18 (1.81)	47 | 4.21 (0.92)	45 | 5.03 (1.03)	44 | 3.88 (0.94)	50 | 1.23 (0.37)	56 | 0.67 (0.22)
48 | 6.99 (1.78)	50 | 6.66 (1.40)	53 | 6.34 (0.84)	51 | 4.65 (0.91)	50 | 2.77 (0.63)	57 | 1.12 (0.51)	63 | 0.55 (0.16)
54 | 5.68 (1.66)	56 | 4.66 (0.99)	61 | 4.94 (0.69)	57 | 4.48 (0.93)	57 | 2.33 (0.58)	65 | 1.24 (0.34)	70 | 0.26 (0.14)
60 | 5.44 (1.72)	62 | 5.79 (1.26)	69 | 4.84 (0.80)	63 | 3.77 (0.86)	63 | 3.43 (0.60)	74 | 1.05 (0.25)	76 | 0.52 (0.17)
65 | 7.82 (1.51)	68 | 7.15 (1.21)	77 | 5.19 (0.91)	69 | 4.94 (0.90)	71 | 3.20 (0.58)	82 | 1.04 (0.31)	82 | 0.11 (0.07)
71 | 7.18 (1.38)	75 | 5.76 (1.01)	87 | 5.31 (0.70)	75 | 4.35 (0.89)	80 | 2.96 (0.46)	88 | 1.06 (0.27)	89 | 0.41 (0.14)
79 | 6.02 (1.14)	81 | 7.56 (1.22)	95 | 6.94 (1.16)	80 | 5.39 (1.00)	89 | 1.79 (0.53)	96 | 0.30 (0.28)	97 | 0.03 (0.03)
85 | 5.84 (1.71)	85 | 6.73 (1.14)	101 | 6.16 (1.10)	84 | 5.86 (0.97)	95 | 2.36 (0.59)	104 | 0.51 (0.42)	107 | 0.04 (0.03)
90 | 9.17 (1.81)	90 | 3.64 (1.23)	108 | 7.92 (1.34)	89 | 3.37 (0.66)	102 | 2.36 (0.59)	113 | 0.89 (0.16)	119 | 0.02 (0.02)
95 | 12.93 (1.89)	95 | 5.99 (1.65)	116 | 10.85 (1.49)	95 | 4.26 (0.88)	110 | 3.32 (0.45)	124 | 0.81 (0.26)	
101 | 14.01 (2.43)	101 | 11.40 (1.76)	125 | 11.25 (1.56)	101 | 3.27 (1.14)	120 | 2.95 (0.55)	137 | 0.17 (0.22)	
107 | 12.51 (2.19)	107 | 14.00 (1.91)	135 | 10.89 (1.61)	109 | 4.87 (1.12)	130 | 2.48 (0.55)		
114 | 14.94 (1.96)	114 | 13.20 (1.49)	146 | 9.24 (1.55)	116 | 4.55 (0.69)	142 | 2.49 (0.50)		
121 | 16.17 (1.56)	121 | 11.28 (2.14)		125 | 3.70 (0.78)			
130 | 11.06 (1.45)	130 | 12.06 (1.96)		135 | 6.34 (1.28)			
139 | 9.03 (1.71)			146 | 4.89 (0.78)			
150 | 10.22 (1.57)						

Table 95. Triton production cross sections for 400 MeV/u krypton on aluminum.

5	10	20	30	40	60	80
41 | 1.52 (0.92)	34 | 3.71 (1.44)	36 | 1.67 (1.01)	27 | 3.43 (1.35)	23 | 1.02 (0.55)	25 | 0.29 (0.67)	
47 | 4.12 (1.18)	38 | 4.38 (1.70)	38 | 0.61 (1.34)	30 | 1.06 (1.18)	26 | 0.71 (0.41)	30 | 1.51 (0.99)	
53 | 5.16 (1.20)	42 | 3.50 (0.96)	39 | 2.77 (1.03)	34 | 1.90 (0.80)	29 | 2.19 (0.63)	34 | 0.42 (0.28)	
59 | 10.06 (2.20)	46 | 3.37 (1.43)	41 | 3.93 (1.34)	38 | 2.77 (1.17)	33 | 1.52 (0.51)	40 | 0.03 (0.18)	
64 | 7.50 (1.81)	50 | 4.28 (1.31)	42 | 1.09 (0.55)	42 | 1.45 (0.71)	38 | 0.38 (0.59)	45 | 0.72 (0.23)	
71 | 5.68 (1.16)	54 | 2.62 (1.06)	44 | 1.52 (0.80)	45 | 2.00 (0.59)	43 | 1.34 (0.34)	50 | 0.65 (0.20)	
76 | 5.49 (1.39)	58 | 1.27 (0.89)	46 | 1.44 (1.66)	49 | 1.26 (0.57)	48 | 0.78 (0.31)	54 | 0.50 (0.23)	
80 | 8.65 (1.98)	60 | 1.09 (1.36)	48 | 3.34 (1.34)	54 | 1.34 (0.39)	53 | 1.16 (0.31)	58 | 0.50 (0.21)	
85 | 3.48 (1.04)	63 | 2.95 (0.95)	50 | 3.28 (1.05)	58 | 2.17 (0.73)	59 | 0.88 (0.24)	62 | 0.29 (0.21)	
	66 | 2.48 (0.83)	52 | 0.94 (0.42)	60 | 2.00 (1.01)	64 | 1.14 (0.37)	66 | 0.09 (0.22)	
		55 | 1.89 (0.66)	64 | 0.93 (0.64)	68 | 0.96 (0.31)		
		58 | 2.13 (0.79)	67 | 1.97 (0.63)	73 | 0.86 (0.28)		
		60 | 1.32 (0.62)	71 | 1.70 (0.48)			
		64 | 2.13 (0.68)	74 | 1.22 (0.46)			
		67 | 1.67 (0.54)				
		71 | 1.06 (0.38)				
		74 | 1.02 (0.38)				

Table 96. ^{3}He production cross sections for 400 MeV/u krypton on aluminum.

5	10	20	30	40	60	80
	94 | 2.66 (0.82)	99 | 2.27 (0.53)	99 | 0.21 (0.38)	100 | 1.07 (0.56)		
	99 | 1.97 (0.67)	105 | 1.84 (0.51)	106 | 0.77 (0.31)	106 | 0.43 (0.19)		
	105 | 0.08 (0.53)	112 | 1.54 (0.36)	112 | 1.50 (0.37)	114 | 0.46 (0.16)		
	111 | 2.01 (0.57)	120 | 1.56 (0.50)	120 | 0.54 (0.32)	123 | 0.17 (0.30)		
	118 | 2.99 (0.74)	128 | 1.59 (0.40)	129 | 0.75 (0.21)	134 | 0.20 (0.24)		
	125 | 2.54 (0.75)	138 | 1.79 (0.38)	138 | 0.53 (0.25)	145 | 0.37 (0.13)		
	133 | 2.08 (0.66)	149 | 1.67 (0.32)		159 | 0.19 (0.07)		
	143 | 2.72 (0.71)	162 | 1.13 (0.33)		175 | 0.17 (0.07)		
	153 | 3.69 (0.70)	177 | 0.85 (0.33)				
	165 | 4.17 (0.59)					
	178 | 1.51 (0.59)					

Table 97. ^{4}He production cross sections for 400 MeV/u krypton on aluminum.

5	10	20	30	40	60	80
	83 | 2.24 (0.78)	82 | 0.64 (0.26)	82 | 0.17 (0.24)	81 | 0.19 (0.14)		
	88 | 2.50 (0.66)	86 | 0.90 (0.33)	87 | 0.66 (0.31)	86 | 0.32 (0.20)		
	92 | 0.94 (0.58)	92 | 0.54 (0.25)	92 | 0.69 (0.30)	91 | 0.25 (0.13)		
	97 | 1.44 (0.57)	97 | 0.94 (0.32)	97 | 0.40 (0.18)	97 | 0.30 (0.14)		
	103 | 1.01 (0.37)	103 | 0.98 (0.33)	103 | 0.93 (0.31)	104 | 0.17 (0.10)		
	109 | 1.83 (0.48)	110 | 0.90 (0.29)	110 | 0.24 (0.17)	112 | 0.31 (0.12)		
	115 | 1.45 (0.40)	118 | 1.33 (0.33)		121 | 0.08 (0.06)		
	123 | 0.99 (0.43)	126 | 1.28 (0.34)		131 | 0.05 (0.05)		
	131 | 1.83 (0.53)	136 | 0.78 (0.22)				
	140 | 1.81 (0.47)	147 | 0.48 (0.19)				

Table 98. Proton production cross sections for 400 MeV/u krypton on carbon.

5	10	20	30	40	60	80
44 | 3.82 (1.00)	44 | 3.86 (0.88)	43 | 3.39 (0.79)	44 | 3.36 (0.55)	45 | 3.95 (0.65)	46 | 1.92 (0.46)	55 | 1.19 (0.27)
49 | 5.34 (0.87)	49 | 6.75 (0.89)	48 | 3.79 (0.64)	50 | 3.61 (0.51)	52 | 3.07 (0.45)	53 | 2.58 (0.44)	61 | 1.41 (0.22)
56 | 5.67 (0.84)	56 | 4.57 (0.70)	54 | 3.96 (0.66)	57 | 3.09 (0.52)	60 | 3.35 (0.50)	61 | 1.97 (0.34)	70 | 0.84 (0.16)
63 | 4.82 (0.82)	63 | 5.01 (0.75)	60 | 5.04 (0.62)	66 | 2.89 (0.54)	69 | 3.48 (0.46)	72 | 1.86 (0.29)	81 | 0.82 (0.13)
71 | 6.29 (0.81)	71 | 5.13 (0.77)	68 | 4.50 (0.52)	75 | 3.54 (0.44)	79 | 3.15 (0.44)	84 | 1.59 (0.25)	95 | 0.58 (0.11)
80 | 5.42 (0.69)	81 | 7.16 (0.70)	79 | 4.84 (0.56)	85 | 3.35 (0.52)	89 | 3.97 (0.53)	96 | 1.59 (0.24)	111 | 0.59 (0.09)
91 | 5.54 (0.68)	91 | 6.71 (0.71)	90 | 6.11 (0.62)	95 | 3.77 (0.46)	102 | 3.19 (0.37)	112 | 1.50 (0.19)	133 | 0.23 (0.05)
101 | 6.03 (0.67)	101 | 6.26 (0.65)	101 | 6.79 (0.60)	108 | 3.67 (0.42)	118 | 3.28 (0.37)	128 | 1.38 (0.20)	156 | 0.25 (0.05)
113 | 6.23 (0.63)	113 | 6.80 (0.67)	115 | 6.29 (0.56)	123 | 3.38 (0.32)	133 | 2.12 (0.38)	140 | 1.13 (0.16)	175 | 0.23 (0.04)
124 | 7.25 (0.75)	124 | 7.55 (0.82)	133 | 5.79 (0.59)	138 | 3.78 (0.49)	145 | 3.32 (0.44)	155 | 1.18 (0.15)	200 | 0.12 (0.03)
132 | 6.26 (0.86)	132 | 6.49 (0.86)	149 | 8.61 (1.03)	149 | 4.68 (0.74)	158 | 3.22 (0.41)	173 | 1.22 (0.14)	232 | 0.10 (0.02)
142 | 6.32 (0.82)	142 | 9.78 (1.18)	161 | 8.75 (0.93)	162 | 4.69 (0.58)	175 | 2.16 (0.28)	195 | 0.78 (0.10)	274 | 0.06 (0.02)
152 | 6.80 (1.00)	152 | 12.07 (1.28)	176 | 7.24 (0.73)	176 | 3.36 (0.52)		222 | 0.58 (0.07)	331 | 0.03 (0.01)
164 | 2.87 (0.94)	164 | 12.30 (1.23)				255 | 0.39 (0.05)	
178 | 3.14 (0.69)					299 | 0.16 (0.03)	
					357 | 0.07 (0.02)	

Table 99. Deuteron production cross sections for 400 MeV/u krypton on carbon.

5	10	20	30	40	60	80
28 | 2.49 (1.03)	29 | 2.24 (0.99)	27 | 1.47 (0.73)	28 | 1.79 (0.47)	27 | 2.18 (0.42)	28 | -0.42 (0.56)	34 | 0.54 (0.15)
31 | 3.62 (1.19)	32 | 2.53 (0.78)	31 | 2.19 (0.61)	32 | 1.65 (0.46)	31 | 1.71 (0.39)	33 | 0.23 (0.42)	40 | 0.34 (0.15)
35 | 2.11 (1.10)	36 | 3.63 (0.89)	35 | 3.39 (0.57)	36 | 1.71 (0.50)	35 | 1.68 (0.33)	38 | 0.88 (0.32)	46 | 0.49 (0.11)
40 | 3.41 (0.96)	40 | 3.78 (0.89)	39 | 2.91 (0.60)	40 | 1.41 (0.38)	41 | 2.01 (0.34)	43 | 0.79 (0.21)	55 | 0.15 (0.07)
45 | 2.33 (0.76)	45 | 4.19 (0.85)	44 | 3.27 (0.60)	45 | 2.63 (0.48)	46 | 1.87 (0.38)	50 | 0.64 (0.18)	64 | 0.17 (0.06)
50 | 2.91 (0.79)	50 | 3.26 (0.65)	49 | 2.77 (0.44)	51 | 1.18 (0.33)	53 | 1.46 (0.25)	57 | 1.10 (0.21)	73 | 0.15 (0.06)
56 | 3.20 (0.72)	56 | 2.51 (0.44)	55 | 2.35 (0.40)	57 | 2.13 (0.44)	60 | 1.07 (0.26)	65 | 0.51 (0.16)	86 | 0.08 (0.03)
62 | 4.66 (0.83)	62 | 2.52 (0.57)	60 | 1.64 (0.32)	63 | 1.72 (0.42)	67 | 1.37 (0.23)	74 | 0.31 (0.10)	98 | 0.01 (0.01)
68 | 2.78 (0.62)	68 | 3.72 (0.61)	66 | 1.77 (0.30)	70 | 2.00 (0.39)	76 | 1.09 (0.21)	82 | 0.24 (0.11)	108 | 0.03 (0.02)
75 | 3.58 (0.59)	75 | 1.73 (0.42)	73 | 1.95 (0.37)	77 | 1.93 (0.32)	83 | 1.15 (0.24)	88 | 0.22 (0.10)	
81 | 1.57 (0.72)	83 | 3.13 (0.42)	80 | 2.44 (0.58)	84 | 2.10 (0.41)	89 | 0.75 (0.24)	96 | 0.21 (0.08)	
85 | 4.43 (0.88)	90 | 3.54 (0.71)	84 | 2.58 (0.44)	90 | 1.54 (0.30)	95 | 0.83 (0.25)	104 | 0.03 (0.15)	
90 | 4.43 (0.92)	95 | 3.61 (0.83)	89 | 2.53 (0.45)	95 | 1.81 (0.35)	103 | 1.00 (0.22)	114 | 0.35 (0.05)	
95 | 6.00 (0.89)	101 | 4.82 (0.80)	95 | 3.78 (0.56)	102 | 1.54 (0.49)	111 | 1.26 (0.22)	125 | 0.48 (0.10)	
101 | 5.17 (1.04)	107 | 5.61 (0.86)	102 | 4.10 (0.64)	109 | 2.55 (0.54)	120 | 1.29 (0.21)	137 | 0.15 (0.12)	
107 | 4.79 (1.01)	114 | 6.52 (0.78)	109 | 4.02 (0.66)	117 | 2.37 (0.30)	130 | 1.28 (0.28)		
114 | 6.80 (0.97)	122 | 6.25 (1.02)	116 | 4.68 (0.59)	125 | 1.90 (0.33)	142 | 0.93 (0.25)		
122 | 6.39 (0.65)	130 | 6.04 (0.89)	125 | 5.29 (0.70)	135 | 3.05 (0.58)			
130 | 5.49 (0.83)		135 | 4.42 (0.75)	147 | 2.38 (0.35)			
140 | 4.85 (0.80)						
150 | 4.90 (0.72)						

Table 100. Triton production cross sections for 400 MeV/u krypton on carbon.

5	10	20	30	40	60	80
45 | 0.02 (0.54)	31 | 0.97 (0.58)	40 | 0.74 (0.24)	28 | 0.77 (0.62)	23 | 0.65 (0.28)	25 | 0.07 (0.14)	
51 | 1.10 (0.56)	34 | 0.52 (0.79)	46 | 0.20 (0.27)	31 | 0.42 (0.34)	26 | 0.45 (0.21)	29 | 0.61 (0.43)	
56 | 2.37 (0.71)	38 | 0.78 (0.65)	53 | 0.30 (0.19)	35 | 1.04 (0.51)	29 | 0.61 (0.22)	33 | 0.21 (0.17)	
62 | 6.05 (1.09)	42 | 0.95 (0.39)	59 | 0.27 (0.16)	39 | 0.53 (0.37)	32 | 0.35 (0.23)	38 | 0.14 (0.19)	
67 | 2.67 (0.64)	47 | 0.86 (0.42)	65 | 0.64 (0.16)	44 | 0.74 (0.20)	36 | 0.47 (0.22)	44 | 0.10 (0.07)	
72 | 1.26 (0.52)	52 | 0.90 (0.42)	71 | 0.28 (0.15)	49 | 0.38 (0.20)	41 | 0.53 (0.17)	50 | 0.19 (0.08)	
76 | 2.19 (0.68)	56 | 0.62 (0.40)	75 | 0.15 (0.09)	54 | 0.43 (0.14)	46 | 0.30 (0.13)	56 | 0.22 (0.07)	
80 | 4.51 (0.96)	62 | 0.46 (0.33)		59 | 0.29 (0.12)	51 | 0.15 (0.10)	62 | 0.02 (0.06)	
85 | 2.14 (0.58)	66 | 0.43 (0.25)		64 | 0.26 (0.24)	56 | 0.40 (0.12)	70 | 0.04 (0.04)	
	69 | 0.39 (0.23)		67 | 0.49 (0.21)	61 | 0.25 (0.13)		
			71 | 0.22 (0.11)	64 | 0.14 (0.08)		
			75 | 0.15 (0.11)	68 | 0.20 (0.11)		
				73 | 0.08 (0.06)		

Table 101. ^{3}He production cross sections for 400 MeV/u krypton on carbon.

5	10	20	30	40	60	80
	95 | 0.58 (0.34)	100 | 0.65 (0.21)	106 | 0.23 (0.12)	94 | 0.00 (0.00)		
	100 | 0.65 (0.34)	106 | 0.51 (0.18)	113 | 0.34 (0.12)	100 | 0.27 (0.24)		
	105 | 0.69 (0.37)	112 | 0.75 (0.18)	120 | 0.10 (0.12)	107 | 0.21 (0.09)		
	111 | 0.54 (0.24)	120 | 0.18 (0.16)	129 | 0.21 (0.08)	115 | 0.17 (0.06)		
	118 | 0.86 (0.26)	129 | 0.57 (0.16)	139 | 0.08 (0.09)	124 | 0.08 (0.08)		
	125 | 0.81 (0.32)	138 | 0.24 (0.11)		134 | 0.08 (0.05)		
	134 | 1.01 (0.31)	150 | 0.58 (0.13)		145 | 0.11 (0.05)		
	143 | 1.00 (0.31)	162 | 0.55 (0.16)		159 | 0.06 (0.03)		
	153 | 1.30 (0.30)			175 | 0.02 (0.02)		
	165 | 1.75 (0.27)			194 | 0.01 (0.02)		
	178 | 0.76 (0.28)					

Table 102. ^{4}He production cross sections for 400 MeV/u krypton on carbon.

5	10	20	30	40	60	80
	80 | 0.18 (0.28)	82 | 0.17 (0.10)	82 | 0.03 (0.10)	86 | 0.03 (0.07)		
	84 | 0.17 (0.22)	87 | 0.35 (0.14)	87 | 0.22 (0.12)	98 | 0.02 (0.02)		
	88 | 0.09 (0.09)	92 | 0.12 (0.07)	92 | 0.16 (0.10)	105 | 0.06 (0.04)		
	97 | 0.58 (0.26)	97 | 0.44 (0.16)	97 | 0.16 (0.09)	131 | 0.04 (0.03)		
	103 | 0.12 (0.17)	103 | 0.11 (0.07)	104 | 0.14 (0.07)			
	109 | 0.34 (0.16)	110 | 0.21 (0.09)				
	116 | 0.47 (0.17)	118 | 0.23 (0.09)				
	123 | 0.49 (0.20)	127 | 0.18 (0.09)				
	131 | 0.27 (0.18)	136 | 0.28 (0.09)				
	141 | 0.45 (0.18)	147 | 0.13 (0.06)				

Table 103. Proton production cross sections for 400 MeV/u krypton on copper.

5	10	20	30	40	60	80
45 | 14.23 (3.08)	45 | 16.64 (2.92)	43 | 18.94 (2.84)	45 | 17.07 (2.08)	45 | 10.32 (2.17)	47 | 9.28 (1.53)	59 | 8.26 (1.11)
50 | 23.16 (2.98)	50 | 17.24 (2.60)	49 | 20.00 (2.29)	50 | 14.15 (1.87)	51 | 13.56 (1.64)	54 | 10.26 (1.29)	66 | 6.09 (0.79)
56 | 15.30 (2.48)	56 | 16.73 (2.27)	54 | 16.48 (2.05)	58 | 16.42 (1.80)	58 | 13.54 (1.57)	62 | 9.61 (1.19)	76 | 5.67 (0.71)
63 | 14.84 (2.47)	63 | 17.48 (2.46)	61 | 18.42 (2.16)	66 | 12.98 (1.73)	67 | 15.00 (1.81)	73 | 9.16 (1.11)	89 | 4.41 (0.52)
71 | 18.76 (2.48)	71 | 15.74 (2.35)	69 | 15.33 (1.70)	76 | 14.13 (1.47)	78 | 13.46 (1.39)	87 | 6.70 (0.78)	104 | 3.66 (0.46)
81 | 15.46 (1.99)	81 | 24.18 (2.26)	77 | 22.17 (2.25)	88 | 15.41 (1.53)	90 | 14.02 (1.65)	104 | 7.33 (0.83)	122 | 2.79 (0.33)
91 | 17.62 (2.11)	91 | 21.51 (2.26)	86 | 18.19 (2.07)	102 | 14.53 (1.52)	102 | 12.62 (1.35)	123 | 6.39 (0.66)	149 | 1.77 (0.22)
101 | 19.57 (2.11)	101 | 20.98 (2.16)	96 | 19.68 (1.82)	116 | 15.04 (1.29)	118 | 11.80 (1.08)	148 | 4.99 (0.49)	176 | 1.33 (0.19)
113 | 20.37 (1.90)	113 | 23.79 (2.04)	105 | 22.14 (2.28)	128 | 13.33 (1.53)	133 | 9.94 (1.22)	173 | 4.96 (0.53)	201 | 0.98 (0.15)
124 | 23.19 (2.19)	124 | 24.86 (2.86)	112 | 22.12 (2.10)	138 | 13.42 (1.63)	145 | 13.74 (1.51)	195 | 4.48 (0.45)	232 | 0.58 (0.10)
133 | 15.24 (2.45)	133 | 20.41 (2.65)	119 | 22.40 (2.49)	149 | 17.29 (2.36)	159 | 11.99 (1.39)	222 | 2.87 (0.32)	273 | 0.48 (0.08)
142 | 15.21 (2.35)	142 | 27.78 (3.48)	128 | 17.39 (2.19)	162 | 15.60 (1.84)	175 | 9.15 (0.97)	255 | 1.76 (0.21)	330 | 0.19 (0.04)
153 | 18.68 (3.04)	153 | 37.97 (4.02)	138 | 24.08 (2.63)	177 | 10.81 (1.66)		299 | 1.05 (0.14)	
164 | 10.63 (3.04)	164 | 38.28 (3.79)	149 | 24.35 (3.06)			357 | 0.57 (0.09)	
178 | 10.79 (2.21)		162 | 27.11 (2.90)				
		176 | 22.12 (2.23)				

Table 104. Deuteron production cross sections for 400 MeV/u krypton on copper.

5	10	20	30	40	60	80
29 | 19.98 (4.17)	29 | 7.49 (3.37)	28 | 13.00 (2.73)	29 | 10.21 (1.91)	27 | 9.15 (1.59)	30 | 5.20 (1.48)	34 | 2.50 (0.60)
32 | 13.53 (3.69)	32 | 12.04 (2.75)	32 | 10.19 (1.77)	33 | 9.74 (1.66)	30 | 8.32 (1.52)	34 | 6.47 (1.09)	39 | 3.23 (0.67)
36 | 12.87 (3.44)	36 | 9.26 (2.68)	36 | 11.58 (1.84)	37 | 9.83 (1.73)	34 | 8.91 (1.42)	40 | 5.52 (0.95)	45 | 2.16 (0.47)
41 | 13.24 (3.40)	41 | 15.54 (3.12)	41 | 13.95 (2.15)	42 | 10.11 (1.77)	39 | 9.32 (1.37)	45 | 4.86 (0.85)	52 | 1.71 (0.33)
45 | 15.21 (3.02)	45 | 18.44 (3.01)	45 | 14.54 (1.89)	47 | 8.88 (1.56)	44 | 11.53 (1.58)	53 | 4.16 (0.76)	60 | 1.72 (0.34)
50 | 13.75 (2.56)	50 | 16.41 (2.46)	51 | 15.39 (1.66)	54 | 8.14 (1.30)	51 | 6.80 (1.07)	61 | 4.34 (0.65)	69 | 1.17 (0.25)
56 | 11.06 (2.45)	56 | 12.37 (1.67)	57 | 11.30 (1.66)	60 | 9.44 (1.55)	57 | 6.52 (1.06)	69 | 4.00 (0.62)	77 | 0.88 (0.26)
63 | 16.68 (2.87)	63 | 11.99 (2.02)	63 | 11.45 (1.38)	66 | 10.11 (1.47)	64 | 9.28 (1.17)	79 | 2.23 (0.48)	83 | 0.84 (0.24)
68 | 16.73 (2.26)	68 | 16.99 (2.16)	70 | 13.34 (1.50)	73 | 11.88 (1.43)	71 | 8.81 (1.05)	89 | 2.17 (0.45)	90 | 0.83 (0.23)
75 | 14.53 (2.02)	75 | 15.68 (1.91)	75 | 11.83 (2.00)	80 | 9.47 (1.99)	78 | 7.51 (1.23)	96 | 3.09 (0.51)	98 | 0.11 (0.07)
83 | 13.77 (1.96)	81 | 14.41 (2.05)	80 | 17.06 (2.38)	84 | 12.63 (1.80)	83 | 6.82 (1.04)	104 | 2.23 (0.60)	108 | 0.30 (0.11)
90 | 15.35 (3.18)	85 | 12.89 (2.10)	84 | 15.46 (1.85)	90 | 9.22 (1.29)	89 | 5.78 (1.03)	114 | 2.86 (0.35)	119 | 0.04 (0.04)
95 | 22.98 (2.95)	90 | 10.57 (2.31)	90 | 11.18 (1.56)	95 | 8.78 (1.27)	95 | 5.04 (0.97)	125 | 2.50 (0.39)	
101 | 15.80 (3.35)	95 | 19.07 (2.95)	95 | 15.95 (1.94)	102 | 6.93 (1.93)	103 | 5.69 (0.95)	137 | 1.84 (0.41)	
107 | 23.35 (3.46)	101 | 21.97 (2.83)	102 | 17.64 (2.04)	109 | 12.42 (1.78)	111 | 5.65 (0.61)		
114 | 28.61 (3.31)	107 | 24.94 (3.03)	109 | 15.30 (1.99)	117 | 10.62 (1.04)	120 | 6.01 (0.75)		
122 | 26.55 (2.43)	114 | 25.73 (2.45)	116 | 17.78 (2.02)	125 | 9.23 (1.29)	130 | 6.08 (0.79)		
130 | 21.70 (2.50)	122 | 24.88 (2.66)	125 | 22.23 (2.46)	135 | 13.13 (1.92)	142 | 5.00 (0.85)		
140 | 21.37 (2.71)	130 | 32.29 (3.34)	135 | 18.92 (2.66)	147 | 10.45 (1.29)			
150 | 20.81 (2.46)						

Table 105. Triton production cross sections for 400 MeV/u krypton on copper.

5	10	20	30	40	60	80
45 | 6.75 (1.97)	32 | 8.86 (2.49)	39 | 6.24 (1.25)	27 | 7.20 (2.36)	23 | 3.94 (1.14)	25 | 2.78 (1.02)	
51 | 10.69 (1.88)	36 | 8.30 (2.28)	44 | 4.75 (1.10)	30 | 7.07 (1.64)	26 | 6.45 (1.24)	29 | 4.20 (1.49)	
58 | 14.84 (2.54)	41 | 7.79 (2.02)	50 | 5.32 (0.90)	34 | 7.26 (1.50)	29 | 5.04 (1.14)	33 | 2.26 (0.71)	
64 | 17.31 (2.96)	45 | 6.43 (1.69)	56 | 5.58 (1.01)	38 | 5.42 (1.72)	32 | 5.20 (1.13)	38 | 1.68 (0.61)	
71 | 13.36 (2.01)	50 | 5.88 (1.78)	62 | 4.80 (0.87)	43 | 8.20 (1.29)	36 | 3.31 (0.88)	43 | 0.72 (0.38)	
76 | 14.63 (2.57)	54 | 3.48 (1.59)	67 | 4.78 (1.09)	47 | 7.72 (1.44)	40 | 5.12 (1.10)	47 | 1.28 (0.35)	
80 | 13.37 (2.82)	59 | 6.64 (1.61)	71 | 4.72 (0.99)	51 | 6.52 (1.15)	44 | 4.48 (0.88)	53 | 1.61 (0.36)	
	63 | 4.20 (1.35)	75 | 3.72 (0.90)	56 | 2.95 (0.67)	48 | 4.55 (0.85)	58 | 1.60 (0.47)	
	66 | 4.91 (1.40)		61 | 3.83 (0.95)	52 | 2.79 (0.82)	62 | 1.10 (0.43)	
	69 | 3.30 (1.07)		64 | 5.23 (1.32)	55 | 2.11 (0.74)	66 | 0.17 (0.32)	
			67 | 5.60 (1.17)	58 | 3.43 (0.87)	70 | 0.10 (0.10)	
			71 | 5.13 (1.07)	61 | 3.31 (0.84)		
				64 | 3.04 (0.76)		
				68 | 3.05 (0.71)		
				73 | 2.34 (0.59)		

Table 106. ^{3}He production cross sections for 400 MeV/u krypton on copper.

5	10	20	30	40	60	80
	100 | 6.91 (1.42)	100 | 4.64 (0.92)	107 | 2.49 (0.61)	95 | 0.82 (0.32)		
	106 | 5.63 (1.34)	106 | 2.88 (0.67)	113 | 2.66 (0.57)	101 | 2.07 (0.86)		
	112 | 5.98 (1.20)	113 | 4.79 (0.78)	121 | 1.98 (0.55)	107 | 1.21 (0.37)		
	118 | 5.67 (1.06)	121 | 3.42 (0.76)	130 | 2.03 (0.44)	115 | 1.02 (0.26)		
	126 | 5.41 (1.20)	129 | 2.76 (0.59)	139 | 0.70 (0.34)	124 | 0.97 (0.35)		
	134 | 4.57 (1.07)	139 | 4.42 (0.70)	150 | 0.01 (0.11)	134 | 0.79 (0.23)		
	143 | 4.96 (1.02)	150 | 4.49 (0.62)		146 | 0.87 (0.23)		
	153 | 7.77 (1.16)	162 | 3.49 (0.59)		159 | 0.77 (0.18)		
	165 | 8.41 (1.03)			175 | 0.46 (0.14)		
	178 | 6.94 (1.14)			193 | 0.23 (0.12)		

Table 107. ^{4}He production cross sections for 400 MeV/u krypton on copper.

5	10	20	30	40	60	80
	84 | 4.90 (1.36)	83 | 4.85 (1.00)	87 | 2.13 (0.59)	86 | 0.81 (0.36)		
	88 | 4.10 (1.06)	87 | 4.48 (0.92)	92 | 2.53 (0.65)	92 | 0.97 (0.31)		
	93 | 3.48 (1.15)	92 | 3.51 (0.75)	98 | 2.38 (0.55)	98 | 1.01 (0.31)		
	98 | 4.38 (1.13)	98 | 4.98 (0.88)	104 | 2.41 (0.56)	105 | 0.84 (0.29)		
	103 | 5.51 (1.10)	104 | 4.56 (0.79)		113 | 0.83 (0.26)		
	109 | 4.87 (0.98)	111 | 3.74 (0.67)		122 | 1.08 (0.28)		
	116 | 6.39 (1.06)	118 | 3.64 (0.64)				
	123 | 5.36 (1.01)	127 | 2.93 (0.56)				
	132 | 5.86 (1.03)	137 | 2.58 (0.46)				
	141 | 6.02 (0.96)	148 | 2.33 (0.44)				

Table 108. Proton production cross sections for 400 MeV/u krypton on lithium.

5	10	20	30	40	60	80
43 | 1.87 (0.63)	44 | 2.11 (0.51)	43 | 2.23 (0.49)	43 | 2.27 (0.40)	43 | 1.48 (0.41)	46 | 1.28 (0.29)	52 | 0.73 (0.16)
47 | 2.12 (0.50)	49 | 2.75 (0.45)	49 | 2.08 (0.37)	49 | 2.02 (0.33)	50 | 1.48 (0.29)	54 | 1.31 (0.24)	59 | 0.74 (0.12)
53 | 2.09 (0.51)	55 | 2.37 (0.39)	55 | 3.00 (0.41)	55 | 2.51 (0.41)	57 | 1.87 (0.26)	64 | 1.25 (0.22)	68 | 0.51 (0.10)
60 | 2.60 (0.50)	62 | 3.71 (0.49)	62 | 2.95 (0.40)	62 | 2.17 (0.35)	66 | 1.78 (0.33)	76 | 1.11 (0.17)	80 | 0.47 (0.08)
67 | 2.59 (0.51)	70 | 2.88 (0.48)	71 | 3.07 (0.36)	71 | 2.26 (0.31)	75 | 1.88 (0.27)	92 | 0.83 (0.12)	94 | 0.29 (0.06)
77 | 2.98 (0.43)	80 | 3.65 (0.42)	80 | 2.69 (0.37)	81 | 1.87 (0.32)	84 | 2.33 (0.29)	112 | 0.73 (0.11)	110 | 0.29 (0.05)
86 | 3.14 (0.46)	90 | 3.61 (0.43)	90 | 3.68 (0.40)	90 | 3.15 (0.35)	95 | 1.82 (0.27)	134 | 0.74 (0.09)	133 | 0.18 (0.03)
95 | 3.56 (0.45)	101 | 3.92 (0.42)	101 | 3.05 (0.32)	101 | 2.25 (0.29)	105 | 1.86 (0.31)	164 | 0.52 (0.06)	156 | 0.09 (0.03)
106 | 3.94 (0.42)	113 | 4.27 (0.43)	111 | 2.89 (0.39)	115 | 2.18 (0.25)	113 | 1.67 (0.33)	209 | 0.28 (0.04)	176 | 0.13 (0.03)
116 | 3.69 (0.46)	124 | 4.09 (0.49)	119 | 2.93 (0.41)	128 | 2.33 (0.35)	122 | 1.82 (0.28)	256 | 0.12 (0.03)	202 | 0.06 (0.02)
124 | 3.84 (0.39)	132 | 3.62 (0.54)	128 | 2.55 (0.44)	138 | 2.65 (0.33)	133 | 1.69 (0.25)	300 | 0.05 (0.02)	234 | 0.04 (0.01)
132 | 2.65 (0.49)	142 | 4.72 (0.70)	137 | 4.01 (0.53)	149 | 2.72 (0.49)	145 | 2.26 (0.29)	359 | 0.04 (0.01)	277 | 0.01 (0.01)
142 | 2.56 (0.48)	152 | 6.43 (0.82)	149 | 5.12 (0.66)	162 | 2.20 (0.35)	158 | 1.98 (0.26)	442 | 0.01 (0.01)	336 | 0.00 (0.00)
152 | 3.39 (0.62)	164 | 6.68 (0.77)	162 | 5.95 (0.63)	176 | 2.33 (0.34)			
164 | 1.69 (0.63)	178 | 2.27 (0.48)	176 | 5.14 (0.50)				
178 | 1.03 (0.43)						

Table 109. Deuteron production cross sections for 400 MeV/u krypton on lithium.

5	10	20	30	40	60	80
29 | 2.72 (0.80)	31 | 1.38 (0.52)	27 | 0.93 (0.41)	28 | 1.04 (0.30)	25 | 0.37 (0.18)	29 | 0.10 (0.23)	33 | 0.19 (0.07)
32 | 1.01 (0.69)	35 | 0.58 (0.46)	30 | 1.49 (0.40)	31 | 0.83 (0.30)	29 | 0.79 (0.23)	34 | 0.41 (0.16)	38 | 0.31 (0.15)
36 | 1.06 (0.74)	40 | 2.13 (0.56)	34 | 1.44 (0.32)	36 | 0.84 (0.31)	33 | 0.59 (0.23)	39 | 0.34 (0.17)	44 | 0.06 (0.06)
41 | 1.55 (0.62)	45 | 1.29 (0.48)	39 | 0.90 (0.38)	40 | 0.55 (0.22)	37 | 0.27 (0.22)	45 | 0.36 (0.13)	50 | 0.11 (0.06)
46 | 1.25 (0.59)	50 | 1.65 (0.38)	43 | 1.47 (0.35)	45 | 0.89 (0.24)	42 | 0.50 (0.32)	53 | 0.10 (0.11)	56 | 0.08 (0.04)
52 | 0.85 (0.50)	56 | 0.89 (0.23)	49 | 1.16 (0.28)	51 | 0.55 (0.20)	48 | 0.81 (0.17)	61 | 0.19 (0.10)	64 | 0.06 (0.03)
59 | 1.16 (0.41)	62 | 1.42 (0.36)	55 | 1.31 (0.23)	59 | 0.75 (0.21)	56 | 0.55 (0.14)	69 | 0.13 (0.08)	71 | 0.08 (0.04)
65 | 1.23 (0.46)	68 | 1.16 (0.30)	60 | 1.06 (0.22)	66 | 1.12 (0.25)	64 | 0.50 (0.14)	79 | 0.13 (0.05)	76 | 0.09 (0.04)
72 | 1.14 (0.34)	75 | 1.32 (0.28)	66 | 1.13 (0.20)	73 | 0.92 (0.19)	71 | 0.48 (0.12)	89 | 0.05 (0.05)	83 | 0.07 (0.03)
79 | 1.51 (0.33)	81 | 1.78 (0.34)	73 | 0.84 (0.22)	82 | 0.77 (0.17)	81 | 0.58 (0.12)	96 | 0.05 (0.08)	90 | 0.02 (0.02)
88 | 3.13 (0.45)	85 | 1.53 (0.34)	80 | 0.62 (0.33)	92 | 0.49 (0.14)	89 | 0.26 (0.14)	104 | 0.06 (0.05)	99 | 0.02 (0.02)
95 | 4.55 (0.61)	90 | 0.96 (0.37)	84 | 1.39 (0.27)	102 | 0.78 (0.32)	95 | 0.36 (0.15)	114 | 0.17 (0.03)	
101 | 3.32 (0.70)	95 | 2.05 (0.50)	90 | 0.94 (0.22)	109 | 1.24 (0.34)	103 | 0.31 (0.12)	125 | 0.20 (0.05)	
107 | 3.33 (0.69)	101 | 2.19 (0.48)	95 | 1.88 (0.35)	117 | 0.85 (0.13)	111 | 0.57 (0.10)	138 | -0.06 (0.07)	
114 | 3.94 (0.61)	107 | 2.82 (0.53)	102 | 2.12 (0.37)	125 | 0.73 (0.16)	120 | 0.52 (0.13)		
122 | 4.09 (0.43)	114 | 3.01 (0.39)	109 | 1.41 (0.41)	135 | 1.16 (0.36)	130 | 0.44 (0.15)		
130 | 3.49 (0.49)	122 | 2.70 (0.47)	117 | 2.44 (0.33)	147 | 0.98 (0.20)	143 | 0.27 (0.14)		
140 | 3.17 (0.55)	130 | 2.60 (0.53)	125 | 2.29 (0.42)		157 | 0.00 (0.00)		
150 | 2.58 (0.44)		135 | 2.55 (0.46)				

Table 110. Triton production cross sections for 400 MeV/u krypton on lithium.

5	10	20	30	40	60	80
45 | 0.31 (0.35)	33 | 1.35 (0.48)	38 | 0.46 (0.19)	27 | 0.82 (0.39)	24 | 0.27 (0.16)	25 | -0.09 (0.24)	
51 | 0.83 (0.35)	37 | 0.29 (0.44)	42 | 0.46 (0.15)	30 | 0.70 (0.30)	27 | 0.31 (0.12)	29 | 0.45 (0.36)	
58 | 2.50 (0.51)	41 | 0.68 (0.31)	47 | -0.08 (0.24)	34 | 0.18 (0.19)	31 | 0.20 (0.16)	33 | 0.08 (0.17)	
64 | 2.87 (0.57)	44 | 0.80 (0.35)	51 | 0.23 (0.09)	38 | 0.60 (0.34)	35 | 0.03 (0.12)	37 | 0.12 (0.08)	
71 | 0.86 (0.30)	48 | 0.49 (0.28)	56 | 0.14 (0.09)	42 | 0.39 (0.22)	38 | 0.14 (0.10)	41 | 0.01 (0.08)	
76 | 1.32 (0.42)	52 | 0.47 (0.26)	61 | 0.18 (0.14)	45 | 0.48 (0.14)	42 | 0.20 (0.10)	45 | 0.08 (0.04)	
80 | 2.24 (0.58)	55 | -0.25 (0.46)	64 | 0.13 (0.08)	49 | 0.08 (0.11)	46 | 0.17 (0.07)	49 | 0.06 (0.04)	
85 | 1.54 (0.37)	58 | -0.10 (0.18)	67 | 0.16 (0.10)	54 | 0.12 (0.06)	49 | 0.06 (0.11)	52 | 0.09 (0.05)	
	60 | 0.08 (0.39)	71 | 0.04 (0.04)	58 | 0.10 (0.07)	52 | 0.09 (0.06)	55 | 0.06 (0.04)	
	63 | 0.14 (0.10)		61 | 0.19 (0.11)	55 | 0.16 (0.08)	58 | 0.08 (0.05)	
	69 | 0.07 (0.07)		64 | 0.02 (0.15)	58 | 0.12 (0.07)		
	73 | 0.00 (0.00)		67 | 0.21 (0.10)	61 | 0.07 (0.05)		
			71 | 0.16 (0.08)	65 | 0.10 (0.06)		
			75 | 0.11 (0.06)			

Table 111. ^{3}He production cross sections for 400 MeV/u krypton on lithium.

5	10	20	30	40	60	80
	93 | 0.27 (0.19)	98 | 0.21 (0.10)	104 | 0.16 (0.08)	92 | 0.02 (0.02)		
	98 | 0.42 (0.20)	104 | 0.22 (0.11)	111 | 0.08 (0.04)	98 | 0.17 (0.16)		
	104 | 0.45 (0.21)	111 | 0.28 (0.08)	119 | 0.02 (0.08)	105 | 0.03 (0.04)		
	110 | 0.15 (0.11)	119 | 0.18 (0.12)	128 | 0.09 (0.04)	113 | 0.04 (0.02)		
	116 | 0.37 (0.14)	127 | 0.19 (0.09)	137 | 0.01 (0.05)	122 | 0.01 (0.05)		
	124 | 0.18 (0.17)	137 | 0.26 (0.09)		132 | 0.02 (0.02)		
	132 | 0.31 (0.17)	149 | 0.17 (0.06)		144 | 0.01 (0.02)		
	142 | 0.43 (0.17)	161 | 0.10 (0.09)		158 | 0.02 (0.01)		
	152 | 0.43 (0.16)	176 | 0.07 (0.09)		194 | 0.03 (0.02)		
	164 | 0.50 (0.12)					
	178 | 0.27 (0.18)					

Table 112. ^{4}He production cross sections for 400 MeV/u krypton on lithium.

5	10	20	30	40	60	80
	82 | 0.13 (0.16)	81 | 0.18 (0.09)	86 | 0.05 (0.05)	90 | 0.02 (0.02)		
	87 | 0.19 (0.10)	91 | 0.12 (0.07)	110 | 0.04 (0.03)	111 | 0.01 (0.01)		
	96 | 0.02 (0.10)	96 | 0.04 (0.04)		120 | 0.02 (0.02)		
	102 | 0.11 (0.06)	102 | 0.13 (0.07)				
	108 | 0.06 (0.11)	109 | 0.04 (0.04)				
	115 | 0.08 (0.11)	117 | 0.11 (0.05)				
	122 | 0.17 (0.11)	126 | 0.04 (0.04)				
	131 | 0.01 (0.10)	136 | 0.11 (0.04)				
	140 | 0.24 (0.11)	147 | 0.09 (0.04)				

Table 113. Proton production cross sections for 400 MeV/u krypton on lead.

5	10	20	30	40	60	80
44 | 32.89 (8.17)	44 | 38.01 (7.93)	41 | 48.15 (7.78)	44 | 36.79 (5.25)	43 | 22.81 (5.39)	46 | 28.77 (4.76)	56 | 21.15 (2.88)
49 | 45.02 (7.61)	49 | 33.14 (6.21)	46 | 30.45 (4.85)	50 | 41.50 (4.97)	48 | 37.88 (5.26)	53 | 29.99 (3.80)	63 | 20.37 (2.52)
55 | 36.55 (6.83)	56 | 35.85 (5.68)	52 | 43.86 (6.32)	56 | 28.76 (5.35)	55 | 25.25 (3.90)	61 | 23.11 (3.22)	73 | 14.37 (1.84)
63 | 42.18 (7.24)	63 | 37.50 (6.21)	58 | 38.28 (5.50)	63 | 28.45 (4.84)	63 | 29.10 (4.61)	72 | 19.76 (2.72)	86 | 14.41 (1.64)
71 | 39.59 (6.44)	71 | 34.36 (6.17)	65 | 36.76 (5.11)	72 | 37.37 (4.24)	71 | 32.00 (4.42)	83 | 19.26 (2.63)	102 | 11.00 (1.34)
80 | 35.22 (5.24)	80 | 48.94 (5.67)	73 | 37.74 (5.45)	81 | 27.55 (4.63)	79 | 33.95 (4.05)	96 | 23.26 (2.57)	121 | 9.26 (1.05)
91 | 38.66 (5.49)	91 | 51.30 (5.95)	81 | 39.81 (5.58)	90 | 39.32 (4.57)	89 | 37.27 (4.50)	112 | 15.68 (1.71)	147 | 4.69 (0.60)
101 | 41.48 (5.38)	101 | 42.16 (5.25)	90 | 44.39 (5.49)	101 | 26.53 (3.74)	98 | 29.95 (4.46)	128 | 14.55 (1.68)	175 | 4.45 (0.61)
113 | 38.05 (4.43)	113 | 41.94 (4.34)	101 | 42.32 (4.43)	111 | 35.41 (4.45)	105 | 30.89 (3.99)	140 | 10.91 (1.57)	199 | 3.22 (0.47)
124 | 44.22 (5.20)	124 | 41.18 (6.61)	111 | 44.00 (5.09)	119 | 29.08 (3.72)	113 | 28.64 (3.86)	155 | 12.63 (1.52)	231 | 2.77 (0.38)
132 | 30.91 (6.64)	132 | 36.18 (6.70)	119 | 41.73 (5.81)	128 | 25.29 (3.41)	122 | 25.29 (3.18)	173 | 11.98 (1.38)	272 | 1.53 (0.24)
142 | 27.14 (6.00)	142 | 73.88 (9.82)	128 | 32.01 (5.56)	138 | 23.82 (3.87)	133 | 24.89 (3.48)	195 | 10.18 (1.10)	329 | 0.78 (0.14)
152 | 34.84 (8.19)	152 | 67.40 (10.14)	137 | 38.59 (6.41)	149 | 25.77 (6.64)	145 | 29.55 (3.68)	221 | 7.11 (0.84)	
164 | 13.34 (8.26)	164 | 66.37 (9.63)	149 | 50.66 (8.45)	162 | 26.87 (4.59)	158 | 21.61 (3.40)	255 | 5.50 (0.64)	
178 | 14.33 (5.90)	178 | 27.25 (6.41)	161 | 58.99 (7.76)	176 | 20.23 (4.35)	175 | 16.92 (2.29)	298 | 2.86 (0.40)	
		176 | 42.07 (5.58)			357 | 1.66 (0.28)	
					439 | 0.73 (0.15)	

Table 114. Deuteron production cross sections for 400 MeV/u krypton on lead.

5	10	20	30	40	60	80
28 | 39.24 (10.05)	28 | 29.24 (9.86)	27 | 23.11 (6.20)	28 | 33.29 (5.77)	27 | 31.01 (4.89)	28 | 23.01 (4.20)	34 | 12.24 (2.27)
31 | 43.72 (11.66)	31 | 33.17 (8.08)	31 | 37.13 (6.62)	32 | 36.52 (5.86)	31 | 36.30 (5.09)	33 | 23.94 (3.74)	39 | 14.06 (2.58)
35 | 19.84 (9.49)	35 | 33.79 (7.88)	35 | 37.47 (5.45)	36 | 31.32 (5.84)	35 | 29.19 (4.00)	38 | 22.74 (3.69)	44 | 9.30 (1.64)
40 | 39.06 (8.49)	39 | 49.35 (9.52)	39 | 40.49 (6.27)	40 | 30.87 (4.97)	41 | 34.98 (4.36)	43 | 18.75 (2.79)	50 | 7.72 (1.55)
45 | 36.39 (8.74)	43 | 48.56 (9.36)	44 | 44.15 (6.75)	45 | 38.36 (5.07)	46 | 36.52 (4.64)	50 | 13.49 (2.29)	56 | 7.58 (1.33)
50 | 50.95 (8.03)	48 | 49.14 (6.87)	49 | 40.43 (5.44)	51 | 27.23 (4.05)	53 | 28.38 (3.52)	57 | 17.09 (2.47)	64 | 8.08 (1.34)
56 | 32.30 (6.57)	54 | 38.53 (5.60)	55 | 27.36 (4.44)	57 | 25.54 (4.19)	60 | 24.08 (3.43)	65 | 15.52 (2.04)	71 | 5.66 (1.23)
64 | 53.71 (6.22)	60 | 23.18 (5.60)	60 | 29.28 (4.19)	63 | 32.87 (4.62)	67 | 24.49 (3.20)	74 | 9.48 (1.47)	76 | 4.14 (1.17)
72 | 34.54 (6.18)	65 | 31.25 (4.71)	66 | 37.88 (4.30)	70 | 29.98 (4.62)	76 | 24.81 (2.96)	82 | 10.43 (1.91)	82 | 4.56 (0.95)
79 | 34.05 (5.32)	72 | 29.07 (5.26)	73 | 33.95 (4.23)	77 | 26.38 (3.22)	83 | 28.28 (3.71)	88 | 5.58 (1.30)	89 | 3.14 (0.74)
88 | 30.23 (5.62)	79 | 34.92 (4.33)	80 | 38.01 (6.17)	84 | 34.28 (4.62)	89 | 17.11 (2.96)	96 | 9.42 (1.57)	98 | 1.57 (0.46)
95 | 47.91 (7.60)	85 | 35.59 (5.93)	84 | 33.88 (4.66)	90 | 15.68 (3.24)	95 | 22.39 (3.36)	104 | 9.24 (1.91)	107 | 1.42 (0.39)
101 | 33.58 (9.17)	90 | 36.19 (6.75)	89 | 33.02 (4.57)	95 | 24.10 (3.62)	103 | 19.81 (2.81)	113 | 9.66 (1.18)	
107 | 52.26 (9.54)	95 | 38.08 (7.48)	95 | 36.28 (5.35)	102 | 17.23 (5.24)	111 | 20.73 (2.96)	124 | 8.16 (1.29)	
114 | 62.15 (8.84)	101 | 42.10 (6.99)	102 | 37.16 (5.51)	109 | 28.84 (5.48)	120 | 17.88 (2.44)	137 | 6.14 (1.14)	
122 | 58.78 (6.45)	107 | 62.99 (8.34)	109 | 38.04 (6.56)	116 | 26.36 (3.17)	130 | 13.46 (1.74)		
130 | 46.70 (6.81)	114 | 63.15 (7.11)	116 | 44.67 (5.34)	125 | 23.12 (3.29)	142 | 13.43 (2.41)		
139 | 40.26 (7.01)	122 | 56.04 (7.67)	125 | 42.84 (5.10)	135 | 31.57 (5.43)			
150 | 40.83 (6.23)	130 | 61.87 (8.34)	135 | 40.41 (6.83)	147 | 26.42 (3.14)			

Table 115. Triton production cross sections for 400 MeV/u krypton on lead.

5	10	20	30	40	60	80
45 | 24.77 (6.03)	33 | 35.46 (7.69)	39 | 21.58 (3.81)	28 | 33.91 (6.83)	23 | 36.49 (5.82)	26 | 16.10 (3.26)	
51 | 28.88 (5.85)	37 | 24.88 (7.20)	44 | 25.15 (4.20)	31 | 37.23 (6.22)	26 | 28.32 (4.53)	30 | 17.94 (4.50)	
56 | 29.48 (7.21)	41 | 35.55 (6.65)	50 | 28.33 (3.73)	35 | 33.21 (6.39)	29 | 26.70 (4.48)	34 | 8.95 (1.91)	
62 | 30.29 (8.43)	44 | 26.88 (7.45)	56 | 22.79 (3.52)	39 | 16.81 (4.67)	32 | 23.40 (4.06)	40 | 12.17 (2.05)	
67 | 51.56 (7.47)	48 | 23.42 (5.54)	62 | 21.66 (3.21)	44 | 20.79 (3.17)	36 | 24.48 (3.79)	45 | 10.64 (1.94)	
72 | 30.70 (6.53)	52 | 29.40 (5.99)	67 | 17.47 (3.46)	49 | 21.29 (3.96)	40 | 14.07 (3.00)	50 | 8.54 (1.60)	
76 | 34.90 (7.52)	55 | 23.49 (8.15)	71 | 18.49 (3.55)	54 | 18.70 (3.16)	44 | 18.12 (3.09)	55 | 7.99 (1.94)	
80 | 29.78 (7.86)	58 | 23.61 (6.61)	75 | 9.53 (2.34)	59 | 20.75 (3.19)	48 | 12.36 (2.40)	58 | 7.59 (1.84)	
85 | 24.29 (5.34)	60 | 15.15 (6.83)	79 | 5.57 (1.70)	64 | 15.69 (3.83)	52 | 12.96 (3.06)	62 | 5.92 (1.59)	
	63 | 27.22 (5.98)		67 | 19.67 (3.73)	55 | 14.36 (3.18)	66 | 1.39 (1.04)	
	66 | 21.83 (5.13)		71 | 20.62 (3.70)	58 | 13.70 (3.07)		
			75 | 7.34 (1.89)	61 | 13.03 (2.69)		
				64 | 18.59 (3.27)		
				68 | 15.53 (2.80)		
				73 | 7.88 (1.85)		

Table 116. ^{3}He production cross sections for 400 MeV/u krypton on lead.

5	10	20	30	40	60	80
	100 | 13.97 (3.79)	100 | 9.41 (2.05)	106 | 8.09 (1.90)	100 | 7.91 (2.51)		
	105 | 14.55 (3.79)	106 | 9.21 (2.14)	113 | 3.78 (1.07)	107 | 4.62 (1.24)		
	111 | 12.42 (2.90)	112 | 6.52 (1.51)	120 | 2.83 (1.31)	115 | 3.80 (0.94)		
	118 | 10.52 (2.56)	120 | 8.33 (2.12)	129 | 4.70 (1.17)	124 | 2.36 (0.94)		
	125 | 7.61 (2.79)	129 | 7.70 (1.70)	138 | 4.56 (1.26)	134 | 2.01 (1.00)		
	133 | 11.13 (3.00)	138 | 8.67 (1.64)		145 | 2.14 (0.61)		
	143 | 9.49 (2.65)	149 | 6.05 (1.23)		159 | 1.97 (0.52)		
	153 | 20.14 (3.22)	162 | 6.84 (1.49)		174 | 1.38 (0.37)		
	164 | 19.80 (2.71)					
	178 | 5.78 (2.69)					

Table 117. ^{4}He production cross sections for 400 MeV/u krypton on lead.

5	10	20	30	40	60	80
	84 | 22.63 (4.89)	82 | 14.56 (2.79)	82 | 3.09 (1.45)	86 | 4.93 (1.48)		
	88 | 17.60 (4.16)	87 | 10.83 (2.44)	87 | 6.31 (1.75)	91 | 5.84 (1.40)		
	92 | 13.60 (3.69)	92 | 13.15 (2.72)	92 | 9.52 (2.15)	98 | 3.41 (0.97)		
	97 | 12.19 (3.20)	97 | 10.17 (2.09)	98 | 7.60 (1.88)	105 | 4.76 (1.14)		
	103 | 15.10 (3.06)	104 | 11.01 (2.06)	104 | 7.65 (1.69)	112 | 1.99 (0.67)		
	109 | 18.37 (3.25)	110 | 8.86 (1.74)		121 | 2.47 (0.70)		
	116 | 8.02 (2.05)	118 | 8.90 (1.71)		131 | 0.50 (0.30)		
	123 | 16.44 (3.05)	127 | 10.36 (1.79)				
	131 | 9.74 (2.38)	136 | 5.92 (1.21)				
	141 | 10.17 (2.23)	147 | 4.75 (1.04)				

Table 118. Proton production cross sections for 230 MeV/u helium on aluminum.

5	10	20	30	40	60	80
68 | 0.62 (0.11)	68 | 1.19 (0.14)	66 | 0.78 (0.11)	67 | 0.81 (0.12)	71 | 0.70 (0.09)		136 | 0.12 (0.03)
73 | 1.08 (0.12)	73 | 1.12 (0.12)	70 | 0.97 (0.11)	71 | 0.88 (0.11)	76 | 0.62 (0.07)		141 | 0.10 (0.02)
78 | 1.04 (0.13)	79 | 1.11 (0.11)	76 | 0.89 (0.09)	75 | 0.74 (0.10)	83 | 0.72 (0.08)		148 | 0.08 (0.02)
84 | 1.08 (0.11)	87 | 1.09 (0.11)	83 | 1.00 (0.10)	80 | 0.90 (0.10)	90 | 0.73 (0.07)		159 | 0.05 (0.01)
92 | 0.86 (0.09)	96 | 1.17 (0.10)	92 | 0.85 (0.08)	87 | 0.77 (0.08)	99 | 0.68 (0.07)		173 | 0.03 (0.01)
101 | 0.77 (0.09)	107 | 1.02 (0.08)	103 | 0.90 (0.08)	94 | 0.86 (0.09)	107 | 0.62 (0.06)		192 | 0.01 (0.00)
109 | 0.72 (0.08)	120 | 1.32 (0.10)	115 | 0.82 (0.07)	102 | 0.77 (0.08)	119 | 0.54 (0.05)		211 | 0.00 (0.00)
119 | 0.62 (0.07)	132 | 1.23 (0.09)	128 | 0.74 (0.06)	111 | 0.69 (0.07)	129 | 0.49 (0.06)		
129 | 0.61 (0.09)	148 | 1.36 (0.10)	144 | 0.80 (0.06)	122 | 0.67 (0.06)	138 | 0.51 (0.06)		
136 | 0.70 (0.08)	163 | 2.04 (0.15)	160 | 1.03 (0.09)	133 | 0.53 (0.05)	147 | 0.35 (0.04)		
144 | 0.54 (0.07)	174 | 2.14 (0.15)	172 | 1.00 (0.08)	141 | 0.49 (0.06)	159 | 0.39 (0.04)		
153 | 0.34 (0.05)	188 | 2.27 (0.15)	187 | 0.50 (0.05)	150 | 0.52 (0.06)	172 | 0.18 (0.02)		
163 | 0.55 (0.06)			161 | 0.54 (0.06)			
174 | 0.37 (0.05)			173 | 0.59 (0.06)			

Table 119. Deuteron production cross sections for 230 MeV/u helium on aluminum.

5	10	20	30	40	60	80
38 | 0.52 (0.13)	37 | 0.60 (0.13)	36 | 0.43 (0.09)	36 | 1.09 (0.16)	37 | 0.37 (0.08)		64 | 0.04 (0.02)
41 | 0.62 (0.11)	39 | 0.60 (0.12)	39 | 0.43 (0.09)	38 | 1.17 (0.15)	40 | 0.31 (0.06)		67 | 0.02 (0.01)
45 | 0.33 (0.09)	43 | 0.47 (0.09)	43 | 0.47 (0.08)	41 | 1.65 (0.20)	44 | 0.22 (0.04)		71 | 0.01 (0.01)
49 | 0.47 (0.09)	47 | 0.67 (0.11)	47 | 0.38 (0.07)	44 | 1.56 (0.18)	49 | 0.21 (0.04)		77 | 0.01 (0.00)
54 | 0.49 (0.09)	51 | 0.71 (0.11)	51 | 0.54 (0.08)	47 | 1.44 (0.18)	54 | 0.19 (0.04)		84 | 0.01 (0.00)
59 | 0.43 (0.08)	55 | 0.51 (0.08)	57 | 0.49 (0.07)		60 | 0.18 (0.03)		93 | 0.01 (0.00)
65 | 0.48 (0.09)	60 | 0.63 (0.10)	64 | 0.31 (0.05)		67 | 0.21 (0.04)		
70 | 0.54 (0.08)	65 | 0.49 (0.08)	71 | 0.36 (0.06)		73 | 0.18 (0.03)		
76 | 0.40 (0.06)	70 | 0.51 (0.08)	78 | 0.37 (0.05)		81 | 0.11 (0.02)		
81 | 0.63 (0.11)	76 | 0.56 (0.08)	86 | 0.30 (0.04)		89 | 0.09 (0.03)		
85 | 0.31 (0.09)	81 | 0.47 (0.09)	94 | 0.06 (0.02)		94 | 0.09 (0.02)		
89 | 0.46 (0.08)	85 | 0.48 (0.09)	99 | 0.18 (0.05)		101 | 0.10 (0.03)		
94 | 0.35 (0.07)	90 | 0.38 (0.05)	106 | 0.33 (0.06)		108 | 0.06 (0.02)		
99 | 0.06 (0.03)	94 | 0.49 (0.08)	113 | 0.23 (0.04)				
105 | 0.18 (0.05)	99 | 0.67 (0.09)					
111 | 0.29 (0.06)	105 | 0.59 (0.08)					
118 | 0.32 (0.06)	111 | 0.65 (0.08)					

Table 120. Triton production cross sections for 230 MeV/u helium on aluminum.

5	10	20	30	40	60	80
29 | 0.17 (0.07)	26 | 0.26 (0.09)	25 | 0.20 (0.08)	25 | 0.14 (0.06)	28 | 0.11 (0.05)		49 | 0.01 (0.01)
32 | 0.16 (0.06)	28 | 0.16 (0.07)	27 | 0.12 (0.05)	27 | 0.09 (0.05)	31 | 0.04 (0.02)		51 | 0.02 (0.02)
36 | 0.12 (0.04)	31 | 0.24 (0.07)	30 | 0.09 (0.04)	30 | 0.11 (0.05)	35 | 0.06 (0.02)		
40 | 0.24 (0.07)	34 | 0.38 (0.08)	32 | 0.16 (0.06)	33 | 0.19 (0.06)	39 | 0.04 (0.02)		
43 | 0.14 (0.04)	37 | 0.48 (0.10)	35 | 0.12 (0.04)	35 | 0.07 (0.03)	43 | 0.05 (0.02)		
47 | 0.13 (0.07)	41 | 0.32 (0.07)	38 | 0.18 (0.05)	39 | 0.07 (0.03)	48 | 0.04 (0.02)		
50 | 0.05 (0.05)	45 | 0.24 (0.06)	42 | 0.14 (0.05)	43 | 0.03 (0.02)	54 | 0.04 (0.02)		
53 | 0.16 (0.07)	50 | 0.10 (0.04)	44 | 0.09 (0.04)	47 | 0.05 (0.02)	59 | 0.01 (0.01)		
55 | 0.14 (0.06)	54 | 0.13 (0.04)	48 | 0.07 (0.03)	52 | 0.03 (0.02)	66 | 0.01 (0.01)		
58 | 0.14 (0.06)	59 | 0.08 (0.05)	51 | 0.06 (0.04)	56 | 0.06 (0.02)	73 | 0.01 (0.01)		
60 | 0.02 (0.02)	64 | 0.05 (0.02)	53 | 0.12 (0.05)	62 | 0.01 (0.01)			
62 | 0.13 (0.05)	68 | 0.08 (0.04)	55 | 0.10 (0.04)	68 | 0.02 (0.01)			
65 | 0.04 (0.03)	71 | 0.05 (0.03)	57 | 0.11 (0.04)				
	75 | 0.03 (0.02)	60 | 0.07 (0.03)				
	78 | 0.21 (0.06)					
	82 | 0.15 (0.05)					
	87 | 0.18 (0.02)					
	91 | 0.17 (0.03)					
	97 | 0.22 (0.05)					
	102 | 0.13 (0.04)					

Table 121. Proton production cross sections for 230 MeV/u helium on copper.

5	10	20	30	40	60	80
65 | 1.51 (0.23)	62 | 2.06 (0.30)	62 | 2.04 (0.27)	64 | 1.61 (0.23)	66 | 1.32 (0.19)		124 | 0.39 (0.08)
70 | 1.48 (0.20)	66 | 1.83 (0.25)	66 | 1.63 (0.21)	68 | 1.79 (0.22)	71 | 1.64 (0.20)		128 | 0.18 (0.04)
76 | 1.54 (0.18)	71 | 1.87 (0.21)	71 | 1.60 (0.21)	74 | 1.35 (0.16)	77 | 1.54 (0.18)		135 | 0.17 (0.04)
84 | 1.51 (0.19)	77 | 1.65 (0.20)	78 | 1.42 (0.17)	82 | 1.27 (0.15)	84 | 1.32 (0.15)		144 | 0.12 (0.02)
93 | 1.46 (0.16)	84 | 1.84 (0.20)	86 | 1.59 (0.17)	90 | 1.36 (0.14)	94 | 1.23 (0.13)		156 | 0.06 (0.02)
105 | 0.94 (0.12)	93 | 1.82 (0.18)	96 | 1.57 (0.15)	99 | 1.44 (0.16)	104 | 1.10 (0.12)		171 | 0.04 (0.01)
117 | 0.94 (0.14)	102 | 1.85 (0.19)	107 | 1.33 (0.14)	108 | 1.22 (0.13)	116 | 1.01 (0.10)		193 | 0.02 (0.01)
130 | 0.79 (0.11)	112 | 1.78 (0.17)	119 | 1.38 (0.13)	120 | 1.09 (0.11)	130 | 0.77 (0.08)		217 | 0.01 (0.00)
146 | 0.50 (0.08)	123 | 1.89 (0.16)	133 | 1.29 (0.11)	134 | 0.90 (0.09)	144 | 0.60 (0.08)		239 | 0.00 (0.00)
161 | 0.66 (0.10)	138 | 1.78 (0.14)	147 | 1.46 (0.15)	148 | 0.97 (0.11)	156 | 0.67 (0.08)		
172 | 0.40 (0.10)	151 | 2.07 (0.20)	158 | 1.57 (0.15)	159 | 1.04 (0.11)	169 | 0.32 (0.05)		
185 | 0.22 (0.06)	161 | 3.01 (0.24)	170 | 1.87 (0.16)	171 | 0.76 (0.09)			
	172 | 3.32 (0.25)		185 | 0.36 (0.06)			
	186 | 3.25 (0.24)					

Table 122. Deuteron production cross sections for 230 MeV/u helium on copper.

5	10	20	30	40	60	80
36 | 0.78 (0.20)	34 | 0.75 (0.21)	34 | 0.83 (0.19)	34 | 2.37 (0.36)	35 | 0.56 (0.14)		59 | 0.06 (0.04)
39 | 1.05 (0.21)	37 | 0.82 (0.19)	37 | 0.96 (0.19)	37 | 2.10 (0.30)	38 | 0.65 (0.14)		62 | 0.07 (0.03)
43 | 1.05 (0.19)	40 | 0.71 (0.16)	41 | 0.94 (0.17)	40 | 2.49 (0.34)	42 | 0.48 (0.10)		67 | 0.05 (0.02)
48 | 0.73 (0.16)	44 | 1.01 (0.18)	45 | 0.70 (0.15)	43 | 2.74 (0.34)	46 | 0.54 (0.11)		72 | 0.02 (0.01)
53 | 0.87 (0.18)	48 | 1.20 (0.20)	49 | 0.80 (0.14)	46 | 2.69 (0.37)	50 | 0.53 (0.10)		80 | 0.01 (0.01)
58 | 0.95 (0.15)	53 | 1.17 (0.18)	54 | 0.84 (0.14)		56 | 0.37 (0.07)		91 | 0.01 (0.01)
65 | 0.67 (0.11)	58 | 0.87 (0.14)	60 | 0.51 (0.09)		63 | 0.37 (0.08)		
72 | 0.96 (0.17)	65 | 0.83 (0.13)	67 | 0.54 (0.10)		69 | 0.36 (0.07)		
79 | 0.85 (0.13)	72 | 0.78 (0.13)	73 | 0.52 (0.11)		76 | 0.27 (0.06)		
86 | 0.66 (0.10)	79 | 0.68 (0.12)	81 | 0.58 (0.09)		83 | 0.30 (0.08)		
96 | 0.41 (0.08)	87 | 0.67 (0.11)	88 | 0.24 (0.07)		88 | 0.27 (0.07)		
104 | 0.18 (0.06)	93 | 0.80 (0.15)	93 | 0.04 (0.03)		93 | 0.15 (0.05)		
110 | 0.58 (0.13)	98 | 0.87 (0.15)	99 | 0.37 (0.09)		99 | 0.22 (0.06)		
117 | 0.26 (0.07)	104 | 0.90 (0.15)	105 | 0.69 (0.11)		106 | 0.22 (0.05)		
	110 | 0.91 (0.14)	112 | 0.27 (0.07)				

Table 123. Triton production cross sections for 230 MeV/u helium on copper.

5	10	20	30	40	60	80
28 | 0.38 (0.24)	26 | 0.52 (0.19)	24 | 0.07 (0.07)	25 | 0.34 (0.14)	26 | 0.20 (0.09)		45 | 0.05 (0.05)
31 | 0.24 (0.10)	28 | 0.26 (0.12)	26 | 0.05 (0.05)	27 | 0.11 (0.08)	29 | 0.15 (0.07)		46 | 0.05 (0.05)
34 | 0.25 (0.10)	31 | 0.42 (0.14)	29 | 0.32 (0.11)	29 | 0.44 (0.13)	32 | 0.14 (0.06)		
38 | 0.46 (0.14)	34 | 0.67 (0.16)	32 | 0.32 (0.12)	32 | 0.22 (0.08)	36 | 0.06 (0.03)		
42 | 0.17 (0.08)	38 | 0.60 (0.16)	34 | 0.39 (0.12)	36 | 0.12 (0.06)	41 | 0.06 (0.04)		
46 | 0.35 (0.10)	42 | 0.34 (0.11)	38 | 0.18 (0.07)	39 | 0.23 (0.08)	46 | 0.09 (0.04)		
50 | 0.10 (0.06)	46 | 0.20 (0.08)	41 | 0.12 (0.07)	43 | 0.04 (0.03)	52 | 0.04 (0.02)		
54 | 0.09 (0.05)	51 | 0.28 (0.08)	44 | 0.14 (0.07)	49 | 0.17 (0.06)	59 | 0.03 (0.02)		
57 | 0.28 (0.13)	56 | 0.18 (0.08)	47 | 0.32 (0.10)	54 | 0.05 (0.04)	65 | 0.06 (0.03)		
59 | 0.05 (0.05)	61 | 0.17 (0.07)	51 | 0.24 (0.08)	58 | 0.09 (0.04)	73 | 0.02 (0.01)		
62 | 0.10 (0.07)	66 | 0.06 (0.04)	56 | 0.12 (0.06)	64 | 0.05 (0.03)			
65 | 0.10 (0.07)	72 | 0.09 (0.04)					
	78 | 0.18 (0.08)					
	82 | 0.22 (0.09)					
	86 | 0.21 (0.04)					
	91 | 0.22 (0.05)					
	96 | 0.23 (0.07)					
	102 | 0.26 (0.08)					

Table 124. Proton production cross sections for 400 MeV/u nitrogen on carbon.

5	10	20	30	40	60	80
53 | 0.93 (0.16)	53 | 1.21 (0.19)	51 | 1.14 (0.19)	51 | 1.20 (0.18)	54 | 1.20 (0.17)		85 | 0.37 (0.08)
58 | 1.34 (0.16)	59 | 1.24 (0.17)	56 | 1.38 (0.18)	56 | 1.52 (0.19)	60 | 1.29 (0.14)		91 | 0.29 (0.05)
65 | 1.18 (0.15)	65 | 1.39 (0.15)	63 | 1.09 (0.13)	62 | 1.41 (0.16)	68 | 1.33 (0.15)		99 | 0.30 (0.06)
73 | 1.18 (0.16)	73 | 1.37 (0.15)	71 | 1.31 (0.15)	69 | 1.45 (0.16)	76 | 1.34 (0.13)		110 | 0.22 (0.03)
82 | 1.26 (0.15)	82 | 1.31 (0.13)	80 | 1.21 (0.13)	77 | 1.34 (0.14)	88 | 1.09 (0.11)		124 | 0.18 (0.03)
93 | 0.91 (0.10)	93 | 1.46 (0.13)	92 | 1.51 (0.14)	88 | 1.27 (0.12)	101 | 1.10 (0.11)		141 | 0.14 (0.02)
108 | 0.60 (0.07)	105 | 1.56 (0.14)	105 | 1.42 (0.14)	100 | 1.25 (0.13)	114 | 1.00 (0.09)		166 | 0.08 (0.01)
124 | 0.48 (0.06)	117 | 1.61 (0.14)	119 | 1.34 (0.12)	112 | 1.14 (0.11)	127 | 0.59 (0.08)		193 | 0.05 (0.01)
140 | 0.32 (0.05)	132 | 1.11 (0.09)	136 | 1.14 (0.10)	128 | 0.96 (0.09)	137 | 0.77 (0.10)		217 | 0.02 (0.01)
156 | 0.41 (0.07)	150 | 1.30 (0.11)	152 | 1.71 (0.17)	141 | 1.05 (0.13)	149 | 1.08 (0.12)		248 | 0.02 (0.01)
167 | 0.31 (0.06)	167 | 1.14 (0.12)	165 | 1.84 (0.18)	153 | 1.26 (0.13)	163 | 0.44 (0.06)		
181 | 0.23 (0.04)	181 | 0.69 (0.09)	179 | 0.85 (0.10)	165 | 1.33 (0.12)			
196 | 0.14 (0.04)	196 | 0.16 (0.04)		180 | 0.53 (0.08)			

Table 125. Deuteron production cross sections for 400 MeV/u nitrogen on carbon.

5	10	20	30	40	60	80
33 | 0.49 (0.17)	31 | 0.54 (0.14)	29 | 0.37 (0.16)	29 | 0.70 (0.17)	30 | 0.39 (0.11)		44 | 0.15 (0.05)
36 | 0.85 (0.16)	34 | 0.85 (0.17)	32 | 0.70 (0.17)	32 | 0.70 (0.15)	34 | 0.59 (0.10)		47 | 0.07 (0.03)
41 | 0.65 (0.12)	37 | 0.63 (0.16)	36 | 0.50 (0.12)	35 | 0.75 (0.14)	38 | 0.49 (0.10)		52 | 0.06 (0.04)
45 | 0.53 (0.11)	42 | 0.65 (0.13)	40 | 0.66 (0.12)	39 | 0.67 (0.13)	43 | 0.43 (0.10)		65 | 0.01 (0.02)
50 | 0.60 (0.11)	47 | 0.35 (0.15)	45 | 0.77 (0.13)	44 | 0.41 (0.12)	48 | 0.40 (0.07)		72 | 0.02 (0.01)
56 | 0.87 (0.13)	52 | 0.64 (0.13)	51 | 0.64 (0.11)	49 | 0.45 (0.10)	55 | 0.27 (0.07)		79 | 0.04 (0.02)
61 | 0.81 (0.13)	58 | 0.47 (0.09)	58 | 0.48 (0.08)	55 | 0.59 (0.10)	62 | 0.40 (0.07)		84 | 0.01 (0.01)
67 | 0.57 (0.12)	65 | 0.50 (0.08)	64 | 0.50 (0.10)	62 | 0.50 (0.10)	69 | 0.48 (0.07)		
73 | 0.65 (0.11)	73 | 0.60 (0.11)	71 | 0.75 (0.11)	68 | 0.42 (0.08)	77 | 0.38 (0.06)		
78 | 0.72 (0.14)	80 | 0.66 (0.10)	79 | 0.50 (0.08)	75 | 0.56 (0.09)	88 | 0.25 (0.05)		
82 | 0.56 (0.13)	89 | 0.63 (0.09)	86 | 0.15 (0.05)	83 | 0.32 (0.06)	97 | 0.34 (0.06)		
87 | 0.39 (0.10)	96 | 0.67 (0.11)	91 | 0.01 (0.01)	91 | 0.30 (0.07)	104 | 0.14 (0.06)		
108 | 0.37 (0.08)	102 | 0.87 (0.13)	97 | 0.40 (0.08)	97 | 0.29 (0.08)	112 | 0.03 (0.01)		
115 | 0.27 (0.08)	108 | 0.73 (0.11)	103 | 0.51 (0.09)	103 | 0.42 (0.09)			
123 | 0.37 (0.06)	115 | 0.52 (0.09)	110 | 0.43 (0.08)	110 | 0.23 (0.06)			
131 | 0.19 (0.04)						
141 | 0.19 (0.06)						
151 | 0.05 (0.06)						

Table 126. Triton production cross sections for 400 MeV/u nitrogen on carbon.

5	10	20	30	40	60	80
26 | 0.26 (0.10)	24 | 0.22 (0.10)	22 | 0.11 (0.14)	23 | 0.17 (0.09)	24 | 0.18 (0.07)		30 | 0.12 (0.07)
29 | 0.16 (0.12)	26 | 0.25 (0.10)	24 | 0.16 (0.08)	25 | 0.21 (0.09)	27 | 0.16 (0.06)		34 | 0.05 (0.02)
32 | 0.27 (0.14)	29 | 0.34 (0.11)	26 | 0.40 (0.12)	28 | 0.15 (0.10)	31 | 0.11 (0.04)		37 | 0.01 (0.01)
35 | 0.38 (0.11)	32 | 0.13 (0.07)	29 | 0.27 (0.11)	31 | 0.28 (0.10)	35 | 0.06 (0.04)		48 | 0.03 (0.02)
39 | 0.19 (0.07)	36 | 0.21 (0.07)	32 | 0.34 (0.11)	34 | 0.09 (0.06)	39 | 0.10 (0.04)		
43 | 0.22 (0.12)	40 | 0.29 (0.09)	35 | 0.20 (0.07)	38 | 0.15 (0.07)	44 | 0.07 (0.03)		
48 | 0.19 (0.07)	44 | 0.08 (0.10)	38 | 0.23 (0.09)	42 | 0.08 (0.04)	51 | 0.06 (0.02)		
53 | 0.19 (0.07)	50 | 0.18 (0.06)	41 | 0.17 (0.07)	46 | 0.10 (0.05)	57 | 0.03 (0.05)		
57 | 0.16 (0.06)	55 | 0.09 (0.04)	44 | 0.14 (0.06)	50 | 0.05 (0.03)	64 | 0.06 (0.02)		
	60 | 0.14 (0.06)	48 | 0.18 (0.06)	55 | 0.07 (0.03)	69 | 0.02 (0.02)		
	65 | 0.13 (0.05)	51 | 0.09 (0.06)	60 | 0.06 (0.03)	73 | 0.02 (0.02)		
	70 | 0.18 (0.07)	53 | 0.07 (0.05)	66 | -0.02 (0.04)	78 | 0.00 (0.00)		
	73 | 0.15 (0.06)	56 | 0.07 (0.08)				
	77 | 0.19 (0.07)	58 | 0.14 (0.07)				
	81 | 0.20 (0.07)	61 | 0.00 (0.00)				
	85 | 0.17 (0.03)					
	90 | 0.06 (0.02)					
	95 | 0.11 (0.08)					
	101 | 0.09 (0.07)					
	107 | 0.08 (0.04)					

Table 127. Proton production cross sections for 400 MeV/u nitrogen on copper.

5	10	20	30	40	60	80
54 | 2.90 (0.60)	53 | 5.25 (0.74)	51 | 5.77 (0.76)	53 | 5.37 (0.68)	54 | 6.04 (0.66)		89 | 1.84 (0.31)
59 | 4.22 (0.52)	58 | 5.95 (0.69)	56 | 5.15 (0.65)	58 | 5.17 (0.61)	60 | 5.04 (0.56)		95 | 1.65 (0.23)
66 | 4.17 (0.50)	64 | 4.53 (0.53)	62 | 5.65 (0.61)	65 | 4.89 (0.52)	66 | 4.36 (0.51)		102 | 1.12 (0.20)
74 | 3.50 (0.49)	71 | 5.54 (0.57)	69 | 6.31 (0.61)	73 | 5.26 (0.55)	74 | 4.63 (0.51)		113 | 1.22 (0.16)
82 | 4.05 (0.44)	79 | 4.93 (0.51)	78 | 5.31 (0.53)	82 | 5.89 (0.53)	84 | 3.95 (0.39)		127 | 0.87 (0.12)
94 | 2.78 (0.33)	90 | 5.10 (0.45)	89 | 5.20 (0.48)	94 | 5.13 (0.45)	96 | 4.13 (0.41)		143 | 0.60 (0.08)
105 | 2.44 (0.34)	100 | 4.55 (0.49)	100 | 5.75 (0.53)	107 | 4.26 (0.42)	108 | 3.76 (0.37)		167 | 0.38 (0.05)
117 | 1.90 (0.25)	111 | 4.80 (0.45)	112 | 4.88 (0.44)	120 | 4.37 (0.38)	119 | 4.35 (0.52)		193 | 0.25 (0.05)
132 | 1.36 (0.17)	124 | 4.55 (0.38)	128 | 3.41 (0.30)	137 | 2.90 (0.29)	128 | 2.22 (0.33)		217 | 0.14 (0.04)
145 | 0.65 (0.17)	141 | 3.43 (0.30)	141 | 5.05 (0.52)	153 | 4.01 (0.43)	138 | 2.97 (0.36)		247 | 0.13 (0.02)
156 | 0.86 (0.21)	156 | 4.44 (0.49)	152 | 5.39 (0.54)	166 | 3.82 (0.37)	149 | 3.31 (0.39)		288 | 0.02 (0.01)
168 | 1.09 (0.20)	168 | 3.13 (0.36)	165 | 5.71 (0.56)	180 | 1.83 (0.28)	163 | 0.95 (0.16)		
181 | 0.61 (0.15)	181 | 1.95 (0.28)	180 | 2.60 (0.31)				
197 | 0.21 (0.12)	197 | 0.31 (0.14)					

Table 128. Deuteron production cross sections for 400 MeV/u nitrogen on copper.

5	10	20	30	40	60	80
33 | 1.41 (0.60)	31 | 3.63 (0.70)	29 | 2.09 (0.58)	31 | 3.13 (0.61)	31 | 3.23 (0.56)		46 | 0.53 (0.16)
36 | 1.78 (0.42)	34 | 3.03 (0.55)	31 | 3.76 (0.75)	34 | 4.21 (0.66)	34 | 3.13 (0.46)		50 | 0.65 (0.14)
40 | 2.83 (0.47)	38 | 3.59 (0.56)	34 | 3.30 (0.56)	38 | 3.33 (0.53)	39 | 2.56 (0.45)		55 | 0.39 (0.12)
44 | 2.32 (0.54)	41 | 2.75 (0.57)	38 | 2.46 (0.46)	42 | 2.98 (0.51)	43 | 2.14 (0.39)		62 | 0.12 (0.12)
48 | 3.07 (0.47)	45 | 3.53 (0.54)	43 | 3.68 (0.54)	46 | 2.75 (0.52)	49 | 2.80 (0.37)		69 | 0.38 (0.09)
54 | 2.33 (0.40)	50 | 3.18 (0.56)	47 | 3.99 (0.52)	51 | 2.19 (0.36)	55 | 2.41 (0.34)		77 | 0.16 (0.05)
59 | 2.36 (0.41)	56 | 2.48 (0.45)	53 | 2.29 (0.36)	58 | 2.74 (0.38)	62 | 2.23 (0.31)		84 | 0.08 (0.04)
64 | 3.28 (0.50)	62 | 2.92 (0.46)	59 | 2.80 (0.42)	65 | 2.27 (0.37)	69 | 1.86 (0.27)		90 | 0.02 (0.02)
70 | 2.18 (0.38)	67 | 3.02 (0.44)	65 | 2.39 (0.41)	71 | 2.56 (0.35)	78 | 1.62 (0.24)		
77 | 3.01 (0.39)	73 | 3.35 (0.46)	71 | 3.09 (0.40)	79 | 2.27 (0.30)	88 | 1.38 (0.22)		
82 | 1.03 (0.31)	80 | 2.73 (0.36)	79 | 2.28 (0.31)	89 | 1.55 (0.22)	97 | 1.21 (0.21)		
87 | 1.70 (0.38)	87 | 3.10 (0.48)	86 | 0.52 (0.18)	97 | 1.42 (0.30)	104 | 0.52 (0.22)		
108 | 1.00 (0.25)	91 | 1.75 (0.32)	91 | 0.33 (0.14)	103 | 1.57 (0.28)	112 | 0.07 (0.04)		
115 | 0.78 (0.27)	97 | 2.79 (0.42)	97 | 1.74 (0.30)	110 | 1.22 (0.23)			
123 | 1.12 (0.18)	102 | 3.10 (0.45)	103 | 2.83 (0.39)				
131 | 0.44 (0.11)	108 | 3.79 (0.47)	110 | 2.43 (0.36)				
141 | 0.54 (0.18)	115 | 1.87 (0.30)					
151 | 0.43 (0.18)						

Table 129. Triton production cross sections for 400 MeV/u nitrogen on copper.

5	10	20	30	40	60	80
26 | 1.37 (0.42)	24 | 2.60 (0.65)	21 | 2.71 (0.68)	24 | 2.46 (0.58)	24 | 1.26 (0.34)		31 | 0.44 (0.23)
29 | 1.01 (0.44)	26 | 1.88 (0.49)	23 | 0.91 (0.35)	26 | 0.97 (0.33)	27 | 1.80 (0.35)		34 | 0.22 (0.09)
32 | 1.10 (0.36)	29 | 1.59 (0.42)	26 | 1.47 (0.43)	29 | 2.64 (0.51)	31 | 1.13 (0.26)		38 | 0.04 (0.04)
34 | 1.31 (0.36)	32 | 1.65 (0.40)	29 | 2.20 (0.47)	32 | 0.79 (0.32)	35 | 1.00 (0.25)		43 | 0.04 (0.11)
38 | 1.63 (0.39)	35 | 1.65 (0.41)	32 | 1.13 (0.37)	35 | 1.25 (0.33)	39 | 1.04 (0.28)		48 | 0.02 (0.03)
42 | 1.09 (0.28)	39 | 1.17 (0.32)	35 | 0.89 (0.27)	39 | 1.35 (0.33)	44 | 0.76 (0.17)		55 | 0.03 (0.03)
45 | 1.09 (0.32)	43 | 1.70 (0.34)	39 | 1.22 (0.30)	44 | 1.09 (0.26)	49 | 0.79 (0.19)		61 | 0.01 (0.01)
49 | 1.02 (0.32)	48 | 0.94 (0.23)	43 | 1.55 (0.38)	48 | 0.64 (0.22)	54 | 0.10 (0.18)		
53 | 0.58 (0.21)	53 | 1.26 (0.31)	46 | 1.07 (0.29)	52 | 0.73 (0.22)	60 | 0.39 (0.11)		
57 | 0.69 (0.23)	57 | 0.65 (0.20)	50 | 1.21 (0.29)	57 | 0.69 (0.20)	65 | 0.53 (0.17)		
	62 | 0.18 (0.14)	53 | 0.48 (0.24)	61 | 0.97 (0.31)	69 | 0.27 (0.11)		
	68 | 0.61 (0.18)	56 | 0.84 (0.38)	64 | 0.23 (0.36)	73 | 0.42 (0.15)		
	73 | 0.70 (0.25)	58 | 0.35 (0.20)	68 | 0.67 (0.24)	78 | 0.03 (0.03)		
	77 | 0.93 (0.28)	61 | 0.00 (0.00)	71 | 0.00 (0.00)			
	81 | 0.67 (0.23)					
	85 | 0.70 (0.12)					
	90 | 0.39 (0.08)					
	95 | 0.22 (0.24)					
	101 | 0.22 (0.25)					
	107 | 0.40 (0.15)					

Table 130. Proton production cross sections for 400 MeV/u xenon on aluminum.

5	10	20	30	40	60	80
58 | 6.08 (2.03)	46 | 8.60 (2.69)	42 | 7.56 (1.92)	43 | 9.25 (2.46)	43 | 13.19 (2.84)		46 | 2.61 (0.89)
68 | 8.27 (2.24)	52 | 11.89 (2.43)	47 | 8.81 (2.20)	49 | 7.70 (1.78)	50 | 3.89 (2.61)		54 | 5.07 (0.86)
79 | 9.43 (2.17)	60 | 10.39 (2.03)	55 | 8.47 (1.71)	56 | 10.60 (2.16)	58 | 9.08 (1.94)		65 | 3.41 (0.67)
92 | 8.18 (1.75)	69 | 17.73 (2.54)	64 | 10.02 (1.89)	64 | 11.16 (1.91)	68 | 9.60 (1.74)		79 | 2.86 (0.54)
106 | 11.76 (1.85)	79 | 12.98 (2.23)	74 | 10.19 (1.81)	74 | 11.05 (1.65)	80 | 8.08 (1.43)		96 | 2.01 (0.41)
119 | 15.95 (2.09)	92 | 9.10 (1.75)	86 | 14.03 (1.68)	86 | 10.49 (1.57)	94 | 8.67 (1.55)		115 | 1.22 (0.27)
131 | 12.97 (2.69)	106 | 12.08 (2.16)	100 | 10.20 (2.02)	100 | 10.42 (1.72)	108 | 7.32 (1.42)		134 | 1.02 (0.25)
141 | 12.20 (2.41)	119 | 17.63 (1.85)	114 | 11.93 (1.66)	114 | 11.88 (1.43)	126 | 8.22 (1.45)		150 | 1.11 (0.29)
151 | 15.50 (3.35)	136 | 12.25 (2.02)	132 | 10.62 (1.96)	132 | 11.71 (1.64)	143 | 7.31 (1.99)		170 | 0.45 (0.16)
163 | 21.61 (3.60)	151 | 13.07 (3.37)	148 | 24.44 (3.64)	148 | 17.30 (2.61)	157 | 7.96 (1.72)		
177 | 17.93 (3.06)	163 | 22.10 (3.52)	161 | 15.04 (3.01)	161 | 12.64 (2.37)			
	177 | 10.99 (2.30)	175 | 16.42 (2.33)				

Table 131.Deuteron production cross sections for 400 MeV/u xenon on aluminum.

5	10	20	30	40	60	80
45 | 7.64 (2.26)	29 | 8.15 (2.94)	27 | 3.47 (2.05)	27 | 3.65 (2.60)	26 | 2.67 (2.31)		26 | 2.59 (0.73)
53 | 3.59 (2.00)	33 | 8.57 (2.43)	31 | 4.30 (1.64)	30 | 4.65 (1.61)	30 | 2.11 (2.03)		31 | 1.79 (0.69)
61 | 7.31 (1.66)	37 | 12.86 (3.43)	35 | 7.02 (1.66)	34 | 9.00 (2.10)	35 | 2.54 (1.69)		36 | 0.58 (0.54)
70 | 6.13 (1.72)	42 | 10.54 (3.22)	40 | 6.32 (1.85)	38 | 5.24 (1.60)	40 | 7.68 (1.67)		41 | 1.85 (0.50)
79 | 13.50 (1.99)	48 | 8.82 (2.19)	45 | 5.61 (1.73)	43 | 8.08 (1.82)	45 | 4.90 (1.58)		47 | 0.93 (0.47)
87 | 15.46 (3.15)	54 | 4.30 (2.27)	51 | 3.52 (1.69)	49 | 4.90 (1.09)	52 | 4.01 (1.19)		54 | 0.27 (0.26)
98 | 24.78 (3.13)	61 | 7.94 (1.84)	57 | 7.14 (1.61)	56 | 1.87 (1.56)	60 | 3.92 (1.28)		61 | 0.58 (0.36)
107 | 8.35 (2.62)	68 | 4.97 (2.24)	62 | 6.65 (1.56)	62 | 5.11 (1.65)	67 | 4.95 (1.12)		68 | 1.45 (0.46)
114 | 9.92 (2.08)	75 | 8.52 (2.07)	69 | 5.30 (1.54)	69 | 5.92 (1.50)	75 | 3.23 (1.32)		74 | 0.48 (0.25)
	83 | 6.91 (1.76)	77 | 5.48 (1.36)	77 | 6.34 (1.44)	83 | 1.91 (1.16)		
	92 | 11.14 (1.73)	84 | 9.81 (2.34)	84 | 6.79 (1.54)	89 | 0.66 (1.17)		
	101 | 11.76 (2.66)	89 | 9.84 (2.45)	89 | 4.79 (1.41)	95 | 1.55 (1.20)		
	107 | 9.98 (2.42)	95 | 13.02 (2.43)	95 | 1.83 (1.52)	102 | 1.45 (1.20)		
	114 | 10.77 (2.40)	101 | 7.46 (1.80)	101 | 5.03 (1.39)			
		108 | 3.76 (1.87)				

Table 132. Triton production cross sections for 400 MeV/u xenon on aluminum.

5	10	20	30	40	60	80
	25 | 1.44 (3.19)	22 | 5.44 (2.20)	21 | 1.88 (1.46)	21 | 4.55 (1.79)		22 | 0.88 (0.61)
	28 | 8.69 (5.38)	25 | 5.80 (2.16)	23 | 2.28 (1.70)	24 | 3.98 (1.23)		29 | 1.07 (0.99)
	32 | 4.35 (3.40)	28 | 0.28 (2.10)	26 | 1.02 (2.06)	27 | 0.55 (1.13)		34 | 0.13 (0.13)
	36 | 5.96 (2.23)	32 | 0.80 (1.44)	30 | 2.06 (1.01)	31 | 3.08 (1.55)		40 | 0.00 (0.00)
	45 | 2.19 (1.58)	36 | 2.68 (1.31)	34 | 1.60 (1.06)	36 | -0.88 (0.91)		46 | 0.38 (0.22)
	51 | 2.46 (1.65)	41 | 1.07 (0.94)	38 | 3.72 (1.15)	41 | 0.92 (1.03)		
	57 | 2.96 (0.99)	45 | 0.50 (0.82)	42 | 1.38 (0.84)	47 | 1.95 (1.06)		
	64 | 3.44 (1.06)	49 | 2.04 (0.85)	47 | 1.72 (1.19)	55 | 0.62 (0.43)		
	71 | 1.36 (0.79)	54 | 1.60 (0.73)	51 | 0.57 (0.40)	62 | 1.52 (0.49)		
	78 | 2.70 (1.30)	59 | 0.45 (0.32)	56 | 1.64 (0.68)	70 | 1.40 (0.54)		
	84 | 3.35 (0.95)		62 | 0.39 (0.86)	80 | 1.04 (0.38)		
	89 | 3.90 (0.92)			88 | 1.85 (0.68)		
	94 | 2.74 (2.41)			94 | 0.45 (0.64)		
	100 | 3.62 (1.65)					
	106 | 4.56 (1.59)					

Table 133. Proton production cross sections for 400 MeV/u xenon on carbon.

5	10	20	30	40	60	80
60 | 4.54 (1.10)	44 | 3.47 (1.08)	45 | 4.70 (0.89)	45 | 4.84 (0.98)	45 | 4.74 (1.30)		48 | 1.57 (0.41)
71 | 4.70 (0.98)	49 | 4.97 (1.29)	51 | 4.70 (0.99)	51 | 5.52 (1.05)	52 | 5.36 (0.93)		56 | 1.82 (0.33)
83 | 5.21 (1.00)	56 | 4.52 (1.00)	59 | 6.72 (1.01)	59 | 6.08 (0.90)	61 | 4.72 (0.92)		66 | 1.56 (0.28)
97 | 6.51 (0.84)	64 | 6.86 (1.27)	67 | 5.97 (0.87)	67 | 5.88 (0.87)	72 | 4.80 (0.76)		80 | 0.85 (0.20)
112 | 6.48 (0.96)	72 | 7.64 (1.18)	76 | 5.54 (0.97)	76 | 5.72 (0.89)	83 | 3.87 (0.77)		97 | 0.59 (0.15)
127 | 6.63 (0.76)	83 | 6.05 (1.05)	84 | 6.54 (0.93)	84 | 5.95 (0.97)	94 | 3.90 (0.65)		116 | 0.56 (0.11)
141 | 6.28 (1.16)	95 | 6.77 (1.09)	94 | 6.65 (0.90)	94 | 4.25 (0.65)	108 | 3.39 (0.54)		135 | 0.35 (0.09)
152 | 11.26 (1.71)	106 | 6.18 (1.03)	103 | 3.87 (1.21)	107 | 5.47 (0.73)	121 | 2.92 (0.56)		151 | 0.30 (0.10)
164 | 15.17 (1.84)	119 | 9.77 (0.99)	110 | 5.85 (1.01)	118 | 5.64 (0.76)	132 | 2.75 (0.90)		171 | 0.10 (0.08)
177 | 13.55 (1.58)	132 | 7.97 (1.47)	118 | 5.88 (0.97)	127 | 5.17 (1.02)	144 | 3.58 (0.90)		
	141 | 7.28 (1.32)	127 | 5.55 (1.14)	137 | 6.11 (0.98)	157 | 4.55 (0.81)		
	152 | 11.74 (1.78)	137 | 8.51 (1.42)	148 | 8.25 (1.23)			
	164 | 11.88 (1.69)	148 | 8.80 (1.58)	161 | 6.27 (1.06)			
	177 | 7.06 (1.13)	161 | 8.76 (1.40)				
	193 | 0.32 (0.54)	176 | 6.33 (0.95)				
	211 | 0.00 (0.00)					

Table 134. Deuteron production cross sections for 400 MeV/u xenon on carbon.

5	10	20	30	40	60	80
47 | 3.54 (1.16)	30 | 5.24 (1.28)	27 | 1.26 (0.84)	26 | 2.10 (1.23)	27 | 3.10 (0.91)		27 | 1.35 (0.34)
54 | 1.36 (1.08)	34 | 3.45 (1.21)	30 | 2.97 (0.84)	29 | 3.34 (0.86)	31 | 1.44 (0.77)		31 | 0.42 (0.38)
61 | 2.55 (0.81)	38 | 7.43 (1.84)	34 | 2.60 (0.95)	33 | 2.66 (0.77)	36 | 2.56 (0.85)		36 | 0.61 (0.27)
68 | 2.35 (0.90)	43 | 2.90 (1.38)	38 | 1.97 (0.64)	37 | 1.71 (0.72)	42 | 2.43 (0.55)		42 | 0.56 (0.17)
75 | 3.28 (0.80)	48 | 2.88 (0.96)	43 | 1.31 (0.89)	41 | 2.32 (0.56)	48 | 1.79 (0.58)		48 | 0.32 (0.17)
83 | 7.19 (1.22)	55 | 3.36 (0.93)	49 | 1.50 (0.68)	47 | 2.78 (0.67)	54 | 1.43 (0.46)		54 | 0.19 (0.13)
90 | 5.45 (2.02)	62 | 4.25 (0.95)	54 | 2.00 (0.73)	52 | 2.12 (0.63)	60 | 1.36 (0.54)		64 | 0.06 (0.15)
95 | 8.30 (1.76)	68 | 3.27 (1.14)	60 | 3.67 (0.78)	57 | 1.18 (0.93)	67 | 1.45 (0.43)		69 | 0.22 (0.12)
101 | 6.46 (1.75)	75 | 4.09 (1.00)	66 | 2.80 (0.59)	63 | 2.09 (0.69)	75 | 0.64 (0.44)		74 | 0.06 (0.06)
107 | 4.23 (1.24)	83 | 3.83 (0.87)	71 | 2.53 (0.98)	69 | 2.09 (0.61)	83 | 0.44 (0.46)		
114 | 4.81 (1.06)	90 | 2.70 (0.78)	75 | 1.61 (0.68)	75 | 1.43 (0.71)	89 | 1.08 (0.46)		
	95 | 5.56 (1.25)	79 | 1.00 (0.71)	79 | 1.68 (0.70)	95 | 1.57 (0.51)		
	101 | 5.96 (1.29)	84 | 3.09 (0.92)	84 | 2.34 (0.59)	102 | 0.77 (0.51)		
	107 | 5.00 (1.18)	89 | 3.39 (0.99)	89 | 1.04 (0.47)			
	114 | 3.70 (1.01)	95 | 5.31 (1.01)	95 | 1.27 (0.68)			
	121 | 1.48 (0.52)	101 | 3.60 (0.88)	101 | 2.12 (0.59)			
		108 | 2.11 (0.78)	108 | 0.32 (0.45)			

Table 135. Triton production cross sections for 400 MeV/u xenon on carbon.

5	10	20	30	40	60	80
	25 | 2.28 (1.05)	22 | 1.74 (0.86)	20 | 1.39 (0.74)	20 | 1.25 (1.67)		20 | 0.32 (0.16)
	27 | 0.29 (2.16)	24 | 1.84 (0.85)	22 | 1.44 (0.79)	26 | 0.32 (0.28)		23 | 0.37 (0.24)
	35 | 2.31 (0.91)	27 | 1.98 (1.07)	25 | 0.51 (0.44)	33 | 0.89 (0.73)		29 | 0.55 (0.44)
	39 | 0.92 (0.60)	29 | 0.32 (0.90)	28 | 0.81 (0.73)	43 | 0.44 (0.25)		34 | 0.23 (0.11)
	44 | 0.95 (0.78)	33 | 0.85 (0.51)	30 | 0.40 (0.37)	48 | 0.97 (0.75)		40 | 0.05 (0.05)
	49 | 0.56 (0.71)	36 | 0.49 (0.66)	34 | 0.77 (0.50)	59 | 0.12 (0.09)		46 | 0.12 (0.07)
	54 | 0.53 (0.45)	38 | 1.58 (0.58)	38 | 0.74 (0.34)	64 | 0.21 (0.15)		53 | 0.03 (0.03)
	59 | 0.46 (0.40)	41 | 0.14 (0.50)	42 | 0.67 (0.35)	68 | 0.48 (0.33)		
	64 | 0.99 (0.38)	45 | 0.14 (0.32)	47 | -0.19 (0.33)	72 | 0.23 (0.24)		
	69 | 0.92 (0.71)	48 | 0.21 (0.21)	51 | 0.29 (0.17)	77 | 0.32 (0.13)		
	72 | 0.23 (0.23)	50 | 1.62 (0.69)	56 | 0.57 (0.26)	82 | 0.18 (0.15)		
	76 | 1.29 (0.59)	52 | 0.56 (0.33)	62 | -0.19 (0.33)	88 | 0.15 (0.36)		
	80 | 1.74 (1.12)	55 | 0.69 (0.41)		94 | 0.20 (0.29)		
	84 | 2.03 (0.63)	57 | 0.55 (0.39)				
	89 | 2.24 (0.95)					
	94 | 1.06 (1.07)					
	100 | 1.45 (0.75)					
	106 | 0.55 (0.59)					

Table 136. Proton production cross sections for 400 MeV/u xenon on copper.

5	10	20	30	40	60	80
61 | 13.65 (3.18)	45 | 21.89 (3.87)	42 | 21.84 (3.54)	43 | 19.68 (3.99)	44 | 28.55 (4.21)		51 | 14.29 (1.93)
71 | 16.60 (2.81)	51 | 20.05 (3.87)	48 | 14.04 (3.10)	48 | 25.45 (3.42)	51 | 19.97 (3.34)		60 | 9.44 (1.35)
84 | 16.22 (2.84)	57 | 19.08 (3.51)	54 | 22.64 (3.42)	55 | 17.83 (3.49)	59 | 20.63 (3.03)		72 | 6.91 (1.04)
98 | 19.83 (2.47)	64 | 26.23 (3.70)	62 | 17.74 (2.92)	62 | 23.26 (3.18)	68 | 15.91 (2.45)		88 | 5.85 (0.80)
112 | 23.28 (2.86)	73 | 27.29 (3.68)	70 | 21.53 (3.05)	71 | 19.17 (2.49)	81 | 16.28 (2.17)		107 | 5.15 (0.69)
128 | 23.73 (2.68)	81 | 22.58 (3.75)	82 | 24.77 (2.74)	80 | 15.79 (2.88)	94 | 15.92 (2.32)		129 | 3.45 (0.46)
141 | 20.69 (3.48)	90 | 20.93 (3.46)	94 | 28.00 (3.25)	89 | 23.37 (2.93)	108 | 19.15 (2.33)		152 | 2.16 (0.44)
152 | 31.52 (4.72)	100 | 23.14 (3.13)	107 | 24.23 (3.13)	100 | 17.01 (2.47)	121 | 15.65 (2.47)		172 | 1.62 (0.31)
164 | 42.36 (5.33)	112 | 22.85 (2.67)	123 | 22.10 (2.49)	111 | 23.35 (2.51)	132 | 15.74 (2.95)		
177 | 32.58 (4.30)	123 | 28.32 (2.85)	137 | 22.80 (4.23)	118 | 20.16 (2.46)	144 | 15.59 (2.92)		
	132 | 22.95 (4.11)	148 | 32.57 (5.03)	127 | 22.84 (3.38)	158 | 21.61 (2.67)		
	141 | 20.10 (3.84)	161 | 33.81 (4.42)	137 | 18.23 (3.08)			
	152 | 39.54 (5.26)	176 | 28.36 (3.46)	148 | 30.49 (3.95)			
	164 | 35.10 (4.87)		161 | 23.21 (3.36)			
	177 | 21.56 (3.41)					

Table 137. Deuteron production cross sections for 400 MeV/u xenon on copper.

5	10	20	30	40	60	80
47 | 14.53 (3.49)	29 | 12.90 (4.43)	28 | 12.75 (3.30)	26 | 12.88 (4.37)	27 | 15.34 (2.84)		30 | 7.23 (1.48)
55 | 7.77 (3.11)	32 | 15.33 (3.42)	32 | 13.34 (3.08)	29 | 13.48 (3.11)	31 | 11.62 (2.91)		34 | 4.64 (1.05)
64 | 19.63 (2.83)	36 | 24.61 (4.55)	37 | 17.95 (2.95)	33 | 16.96 (3.23)	36 | 15.38 (3.22)		40 | 4.93 (1.06)
73 | 16.10 (2.45)	40 | 19.27 (6.40)	42 | 14.72 (3.15)	37 | 16.68 (3.37)	42 | 11.45 (1.98)		47 | 2.79 (0.75)
83 | 36.40 (4.23)	44 | 18.52 (4.05)	47 | 12.91 (2.78)	42 | 18.69 (2.97)	48 | 10.42 (2.10)		54 | 2.60 (0.69)
92 | 35.39 (4.52)	50 | 18.09 (3.53)	53 | 15.10 (2.88)	47 | 12.47 (2.43)	54 | 10.46 (2.49)		62 | 1.66 (0.58)
101 | 43.28 (6.16)	56 | 14.29 (3.48)	60 | 16.13 (2.80)	52 | 14.54 (2.81)	60 | 11.82 (2.16)		69 | 1.31 (0.48)
107 | 16.45 (3.73)	62 | 20.97 (3.29)	66 | 17.98 (2.69)	57 | 9.88 (3.34)	67 | 8.78 (1.65)		75 | 1.19 (0.44)
114 | 19.29 (3.16)	68 | 19.56 (3.79)	73 | 15.70 (2.54)	63 | 12.06 (2.62)	73 | 5.03 (2.17)		
	75 | 18.91 (3.26)	79 | 17.65 (3.53)	69 | 16.30 (2.64)	78 | 9.48 (2.53)		
	81 | 17.79 (4.47)	84 | 31.49 (4.45)	75 | 14.29 (3.60)	83 | 6.56 (1.88)		
	85 | 16.82 (3.92)	89 | 26.83 (4.18)	79 | 12.00 (2.88)	89 | 6.05 (1.65)		
	90 | 22.06 (3.50)	95 | 37.53 (4.54)	84 | 11.53 (2.29)	95 | 9.50 (2.09)		
	95 | 19.28 (3.62)	101 | 18.93 (3.04)	89 | 10.01 (2.26)	102 | 6.44 (2.02)		
	101 | 27.75 (4.26)		95 | 9.72 (2.61)			
	107 | 21.23 (3.71)		101 | 15.38 (2.56)			
	114 | 16.13 (3.20)					

Table 138. Triton production cross sections for 400 MeV/u xenon on copper.

5	10	20	30	40	60	80
	25 | 8.53 (3.32)	22 | 5.63 (2.74)	21 | 8.43 (3.18)	21 | 11.28 (2.96)		20 | 2.11 (0.88)
	27 | 10.11 (7.44)	24 | 11.05 (3.39)	23 | 5.44 (2.47)	24 | 7.28 (2.75)		23 | 3.20 (1.10)
	31 | 12.47 (5.21)	27 | 4.65 (3.27)	26 | 7.19 (3.41)	27 | 2.59 (1.76)		26 | 0.32 (0.87)
	35 | 9.87 (2.73)	30 | 5.03 (2.47)	29 | 8.98 (2.77)	31 | 6.44 (2.93)		30 | 3.20 (1.51)
	39 | 6.06 (2.20)	34 | 4.36 (1.77)	32 | 5.88 (1.90)	35 | 4.24 (1.32)		33 | 2.51 (0.87)
	44 | 4.74 (2.40)	37 | 6.20 (2.54)	35 | 6.92 (2.16)	39 | 2.11 (1.47)		37 | 0.96 (0.49)
	49 | 4.87 (2.47)	40 | 8.10 (2.66)	38 | 3.99 (1.66)	45 | 5.58 (1.73)		40 | 1.28 (0.75)
	54 | 8.80 (2.20)	43 | 7.13 (2.19)	41 | 3.28 (1.35)	51 | 2.86 (1.05)		42 | 0.32 (0.32)
	59 | 7.31 (1.99)	47 | 8.37 (2.31)	45 | 4.39 (2.02)	56 | 3.38 (1.02)		45 | 0.28 (0.28)
	64 | 9.96 (2.03)	50 | 9.90 (2.93)	48 | 7.59 (3.07)	63 | 5.84 (1.13)		48 | 0.26 (0.26)
	69 | 5.53 (2.42)	52 | 3.98 (1.80)	50 | 9.09 (2.94)	70 | 1.98 (0.72)		51 | 0.83 (0.49)
	72 | 5.73 (1.95)	55 | 6.99 (2.38)	52 | 6.18 (2.22)	77 | 3.03 (0.82)		
	76 | 19.89 (3.53)	57 | 5.94 (2.14)	55 | 2.87 (1.44)	82 | 1.75 (0.80)		
	80 | 9.61 (3.45)		57 | 2.12 (1.24)	88 | 3.27 (1.00)		
	84 | 10.35 (3.38)		60 | 2.85 (2.72)	94 | 2.69 (1.11)		
	89 | 10.81 (1.86)		63 | 5.07 (1.72)			
	94 | 5.35 (3.30)					
	100 | 7.29 (2.35)					
	106 | 10.62 (2.53)					

Table 139. Proton production cross sections for 400 MeV/u xenon on lithium.

5	10	20	30	40	60	80
61 | 2.74 (0.44)	46 | 3.37 (0.56)	43 | 3.29 (0.47)	44 | 2.35 (0.48)	50 | 3.56 (0.52)		52 | 0.86 (0.19)
72 | 3.70 (0.42)	52 | 3.32 (0.53)	49 | 2.87 (0.44)	49 | 2.77 (0.38)	59 | 2.56 (0.36)		59 | 0.88 (0.15)
84 | 3.35 (0.42)	58 | 3.47 (0.54)	55 | 2.46 (0.38)	55 | 3.88 (0.50)	69 | 2.55 (0.31)		68 | 0.83 (0.14)
98 | 4.20 (0.39)	65 | 4.07 (0.51)	62 | 3.46 (0.41)	62 | 2.93 (0.38)	81 | 2.54 (0.30)		80 | 0.67 (0.10)
113 | 5.21 (0.48)	73 | 4.40 (0.50)	71 | 3.14 (0.37)	71 | 3.26 (0.36)	95 | 2.61 (0.29)		94 | 0.36 (0.08)
128 | 5.25 (0.45)	84 | 3.92 (0.44)	80 | 3.71 (0.42)	81 | 2.99 (0.40)	109 | 2.19 (0.27)		110 | 0.33 (0.06)
147 | 6.89 (0.54)	95 | 3.83 (0.45)	90 | 4.35 (0.43)	90 | 3.00 (0.35)	122 | 1.98 (0.31)		126 | 0.24 (0.05)
164 | 8.72 (0.77)	107 | 4.24 (0.45)	101 | 3.84 (0.42)	101 | 3.29 (0.36)	133 | 2.38 (0.37)		140 | 0.10 (0.03)
178 | 7.86 (0.67)	120 | 5.19 (0.43)	111 | 4.56 (0.56)	111 | 4.26 (0.48)	145 | 2.43 (0.39)		156 | 0.12 (0.04)
	132 | 5.58 (0.62)	119 | 4.68 (0.48)	119 | 2.97 (0.33)	158 | 2.68 (0.33)		176 | 0.06 (0.02)
	142 | 4.99 (0.58)	128 | 4.52 (0.50)	128 | 3.26 (0.42)			
	152 | 7.43 (0.75)	137 | 4.86 (0.57)	138 | 3.48 (0.41)			
	164 | 7.68 (0.71)	149 | 6.99 (0.69)	149 | 4.53 (0.50)			
	178 | 4.66 (0.48)	162 | 6.83 (0.64)	162 | 4.75 (0.46)			

Table 140. Deuteron production cross sections for 400 MeV/u xenon on lithium.

5	10	20	30	40	60	80
47 | 1.56 (0.38)	29 | 1.85 (0.55)	27 | 0.94 (0.35)	27 | 0.37 (0.38)	26 | 1.22 (0.50)		29 | 0.41 (0.12)
55 | 1.05 (0.33)	32 | 1.69 (0.42)	30 | 1.21 (0.31)	30 | 0.65 (0.35)	30 | 0.28 (0.49)		33 | 0.34 (0.12)
64 | 1.84 (0.31)	36 | 3.30 (0.63)	35 | 1.38 (0.31)	33 | 1.40 (0.32)	34 | 0.93 (0.30)		38 | 0.10 (0.08)
73 | 1.53 (0.28)	41 | 2.47 (0.60)	39 | 1.47 (0.31)	38 | 0.87 (0.28)	39 | 0.97 (0.24)		44 | 0.17 (0.06)
83 | 5.29 (0.59)	46 | 1.99 (0.44)	43 | 1.02 (0.31)	42 | 1.28 (0.25)	44 | 0.64 (0.25)		50 | 0.19 (0.08)
93 | 4.93 (0.57)	52 | 0.87 (0.37)	49 | 0.96 (0.27)	47 | 0.84 (0.22)	50 | 0.88 (0.20)		56 | 0.05 (0.04)
101 | 7.03 (0.84)	59 | 1.89 (0.34)	55 | 1.02 (0.29)	52 | 0.60 (0.21)	57 | 1.16 (0.23)		62 | 0.01 (0.07)
107 | 2.72 (0.50)	65 | 2.40 (0.40)	60 | 1.15 (0.26)	57 | 0.49 (0.32)	64 | 0.77 (0.19)		66 | 0.04 (0.06)
114 | 1.84 (0.37)	72 | 0.67 (0.35)	66 | 1.73 (0.29)	63 | 1.14 (0.28)	71 | 0.27 (0.16)		71 | 0.15 (0.06)
	79 | 1.80 (0.34)	71 | 1.37 (0.39)	68 | 1.15 (0.33)	78 | 0.64 (0.27)		77 | 0.03 (0.02)
	85 | 1.61 (0.43)	75 | 1.43 (0.34)	71 | 1.05 (0.34)	83 | 0.30 (0.17)		
	90 | 1.84 (0.33)	80 | 1.36 (0.35)	75 | 1.01 (0.32)	89 | 0.56 (0.21)		
	95 | 1.14 (0.34)	84 | 2.01 (0.39)	80 | 0.81 (0.27)	95 | 0.54 (0.17)		
	101 | 2.98 (0.49)	90 | 1.33 (0.36)	84 | 0.75 (0.21)	103 | 0.39 (0.23)		
	107 | 2.82 (0.46)	95 | 2.03 (0.37)	90 | 0.66 (0.20)			
	114 | 2.47 (0.42)	102 | 1.69 (0.31)	95 | 0.92 (0.28)			
			102 | 1.11 (0.27)			
			109 | 0.19 (0.16)			

Table 141.Triton production cross sections for 400 MeV/u xenon on lithium.

5	10	20	30	40	60	80
	25 | 1.51 (0.54)	22 | 1.00 (0.36)	20 | 0.31 (0.24)	21 | 0.83 (0.64)		22 | 0.18 (0.09)
	28 | 2.18 (0.89)	24 | 0.65 (0.30)	22 | 0.08 (0.17)	23 | 0.06 (0.39)		26 | 0.21 (0.13)
	32 | 1.98 (0.53)	27 | 0.58 (0.36)	25 | 0.23 (0.17)	26 | 0.33 (0.15)		29 | 0.19 (0.17)
	36 | 0.72 (0.31)	31 | 0.91 (0.33)	28 | 0.12 (0.20)	30 | 0.15 (0.29)		34 | 0.06 (0.04)
	45 | 0.24 (0.16)	34 | 0.41 (0.19)	31 | 0.47 (0.21)	45 | 0.32 (0.16)		38 | 0.03 (0.03)
	51 | 0.74 (0.31)	37 | 0.56 (0.24)	34 | 0.45 (0.21)	51 | 0.11 (0.08)		42 | 0.06 (0.04)
	56 | 0.39 (0.16)	40 | 0.12 (0.18)	37 | 0.12 (0.08)	56 | 0.03 (0.05)		48 | 0.02 (0.02)
	62 | 0.34 (0.17)	43 | 0.02 (0.10)	40 | 0.31 (0.16)	63 | 0.12 (0.05)		54 | 0.01 (0.01)
	68 | 0.19 (0.12)	47 | 0.07 (0.11)	43 | 0.12 (0.14)	77 | 0.19 (0.09)		
	73 | 0.18 (0.13)	51 | 0.27 (0.12)	48 | 0.03 (0.17)	83 | 0.23 (0.11)		
	76 | 0.56 (0.21)	56 | 0.03 (0.03)	50 | 0.20 (0.14)	88 | 0.12 (0.08)		
	80 | 0.13 (0.30)		53 | 0.53 (0.22)	95 | 0.07 (0.09)		
	85 | 0.68 (0.23)		58 | 0.01 (0.09)			
	89 | 0.83 (0.21)		64 | 0.05 (0.05)			
	95 | 0.51 (0.39)					
	100 | 0.37 (0.23)					
	107 | 0.11 (0.18)					

Table 142. Proton production cross sections for 400 MeV/u xenon on lead.

5	10	20	30	40	60	80
58 | 23.82 (8.03)	45 | 52.52 (10.78)	42 | 39.54 (7.91)	45 | 36.99 (7.86)	43 | 53.83 (11.56)		50 | 33.11 (5.33)
68 | 28.39 (8.54)	51 | 42.56 (10.14)	48 | 46.79 (8.71)	52 | 50.86 (8.73)	50 | 28.16 (9.37)		59 | 25.82 (3.84)
79 | 38.19 (7.54)	58 | 36.11 (8.63)	55 | 41.89 (6.93)	59 | 62.91 (8.49)	59 | 50.02 (7.98)		71 | 19.67 (3.02)
92 | 26.71 (6.16)	67 | 61.13 (9.49)	64 | 54.26 (7.87)	67 | 52.20 (7.15)	68 | 41.63 (7.51)		87 | 16.46 (2.27)
106 | 39.53 (7.06)	76 | 39.65 (8.66)	74 | 42.56 (7.31)	76 | 45.40 (8.66)	78 | 41.28 (7.90)		106 | 16.47 (2.25)
120 | 49.73 (6.79)	88 | 41.79 (8.19)	87 | 51.41 (6.46)	84 | 39.32 (7.13)	88 | 34.12 (5.96)		129 | 10.55 (1.52)
136 | 33.79 (6.73)	100 | 37.69 (7.87)	100 | 41.09 (7.32)	94 | 43.49 (6.05)	101 | 30.34 (5.60)		152 | 8.96 (1.65)
152 | 58.33 (12.58)	112 | 66.41 (9.08)	114 | 56.76 (6.31)	107 | 56.32 (6.60)	112 | 33.59 (4.84)		171 | 6.05 (1.20)
164 | 57.04 (12.50)	123 | 76.32 (10.03)	127 | 35.00 (8.09)	118 | 44.92 (6.42)	121 | 45.51 (8.83)		
177 | 52.02 (11.13)	132 | 53.86 (12.17)	137 | 55.22 (11.25)	127 | 48.59 (8.20)	132 | 43.97 (8.38)		
	141 | 49.41 (10.06)	148 | 77.76 (12.16)	137 | 37.63 (7.20)	144 | 44.29 (8.73)		
	152 | 73.86 (14.05)	161 | 74.06 (11.64)	148 | 56.21 (9.43)	158 | 43.65 (7.21)		
	164 | 76.27 (13.25)	176 | 51.12 (7.66)	161 | 50.94 (8.22)	174 | 6.41 (2.69)		
	177 | 31.91 (8.46)					

Table 143. Deuteron production cross sections for 400 MeV/u xenon on lead.

5	10	20	30	40	60	80
45 | 32.92 (8.87)	29 | 35.69 (12.34)	28 | 23.00 (8.30)	27 | 45.96 (12.10)	27 | 60.32 (10.86)		28 | 26.56 (4.95)
53 | 31.14 (10.30)	32 | 41.73 (12.24)	31 | 43.39 (8.66)	30 | 53.50 (9.48)	31 | 36.71 (10.16)		33 | 26.69 (4.64)
61 | 38.59 (7.77)	36 | 58.01 (13.10)	35 | 48.89 (8.16)	34 | 47.94 (8.70)	35 | 54.63 (11.10)		38 | 19.09 (3.66)
70 | 39.91 (7.35)	41 | 68.11 (15.73)	40 | 57.82 (9.41)	39 | 29.80 (7.00)	40 | 41.22 (9.16)		44 | 13.86 (2.87)
79 | 50.69 (7.94)	46 | 58.91 (10.86)	45 | 58.14 (9.13)	43 | 59.29 (8.86)	46 | 41.51 (7.34)		51 | 15.11 (3.34)
87 | 74.96 (12.22)	52 | 30.47 (9.84)	51 | 41.16 (7.86)	49 | 50.81 (7.05)	51 | 27.16 (6.14)		58 | 8.78 (2.00)
95 | 101.41 (16.67)	58 | 47.01 (8.03)	57 | 38.87 (7.00)	54 | 23.69 (8.10)	57 | 32.14 (7.02)		64 | 9.40 (3.39)
101 | 114.28 (17.93)	65 | 59.24 (11.23)	63 | 44.57 (7.17)	60 | 46.96 (9.55)	63 | 30.98 (5.65)		69 | 5.15 (1.40)
107 | 46.61 (12.17)	71 | 36.11 (9.95)	69 | 53.78 (7.81)	66 | 40.27 (6.41)	69 | 26.48 (5.60)		75 | 5.88 (2.12)
114 | 47.91 (9.16)	79 | 39.96 (8.51)	75 | 41.27 (8.51)	71 | 43.18 (9.54)	73 | 18.54 (7.24)		
	85 | 25.64 (5.91)	79 | 52.67 (9.72)	75 | 45.26 (9.35)	78 | 21.38 (4.68)		
	90 | 40.48 (6.86)	84 | 96.76 (12.60)	79 | 22.21 (4.32)	83 | 20.80 (4.66)		
	95 | 62.88 (11.90)	89 | 84.40 (11.70)	84 | 29.06 (4.24)	89 | 17.66 (4.53)		
	101 | 72.36 (12.81)	95 | 87.24 (11.26)	89 | 24.76 (5.68)	95 | 29.05 (6.38)		
	107 | 47.47 (9.12)	101 | 55.89 (8.21)	95 | 35.07 (7.44)	102 | 21.86 (5.13)		
	114 | 41.59 (9.83)		101 | 39.18 (6.68)			

Table 144. Triton production cross sections for 400 MeV/u xenon on lead.

5	10	20	30	40	60	80
	24 | 38.85 (12.31)	22 | 48.79 (11.45)	21 | 38.60 (10.28)	21 | 55.00 (13.47)		21 | 9.58 (2.60)
	27 | 43.33 (22.43)	24 | 44.65 (10.47)	23 | 26.27 (8.45)	24 | 35.52 (9.12)		24 | 13.94 (4.20)
	30 | 20.52 (16.48)	27 | 36.35 (11.01)	26 | 27.89 (8.44)	27 | 25.83 (8.93)		27 | 12.52 (4.44)
	34 | 42.38 (13.47)	30 | 21.59 (7.52)	29 | 34.71 (8.70)	31 | 28.43 (8.90)		31 | 13.98 (4.62)
	38 | 28.61 (7.51)	34 | 41.31 (8.21)	32 | 29.43 (7.01)	35 | 21.81 (6.86)		35 | 6.96 (2.68)
	42 | 25.58 (7.07)	38 | 33.41 (7.24)	35 | 22.75 (6.13)	39 | 14.78 (4.88)		39 | 9.39 (2.64)
	47 | 21.76 (5.94)	41 | 27.10 (7.65)	38 | 29.19 (7.33)	44 | 26.00 (5.50)		42 | 2.06 (1.20)
	52 | 24.29 (8.88)	45 | 31.79 (7.29)	41 | 25.78 (6.46)	48 | 23.64 (6.08)		45 | 1.23 (0.87)
	56 | 27.69 (6.45)	48 | 30.79 (8.77)	45 | 34.95 (7.98)	53 | 11.51 (3.08)		48 | 5.67 (2.95)
	61 | 39.06 (9.16)	50 | 17.48 (6.30)	49 | 15.24 (4.66)	57 | 25.03 (6.26)		51 | 3.18 (1.33)
	66 | 20.46 (8.19)	52 | 41.35 (9.61)	52 | 17.21 (6.19)	61 | 33.28 (7.53)		
	69 | 19.65 (6.22)	55 | 22.88 (6.79)	55 | 20.62 (6.36)	64 | 25.59 (6.50)		
	72 | 30.57 (9.65)	57 | 14.74 (5.30)	57 | 33.13 (8.08)	68 | 17.26 (4.95)		
	76 | 49.47 (11.40)		60 | 19.05 (8.17)	72 | 6.91 (3.58)		
	80 | 30.82 (9.75)		63 | 13.81 (4.70)	77 | 9.08 (1.70)		
	84 | 26.75 (5.99)		67 | 12.32 (4.43)	82 | 7.06 (2.45)		
	89 | 34.03 (6.48)			88 | 13.95 (3.99)		
	94 | 16.02 (8.84)			94 | 7.51 (3.88)		
	100 | 26.16 (8.13)					
	106 | 19.58 (5.34)					

Table 145. Proton production cross sections for 400 MeV/u xenon on aluminum.

5	10	20	30	40	60	80
50 | 6.29 (6.06)	45 | 7.26 (5.08)	46 | 12.55 (3.09)		43 | 9.77 (3.28)		50 | 1.47 (0.64)
58 | 18.71 (6.31)	50 | 21.65 (5.95)	53 | 9.35 (3.12)		50 | 6.77 (2.47)		60 | 2.26 (0.77)
66 | 13.60 (5.50)	57 | 13.18 (5.74)	61 | 7.71 (2.69)		58 | 9.28 (2.95)		74 | 4.60 (0.99)
76 | 16.13 (4.89)	64 | 14.11 (5.80)	70 | 12.05 (3.37)		68 | 6.67 (2.05)		92 | 1.52 (0.48)
85 | 21.52 (5.44)	72 | 20.81 (5.04)	79 | 12.83 (3.60)		78 | 12.05 (2.92)		115 | 2.48 (0.56)
94 | 14.85 (4.36)	81 | 9.89 (5.57)	89 | 16.31 (3.57)		88 | 9.82 (2.60)		142 | 0.68 (0.26)
103 | 18.59 (6.40)	90 | 22.85 (6.13)	100 | 17.93 (2.92)		97 | 15.14 (4.51)		170 | 1.25 (0.36)
109 | 13.80 (5.06)	100 | 31.12 (5.91)	110 | 15.15 (3.01)		104 | 4.32 (4.15)		195 | 0.72 (0.23)
116 | 26.17 (6.90)	109 | 20.10 (7.04)	118 | 9.39 (4.68)		112 | 8.97 (2.72)		227 | 0.18 (0.09)
123 | 22.70 (6.47)	116 | 21.19 (7.82)	127 | 11.63 (3.69)		121 | 11.22 (3.13)		
131 | 26.96 (8.82)	123 | 16.39 (5.41)	137 | 14.27 (4.33)		131 | 7.33 (2.94)		
141 | 41.79 (9.63)	131 | 7.97 (6.67)	148 | 23.01 (5.32)		143 | 9.17 (3.11)		
151 | 42.98 (10.29)	141 | 15.04 (6.77)	161 | 7.87 (5.66)				
	151 | 28.24 (7.82)	175 | 11.42 (3.59)				
	163 | 22.32 (7.65)					

Table 146. Deuteron production cross sections for 400 MeV/u xenon on aluminum.

5	10	20	30	40	60	80
37 | 24.15 (8.87)	36 | 2.70 (5.90)	32 | 8.26 (3.07)		29 | 5.24 (2.42)		48 | 0.21 (0.19)
42 | 19.02 (6.45)	41 | 7.34 (5.49)	36 | 4.02 (3.50)		33 | 3.02 (1.63)		59 | 0.76 (0.36)
48 | 9.81 (6.45)	47 | 15.29 (5.20)	42 | 5.44 (3.38)		38 | 0.73 (3.23)		74 | 0.64 (0.29)
54 | 12.49 (5.92)	54 | 12.12 (4.34)	49 | 4.59 (2.30)		43 | 3.42 (1.63)		92 | 0.04 (0.04)
59 | 6.48 (4.49)	61 | 7.34 (3.10)	55 | 8.62 (2.75)		50 | 8.01 (1.98)		111 | 0.18 (0.13)
65 | 8.52 (4.24)	68 | 13.36 (5.46)	64 | 9.01 (2.12)		57 | 2.78 (1.36)		
71 | 34.50 (7.58)	75 | 4.63 (3.78)	73 | 6.22 (2.75)		63 | 2.30 (1.53)		
79 | 21.51 (7.34)	83 | 2.27 (3.83)	82 | 6.35 (2.25)		71 | 4.35 (1.29)		
85 | 33.54 (10.65)	90 | 5.87 (5.63)	92 | 8.60 (2.10)		78 | 3.32 (2.33)		
90 | 12.55 (9.50)	95 | 18.58 (7.75)	101 | 7.46 (3.69)		83 | 4.76 (1.65)		
95 | 21.88 (9.85)	101 | 5.08 (5.90)	108 | 11.77 (3.89)		89 | 3.24 (1.62)		
101 | 16.71 (8.56)	107 | 16.73 (6.53)	116 | 8.83 (3.69)		95 | 4.82 (1.95)		
107 | 21.67 (9.94)	114 | 21.64 (7.81)	125 | 10.90 (3.43)		102 | 3.00 (3.10)		
114 | 27.02 (7.52)	121 | 23.55 (7.18)	135 | 13.68 (3.73)		110 | 3.57 (0.88)		
121 | 34.01 (8.00)	130 | 13.15 (6.57)	146 | 11.69 (4.33)		119 | 3.39 (0.92)		
130 | 10.94 (7.25)	139 | 39.53 (7.75)			130 | 3.12 (2.04)		
	150 | 24.33 (6.97)			142 | 1.33 (1.89)		

Table 147. Triton production cross sections for 400 MeV/u xenon on aluminum.

5	10	20	30	40	60	80
		33 | 1.83 (2.75)		23 | 7.15 (2.72)		
		39 | 1.22 (1.36)		26 | 1.37 (0.69)		
		44 | 5.35 (2.15)		30 | 0.98 (0.96)		
		51 | 2.39 (1.61)		34 | 1.16 (0.91)		
		57 | 2.51 (1.28)		39 | 0.48 (0.34)		
		63 | 3.53 (1.56)		45 | 2.24 (1.11)		
		68 | 0.43 (0.43)		50 | 0.48 (1.26)		
		71 | 1.05 (0.94)		54 | 1.95 (1.86)		
				57 | 3.48 (2.02)		
				64 | 2.58 (1.45)		

Table 148. Proton production cross sections for 400 MeV/u xenon on lithium.

5	10	20	30	40	60	80
50 | 2.09 (1.03)	46 | 2.57 (1.00)	51 | 4.19 (0.67)		45 | 1.73 (0.55)		59 | 0.32 (0.12)
57 | 2.36 (1.00)	52 | 4.39 (0.98)	59 | 2.77 (0.55)		52 | 2.11 (0.51)		70 | 0.30 (0.10)
65 | 4.47 (1.13)	59 | 4.71 (0.96)	68 | 3.70 (0.60)		60 | 2.91 (0.50)		85 | 0.39 (0.12)
73 | 6.80 (1.07)	67 | 5.25 (1.05)	79 | 5.11 (0.65)		69 | 2.79 (0.45)		106 | 0.36 (0.08)
82 | 3.25 (0.91)	77 | 7.97 (1.15)	90 | 4.06 (0.72)		79 | 2.35 (0.45)		133 | 0.20 (0.06)
91 | 3.14 (0.79)	88 | 5.96 (0.91)	101 | 4.39 (0.60)		89 | 2.55 (0.49)		166 | 0.12 (0.03)
98 | 5.45 (1.20)	101 | 5.96 (0.97)	111 | 3.65 (0.51)		98 | 4.18 (0.74)		202 | 0.07 (0.03)
103 | 5.48 (1.21)	113 | 6.47 (0.86)	119 | 4.79 (0.83)		105 | 2.82 (0.61)		234 | 0.01 (0.01)
110 | 6.93 (1.20)	124 | 8.10 (1.26)	128 | 3.67 (0.60)		113 | 2.65 (0.48)		
116 | 8.06 (1.38)	132 | 7.45 (1.36)	137 | 6.06 (0.86)		122 | 3.19 (0.57)		
124 | 8.79 (1.35)	142 | 8.77 (1.38)	149 | 6.71 (0.99)		133 | 2.66 (0.53)		
132 | 10.18 (1.63)	152 | 10.36 (1.46)	162 | 4.74 (1.02)		145 | 1.70 (0.52)		
142 | 11.85 (1.71)	164 | 10.88 (1.49)					
152 | 15.73 (1.94)						

Table 149. Deuteron production cross sections for 400 MeV/u xenon on lithium.

5	10	20	30	40	60	80
36 | 6.79 (1.66)	36 | 2.58 (1.17)	33 | 2.19 (0.57)		28 | 0.67 (0.38)		46 | 0.02 (0.02)
41 | 1.84 (1.10)	41 | 2.19 (1.04)	38 | 0.98 (0.48)		32 | 0.93 (0.39)		62 | 0.02 (0.02)
46 | 2.29 (1.08)	47 | 0.70 (0.66)	43 | 1.53 (0.62)		37 | 1.37 (0.41)		77 | 0.05 (0.03)
52 | 1.77 (0.87)	54 | 1.32 (0.66)	49 | 1.38 (0.45)		42 | 0.54 (0.34)		110 | 0.01 (0.00)
59 | 2.30 (0.81)	61 | 1.59 (0.56)	56 | 1.72 (0.47)		48 | 0.75 (0.28)		
67 | 3.87 (0.87)	70 | 1.77 (0.63)	63 | 1.14 (0.44)		56 | 0.60 (0.20)		
75 | 6.37 (1.23)	79 | 1.39 (0.71)	70 | 1.17 (0.39)		64 | 0.75 (0.30)		
83 | 6.42 (1.29)	88 | 2.41 (0.72)	77 | 1.60 (0.36)		71 | 0.88 (0.26)		
93 | 6.20 (1.22)	98 | 4.23 (0.89)	84 | 0.93 (0.51)		81 | 0.92 (0.24)		
101 | 5.37 (1.53)	107 | 7.69 (1.40)	90 | 0.96 (0.46)		89 | 0.39 (0.36)		
107 | 4.43 (1.56)	114 | 5.23 (0.83)	95 | 1.87 (0.50)		95 | 0.58 (0.30)		
114 | 7.74 (1.42)	122 | 5.70 (1.22)	102 | 3.54 (0.69)		111 | 0.68 (0.16)		
122 | 11.77 (1.62)	130 | 5.16 (1.20)	109 | 2.27 (0.51)		120 | 0.84 (0.16)		
	140 | 6.76 (1.24)	117 | 2.27 (0.50)		130 | 1.30 (0.37)		
	150 | 7.63 (1.26)	125 | 2.19 (0.56)		143 | 0.73 (0.35)		
		135 | 2.74 (0.57)				
		147 | 2.45 (0.74)				

Table 150. Triton production cross sections for 400 MeV/u xenon on lithium.

5	10	20	30	40	60	80
		33 | -0.24 (0.30)		23 | 0.29 (0.24)		
		38 | 0.20 (0.11)		26 | 0.21 (0.10)		
		43 | 0.23 (0.32)		30 | 0.34 (0.19)		
		49 | 0.24 (0.22)		35 | 0.25 (0.17)		
		54 | 0.30 (0.18)		39 | 0.18 (0.08)		
		60 | 0.12 (0.07)		45 | 0.32 (0.17)		
		64 | 0.62 (0.39)		66 | 0.05 (0.03)		
		68 | 0.06 (0.06)				
		72 | 0.35 (0.31)				

Table 151. Proton production cross sections for 600 MeV/u neon on aluminum.

5	10	20	30	40	60	80
56 | 4.73 (0.60)	57 | 3.47 (0.49)	56 | 2.86 (0.52)		59 | 3.24 (0.48)		119 | 0.74 (0.12)
59 | 4.01 (0.49)	61 | 4.76 (0.53)	60 | 3.93 (0.52)		63 | 3.43 (0.42)		132 | 0.81 (0.11)
65 | 4.14 (0.44)	66 | 3.80 (0.43)	66 | 3.47 (0.40)		69 | 2.83 (0.38)		152 | 0.48 (0.07)
71 | 3.35 (0.41)	73 | 4.56 (0.44)	73 | 3.45 (0.41)		76 | 2.32 (0.30)		180 | 0.27 (0.04)
77 | 3.49 (0.37)	80 | 3.78 (0.41)	81 | 3.58 (0.39)		85 | 2.77 (0.29)		217 | 0.21 (0.03)
86 | 3.97 (0.36)	87 | 4.60 (0.45)	92 | 3.36 (0.33)		95 | 2.92 (0.34)		260 | 0.16 (0.03)
94 | 3.95 (0.38)	95 | 3.83 (0.42)	103 | 3.35 (0.36)		105 | 2.58 (0.28)		301 | 0.09 (0.02)
103 | 3.39 (0.34)	103 | 4.65 (0.41)	115 | 2.82 (0.28)		118 | 2.04 (0.20)		359 | 0.04 (0.01)
114 | 3.76 (0.32)	111 | 4.36 (0.44)	126 | 2.57 (0.29)		131 | 2.16 (0.26)		444 | 0.01 (0.00)
123 | 3.58 (0.34)	117 | 4.22 (0.41)	134 | 2.22 (0.29)		141 | 2.05 (0.26)		
131 | 3.44 (0.32)	123 | 3.99 (0.36)	144 | 3.00 (0.33)		152 | 2.18 (0.25)		
139 | 3.44 (0.34)	131 | 3.71 (0.37)	155 | 3.77 (0.39)		166 | 1.61 (0.20)		
148 | 4.07 (0.39)	139 | 3.68 (0.36)	167 | 1.99 (0.26)				
158 | 4.98 (0.44)	148 | 4.51 (0.42)					
170 | 4.11 (0.37)	158 | 4.21 (0.41)					
183 | 3.60 (0.33)						
199 | 0.36 (0.12)						

Table 152. Deuteron production cross sections for 600 MeV/u neon on aluminum.

5	10	20	30	40	60	80
32 | 1.78 (0.44)	31 | 1.18 (0.33)	32 | 1.59 (0.40)		33 | 1.36 (0.33)		72 | 0.10 (0.06)
34 | 1.40 (0.39)	33 | 1.75 (0.43)	35 | 1.74 (0.37)		36 | 1.16 (0.25)		78 | 0.14 (0.06)
37 | 1.66 (0.32)	36 | 1.59 (0.53)	39 | 1.59 (0.32)		40 | 1.26 (0.28)		87 | 0.08 (0.04)
41 | 2.36 (0.40)	40 | 2.79 (0.50)	43 | 1.57 (0.27)		45 | 1.15 (0.26)		96 | 0.06 (0.04)
45 | 2.04 (0.35)	44 | 1.79 (0.34)	49 | 1.34 (0.27)		50 | 1.19 (0.23)		103 | 0.03 (0.03)
50 | 2.12 (0.34)	48 | 2.69 (0.37)	54 | 1.19 (0.22)		57 | 1.07 (0.20)		110 | 0.01 (0.01)
55 | 1.69 (0.29)	53 | 2.00 (0.30)	62 | 1.35 (0.22)		64 | 1.11 (0.22)		120 | 0.09 (0.03)
61 | 2.19 (0.27)	58 | 1.78 (0.31)	69 | 1.36 (0.23)		71 | 0.73 (0.13)		
68 | 2.38 (0.31)	63 | 1.78 (0.29)	76 | 1.21 (0.22)		79 | 0.72 (0.12)		
74 | 2.49 (0.33)	68 | 2.20 (0.29)	84 | 1.22 (0.20)		86 | 0.44 (0.16)		
81 | 2.36 (0.30)	74 | 2.00 (0.27)	92 | 1.07 (0.23)		92 | 0.77 (0.19)		
90 | 2.33 (0.28)	79 | 1.84 (0.34)	98 | 1.92 (0.36)		98 | 0.69 (0.17)		
97 | 2.29 (0.34)	83 | 1.63 (0.31)	104 | 1.61 (0.28)		105 | 0.78 (0.15)		
103 | 2.13 (0.34)	88 | 1.61 (0.28)	111 | 1.08 (0.17)		113 | 1.09 (0.13)		
109 | 3.00 (0.37)	92 | 1.40 (0.29)	119 | 1.58 (0.19)		122 | 1.01 (0.16)		
116 | 2.58 (0.31)	97 | 2.39 (0.34)			133 | 0.82 (0.14)		
124 | 1.39 (0.13)	103 | 2.52 (0.32)					
	109 | 1.71 (0.29)					
	116 | 1.79 (0.17)					
	124 | 1.47 (0.22)					

Table 153. Triton production cross sections for 600 MeV/u neon on aluminum.

5	10	20	30	40	60	80
24 | -0.01 (0.40)	25 | 1.27 (0.36)	23 | 0.37 (0.22)		24 | 0.19 (0.10)		
26 | 1.27 (0.64)	27 | 0.76 (0.43)	25 | 0.49 (0.26)		26 | 0.32 (0.17)		
28 | 0.74 (0.37)	30 | 1.11 (0.35)	28 | 0.48 (0.31)		29 | 0.57 (0.24)		
31 | 0.05 (0.41)	33 | 0.66 (0.26)	31 | 0.83 (0.22)		33 | 0.43 (0.16)		
35 | 0.69 (0.25)	36 | 0.40 (0.21)	35 | 0.88 (0.33)		37 | 0.36 (0.17)		
38 | 0.56 (0.38)	40 | 0.69 (0.19)	38 | 0.97 (0.29)		41 | 0.24 (0.10)		
42 | 0.47 (0.15)	44 | 0.54 (0.16)	42 | 0.71 (0.24)		47 | 0.15 (0.08)		
47 | 0.70 (0.22)	49 | 0.47 (0.26)	47 | 0.58 (0.22)		52 | 0.19 (0.07)		
52 | 1.54 (0.26)	53 | 0.48 (0.15)	51 | 0.16 (0.14)		58 | 0.21 (0.11)		
58 | 0.83 (0.27)	58 | 0.30 (0.15)	55 | 0.65 (0.21)		64 | 0.26 (0.09)		
63 | 1.54 (0.26)	63 | 0.44 (0.15)	59 | 0.60 (0.28)		70 | 0.21 (0.11)		
69 | 1.40 (0.25)	69 | 0.38 (0.11)	62 | 0.13 (0.08)		74 | 0.33 (0.13)		
75 | 2.65 (0.33)	76 | 0.56 (0.15)	65 | 0.30 (0.15)		79 | 0.18 (0.05)		
81 | 2.16 (0.38)	81 | 0.67 (0.12)	68 | 0.29 (0.11)		84 | 0.16 (0.17)		
86 | 2.56 (0.39)	86 | 0.42 (0.08)	72 | 0.11 (0.06)		90 | 0.10 (0.09)		
90 | 2.24 (0.37)	90 | 0.41 (0.19)	76 | 0.49 (0.13)		96 | 0.06 (0.10)		
96 | 2.63 (0.37)	96 | 0.69 (0.16)	80 | 0.50 (0.12)		103 | 0.42 (0.06)		
101 | 0.87 (0.23)	101 | 0.65 (0.18)	85 | 0.49 (0.10)		111 | 0.26 (0.14)		
108 | 0.30 (0.15)	108 | 1.06 (0.11)	90 | 0.37 (0.14)		121 | 0.06 (0.10)		
114 | 0.92 (0.11)	114 | 0.81 (0.17)	96 | 0.56 (0.18)				
122 | 0.18 (0.09)		102 | 0.69 (0.19)				
		109 | 0.42 (0.06)				
		117 | 0.31 (0.09)				

Table 154. Proton production cross sections for 600 MeV/u neon on lithium.

5	10	20	30	40	60	80
45 | 3.41 (0.48)	46 | 4.19 (0.50)	44 | 3.32 (0.43)		45 | 2.53 (0.32)		60 | 0.30 (0.06)
50 | 3.78 (0.45)	51 | 4.90 (0.52)	50 | 3.74 (0.41)		51 | 2.86 (0.31)		68 | 0.29 (0.06)
56 | 4.59 (0.44)	57 | 5.21 (0.55)	56 | 3.92 (0.41)		58 | 2.79 (0.30)		79 | 0.91 (0.11)
63 | 4.80 (0.46)	63 | 4.78 (0.46)	63 | 3.70 (0.37)		67 | 3.17 (0.30)		95 | 0.80 (0.09)
71 | 3.91 (0.38)	71 | 4.44 (0.42)	70 | 4.34 (0.45)		75 | 2.83 (0.29)		114 | 0.66 (0.08)
81 | 4.12 (0.36)	79 | 4.28 (0.42)	77 | 4.22 (0.41)		85 | 2.99 (0.30)		136 | 0.46 (0.05)
91 | 3.89 (0.39)	87 | 4.86 (0.44)	85 | 4.01 (0.36)		93 | 3.23 (0.36)		159 | 0.34 (0.05)
101 | 4.95 (0.40)	96 | 4.57 (0.42)	96 | 4.04 (0.35)		99 | 2.98 (0.34)		179 | 0.28 (0.04)
114 | 4.43 (0.34)	104 | 5.17 (0.49)	105 | 4.02 (0.42)		106 | 2.29 (0.28)		205 | 0.20 (0.03)
124 | 4.39 (0.39)	110 | 5.23 (0.48)	112 | 3.98 (0.39)		114 | 2.44 (0.26)		238 | 0.14 (0.02)
133 | 4.87 (0.42)	117 | 4.81 (0.43)	119 | 3.77 (0.33)		123 | 2.79 (0.29)		281 | 0.07 (0.01)
142 | 5.19 (0.47)	124 | 4.75 (0.44)	128 | 3.59 (0.35)		133 | 2.55 (0.26)		341 | 0.05 (0.01)
153 | 7.14 (0.56)	133 | 5.11 (0.46)	138 | 4.44 (0.39)		145 | 3.27 (0.30)		427 | 0.01 (0.00)
165 | 5.94 (0.48)	142 | 6.56 (0.54)	149 | 5.97 (0.47)		159 | 2.69 (0.26)		
178 | 5.46 (0.44)	153 | 6.38 (0.54)	162 | 4.04 (0.36)				

Table 155. Deuteron production cross sections for 600 MeV/u neon on lithium.

5	10	20	30	40	60	80
27 | 1.80 (0.38)	27 | 1.98 (0.45)	27 | 1.27 (0.32)		27 | 1.22 (0.27)		56 | 0.09 (0.03)
30 | 1.61 (0.45)	30 | 1.26 (0.47)	30 | 1.43 (0.36)		30 | 0.80 (0.20)		65 | 0.09 (0.03)
33 | 1.72 (0.31)	33 | 2.50 (0.46)	34 | 1.31 (0.29)		34 | 0.81 (0.19)		75 | 0.06 (0.03)
37 | 2.01 (0.43)	38 | 2.99 (0.47)	38 | 1.36 (0.25)		39 | 0.73 (0.15)		84 | 0.06 (0.03)
42 | 1.75 (0.36)	42 | 1.74 (0.32)	42 | 1.43 (0.25)		44 | 1.00 (0.18)		92 | 0.04 (0.02)
47 | 1.95 (0.36)	47 | 1.90 (0.29)	47 | 1.39 (0.23)		51 | 0.84 (0.17)		100 | 0.02 (0.01)
52 | 1.25 (0.26)	52 | 1.59 (0.26)	52 | 1.17 (0.21)		57 | 0.70 (0.16)		110 | 0.03 (0.01)
57 | 1.63 (0.29)	59 | 1.82 (0.27)	57 | 1.20 (0.23)		64 | 0.58 (0.12)		122 | 0.01 (0.01)
63 | 1.44 (0.24)	65 | 2.09 (0.29)	63 | 1.21 (0.20)		72 | 0.50 (0.10)		
68 | 1.59 (0.24)	72 | 2.38 (0.30)	70 | 1.17 (0.18)		81 | 0.41 (0.08)		
73 | 4.18 (0.63)	79 | 1.12 (0.17)	76 | 1.16 (0.23)		89 | 0.52 (0.13)		
77 | 3.71 (0.52)	88 | 1.68 (0.23)	80 | 1.01 (0.18)		96 | 0.48 (0.17)		
81 | 3.30 (0.48)	95 | 2.18 (0.33)	85 | 0.95 (0.19)		103 | 0.54 (0.14)		
86 | 4.16 (0.51)	101 | 2.85 (0.35)	90 | 0.81 (0.19)		111 | 0.60 (0.06)		
90 | 3.58 (0.47)	107 | 2.05 (0.28)	96 | 1.19 (0.24)		120 | 0.54 (0.07)		
95 | 3.38 (0.43)	114 | 1.15 (0.10)	102 | 1.45 (0.22)		131 | 0.59 (0.10)		
101 | 3.95 (0.47)	122 | 1.84 (0.26)	109 | 1.74 (0.25)				
107 | 3.48 (0.42)		117 | 0.85 (0.08)				
114 | 3.03 (0.35)		126 | 1.41 (0.22)				
122 | 1.17 (0.10)						

Table 156. Triton production cross sections for 600 MeV/u neon on lithium.

5	10	20	30	40	60	80
22 | -0.05 (0.42)	23 | 0.81 (0.34)	21 | 0.57 (0.32)		21 | 0.27 (0.12)		
24 | 0.79 (0.58)	26 | 2.46 (0.60)	24 | 1.30 (0.36)		24 | 0.20 (0.14)		
27 | 0.79 (0.38)	28 | 1.12 (0.34)	27 | 1.07 (0.24)		28 | 0.14 (0.13)		
30 | 0.89 (0.37)	32 | 0.79 (0.31)	30 | 0.26 (0.14)		32 | 0.14 (0.14)		
34 | 0.28 (0.22)	36 | 0.49 (0.23)	34 | 0.40 (0.23)		36 | 0.18 (0.08)		
38 | 0.32 (0.22)	39 | 0.29 (0.16)	38 | 0.10 (0.11)		41 | 0.09 (0.07)		
42 | 0.32 (0.19)	44 | 0.18 (0.09)	43 | 0.09 (0.05)		47 | 0.05 (0.05)		
47 | 1.75 (0.33)	49 | 0.26 (0.17)	47 | 0.05 (0.10)		54 | 0.03 (0.06)		
53 | 2.76 (0.36)	54 | 0.43 (0.14)	51 | 0.11 (0.06)		60 | 0.04 (0.03)		
59 | 2.08 (0.36)	59 | 0.13 (0.13)	56 | 0.27 (0.09)		67 | 0.04 (0.03)		
65 | 2.78 (0.34)	65 | 0.08 (0.10)	62 | 0.00 (0.06)		73 | 0.12 (0.10)		
71 | 2.86 (0.38)	71 | 0.15 (0.10)	67 | 0.28 (0.12)		78 | 0.09 (0.03)		
78 | 3.56 (0.38)	78 | 0.67 (0.14)	71 | 0.09 (0.06)		83 | 0.09 (0.03)		
85 | 4.27 (0.52)	85 | 0.66 (0.20)	75 | 0.07 (0.05)		89 | 0.03 (0.08)		
90 | 3.64 (0.48)	90 | 0.58 (0.24)	79 | 0.24 (0.04)		102 | 0.12 (0.01)		
95 | 3.81 (0.47)	95 | 0.42 (0.12)	84 | 0.17 (0.04)		110 | 0.14 (0.08)		
100 | 1.00 (0.26)	100 | 0.38 (0.17)	89 | 0.26 (0.09)		120 | 0.11 (0.09)		
107 | 0.25 (0.17)	107 | 0.23 (0.02)	95 | 0.14 (0.11)				
114 | 0.71 (0.08)	114 | 0.62 (0.15)	101 | 0.41 (0.15)				
121 | 0.08 (0.08)		108 | 0.15 (0.02)				
		116 | 0.21 (0.08)				

Table 157. Proton production cross sections for 600 MeV/u silicon on carbon.

5	10	20	30	40	60	80
	52 | 1.30 (0.28)	52 | 2.03 (0.25)	52 | 1.48 (0.24)	50 | 1.07 (0.20)	58 | 1.20 (0.21)	85 | 0.36 (0.08)
	57 | 2.35 (0.29)	58 | 1.78 (0.22)	57 | 1.71 (0.22)	54 | 1.71 (0.23)	63 | 1.37 (0.19)	90 | 0.34 (0.07)
	62 | 2.25 (0.30)	64 | 1.79 (0.22)	63 | 1.92 (0.23)	59 | 2.06 (0.23)	70 | 1.30 (0.16)	96 | 0.46 (0.07)
	68 | 2.59 (0.30)	71 | 1.85 (0.20)	69 | 1.68 (0.21)	65 | 1.50 (0.18)	78 | 1.18 (0.13)	104 | 0.51 (0.07)
	76 | 2.37 (0.25)	78 | 2.01 (0.21)	76 | 1.55 (0.19)	73 | 1.51 (0.16)	88 | 1.14 (0.13)	112 | 0.44 (0.06)
	83 | 1.91 (0.26)	86 | 1.73 (0.19)	82 | 1.57 (0.18)	81 | 1.56 (0.17)	98 | 1.10 (0.12)	121 | 0.41 (0.07)
	91 | 2.06 (0.24)	95 | 2.13 (0.20)	90 | 1.94 (0.20)	90 | 1.56 (0.16)	108 | 0.86 (0.11)	128 | 0.28 (0.05)
	100 | 2.08 (0.22)	102 | 1.97 (0.24)	98 | 1.61 (0.22)	101 | 1.44 (0.15)	115 | 1.00 (0.11)	136 | 0.22 (0.04)
	108 | 2.47 (0.30)	108 | 1.80 (0.21)	103 | 1.88 (0.22)	111 | 1.17 (0.16)	124 | 0.72 (0.08)	146 | 0.22 (0.04)
	114 | 2.30 (0.26)	115 | 1.60 (0.19)	109 | 1.18 (0.18)	118 | 1.16 (0.12)	135 | 0.57 (0.07)	159 | 0.20 (0.03)
	120 | 2.29 (0.23)	123 | 1.75 (0.18)	116 | 1.46 (0.17)	127 | 0.90 (0.11)	147 | 0.55 (0.07)	174 | 0.20 (0.03)
	128 | 2.05 (0.24)	131 | 1.83 (0.19)	123 | 1.37 (0.15)	137 | 1.12 (0.13)	162 | 0.72 (0.08)	
	136 | 2.26 (0.26)	141 | 2.11 (0.22)	132 | 1.56 (0.17)	149 | 1.41 (0.15)	179 | 0.60 (0.07)	
	145 | 2.79 (0.29)	152 | 2.18 (0.23)	141 | 1.63 (0.17)	163 | 1.51 (0.15)	201 | 0.22 (0.03)	
	156 | 3.16 (0.29)	165 | 2.25 (0.22)	153 | 1.87 (0.21)			
	167 | 3.12 (0.28)		165 | 1.89 (0.18)			

Table 158. Deuteron production cross sections for 600 MeV/u silicon on carbon.

5	10	20	30	40	60	80
	30 | 1.27 (0.33)	29 | 0.49 (0.23)	31 | 0.54 (0.16)	30 | 0.73 (0.16)	32 | 0.41 (0.11)	43 | 0.17 (0.07)
	33 | 1.02 (0.26)	31 | 0.70 (0.16)	34 | 1.06 (0.22)	33 | 0.68 (0.13)	35 | 0.52 (0.10)	46 | 0.08 (0.04)
	36 | 1.77 (0.37)	35 | 1.15 (0.20)	38 | 0.77 (0.15)	37 | 0.61 (0.14)	39 | 0.25 (0.12)	51 | 0.06 (0.03)
	40 | 1.42 (0.29)	39 | 1.16 (0.20)	43 | 0.58 (0.14)	41 | 0.67 (0.12)	43 | 0.45 (0.09)	56 | 0.15 (0.06)
	44 | 0.60 (0.19)	42 | 0.70 (0.13)	47 | 0.90 (0.16)	46 | 0.57 (0.10)	49 | 0.32 (0.07)	62 | 0.00 (0.03)
	48 | 0.76 (0.16)	47 | 0.91 (0.15)	53 | 0.83 (0.12)	53 | 0.65 (0.12)	55 | 0.25 (0.07)	68 | 0.07 (0.02)
	54 | 0.72 (0.15)	52 | 0.77 (0.14)	59 | 0.28 (0.08)	59 | 0.35 (0.08)	60 | 0.26 (0.05)	76 | 0.04 (0.02)
	59 | 0.99 (0.21)	56 | 0.65 (0.13)	65 | 0.39 (0.08)	65 | 0.41 (0.08)	68 | 0.18 (0.06)	84 | 0.03 (0.02)
	64 | 0.65 (0.15)	62 | 0.70 (0.12)	71 | 0.46 (0.10)	73 | 0.27 (0.05)	74 | 0.18 (0.05)	90 | 0.04 (0.02)
	70 | 0.96 (0.16)	66 | 0.66 (0.18)	77 | 0.38 (0.10)	80 | 0.22 (0.05)	79 | 0.05 (0.06)	97 | 0.01 (0.01)
	76 | 1.26 (0.18)	69 | 0.71 (0.16)	81 | 0.30 (0.07)	85 | 0.19 (0.06)	85 | 0.08 (0.04)	105 | 0.02 (0.01)
	82 | 0.87 (0.18)	73 | 0.57 (0.14)	86 | 0.38 (0.08)	91 | 0.23 (0.06)	91 | 0.15 (0.04)	115 | 0.02 (0.01)
	87 | 0.61 (0.14)	77 | 0.50 (0.10)	91 | 0.44 (0.11)	97 | 0.39 (0.09)	98 | 0.17 (0.04)	126 | 0.02 (0.00)
	91 | 0.90 (0.19)	81 | 0.58 (0.14)	97 | 0.46 (0.11)	104 | 0.35 (0.07)	106 | 0.25 (0.06)	
	96 | 0.62 (0.17)	86 | 0.62 (0.12)	103 | 0.62 (0.15)	112 | 0.54 (0.07)	116 | 0.05 (0.01)	
	102 | 1.10 (0.21)	91 | 0.48 (0.14)	110 | 0.67 (0.12)	121 | 0.42 (0.06)	127 | 0.07 (0.01)	
	108 | 1.04 (0.18)	97 | 0.67 (0.13)	118 | 0.37 (0.04)			
	115 | 0.91 (0.09)	103 | 1.02 (0.15)				
	123 | 0.61 (0.13)	110 | 0.54 (0.10)				
		118 | 0.77 (0.08)				

Table 159. Triton production cross sections for 600 MeV/u silicon on carbon.

5	10	20	30	40	60	80
	22 | 0.51 (0.34)	21 | 0.39 (0.32)	23 | 0.24 (0.11)	21 | 0.29 (0.14)	23 | 0.12 (0.05)	27 | 0.00 (0.00)
	24 | 0.39 (0.21)	23 | 0.19 (0.16)	25 | 0.31 (0.13)	24 | 0.09 (0.07)	25 | 0.21 (0.09)	29 | 0.02 (0.02)
	26 | 1.40 (0.33)	26 | 0.34 (0.17)	28 | 0.33 (0.12)	26 | 0.14 (0.06)	29 | 0.12 (0.06)	37 | 0.01 (0.01)
	29 | 1.36 (0.35)	29 | 0.47 (0.14)	31 | 0.21 (0.09)	30 | 0.23 (0.07)	32 | 0.16 (0.06)	42 | 0.02 (0.03)
	31 | 0.90 (0.27)	32 | 0.45 (0.13)	35 | 0.10 (0.07)	33 | 0.14 (0.06)	36 | 0.04 (0.03)	48 | 0.05 (0.05)
	34 | 0.45 (0.22)	35 | 0.36 (0.10)	39 | 0.00 (0.07)	37 | 0.09 (0.04)	41 | 0.03 (0.02)	
	38 | 0.37 (0.13)	39 | 0.05 (0.06)	43 | 0.21 (0.06)	42 | 0.13 (0.05)	47 | 0.05 (0.05)	
	42 | 0.36 (0.17)	43 | 0.14 (0.05)	48 | 0.09 (0.06)	47 | 0.08 (0.03)	52 | 0.06 (0.03)	
	45 | 0.04 (0.15)	48 | 0.05 (0.03)	52 | 0.11 (0.05)	52 | 0.10 (0.05)	58 | 0.03 (0.02)	
	49 | 0.45 (0.14)	52 | 0.14 (0.05)	57 | 0.04 (0.03)	57 | 0.06 (0.03)	65 | 0.05 (0.02)	
	53 | 0.41 (0.14)	57 | 0.11 (0.04)	63 | 0.02 (0.01)	64 | 0.08 (0.03)	72 | 0.03 (0.02)	
	57 | 0.12 (0.06)	63 | 0.01 (0.04)	68 | 0.02 (0.02)	71 | 0.01 (0.01)	77 | 0.03 (0.02)	
	61 | 0.22 (0.11)	68 | 0.21 (0.08)	71 | 0.08 (0.04)	78 | 0.17 (0.04)	83 | 0.01 (0.03)	
	64 | 0.08 (0.12)	71 | 0.03 (0.02)	75 | 0.12 (0.05)	83 | 0.03 (0.04)	89 | 0.01 (0.00)	
	67 | 0.10 (0.07)	75 | 0.23 (0.09)	80 | 0.16 (0.04)	89 | 0.04 (0.04)	96 | 0.06 (0.05)	
	70 | 0.13 (0.07)	80 | 0.41 (0.10)	84 | 0.24 (0.05)	96 | -0.01 (0.02)	105 | 0.03 (0.02)	
	73 | 0.25 (0.10)	84 | 0.42 (0.09)	90 | 0.13 (0.07)	103 | 0.05 (0.01)	114 | 0.02 (0.00)	
	77 | 0.02 (0.08)	89 | 0.19 (0.09)	95 | 0.15 (0.08)	111 | 0.10 (0.02)		
	81 | 0.16 (0.04)	95 | 0.23 (0.07)	102 | 0.01 (0.07)			
	85 | 0.57 (0.15)	102 | 0.28 (0.07)	109 | 0.32 (0.04)			
	90 | 0.24 (0.13)	109 | 0.22 (0.03)	117 | 0.29 (0.08)			
	95 | 0.14 (0.10)					
	101 | 0.25 (0.10)					
	107 | 0.21 (0.03)					
	114 | 0.20 (0.07)					

Table 160. Proton production cross sections for 600 MeV/u silicon on copper.

5	10	20	30	40	60	80
	57 | 8.05 (1.02)	56 | 10.54 (1.04)	58 | 6.64 (0.79)	57 | 6.59 (0.76)	66 | 5.06 (0.61)	101 | 1.83 (0.28)
	61 | 8.27 (0.85)	61 | 9.07 (0.86)	63 | 8.43 (0.80)	62 | 6.25 (0.62)	72 | 5.09 (0.54)	105 | 1.24 (0.19)
	66 | 7.94 (0.86)	66 | 7.69 (0.79)	69 | 7.30 (0.76)	68 | 7.10 (0.66)	79 | 5.36 (0.53)	112 | 1.62 (0.23)
	72 | 8.18 (0.83)	72 | 8.82 (0.79)	76 | 7.95 (0.71)	75 | 6.57 (0.59)	88 | 4.83 (0.45)	120 | 2.14 (0.23)
	79 | 7.84 (0.73)	79 | 8.45 (0.80)	83 | 8.60 (0.77)	82 | 6.00 (0.55)	98 | 3.85 (0.38)	131 | 1.66 (0.20)
	87 | 7.40 (0.77)	85 | 7.58 (0.71)	90 | 7.13 (0.66)	89 | 5.25 (0.48)	109 | 3.58 (0.33)	144 | 1.30 (0.14)
	94 | 7.11 (0.72)	91 | 10.24 (1.03)	98 | 6.86 (0.60)	99 | 5.49 (0.48)	120 | 2.95 (0.31)	157 | 1.01 (0.12)
	100 | 6.26 (0.80)	95 | 9.71 (0.93)	106 | 7.48 (0.75)	107 | 4.90 (0.51)	129 | 2.16 (0.22)	169 | 0.81 (0.11)
	105 | 7.77 (0.83)	100 | 7.60 (0.84)	112 | 6.43 (0.70)	114 | 4.70 (0.48)	139 | 1.47 (0.17)	183 | 0.97 (0.12)
	110 | 7.57 (0.81)	105 | 6.71 (0.72)	119 | 5.15 (0.48)	121 | 3.76 (0.33)	151 | 2.04 (0.23)	201 | 0.38 (0.05)
	116 | 6.47 (0.64)	111 | 8.61 (0.78)	126 | 5.61 (0.50)	130 | 4.45 (0.44)	165 | 2.76 (0.26)	
	123 | 6.99 (0.59)	118 | 6.56 (0.62)	134 | 6.19 (0.58)	140 | 4.14 (0.39)	183 | 2.10 (0.20)	
	130 | 7.49 (0.72)	125 | 5.60 (0.47)	144 | 5.84 (0.53)	151 | 4.94 (0.47)	204 | 0.98 (0.11)	
	138 | 6.33 (0.68)	134 | 6.66 (0.61)	155 | 7.09 (0.64)	165 | 4.23 (0.41)		
	147 | 8.65 (0.80)	143 | 7.20 (0.65)	167 | 7.16 (0.60)			
	158 | 8.68 (0.75)	154 | 9.26 (0.75)				
	169 | 7.71 (0.69)	167 | 8.20 (0.67)				

Table 161. Deuteron production cross sections for 600 MeV/u silicon on copper.

5	10	20	30	40	60	80
	31 | 5.34 (1.03)	31 | 5.49 (0.86)	34 | 5.64 (0.78)	33 | 3.68 (0.54)	35 | 2.09 (0.37)	50 | 0.62 (0.18)
	34 | 2.50 (0.71)	34 | 4.76 (0.69)	38 | 5.95 (0.73)	36 | 2.43 (0.39)	38 | 2.99 (0.43)	54 | 0.43 (0.12)
	37 | 6.59 (1.14)	37 | 6.53 (0.78)	42 | 4.85 (0.58)	40 | 4.08 (0.47)	41 | 2.12 (0.44)	58 | 0.96 (0.25)
	41 | 6.14 (0.84)	41 | 6.64 (0.79)	47 | 5.63 (0.65)	45 | 3.14 (0.41)	46 | 2.20 (0.31)	64 | 0.28 (0.09)
	45 | 4.59 (0.74)	45 | 5.73 (0.68)	52 | 3.95 (0.48)	50 | 2.65 (0.33)	51 | 1.73 (0.25)	70 | 0.32 (0.10)
	49 | 5.32 (0.67)	50 | 4.76 (0.55)	59 | 3.15 (0.38)	57 | 2.77 (0.37)	57 | 1.47 (0.24)	77 | 0.35 (0.08)
	55 | 3.95 (0.56)	55 | 4.02 (0.56)	66 | 3.89 (0.48)	63 | 2.99 (0.35)	62 | 1.55 (0.25)	83 | 0.30 (0.09)
	60 | 3.69 (0.58)	60 | 4.87 (0.57)	72 | 3.90 (0.46)	70 | 2.07 (0.28)	69 | 1.29 (0.22)	88 | 0.33 (0.08)
	65 | 5.34 (0.64)	65 | 5.07 (0.57)	80 | 2.59 (0.31)	76 | 2.05 (0.33)	76 | 1.38 (0.24)	94 | 0.11 (0.04)
	71 | 5.20 (0.60)	70 | 4.53 (0.66)	87 | 1.29 (0.19)	81 | 1.41 (0.23)	81 | 0.87 (0.18)	100 | 0.18 (0.06)
	76 | 4.84 (0.75)	74 | 3.79 (0.58)	92 | 2.66 (0.42)	86 | 2.03 (0.31)	86 | 0.70 (0.16)	109 | 0.16 (0.05)
	79 | 4.37 (0.68)	78 | 3.69 (0.54)	97 | 3.16 (0.44)	92 | 1.30 (0.22)	92 | 0.90 (0.14)	118 | 0.18 (0.05)
	83 | 2.57 (0.40)	82 | 1.87 (0.30)	104 | 3.02 (0.47)	98 | 1.82 (0.27)	100 | 0.95 (0.15)	129 | 0.16 (0.02)
	87 | 2.34 (0.32)	86 | 1.41 (0.21)	111 | 2.79 (0.31)	105 | 2.12 (0.27)	108 | 1.20 (0.19)	
	92 | 3.05 (0.52)	92 | 2.14 (0.43)	118 | 2.69 (0.23)	113 | 2.68 (0.28)	117 | 0.41 (0.05)	
	97 | 4.11 (0.59)	97 | 3.68 (0.48)		122 | 2.44 (0.31)	128 | 0.40 (0.05)	
	103 | 5.10 (0.65)	104 | 4.21 (0.48)				
	109 | 4.28 (0.58)	110 | 3.66 (0.37)				
	116 | 4.40 (0.38)	118 | 3.41 (0.29)				
		127 | 0.87 (0.21)				

Table 162. Triton production cross sections for 600 MeV/u silicon on copper.

5	10	20	30	40	60	80
	24 | 2.85 (0.79)	24 | 2.34 (0.59)	24 | 2.67 (0.62)	23 | 1.16 (0.32)	23 | 0.66 (0.21)	33 | 0.25 (0.11)
	26 | 2.97 (0.75)	26 | 4.17 (0.81)	26 | 2.37 (0.57)	25 | 1.91 (0.40)	25 | 0.70 (0.21)	35 | 0.06 (0.10)
	28 | 4.18 (1.05)	29 | 2.53 (0.59)	29 | 2.21 (0.48)	28 | 2.22 (0.39)	28 | 0.90 (0.24)	38 | 0.21 (0.08)
	31 | 2.88 (0.72)	31 | 2.85 (0.56)	32 | 2.16 (0.42)	32 | 1.05 (0.23)	31 | 0.32 (0.17)	42 | 0.19 (0.07)
	34 | 2.68 (0.67)	34 | 2.25 (0.46)	36 | 1.60 (0.37)	35 | 0.96 (0.22)	35 | 0.56 (0.16)	47 | 0.03 (0.06)
	37 | 1.87 (0.50)	38 | 1.76 (0.41)	40 | 1.52 (0.38)	40 | 0.94 (0.20)	39 | 0.67 (0.15)	52 | 0.23 (0.16)
	41 | 1.92 (0.58)	41 | 1.81 (0.41)	44 | 1.18 (0.25)	45 | 1.31 (0.22)	43 | 0.83 (0.19)	57 | 0.02 (0.05)
	45 | 1.54 (0.41)	45 | 1.94 (0.41)	49 | 1.30 (0.31)	50 | 0.60 (0.17)	47 | 0.29 (0.13)	63 | 0.04 (0.03)
	49 | 1.24 (0.34)	48 | 1.43 (0.33)	53 | 0.88 (0.22)	55 | 1.15 (0.21)	53 | 0.34 (0.10)	74 | 0.03 (0.02)
	53 | 0.69 (0.29)	53 | 1.25 (0.28)	58 | 1.31 (0.27)	61 | 0.91 (0.17)	57 | 0.21 (0.10)	80 | 0.05 (0.03)
	58 | 1.69 (0.36)	56 | 1.63 (0.42)	62 | 0.83 (0.29)	66 | 0.76 (0.21)	60 | 0.22 (0.12)	86 | 0.01 (0.01)
	61 | 1.13 (0.37)	59 | 1.97 (0.46)	65 | 1.16 (0.31)	70 | 0.19 (0.10)	64 | 0.10 (0.05)	93 | 0.04 (0.03)
	64 | 0.94 (0.43)	62 | 2.93 (0.59)	68 | 1.46 (0.35)	74 | 0.37 (0.10)	68 | 0.25 (0.11)	111 | 0.07 (0.01)
	67 | 1.48 (0.42)	65 | 1.72 (0.38)	72 | 1.03 (0.27)	79 | 0.25 (0.05)	72 | 0.32 (0.11)	
	70 | 0.73 (0.25)	68 | 2.02 (0.42)	76 | 1.40 (0.31)	84 | 0.36 (0.21)	77 | 0.00 (0.00)	
	73 | 1.75 (0.41)	72 | 1.19 (0.29)	80 | 1.22 (0.20)	89 | 0.33 (0.12)	83 | 0.11 (0.08)	
	77 | 1.03 (0.36)	76 | 2.26 (0.42)	85 | 1.41 (0.21)	96 | 0.16 (0.09)	89 | 0.08 (0.01)	
	81 | 1.64 (0.28)	80 | 1.44 (0.21)	90 | 1.22 (0.28)	103 | 0.12 (0.02)	97 | 0.38 (0.14)	
	86 | 1.75 (0.28)	85 | 1.55 (0.22)	96 | 1.17 (0.25)	111 | 0.20 (0.03)	105 | 0.13 (0.05)	
	90 | 1.70 (0.40)	90 | 1.86 (0.36)	102 | 1.14 (0.28)		114 | 0.13 (0.02)	
	95 | 1.64 (0.34)	95 | 1.09 (0.23)	109 | 1.48 (0.14)			
	101 | 1.37 (0.33)	102 | 1.17 (0.24)	117 | 1.68 (0.26)			
	107 | 1.25 (0.13)	109 | 0.82 (0.10)				
	114 | 0.74 (0.19)	117 | 0.24 (0.15)				

Table 163. Proton production cross sections for 600 MeV/u silicon on lead.

5	10	20	30	40	60	80
	55 | 26.79 (2.94)	55 | 25.38 (2.63)	57 | 20.51 (2.28)	55 | 18.64 (2.12)	64 | 15.76 (1.84)	98 | 5.51 (0.82)
	60 | 19.98 (2.17)	59 | 27.19 (2.51)	62 | 23.41 (2.23)	61 | 21.28 (1.96)	70 | 17.32 (1.69)	103 | 4.51 (0.60)
	65 | 22.11 (2.42)	65 | 25.13 (2.42)	68 | 17.91 (1.96)	67 | 20.52 (1.84)	77 | 15.80 (1.49)	111 | 7.23 (0.81)
	71 | 20.21 (2.25)	71 | 22.41 (2.08)	75 | 17.87 (1.71)	73 | 18.16 (1.62)	86 | 13.45 (1.22)	121 | 6.45 (0.67)
	78 | 19.29 (1.83)	78 | 21.35 (2.09)	82 | 16.52 (1.71)	81 | 18.52 (1.63)	97 | 11.52 (1.10)	134 | 4.96 (0.54)
	86 | 21.71 (2.18)	84 | 17.82 (1.78)	89 | 19.16 (1.78)	88 | 16.32 (1.43)	108 | 10.70 (0.95)	150 | 3.45 (0.36)
	93 | 18.62 (1.88)	92 | 18.72 (1.68)	98 | 18.74 (1.63)	95 | 19.29 (1.90)	119 | 10.24 (1.02)	167 | 2.32 (0.31)
	102 | 19.74 (1.74)	99 | 17.64 (2.12)	105 | 18.42 (1.93)	100 | 16.00 (1.59)	128 | 7.89 (0.77)	181 | 3.18 (0.37)
	110 | 20.18 (2.14)	105 | 15.96 (1.78)	111 | 15.61 (1.75)	106 | 15.56 (1.51)	138 | 5.78 (0.60)	200 | 1.59 (0.20)
	116 | 17.88 (1.74)	111 | 18.47 (1.85)	118 | 15.72 (1.48)	113 | 13.54 (1.30)	150 | 5.93 (0.64)	
	122 | 17.75 (1.52)	117 | 14.55 (1.44)	125 | 11.21 (1.06)	121 | 11.01 (0.96)	165 | 8.24 (0.77)	
	130 | 17.26 (1.80)	125 | 12.84 (1.16)	134 | 13.98 (1.41)	129 | 13.88 (1.29)	182 | 6.61 (0.61)	
	138 | 16.76 (1.74)	133 | 14.27 (1.47)	143 | 13.96 (1.35)	139 | 12.17 (1.09)	203 | 3.04 (0.31)	
	147 | 21.32 (2.04)	143 | 14.72 (1.53)	154 | 16.27 (1.62)	151 | 12.35 (1.13)		
	157 | 21.72 (1.93)	154 | 19.49 (1.75)	167 | 14.68 (1.39)	164 | 12.84 (1.15)		
	169 | 18.65 (1.72)	166 | 18.87 (1.66)	181 | 10.37 (0.99)			

Table 164. Deuteron production cross sections for 600 MeV/u silicon on lead.

5	10	20	30	40	60	80
	31 | 22.24 (3.40)	31 | 19.07 (2.59)	32 | 14.93 (2.23)	31 | 15.55 (1.95)	34 | 9.88 (1.39)	48 | 1.68 (0.82)
	33 | 17.06 (3.01)	33 | 15.83 (2.12)	36 | 13.65 (1.90)	34 | 15.20 (1.73)	37 | 12.48 (1.46)	52 | 2.09 (0.47)
	37 | 20.65 (3.16)	37 | 16.99 (2.03)	40 | 17.89 (2.06)	38 | 13.05 (1.45)	41 | 6.95 (1.09)	56 | 2.64 (0.48)
	40 | 17.83 (2.25)	41 | 15.06 (1.98)	44 | 13.94 (1.81)	43 | 11.42 (1.34)	45 | 8.89 (1.08)	61 | 2.79 (0.53)
	45 | 19.45 (2.50)	45 | 16.96 (1.94)	48 | 18.81 (1.96)	48 | 13.06 (1.35)	49 | 8.17 (1.12)	66 | 1.56 (0.38)
	49 | 17.95 (2.07)	50 | 17.55 (1.87)	54 | 12.55 (1.40)	54 | 13.02 (1.36)	54 | 8.13 (1.01)	72 | 2.13 (0.36)
	54 | 15.66 (1.72)	55 | 14.27 (1.77)	60 | 11.96 (1.48)	60 | 11.86 (1.27)	59 | 7.26 (0.89)	80 | 1.97 (0.31)
	60 | 13.44 (1.78)	60 | 14.99 (1.69)	66 | 12.18 (1.40)	66 | 8.78 (1.00)	64 | 5.54 (0.88)	87 | 2.16 (0.42)
	65 | 14.92 (1.77)	65 | 17.71 (1.84)	70 | 10.46 (1.67)	74 | 7.36 (0.82)	67 | 7.21 (1.07)	93 | 0.98 (0.22)
	70 | 15.19 (1.67)	70 | 12.88 (1.86)	74 | 12.90 (1.94)	81 | 4.44 (0.62)	71 | 6.32 (0.95)	100 | 0.92 (0.21)
	75 | 12.12 (1.91)	74 | 12.59 (1.85)	78 | 10.51 (1.52)	86 | 5.91 (0.96)	75 | 5.00 (0.74)	108 | 0.70 (0.17)
	79 | 15.38 (2.14)	77 | 9.85 (1.50)	82 | 4.63 (0.69)	91 | 4.31 (0.68)	80 | 3.83 (0.61)	117 | 0.71 (0.16)
	83 | 9.94 (1.29)	82 | 8.79 (1.13)	87 | 3.69 (0.59)	98 | 6.76 (0.83)	86 | 2.71 (0.43)	128 | 0.57 (0.07)
	87 | 5.66 (0.78)	86 | 7.20 (0.90)	92 | 7.43 (1.16)	105 | 7.82 (0.87)	92 | 2.42 (0.36)	
	92 | 10.41 (1.59)	91 | 6.39 (1.20)	97 | 7.64 (1.16)	113 | 5.70 (0.56)	99 | 3.31 (0.47)	
	97 | 13.81 (1.75)	97 | 9.70 (1.34)	104 | 11.02 (1.43)	122 | 4.76 (0.52)	107 | 3.50 (0.57)	
	103 | 13.37 (1.71)	103 | 13.25 (1.44)	111 | 12.14 (1.38)		117 | 2.07 (0.25)	
	109 | 14.28 (1.65)	110 | 11.13 (1.26)	118 | 8.61 (0.77)		128 | 1.91 (0.22)	
	116 | 11.40 (0.99)	118 | 8.84 (0.77)				

Table 165. Triton production cross sections for 600 MeV/u silicon on lead.

5	10	20	30	40	60	80
	23 | 20.28 (3.61)	22 | 15.36 (3.25)	24 | 8.55 (2.01)	22 | 10.57 (1.88)	24 | 5.00 (1.03)	33 | 1.04 (0.37)
	25 | 18.73 (3.11)	24 | 11.65 (2.55)	26 | 14.18 (2.27)	24 | 11.07 (1.68)	26 | 6.91 (1.13)	35 | 0.15 (0.45)
	27 | 22.49 (3.31)	26 | 14.14 (2.37)	29 | 11.01 (1.80)	27 | 10.03 (1.45)	29 | 6.03 (1.15)	40 | 1.25 (0.40)
	30 | 10.72 (2.36)	29 | 10.58 (1.73)	32 | 7.03 (1.36)	30 | 8.04 (1.14)	32 | 3.74 (0.70)	44 | 1.05 (0.30)
	33 | 14.67 (2.64)	32 | 12.97 (1.99)	36 | 9.82 (1.61)	34 | 7.01 (1.07)	36 | 4.34 (0.73)	50 | 0.81 (0.31)
	36 | 10.58 (1.94)	35 | 14.32 (1.95)	39 | 6.55 (1.26)	38 | 6.69 (0.97)	40 | 4.15 (0.63)	57 | 0.27 (0.17)
	39 | 8.55 (1.95)	39 | 11.94 (1.67)	44 | 7.71 (1.21)	43 | 4.02 (0.66)	45 | 2.18 (0.49)	63 | 0.26 (0.12)
	43 | 9.10 (1.62)	44 | 8.00 (1.17)	48 | 4.42 (0.97)	48 | 5.22 (0.83)	50 | 2.52 (0.51)	69 | 0.19 (0.19)
	47 | 7.12 (1.43)	48 | 6.91 (1.20)	53 | 6.85 (1.12)	52 | 4.11 (0.73)	55 | 2.41 (0.44)	74 | 0.11 (0.08)
	51 | 6.96 (1.36)	53 | 6.69 (1.13)	58 | 5.60 (0.96)	58 | 4.93 (0.70)	60 | 1.52 (0.47)	79 | 0.04 (0.04)
	55 | 7.03 (1.26)	57 | 7.06 (1.06)	62 | 4.61 (1.14)	62 | 4.52 (0.86)	64 | 1.11 (0.32)	86 | 0.15 (0.04)
	59 | 5.11 (1.42)	62 | 7.02 (1.61)	65 | 4.96 (1.09)	66 | 4.40 (0.84)	68 | 1.17 (0.35)	93 | 0.16 (0.07)
	61 | 7.46 (1.67)	65 | 5.88 (1.20)	68 | 4.33 (1.01)	70 | 0.57 (0.26)	72 | 1.42 (0.35)	101 | 0.39 (0.11)
	64 | 4.81 (1.39)	68 | 7.25 (1.32)	72 | 4.24 (0.95)	74 | 1.18 (0.39)	77 | 0.42 (0.16)	111 | 0.36 (0.06)
	67 | 4.84 (1.17)	72 | 7.31 (1.26)	76 | 4.60 (0.94)	78 | 1.29 (0.21)	83 | 0.52 (0.12)	122 | 0.14 (0.06)
	70 | 3.57 (1.00)	76 | 8.68 (1.37)	80 | 3.82 (0.62)	84 | 1.93 (0.51)	89 | 0.74 (0.13)	
	73 | 5.93 (1.25)	80 | 5.25 (0.64)	85 | 5.58 (0.76)	89 | 2.09 (0.47)	97 | 1.25 (0.39)	
	77 | 4.66 (1.20)	85 | 5.53 (0.65)	90 | 4.50 (0.88)	96 | 1.43 (0.36)	105 | 0.59 (0.17)	
	81 | 6.23 (0.86)	90 | 5.14 (0.98)	96 | 4.94 (0.89)	103 | 0.83 (0.12)	114 | 0.80 (0.10)	
	85 | 5.19 (0.83)	95 | 2.54 (0.67)	102 | 2.29 (0.70)	111 | 1.45 (0.17)		
	90 | 6.70 (1.39)	102 | 2.83 (0.58)	109 | 3.73 (0.36)			
	95 | 5.72 (1.08)	109 | 2.28 (0.27)	117 | 5.55 (0.78)			
	101 | 5.01 (1.01)					
	107 | 3.42 (0.36)					

Table 166. Proton production cross sections for 400 MeV/u carbon on aluminum.

5	10	20	30	40	60	80
61 | 2.08 (0.28)	62 | 3.34 (0.38)	59 | 3.12 (0.32)	61 | 2.39 (0.30)	63 | 2.27 (0.25)	74 | 2.18 (0.23)	117 | 0.63 (0.14)
66 | 1.95 (0.24)	66 | 3.73 (0.36)	63 | 3.01 (0.30)	65 | 2.74 (0.27)	68 | 2.65 (0.24)	79 | 1.73 (0.19)	121 | 0.66 (0.12)
71 | 2.33 (0.27)	72 | 3.94 (0.36)	68 | 2.84 (0.27)	70 | 2.61 (0.27)	74 | 2.57 (0.23)	85 | 1.44 (0.15)	128 | 0.48 (0.09)
77 | 1.53 (0.20)	78 | 3.71 (0.32)	74 | 3.37 (0.29)	75 | 2.81 (0.26)	82 | 2.50 (0.21)	92 | 1.62 (0.16)	135 | 0.48 (0.08)
83 | 1.30 (0.22)	85 | 2.94 (0.26)	79 | 3.07 (0.29)	81 | 2.87 (0.27)	89 | 2.52 (0.22)	99 | 1.30 (0.13)	144 | 0.44 (0.06)
89 | 2.17 (0.24)	93 | 2.89 (0.28)	85 | 2.93 (0.26)	86 | 2.75 (0.25)	97 | 2.15 (0.19)	106 | 1.45 (0.15)	153 | 0.36 (0.07)
95 | 1.55 (0.24)	101 | 3.27 (0.27)	90 | 3.36 (0.35)	93 | 2.56 (0.23)	105 | 2.38 (0.22)	112 | 1.13 (0.13)	161 | 0.24 (0.05)
99 | 1.01 (0.17)	110 | 3.37 (0.26)	94 | 3.14 (0.34)	99 | 2.96 (0.30)	111 | 2.25 (0.21)	118 | 1.30 (0.14)	170 | 0.22 (0.04)
103 | 0.87 (0.15)	119 | 3.17 (0.31)	98 | 3.03 (0.31)	104 | 2.59 (0.26)	117 | 2.55 (0.22)	125 | 1.32 (0.13)	181 | 0.17 (0.03)
108 | 1.04 (0.18)	125 | 2.52 (0.22)	103 | 3.40 (0.31)	109 | 2.70 (0.26)	125 | 1.93 (0.16)	134 | 1.01 (0.10)	196 | 0.18 (0.03)
113 | 1.17 (0.16)	132 | 2.31 (0.20)	108 | 3.22 (0.30)	115 | 3.08 (0.27)	133 | 1.53 (0.13)	144 | 0.84 (0.09)	214 | 0.14 (0.02)
119 | 1.20 (0.17)	140 | 2.48 (0.24)	114 | 3.45 (0.30)	121 | 2.60 (0.22)	143 | 1.46 (0.14)	156 | 0.62 (0.07)	237 | 0.10 (0.02)
	150 | 2.58 (0.24)	121 | 2.98 (0.25)	129 | 2.37 (0.19)	155 | 1.94 (0.17)	170 | 0.75 (0.07)	268 | 0.07 (0.01)
	160 | 2.80 (0.24)	128 | 2.81 (0.22)	137 | 2.26 (0.20)	168 | 1.09 (0.10)	187 | 0.35 (0.04)	309 | 0.03 (0.01)
		136 | 2.71 (0.22)	147 | 2.29 (0.20)			367 | 0.01 (0.00)
		146 | 2.87 (0.23)	157 | 2.52 (0.20)			
		157 | 3.36 (0.26)				

Table 167. Deuteron production cross sections for 400 MeV/u carbon on aluminum.

5	10	20	30	40	60	80
35 | 0.52 (0.28)	33 | 2.02 (0.37)	32 | 0.94 (0.20)	33 | 1.26 (0.27)	35 | 1.60 (0.20)	39 | 1.12 (0.17)	56 | 0.28 (0.09)
37 | 1.10 (0.23)	36 | 2.23 (0.31)	35 | 1.19 (0.25)	36 | 1.08 (0.24)	38 | 1.08 (0.15)	42 | 0.79 (0.14)	59 | 0.20 (0.09)
40 | 0.76 (0.24)	39 | 2.11 (0.30)	38 | 1.30 (0.22)	39 | 1.39 (0.22)	42 | 1.24 (0.17)	47 | 0.58 (0.10)	63 | 0.20 (0.08)
44 | 0.69 (0.21)	43 | 1.44 (0.27)	41 | 1.51 (0.22)	43 | 1.19 (0.21)	46 | 1.29 (0.16)	51 | 0.57 (0.09)	66 | 0.26 (0.08)
47 | 0.95 (0.21)	46 | 1.42 (0.21)	45 | 1.52 (0.19)	47 | 1.63 (0.20)	50 | 1.15 (0.16)	56 | 0.51 (0.09)	70 | 0.13 (0.04)
51 | 0.68 (0.17)	51 | 2.10 (0.25)	50 | 1.58 (0.19)	52 | 1.38 (0.16)	54 | 0.86 (0.12)	62 | 0.34 (0.06)	74 | 0.08 (0.06)
55 | 0.66 (0.16)	55 | 1.91 (0.28)	54 | 1.52 (0.21)	57 | 1.11 (0.17)	59 | 1.17 (0.14)	66 | 0.33 (0.09)	77 | 0.05 (0.05)
59 | 0.54 (0.17)	59 | 1.52 (0.24)	59 | 1.25 (0.17)	61 | 1.16 (0.16)	63 | 0.80 (0.15)	70 | 0.43 (0.08)	80 | 0.06 (0.04)
80 | 1.15 (0.22)	63 | 1.48 (0.22)	64 | 1.74 (0.20)	67 | 1.10 (0.14)	66 | 0.81 (0.14)	73 | 0.32 (0.07)	84 | 0.05 (0.03)
84 | 1.08 (0.19)	67 | 1.49 (0.29)	68 | 1.18 (0.21)	72 | 0.73 (0.17)	70 | 0.90 (0.14)	78 | 0.29 (0.06)	93 | 0.08 (0.03)
88 | 0.91 (0.16)	70 | 1.59 (0.26)	71 | 1.20 (0.20)	75 | 0.96 (0.17)	73 | 0.83 (0.13)	83 | 0.24 (0.05)	99 | 0.02 (0.02)
93 | 0.82 (0.15)	73 | 1.52 (0.27)	75 | 1.64 (0.21)	79 | 1.30 (0.17)	78 | 0.76 (0.10)	88 | 0.22 (0.04)	106 | 0.05 (0.02)
98 | 0.99 (0.17)	76 | 1.66 (0.25)	79 | 1.79 (0.22)	83 | 1.01 (0.15)	82 | 0.66 (0.11)	94 | 0.18 (0.04)	114 | 0.01 (0.01)
104 | 1.11 (0.15)	80 | 1.82 (0.26)	83 | 1.30 (0.14)	88 | 0.96 (0.12)	87 | 0.59 (0.08)	101 | 0.12 (0.03)	123 | 0.04 (0.01)
110 | 1.13 (0.16)	84 | 1.81 (0.24)	87 | 1.32 (0.18)	93 | 0.75 (0.12)	93 | 0.60 (0.09)	110 | 0.16 (0.03)	134 | 0.01 (0.01)
	88 | 1.59 (0.19)	93 | 1.15 (0.17)	99 | 1.05 (0.14)	99 | 0.69 (0.11)	119 | 0.14 (0.03)	
	93 | 1.63 (0.22)	98 | 1.42 (0.18)	105 | 1.13 (0.13)	106 | 0.68 (0.08)		
	98 | 1.79 (0.23)					
	104 | 2.50 (0.26)					
	110 | 1.97 (0.23)					

Table 168. Triton production cross sections for 400 MeV/u carbon on aluminum.

5	10	20	30	40	60	80
	24 | 0.50 (0.23)	24 | 0.53 (0.14)	25 | 0.83 (0.21)	26 | 0.66 (0.14)	27 | 0.36 (0.09)	39 | 0.19 (0.09)
	26 | 0.63 (0.21)	26 | 0.65 (0.15)	27 | 0.85 (0.17)	28 | 0.51 (0.11)	30 | 0.29 (0.08)	42 | 0.13 (0.06)
	28 | 0.70 (0.21)	29 | 0.75 (0.16)	30 | 0.92 (0.17)	31 | 0.39 (0.12)	33 | 0.24 (0.06)	45 | 0.09 (0.03)
	31 | 0.51 (0.17)	31 | 0.58 (0.13)	32 | 0.62 (0.15)	34 | 0.46 (0.10)	36 | 0.16 (0.06)	49 | 0.05 (0.03)
	34 | 0.75 (0.20)	34 | 0.77 (0.16)	35 | 0.74 (0.13)	38 | 0.53 (0.11)	39 | 0.27 (0.06)	53 | 0.03 (0.02)
	37 | 0.26 (0.13)	37 | 0.97 (0.17)	39 | 0.54 (0.12)	41 | 0.36 (0.08)	43 | 0.21 (0.06)	56 | 0.02 (0.02)
	40 | 0.54 (0.17)	41 | 0.69 (0.14)	42 | 0.13 (0.09)	44 | 0.53 (0.11)	46 | 0.20 (0.05)	59 | 0.06 (0.04)
	43 | 0.46 (0.15)	44 | 0.65 (0.12)	45 | 0.20 (0.10)	48 | 0.41 (0.08)	50 | 0.09 (0.05)	69 | 0.02 (0.01)
	46 | 0.55 (0.18)	47 | 0.47 (0.11)	49 | 0.47 (0.10)	52 | 0.33 (0.09)	52 | 0.21 (0.07)	73 | 0.00 (0.00)
	50 | 0.62 (0.16)	50 | 0.34 (0.15)	52 | 0.41 (0.12)	54 | 0.20 (0.06)	55 | 0.10 (0.05)	78 | 0.02 (0.01)
	53 | 0.35 (0.16)	52 | 0.46 (0.12)	55 | 0.20 (0.08)	57 | 0.23 (0.07)	58 | 0.09 (0.04)	
	55 | 0.53 (0.18)	54 | 0.34 (0.13)	57 | 0.33 (0.10)	60 | 0.29 (0.08)	61 | 0.05 (0.03)	
	57 | 0.50 (0.20)	57 | 0.38 (0.12)	60 | 0.22 (0.08)	63 | 0.24 (0.07)	65 | 0.16 (0.04)	
	59 | 0.36 (0.12)	59 | 0.23 (0.08)	62 | 0.31 (0.10)	67 | 0.14 (0.04)	69 | 0.05 (0.02)	
	62 | 0.46 (0.13)	62 | 0.26 (0.08)	65 | 0.36 (0.09)	70 | 0.13 (0.04)	73 | 0.03 (0.02)	
	64 | 0.49 (0.15)	65 | 0.18 (0.06)	69 | 0.15 (0.05)	75 | 0.13 (0.04)	79 | 0.01 (0.01)	
	67 | 0.38 (0.11)	69 | 0.43 (0.10)	72 | 0.14 (0.05)		84 | 0.02 (0.01)	
	71 | 0.33 (0.10)	72 | 0.35 (0.09)	76 | 0.25 (0.08)			
	74 | 0.51 (0.15)	76 | 0.37 (0.08)	81 | 0.05 (0.03)			
	78 | 0.92 (0.17)					
	82 | 0.23 (0.09)					

Table 169. ^{3}He production cross sections for 400 MeV/u carbon on aluminum.

5	10	20	30	40	60	80
	125 | 0.38 (0.09)	114 | 0.24 (0.07)	116 | 0.22 (0.06)	118 | 0.03 (0.01)		
	131 | 0.45 (0.10)	120 | 0.26 (0.06)	122 | 0.11 (0.04)	125 | 0.08 (0.03)		
	137 | 0.54 (0.10)	126 | 0.31 (0.06)	127 | 0.06 (0.06)	131 | 0.04 (0.02)		
	145 | 0.36 (0.08)	134 | 0.23 (0.05)	134 | 0.19 (0.05)	140 | 0.02 (0.02)		
	155 | 0.39 (0.08)	141 | 0.24 (0.05)	143 | 0.06 (0.04)	149 | 0.04 (0.02)		
	164 | 0.47 (0.07)	150 | 0.17 (0.04)	152 | 0.12 (0.03)	159 | 0.03 (0.01)		
	176 | 0.48 (0.07)	161 | 0.16 (0.04)	162 | 0.08 (0.03)	173 | 0.04 (0.01)		
		173 | 0.21 (0.04)	174 | 0.11 (0.03)	189 | 0.03 (0.01)		
			188 | 0.05 (0.02)	200 | 0.24 (0.07)		

Table 170. ^{4}He production cross sections for 400 MeV/u carbon on aluminum.

5	10	20	30	40	60	80
	98 | 0.16 (0.07)	93 | 0.11 (0.04)	99 | 0.08 (0.04)	99 | 0.04 (0.02)		
	102 | 0.18 (0.08)	98 | 0.04 (0.04)	103 | 0.13 (0.04)	104 | 0.05 (0.02)		
	107 | 0.14 (0.06)	102 | 0.14 (0.05)	108 | 0.10 (0.04)	110 | 0.07 (0.02)		
	112 | 0.14 (0.05)	108 | 0.17 (0.06)	114 | 0.08 (0.04)	117 | 0.04 (0.02)		
	118 | 0.11 (0.05)	113 | 0.03 (0.04)	121 | 0.06 (0.03)	124 | 0.02 (0.01)		
	124 | 0.13 (0.04)	120 | 0.08 (0.03)	128 | 0.09 (0.03)			
	131 | 0.14 (0.06)	127 | 0.11 (0.03)	136 | 0.01 (0.01)			
	139 | 0.18 (0.05)	135 | 0.09 (0.04)	156 | 0.03 (0.01)			
	148 | 0.13 (0.04)	144 | 0.09 (0.03)				
	158 | 0.09 (0.04)	155 | 0.06 (0.02)				

Table 171. Proton production cross sections for 400 MeV/u carbon on carbon.

5	10	20	30	40	60	80
62 | 0.96 (0.15)	61 | 1.64 (0.20)	61 | 1.51 (0.16)	61 | 1.28 (0.16)	64 | 1.18 (0.13)	74 | 0.95 (0.11)	119 | 0.44 (0.08)
67 | 0.94 (0.12)	65 | 1.62 (0.17)	65 | 1.57 (0.15)	65 | 1.45 (0.15)	69 | 1.42 (0.13)	78 | 0.96 (0.11)	125 | 0.32 (0.06)
72 | 0.78 (0.12)	70 | 1.65 (0.17)	70 | 1.52 (0.14)	70 | 1.43 (0.15)	75 | 1.39 (0.12)	84 | 0.91 (0.10)	132 | 0.25 (0.04)
78 | 0.66 (0.10)	76 | 2.02 (0.18)	76 | 1.78 (0.15)	75 | 1.25 (0.13)	82 | 1.30 (0.11)	90 | 0.74 (0.08)	141 | 0.15 (0.03)
84 | 0.71 (0.11)	83 | 1.75 (0.15)	83 | 1.66 (0.15)	81 | 1.51 (0.14)	90 | 1.22 (0.11)	96 | 0.85 (0.09)	151 | 0.17 (0.03)
90 | 0.86 (0.11)	90 | 1.75 (0.17)	89 | 1.46 (0.13)	87 | 1.38 (0.13)	98 | 1.23 (0.10)	102 | 0.61 (0.08)	162 | 0.13 (0.03)
95 | 0.69 (0.12)	97 | 1.64 (0.14)	94 | 1.51 (0.17)	94 | 1.35 (0.12)	105 | 1.19 (0.12)	107 | 0.65 (0.07)	172 | 0.11 (0.02)
99 | 0.33 (0.07)	106 | 1.69 (0.14)	99 | 1.21 (0.15)	102 | 1.24 (0.11)	111 | 1.12 (0.11)	112 | 0.56 (0.07)	183 | 0.07 (0.02)
103 | 0.37 (0.07)	113 | 1.91 (0.18)	103 | 1.53 (0.15)	110 | 1.39 (0.14)	118 | 1.35 (0.12)	119 | 0.64 (0.07)	198 | 0.07 (0.01)
108 | 0.35 (0.08)	119 | 1.69 (0.16)	109 | 1.76 (0.17)	115 | 1.43 (0.13)	125 | 1.01 (0.09)	126 | 0.60 (0.06)	216 | 0.05 (0.01)
113 | 0.68 (0.09)	126 | 1.82 (0.15)	114 | 1.74 (0.15)	122 | 1.27 (0.11)	134 | 0.81 (0.07)	134 | 0.57 (0.06)	240 | 0.03 (0.01)
119 | 0.61 (0.09)	133 | 1.57 (0.13)	121 | 1.53 (0.13)	129 | 1.18 (0.10)	144 | 0.96 (0.08)	144 | 0.45 (0.05)	271 | 0.02 (0.00)
125 | 0.22 (0.05)	141 | 1.49 (0.13)	128 | 1.46 (0.11)	138 | 1.23 (0.11)	155 | 1.05 (0.09)	156 | 0.30 (0.03)	313 | 0.01 (0.00)
	150 | 1.61 (0.14)	137 | 1.37 (0.12)	147 | 1.18 (0.10)		171 | 0.38 (0.04)	
	160 | 1.60 (0.13)	146 | 1.63 (0.13)	158 | 1.37 (0.11)		188 | 0.16 (0.02)	
		157 | 2.01 (0.15)				

Table 172. Deuteron production cross sections for 400 MeV/u carbon on carbon.

5	10	20	30	40	60	80
35 | 0.61 (0.16)	34 | 1.01 (0.20)	34 | 0.60 (0.13)	34 | 0.72 (0.15)	35 | 0.53 (0.09)	39 | 0.33 (0.07)	56 | 0.14 (0.06)
38 | 0.61 (0.14)	36 | 0.82 (0.14)	36 | 0.65 (0.12)	37 | 0.37 (0.11)	38 | 0.72 (0.09)	43 | 0.31 (0.07)	59 | 0.09 (0.04)
42 | 0.34 (0.12)	39 | 0.68 (0.13)	40 | 0.56 (0.10)	40 | 0.47 (0.11)	41 | 0.64 (0.09)	47 | 0.19 (0.04)	63 | 0.07 (0.04)
45 | 0.64 (0.13)	43 | 0.74 (0.15)	44 | 0.76 (0.11)	43 | 0.63 (0.11)	45 | 0.42 (0.08)	52 | 0.17 (0.04)	68 | 0.05 (0.02)
48 | 0.41 (0.12)	46 | 1.10 (0.14)	48 | 0.84 (0.10)	47 | 0.50 (0.08)	49 | 0.52 (0.09)	57 | 0.22 (0.05)	74 | 0.04 (0.02)
51 | 0.44 (0.10)	51 | 0.83 (0.12)	53 | 0.83 (0.10)	51 | 0.56 (0.09)	53 | 0.55 (0.08)	62 | 0.15 (0.03)	79 | 0.04 (0.01)
54 | 0.15 (0.12)	55 | 0.84 (0.13)	59 | 0.58 (0.08)	55 | 0.49 (0.09)	57 | 0.49 (0.07)	66 | 0.18 (0.05)	85 | 0.04 (0.02)
56 | 0.29 (0.11)	59 | 0.74 (0.12)	64 | 0.53 (0.08)	59 | 0.49 (0.08)	61 | 0.48 (0.09)	70 | 0.16 (0.04)	89 | 0.00 (0.02)
58 | 0.44 (0.15)	63 | 0.75 (0.12)	70 | 0.68 (0.08)	63 | 0.36 (0.09)	63 | 0.36 (0.08)	74 | 0.11 (0.03)	94 | 0.01 (0.01)
60 | 0.11 (0.11)	67 | 0.73 (0.15)	75 | 0.78 (0.11)	66 | 0.52 (0.10)	67 | 0.39 (0.07)	78 | 0.11 (0.03)	100 | 0.02 (0.01)
77 | 0.32 (0.08)	70 | 0.58 (0.11)	79 | 0.70 (0.10)	69 | 0.47 (0.08)	70 | 0.37 (0.07)	83 | 0.11 (0.03)	107 | 0.01 (0.00)
80 | 0.43 (0.10)	73 | 0.77 (0.14)	83 | 0.64 (0.07)	72 | 0.33 (0.09)	74 | 0.32 (0.06)	88 | 0.11 (0.02)	115 | 0.01 (0.01)
84 | 0.43 (0.09)	77 | 0.65 (0.11)	88 | 0.53 (0.08)	75 | 0.46 (0.09)	78 | 0.46 (0.06)	95 | 0.08 (0.02)	125 | 0.01 (0.01)
88 | 0.30 (0.06)	80 | 0.50 (0.10)	93 | 0.51 (0.08)	79 | 0.42 (0.07)	82 | 0.36 (0.06)	102 | 0.05 (0.02)	
93 | 0.35 (0.07)	84 | 0.84 (0.11)	98 | 0.68 (0.09)	83 | 0.45 (0.07)	87 | 0.28 (0.05)	110 | 0.08 (0.02)	
98 | 0.34 (0.07)	88 | 0.78 (0.09)		88 | 0.47 (0.07)	93 | 0.27 (0.04)	119 | 0.04 (0.01)	
104 | 0.64 (0.09)	93 | 0.84 (0.11)		93 | 0.46 (0.07)	99 | 0.37 (0.05)		
110 | 0.58 (0.08)	98 | 1.05 (0.12)		99 | 0.46 (0.07)	106 | 0.27 (0.04)		
117 | 0.21 (0.05)	104 | 1.04 (0.12)		105 | 0.60 (0.07)			
	110 | 1.14 (0.12)					

Table 173. Triton production cross sections for 400 MeV/u carbon on carbon.

5	10	20	30	40	60	80
	25 | 0.45 (0.14)	23 | 0.30 (0.08)	24 | 0.19 (0.09)	26 | 0.15 (0.06)	26 | 0.14 (0.04)	37 | 0.01 (0.04)
	27 | 0.51 (0.13)	25 | 0.20 (0.07)	26 | 0.13 (0.06)	29 | 0.21 (0.06)	29 | 0.10 (0.05)	39 | 0.07 (0.04)
	29 | 0.28 (0.10)	28 | 0.34 (0.08)	29 | 0.34 (0.08)	32 | 0.31 (0.06)	32 | 0.08 (0.02)	42 | 0.04 (0.03)
	32 | 0.31 (0.09)	30 | 0.31 (0.08)	32 | 0.37 (0.09)	35 | 0.26 (0.05)	35 | 0.04 (0.03)	44 | 0.04 (0.02)
	35 | 0.44 (0.10)	33 | 0.32 (0.09)	34 | 0.22 (0.08)	38 | 0.17 (0.07)	38 | 0.08 (0.03)	46 | 0.05 (0.02)
	38 | 0.30 (0.08)	36 | 0.38 (0.08)	38 | 0.21 (0.06)	41 | 0.23 (0.05)	41 | 0.10 (0.03)	49 | 0.05 (0.02)
	41 | 0.41 (0.13)	39 | 0.28 (0.07)	41 | 0.16 (0.06)	45 | 0.24 (0.06)	44 | 0.01 (0.03)	53 | 0.02 (0.01)
	43 | 0.28 (0.08)	42 | 0.19 (0.05)	44 | 0.04 (0.05)	47 | 0.03 (0.03)	46 | 0.08 (0.04)	58 | 0.00 (0.00)
	46 | 0.18 (0.08)	45 | 0.35 (0.07)	47 | 0.18 (0.05)	50 | 0.14 (0.05)	48 | 0.09 (0.04)	64 | 0.01 (0.01)
	49 | 0.09 (0.11)	49 | 0.07 (0.04)	50 | 0.09 (0.06)	52 | 0.18 (0.05)	50 | 0.04 (0.03)	
	51 | 0.26 (0.08)	52 | 0.08 (0.04)	52 | 0.15 (0.05)	54 | 0.11 (0.04)	52 | 0.04 (0.03)	
	53 | 0.19 (0.09)	54 | 0.26 (0.08)	55 | 0.05 (0.03)	57 | 0.13 (0.04)	55 | 0.05 (0.03)	
	55 | 0.26 (0.09)	57 | 0.16 (0.06)	57 | 0.09 (0.04)	60 | 0.15 (0.04)	58 | 0.07 (0.03)	
	57 | 0.03 (0.06)	59 | 0.11 (0.04)	60 | 0.02 (0.01)	63 | 0.11 (0.04)	61 | 0.03 (0.02)	
	59 | 0.29 (0.09)	62 | 0.13 (0.04)	62 | 0.07 (0.04)	67 | 0.11 (0.03)	65 | 0.03 (0.01)	
	62 | 0.21 (0.08)	65 | 0.17 (0.05)	66 | 0.11 (0.04)	71 | 0.09 (0.03)	71 | 0.01 (0.01)	
	65 | 0.24 (0.08)	69 | 0.07 (0.03)	69 | 0.08 (0.03)	75 | 0.06 (0.02)	79 | 0.02 (0.01)	
	68 | 0.34 (0.08)	72 | 0.17 (0.05)	72 | 0.06 (0.03)		85 | 0.04 (0.01)	
	71 | 0.27 (0.06)	76 | 0.08 (0.03)	76 | 0.08 (0.03)			
	74 | 0.25 (0.08)		81 | 0.03 (0.02)			
	78 | 0.31 (0.08)					

Table 174. ^{3}He production cross sections for 400 MeV/u carbon on carbon.

5	10	20	30	40	60	80
	118 | 0.16 (0.04) 124 | 0.17 (0.05) 131 | 0.10 (0.04) 138 | 0.27 (0.06) 146 | 0.22 (0.04) 154 | 0.22 (0.04) 164 | 0.17 (0.03) 175 | 0.27 (0.04) 189 | 0.16 (0.03)	114 | 0.09 (0.03) 120 | 0.05 (0.03) 126 | 0.12 (0.03) 134 | 0.11 (0.03) 141 | 0.10 (0.02) 150 | 0.07 (0.02) 161 | 0.13 (0.02) 174 | 0.07 (0.02)	116 | 0.06 (0.02) 121 | 0.06 (0.02) 127 | 0.03 (0.03) 135 | 0.07 (0.02) 143 | 0.05 (0.02) 153 | 0.03 (0.01) 162 | 0.04 (0.01) 175 | 0.03 (0.01) 189 | 0.02 (0.01)	124 | 0.03 (0.01) 132 | 0.03 (0.01) 139 | 0.01 (0.01) 149 | 0.02 (0.01) 160 | 0.01 (0.01) 173 | 0.01 (0.01) 199 | 0.14 (0.06)		

Table 175. ^{4}He production cross sections for 400 MeV/u carbon on carbon.

5	10	20	30	40	60	80
	98 | 0.07 (0.03) 102 | 0.15 (0.05) 107 | 0.11 (0.04) 112 | 0.05 (0.02) 118 | 0.09 (0.03) 124 | 0.16 (0.04) 131 | 0.10 (0.03) 139 | 0.09 (0.03) 148 | 0.07 (0.02) 158 | 0.03 (0.02)	98 | 0.06 (0.03) 102 | 0.10 (0.03) 107 | 0.05 (0.02) 113 | 0.01 (0.02) 120 | 0.06 (0.02) 127 | 0.05 (0.02) 135 | 0.00 (0.01) 144 | 0.03 (0.01) 155 | 0.01 (0.01)	94 | 0.04 (0.02) 99 | 0.01 (0.01) 103 | 0.04 (0.02) 114 | 0.02 (0.02) 121 | 0.03 (0.02) 128 | 0.03 (0.01) 135 | 0.01 (0.01) 145 | 0.01 (0.01)	99 | 0.01 (0.01) 104 | 0.02 (0.01)		

Table 176. Proton production cross sections for 400 MeV/u carbon on copper.

5	10	20	30	40	60	80
61 | 4.08 (0.56)	61 | 7.30 (0.86)	59 | 6.58 (0.73)	60 | 5.59 (0.72)	62 | 5.75 (0.59)	72 | 3.42 (0.41)	112 | 0.67 (0.26)
65 | 4.34 (0.54)	65 | 6.68 (0.69)	64 | 6.90 (0.69)	64 | 6.09 (0.63)	67 | 5.38 (0.51)	77 | 3.72 (0.40)	117 | 1.34 (0.25)
71 | 3.25 (0.45)	71 | 6.21 (0.67)	69 | 6.51 (0.63)	69 | 6.40 (0.66)	73 | 4.39 (0.46)	84 | 3.41 (0.35)	122 | 1.06 (0.18)
77 | 2.90 (0.41)	77 | 5.85 (0.58)	75 | 7.01 (0.65)	74 | 5.64 (0.57)	81 | 4.85 (0.44)	93 | 3.25 (0.32)	131 | 0.76 (0.13)
83 | 2.88 (0.47)	83 | 5.67 (0.59)	81 | 6.33 (0.61)	80 | 5.00 (0.51)	89 | 5.30 (0.50)	102 | 2.48 (0.26)	141 | 0.82 (0.12)
89 | 4.04 (0.48)	89 | 5.94 (0.64)	88 | 5.48 (0.53)	86 | 5.46 (0.54)	97 | 5.29 (0.45)	113 | 2.54 (0.25)	154 | 0.66 (0.10)
94 | 2.43 (0.45)	94 | 7.43 (0.90)	93 | 5.97 (0.73)	91 | 5.36 (0.72)	104 | 4.02 (0.43)	124 | 2.15 (0.23)	167 | 0.59 (0.11)
98 | 1.91 (0.35)	98 | 5.52 (0.69)	98 | 5.76 (0.66)	94 | 4.96 (0.65)	110 | 4.22 (0.45)	132 | 1.94 (0.21)	178 | 0.39 (0.07)
102 | 1.36 (0.30)	102 | 6.53 (0.72)	102 | 5.70 (0.62)	99 | 4.54 (0.58)	116 | 4.54 (0.44)	142 | 1.56 (0.17)	192 | 0.25 (0.04)
107 | 1.49 (0.33)	107 | 4.99 (0.62)	107 | 6.02 (0.66)	103 | 5.63 (0.63)	124 | 3.21 (0.31)	154 | 1.28 (0.15)	209 | 0.32 (0.05)
112 | 2.50 (0.36)	112 | 5.65 (0.59)	113 | 6.35 (0.60)	108 | 4.91 (0.55)	132 | 2.88 (0.27)	168 | 1.51 (0.16)	232 | 0.21 (0.04)
118 | 1.99 (0.34)	118 | 6.17 (0.66)	120 | 5.73 (0.53)	114 | 5.59 (0.58)	142 | 2.91 (0.31)	185 | 0.65 (0.08)	262 | 0.13 (0.02)
125 | 0.64 (0.20)	125 | 6.13 (0.58)	127 | 4.65 (0.41)	121 | 4.46 (0.45)	154 | 3.75 (0.34)		302 | 0.06 (0.01)
	132 | 4.62 (0.45)	136 | 5.12 (0.47)	128 | 4.10 (0.38)	167 | 1.84 (0.19)		357 | 0.02 (0.01)
	140 | 4.03 (0.43)	145 | 4.99 (0.47)	136 | 4.80 (0.46)			
	149 | 4.77 (0.49)	156 | 5.94 (0.50)	146 | 4.27 (0.42)			
	159 | 3.98 (0.43)		157 | 4.62 (0.42)			
	171 | 2.62 (0.29)					

Table 177. Deuteron production cross sections for 400 MeV/u carbon on copper.

5	10	20	30	40	60	80
36 | 1.47 (0.47)	34 | 3.85 (0.73)	33 | 3.46 (0.63)	33 | 3.34 (0.75)	34 | 2.99 (0.54)	38 | 1.69 (0.37)	55 | 0.73 (0.20)
38 | 2.15 (0.56)	36 | 3.87 (0.68)	36 | 3.65 (0.60)	36 | 2.35 (0.50)	37 | 3.38 (0.47)	41 | 1.54 (0.29)	59 | 0.29 (0.12)
41 | 2.25 (0.52)	40 | 3.88 (0.59)	39 | 3.16 (0.52)	39 | 3.12 (0.54)	41 | 3.09 (0.44)	45 | 1.73 (0.31)	63 | 0.42 (0.15)
43 | 1.34 (0.38)	43 | 3.80 (0.62)	42 | 3.51 (0.54)	43 | 3.92 (0.63)	44 | 2.10 (0.34)	49 | 1.10 (0.17)	68 | 0.22 (0.07)
45 | 1.31 (0.55)	47 | 3.58 (0.48)	46 | 3.64 (0.49)	47 | 3.44 (0.48)	48 | 2.00 (0.33)	54 | 1.60 (0.29)	74 | 0.22 (0.09)
46 | 1.47 (0.80)	52 | 4.66 (0.59)	50 | 4.66 (0.61)	52 | 3.22 (0.41)	52 | 2.07 (0.35)	58 | 0.89 (0.15)	81 | 0.24 (0.06)
47 | 1.41 (0.63)	56 | 4.08 (0.62)	54 | 4.02 (0.57)	56 | 2.51 (0.42)	56 | 1.90 (0.29)	64 | 1.00 (0.17)	92 | 0.14 (0.05)
49 | 1.18 (0.41)	61 | 3.77 (0.53)	58 | 3.80 (0.50)	61 | 2.50 (0.38)	60 | 1.96 (0.38)	69 | 0.96 (0.19)	98 | 0.04 (0.03)
50 | 1.28 (0.44)	66 | 2.51 (0.45)	62 | 3.04 (0.58)	67 | 2.01 (0.30)	63 | 1.54 (0.32)	73 | 1.09 (0.20)	104 | 0.04 (0.02)
52 | 1.30 (0.46)	70 | 3.20 (0.50)	65 | 2.44 (0.49)	71 | 2.02 (0.43)	66 | 1.66 (0.26)	77 | 0.78 (0.16)	112 | 0.03 (0.03)
54 | 0.71 (0.33)	73 | 3.22 (0.55)	68 | 4.16 (0.64)	75 | 2.42 (0.45)	69 | 1.57 (0.29)	82 | 0.71 (0.15)	121 | 0.05 (0.02)
55 | 0.91 (0.46)	76 | 3.13 (0.53)	71 | 3.45 (0.54)	79 | 2.60 (0.38)	73 | 1.83 (0.31)	88 | 0.50 (0.11)	132 | 0.01 (0.01)
57 | 0.92 (0.48)	80 | 3.07 (0.51)	74 | 3.32 (0.46)	83 | 2.45 (0.39)	77 | 1.96 (0.29)	94 | 0.35 (0.08)	
76 | 1.14 (0.25)	84 | 3.88 (0.48)	78 | 3.49 (0.46)	87 | 2.03 (0.31)	82 | 2.08 (0.30)	101 | 0.27 (0.07)	
80 | 1.67 (0.42)	88 | 2.62 (0.35)	83 | 2.48 (0.31)	93 | 2.15 (0.34)	87 | 2.07 (0.28)	109 | 0.41 (0.08)	
84 | 1.65 (0.35)	93 | 3.26 (0.47)	87 | 2.79 (0.40)	98 | 1.41 (0.26)	92 | 1.18 (0.19)	118 | 0.32 (0.06)	
88 | 1.75 (0.32)	98 | 3.78 (0.49)	92 | 2.58 (0.40)	104 | 2.18 (0.29)	99 | 1.48 (0.22)		
93 | 1.28 (0.28)	103 | 3.46 (0.43)	98 | 3.15 (0.43)		106 | 1.15 (0.18)		
98 | 1.41 (0.31)	110 | 2.44 (0.38)					
103 | 2.36 (0.34)						
109 | 1.93 (0.33)						
116 | 0.62 (0.19)						

Table 178. Triton production cross sections for 400 MeV/u carbon on copper.

5	10	20	30	40	60	80
	24 | 2.77 (0.61)	24 | 2.02 (0.44)	24 | 0.90 (0.32)	26 | 0.95 (0.21)	27 | 0.80 (0.21)	36 | 0.25 (0.17)
	26 | 2.19 (0.60)	26 | 1.58 (0.37)	27 | 2.12 (0.47)	29 | 1.46 (0.31)	29 | 0.61 (0.16)	39 | 0.26 (0.11)
	29 | 1.49 (0.39)	28 | 2.21 (0.49)	29 | 1.63 (0.33)	32 | 1.93 (0.32)	32 | 0.53 (0.12)	42 | 0.06 (0.07)
	31 | 3.05 (0.61)	31 | 1.10 (0.26)	32 | 1.71 (0.39)	35 | 1.35 (0.26)	36 | 0.65 (0.15)	46 | 0.05 (0.06)
	34 | 2.16 (0.50)	34 | 1.88 (0.33)	35 | 1.01 (0.22)	39 | 1.26 (0.25)	39 | 0.64 (0.16)	50 | 0.16 (0.05)
	36 | 1.46 (0.47)	37 | 1.48 (0.30)	39 | 1.46 (0.30)	43 | 1.10 (0.22)	42 | 0.23 (0.12)	54 | 0.04 (0.03)
	39 | 1.83 (0.46)	40 | 1.29 (0.45)	42 | 1.02 (0.33)	46 | 1.01 (0.20)	46 | 0.30 (0.08)	58 | 0.12 (0.05)
	42 | 0.99 (0.47)	43 | 1.45 (0.27)	45 | 1.22 (0.37)	50 | 0.63 (0.14)	49 | 0.14 (0.09)	60 | 0.00 (0.05)
	45 | 1.71 (0.42)	47 | 1.49 (0.32)	49 | 0.78 (0.22)	54 | 0.55 (0.14)	52 | 0.45 (0.17)	64 | 0.01 (0.01)
	48 | 1.30 (0.36)	50 | 0.87 (0.36)	52 | 0.61 (0.25)	57 | 0.64 (0.16)	55 | 0.50 (0.15)	67 | 0.01 (0.01)
	51 | 0.80 (0.23)	52 | 1.06 (0.30)	54 | 0.86 (0.27)	60 | 0.21 (0.09)	58 | 0.30 (0.09)	71 | 0.02 (0.01)
	52 | 1.10 (0.43)	54 | 1.26 (0.34)	57 | 0.65 (0.24)	63 | 0.29 (0.11)	61 | 0.19 (0.07)	76 | 0.02 (0.01)
	55 | 1.54 (0.49)	57 | 1.03 (0.39)	59 | 0.54 (0.21)	66 | 0.39 (0.10)	64 | 0.22 (0.06)	81 | 0.00 (0.00)
	57 | 1.11 (0.34)	59 | 0.54 (0.15)	62 | 1.00 (0.32)	70 | 0.63 (0.19)	68 | 0.17 (0.05)	88 | 0.01 (0.01)
	59 | 1.14 (0.32)	62 | 0.96 (0.30)	65 | 0.62 (0.20)	74 | 0.32 (0.08)	73 | 0.01 (0.04)	95 | 0.00 (0.00)
	62 | 1.49 (0.42)	65 | 0.71 (0.21)	68 | 0.47 (0.19)	79 | 0.07 (0.03)	78 | 0.15 (0.04)	
	64 | 0.80 (0.25)	68 | 0.75 (0.22)	72 | 0.37 (0.14)			
	67 | 1.48 (0.33)	72 | 1.00 (0.24)	76 | 0.60 (0.18)			
	70 | 1.41 (0.32)	76 | 0.63 (0.18)	80 | 0.38 (0.13)			
	74 | 1.15 (0.34)					
	78 | 1.11 (0.26)					

Table 179. ^{3}He production cross sections for 400 MeV/u carbon on copper.

5	10	20	30	40	60	80
	119 | 0.46 (0.13)	114 | 0.36 (0.13)	116 | 0.26 (0.10)	122 | 0.07 (0.05)		
	124 | 0.54 (0.14)	120 | 0.41 (0.14)	122 | 0.37 (0.15)	129 | 0.17 (0.04)		
	130 | 0.89 (0.27)	127 | 0.58 (0.14)	128 | 0.20 (0.11)	139 | 0.08 (0.05)		
	135 | 0.75 (0.17)	132 | 0.28 (0.09)	132 | 0.49 (0.13)	148 | 0.06 (0.04)		
	145 | 0.52 (0.13)	140 | 0.56 (0.12)	140 | 0.33 (0.12)	159 | 0.03 (0.01)		
	156 | 0.61 (0.15)	150 | 0.44 (0.10)	152 | 0.19 (0.05)	174 | 0.11 (0.04)		
	165 | 0.82 (0.18)	162 | 0.30 (0.09)	164 | 0.13 (0.05)	187 | 0.04 (0.01)		
	173 | 0.54 (0.12)	172 | 0.31 (0.10)	175 | 0.20 (0.07)	200 | 0.37 (0.12)		
	186 | 0.57 (0.10)	185 | 0.13 (0.06)	188 | 0.15 (0.06)			
			199 | 0.04 (0.10)			

Table 180. ^{4}He production cross sections for 400 MeV/u carbon on copper.

5	10	20	30	40	60	80
	98 | 0.39 (0.17)	93 | 0.49 (0.18)	94 | 0.22 (0.12)	98 | 0.07 (0.03)		
	102 | 0.24 (0.12)	97 | 0.27 (0.13)	98 | 0.05 (0.03)	103 | 0.10 (0.04)		
	106 | 0.15 (0.09)	102 | 0.31 (0.13)	103 | 0.12 (0.05)	109 | 0.04 (0.02)		
	112 | 0.16 (0.06)	107 | 0.15 (0.10)	108 | 0.20 (0.09)	116 | 0.05 (0.03)		
	117 | 0.33 (0.14)	113 | 0.19 (0.10)	114 | 0.12 (0.07)	123 | 0.01 (0.02)		
	124 | 0.38 (0.10)	119 | 0.24 (0.09)	120 | 0.06 (0.07)	165 | 0.01 (0.01)		
	131 | 0.54 (0.17)	126 | 0.15 (0.04)	127 | 0.14 (0.07)			
	138 | 0.21 (0.08)	134 | 0.03 (0.05)	135 | 0.07 (0.03)			
	147 | 0.29 (0.10)	144 | 0.18 (0.06)	144 | 0.02 (0.01)			
	158 | 0.26 (0.08)	154 | 0.05 (0.04)	155 | 0.07 (0.04)			

Table 181. Proton production cross sections for 400 MeV/u carbon on lithium.

5	10	20	30	40	60	80
59 | 0.68 (0.10)	59 | 1.05 (0.13)	56 | 0.87 (0.11)	57 | 0.67 (0.10)	62 | 0.87 (0.09)	68 | 0.83 (0.09)	107 | 0.51 (0.07)
63 | 0.59 (0.08)	64 | 1.12 (0.11)	60 | 1.00 (0.11)	62 | 0.87 (0.09)	69 | 0.74 (0.07)	74 | 0.66 (0.07)	113 | 0.41 (0.05)
69 | 0.61 (0.08)	69 | 1.05 (0.11)	66 | 0.97 (0.10)	67 | 0.70 (0.09)	76 | 0.86 (0.07)	81 | 0.76 (0.07)	123 | 0.27 (0.04)
75 | 0.47 (0.07)	75 | 1.07 (0.10)	71 | 0.98 (0.09)	72 | 0.80 (0.08)	85 | 0.84 (0.07)	90 | 0.60 (0.06)	137 | 0.24 (0.03)
81 | 0.63 (0.09)	82 | 1.18 (0.11)	79 | 1.04 (0.09)	78 | 1.03 (0.10)	96 | 0.80 (0.07)	101 | 0.54 (0.05)	154 | 0.13 (0.02)
88 | 0.66 (0.08)	88 | 1.05 (0.11)	87 | 0.81 (0.08)	84 | 0.88 (0.09)	106 | 0.83 (0.07)	113 | 0.45 (0.04)	177 | 0.08 (0.01)
93 | 0.36 (0.07)	95 | 1.16 (0.10)	94 | 0.97 (0.09)	89 | 1.00 (0.12)	116 | 0.88 (0.08)	124 | 0.45 (0.05)	201 | 0.05 (0.01)
97 | 0.36 (0.06)	102 | 1.28 (0.13)	104 | 0.98 (0.08)	93 | 0.97 (0.11)	124 | 0.92 (0.08)	133 | 0.38 (0.04)	222 | 0.05 (0.01)
101 | 0.35 (0.06)	106 | 1.10 (0.12)	113 | 1.31 (0.12)	98 | 1.00 (0.11)	133 | 0.71 (0.06)	144 | 0.33 (0.03)	250 | 0.03 (0.01)
106 | 0.30 (0.06)	112 | 1.09 (0.11)	120 | 1.02 (0.09)	102 | 0.89 (0.10)	143 | 0.64 (0.06)	156 | 0.21 (0.02)	286 | 0.02 (0.00)
112 | 0.43 (0.06)	118 | 1.28 (0.12)	127 | 0.84 (0.07)	108 | 0.93 (0.10)	155 | 0.73 (0.06)	171 | 0.24 (0.02)	335 | 0.01 (0.00)
118 | 0.24 (0.05)	124 | 1.34 (0.11)	136 | 1.02 (0.09)	114 | 1.00 (0.10)		189 | 0.09 (0.01)	
124 | 0.14 (0.03)	132 | 1.06 (0.09)	145 | 1.09 (0.09)	120 | 1.03 (0.10)			
	140 | 1.05 (0.09)	157 | 1.46 (0.11)	128 | 1.01 (0.09)			
	149 | 1.06 (0.09)		137 | 0.95 (0.08)			
	160 | 1.03 (0.09)		146 | 0.86 (0.08)			
			157 | 0.87 (0.07)			

Table 182. Deuteron production cross sections for 400 MeV/u carbon on lithium.

5	10	20	30	40	60	80
34 | 0.41 (0.12)	34 | 0.46 (0.09)	32 | 0.30 (0.08)	33 | 0.21 (0.08)	35 | 0.34 (0.06)	36 | 0.22 (0.05)	54 | 0.20 (0.04)
36 | 0.51 (0.10)	37 | 0.49 (0.09)	34 | 0.33 (0.08)	36 | 0.20 (0.07)	38 | 0.30 (0.05)	40 | 0.19 (0.04)	59 | 0.09 (0.03)
40 | 0.30 (0.09)	40 | 0.36 (0.07)	38 | 0.42 (0.07)	39 | 0.30 (0.07)	43 | 0.26 (0.05)	44 | 0.29 (0.05)	66 | 0.05 (0.02)
43 | 0.24 (0.08)	44 | 0.45 (0.08)	42 | 0.32 (0.07)	43 | 0.50 (0.08)	47 | 0.27 (0.05)	49 | 0.22 (0.04)	74 | 0.08 (0.02)
46 | 0.26 (0.10)	48 | 0.54 (0.08)	46 | 0.51 (0.07)	48 | 0.32 (0.06)	52 | 0.32 (0.05)	53 | 0.09 (0.03)	83 | 0.03 (0.01)
49 | 0.33 (0.08)	53 | 0.46 (0.07)	51 | 0.46 (0.06)	53 | 0.27 (0.05)	56 | 0.23 (0.04)	58 | 0.16 (0.03)	93 | 0.01 (0.01)
52 | 0.25 (0.08)	58 | 0.45 (0.08)	56 | 0.37 (0.07)	59 | 0.25 (0.05)	62 | 0.23 (0.04)	64 | 0.09 (0.02)	102 | 0.01 (0.01)
53 | 0.17 (0.08)	63 | 0.40 (0.07)	61 | 0.32 (0.06)	64 | 0.29 (0.05)	66 | 0.12 (0.05)	70 | 0.13 (0.03)	110 | 0.01 (0.00)
55 | 0.20 (0.07)	68 | 0.53 (0.07)	66 | 0.34 (0.05)	70 | 0.27 (0.05)	70 | 0.21 (0.05)	74 | 0.10 (0.03)	119 | 0.01 (0.01)
57 | 0.25 (0.10)	73 | 0.34 (0.08)	71 | 0.51 (0.08)	75 | 0.27 (0.06)	73 | 0.26 (0.05)	78 | 0.08 (0.02)	130 | 0.01 (0.00)
59 | 0.08 (0.07)	76 | 0.53 (0.08)	75 | 0.39 (0.07)	79 | 0.27 (0.05)	78 | 0.26 (0.04)	83 | 0.05 (0.02)	
62 | 0.16 (0.06)	80 | 0.70 (0.09)	79 | 0.40 (0.06)	83 | 0.24 (0.05)	82 | 0.21 (0.04)	89 | 0.08 (0.02)	
76 | 0.33 (0.06)	84 | 0.65 (0.09)	83 | 0.27 (0.04)	88 | 0.22 (0.04)	88 | 0.15 (0.03)	95 | 0.05 (0.01)	
80 | 0.27 (0.07)	88 | 0.45 (0.06)	88 | 0.24 (0.05)	93 | 0.21 (0.04)	93 | 0.15 (0.03)	103 | 0.04 (0.01)	
84 | 0.23 (0.05)	93 | 0.45 (0.07)	93 | 0.18 (0.05)	99 | 0.24 (0.04)	100 | 0.18 (0.03)	111 | 0.04 (0.01)	
88 | 0.33 (0.06)	98 | 0.61 (0.08)	99 | 0.34 (0.06)	105 | 0.27 (0.04)	107 | 0.14 (0.02)	121 | 0.04 (0.01)	
93 | 0.33 (0.06)	104 | 0.72 (0.08)	105 | 0.13 (0.03)				
98 | 0.29 (0.06)	110 | 0.62 (0.08)					
104 | 0.42 (0.06)						
110 | 0.23 (0.05)						
117 | 0.14 (0.03)						

Table 183. Triton production cross sections for 400 MeV/u carbon on lithium.

5	10	20	30	40	60	80
	24 | 0.16 (0.08)	23 | 0.24 (0.07)	25 | 0.12 (0.06)	27 | 0.11 (0.04)	26 | 0.10 (0.03)	36 | 0.09 (0.04)
	26 | 0.18 (0.06)	26 | 0.07 (0.05)	27 | 0.14 (0.05)	30 | 0.18 (0.04)	29 | 0.08 (0.03)	39 | 0.06 (0.03)
	28 | 0.16 (0.06)	28 | 0.12 (0.05)	30 | 0.30 (0.06)	34 | 0.20 (0.04)	32 | 0.06 (0.03)	41 | 0.04 (0.03)
	31 | 0.21 (0.06)	31 | 0.10 (0.03)	33 | 0.21 (0.05)	37 | 0.07 (0.04)	36 | 0.09 (0.03)	44 | 0.04 (0.02)
	33 | 0.11 (0.05)	34 | 0.24 (0.06)	36 | 0.20 (0.04)	41 | 0.10 (0.03)	39 | 0.09 (0.02)	47 | 0.04 (0.02)
	36 | 0.14 (0.04)	37 | 0.18 (0.05)	40 | 0.12 (0.03)	45 | 0.14 (0.04)	43 | 0.08 (0.03)	51 | 0.00 (0.00)
	39 | 0.08 (0.05)	41 | 0.11 (0.04)	44 | 0.04 (0.04)	49 | 0.05 (0.02)	46 | 0.05 (0.02)	56 | 0.01 (0.01)
	42 | 0.18 (0.08)	44 | 0.13 (0.04)	47 | 0.09 (0.03)	52 | 0.04 (0.01)	48 | 0.06 (0.03)	62 | 0.00 (0.01)
	45 | 0.07 (0.04)	47 | 0.10 (0.03)	51 | 0.05 (0.02)	55 | 0.11 (0.03)	50 | 0.01 (0.02)	
	48 | 0.07 (0.06)	50 | 0.02 (0.04)	55 | 0.07 (0.03)	57 | 0.05 (0.02)	53 | 0.01 (0.02)	
	51 | 0.06 (0.04)	52 | 0.11 (0.04)	57 | 0.04 (0.02)	60 | 0.01 (0.01)	56 | 0.06 (0.02)	
	53 | 0.14 (0.06)	54 | 0.06 (0.04)	60 | 0.06 (0.03)	63 | 0.01 (0.02)	59 | 0.04 (0.02)	
	55 | 0.07 (0.04)	57 | 0.09 (0.04)	63 | 0.03 (0.02)	67 | 0.05 (0.02)	62 | 0.02 (0.01)	
	57 | 0.05 (0.05)	60 | 0.06 (0.02)	66 | 0.02 (0.01)	71 | 0.04 (0.02)	66 | 0.03 (0.01)	
	59 | 0.09 (0.05)	62 | 0.07 (0.03)	69 | 0.02 (0.01)	75 | 0.03 (0.01)	70 | 0.03 (0.01)	
	62 | 0.12 (0.04)	66 | 0.07 (0.03)	73 | 0.04 (0.02)	80 | 0.00 (0.00)	75 | 0.01 (0.01)	
	65 | 0.13 (0.05)	69 | 0.05 (0.02)	77 | 0.06 (0.03)		80 | 0.01 (0.01)	
	68 | 0.10 (0.04)	73 | 0.08 (0.03)	81 | 0.03 (0.02)			
	71 | 0.15 (0.04)	77 | 0.03 (0.01)				
	74 | 0.05 (0.04)					
	78 | 0.22 (0.05)					

Table 184. ^{3}He production cross sections for 400 MeV/u carbon on lithium.

5	10	20	30	40	60	80
	109 | 0.05 (0.02) 115 | 0.08 (0.03) 122 | 0.05 (0.02) 130 | 0.09 (0.03) 138 | 0.08 (0.02) 147 | 0.10 (0.03) 158 | 0.08 (0.02) 170 | 0.10 (0.02) 184 | 0.06 (0.01)	104 | 0.06 (0.02) 110 | 0.05 (0.02) 117 | 0.04 (0.01) 125 | 0.02 (0.01) 134 | 0.04 (0.01) 143 | 0.03 (0.01) 155 | 0.06 (0.01) 168 | 0.03 (0.01)	105 | 0.03 (0.01) 111 | 0.05 (0.02) 125 | 0.02 (0.01) 134 | 0.01 (0.01) 144 | 0.01 (0.01) 155 | 0.01 (0.01) 168 | 0.01 (0.01) 183 | 0.02 (0.01)	121 | 0.01 (0.01) 200 | 0.01 (0.01)		

Table 185. ^{4}He production cross sections for 400 MeV/u carbon on lithium.

5	10	20	30	40	60	80
	101 | 0.05 (0.02) 106 | 0.04 (0.02) 112 | 0.04 (0.02) 119 | 0.03 (0.01) 127 | 0.02 (0.02) 135 | 0.02 (0.01) 144 | 0.01 (0.01)	90 | 0.01 (0.01) 95 | 0.01 (0.01) 101 | 0.00 (0.01) 114 | 0.01 (0.01) 122 | 0.01 (0.01) 130 | 0.01 (0.01) 140 | 0.02 (0.01)	91 | 0.01 (0.01) 96 | 0.01 (0.01) 141 | 0.01 (0.00)			

Table 186. Proton production cross sections for 400 MeV/u carbon on lead.

5	10	20	30	40	60	80
56 | 9.80 (1.48)	56 | 17.57 (2.09)	53 | 11.77 (1.44)	55 | 10.19 (1.54)	57 | 12.86 (1.46)	64 | 10.73 (1.25)	99 | 4.01 (0.80)
61 | 10.72 (1.38)	61 | 16.20 (1.68)	58 | 13.46 (1.53)	59 | 14.81 (1.56)	62 | 12.71 (1.26)	70 | 10.75 (1.09)	105 | 3.51 (0.54)
67 | 8.55 (1.23)	67 | 14.24 (1.57)	63 | 16.11 (1.58)	64 | 12.02 (1.37)	69 | 11.51 (1.14)	77 | 7.63 (0.84)	114 | 2.69 (0.43)
73 | 5.78 (1.02)	73 | 13.97 (1.48)	69 | 15.86 (1.49)	70 | 12.60 (1.32)	76 | 12.24 (1.06)	86 | 7.18 (0.71)	126 | 2.63 (0.33)
79 | 6.63 (1.24)	80 | 14.18 (1.62)	75 | 13.73 (1.52)	76 | 12.93 (1.39)	84 | 11.29 (1.08)	97 | 6.73 (0.66)	142 | 1.60 (0.24)
86 | 9.92 (1.24)	86 | 12.08 (1.53)	81 | 13.54 (1.37)	82 | 10.79 (1.22)	93 | 11.28 (1.01)	108 | 5.60 (0.57)	161 | 1.45 (0.19)
91 | 5.51 (1.22)	91 | 8.69 (1.65)	86 | 13.53 (1.67)	87 | 10.52 (1.53)	100 | 9.11 (1.01)	119 | 5.76 (0.62)	181 | 1.00 (0.16)
95 | 4.71 (0.89)	95 | 14.36 (1.77)	90 | 12.57 (1.72)	91 | 12.70 (1.62)	106 | 10.28 (1.08)	128 | 5.17 (0.55)	200 | 0.88 (0.14)
99 | 4.57 (0.90)	100 | 11.74 (1.52)	94 | 10.24 (1.41)	95 | 9.97 (1.30)	113 | 9.87 (1.03)	138 | 4.31 (0.48)	223 | 0.83 (0.12)
104 | 4.80 (0.97)	104 | 10.24 (1.51)	99 | 13.23 (1.49)	100 | 10.94 (1.31)	121 | 7.66 (0.79)	150 | 3.05 (0.37)	253 | 0.53 (0.07)
110 | 5.54 (0.83)	110 | 13.90 (1.51)	105 | 10.86 (1.39)	105 | 9.98 (1.24)	129 | 6.93 (0.71)	165 | 3.06 (0.34)	293 | 0.22 (0.05)
116 | 4.36 (0.85)	116 | 12.27 (1.52)	111 | 11.51 (1.32)	111 | 10.64 (1.25)	139 | 6.42 (0.75)	182 | 1.46 (0.20)	350 | 0.05 (0.01)
	122 | 11.60 (1.23)	117 | 11.20 (1.20)	118 | 8.87 (0.99)	151 | 7.30 (0.77)		
	130 | 9.93 (1.10)	125 | 10.13 (0.94)	125 | 9.21 (0.89)	164 | 4.51 (0.49)		
	138 | 9.58 (1.09)	133 | 10.38 (1.07)	134 | 8.63 (0.98)			
	147 | 9.28 (1.10)	143 | 9.70 (1.06)	143 | 7.81 (0.90)			
	157 | 7.05 (1.00)	154 | 13.40 (1.21)	154 | 8.94 (0.93)			

Table 187. Deuteron production cross sections for 400 MeV/u carbon on lead.

5	10	20	30	40	60	80
33 | 5.22 (1.78)	31 | 10.77 (2.01)	31 | 12.17 (1.80)	31 | 10.47 (1.83)	34 | 11.13 (1.24)	35 | 6.95 (1.04)	50 | 2.90 (0.55)
36 | 7.06 (1.35)	34 | 13.97 (1.79)	33 | 12.32 (1.66)	34 | 7.75 (1.50)	38 | 8.56 (1.00)	38 | 5.18 (0.88)	54 | 1.40 (0.39)
39 | 6.96 (1.63)	37 | 9.94 (1.47)	37 | 11.25 (1.80)	37 | 8.78 (1.36)	43 | 7.85 (1.00)	42 | 5.56 (0.83)	59 | 1.24 (0.34)
42 | 5.91 (1.40)	41 | 9.27 (1.66)	40 | 10.62 (1.50)	41 | 6.13 (1.25)	48 | 7.76 (0.88)	47 | 4.10 (0.60)	65 | 0.91 (0.20)
45 | 3.96 (1.45)	45 | 10.25 (1.34)	43 | 9.08 (1.38)	45 | 9.31 (1.18)	53 | 7.58 (0.91)	52 | 4.02 (0.63)	72 | 0.79 (0.20)
48 | 3.94 (1.05)	49 | 11.49 (1.41)	46 | 9.07 (1.33)	50 | 7.69 (0.98)	57 | 6.77 (0.83)	56 | 4.16 (0.56)	80 | 0.37 (0.15)
52 | 4.64 (1.02)	53 | 11.31 (1.59)	49 | 10.43 (1.41)	55 | 9.24 (1.24)	62 | 5.13 (0.94)	60 | 3.85 (0.63)	87 | 0.60 (0.18)
54 | 4.51 (1.24)	57 | 9.23 (1.46)	53 | 9.75 (1.35)	60 | 6.42 (0.94)	65 | 5.24 (0.86)	64 | 1.85 (0.58)	93 | 0.38 (0.15)
56 | 2.74 (1.43)	62 | 7.08 (1.19)	56 | 8.44 (1.45)	66 | 6.92 (0.88)	68 | 4.08 (0.76)	67 | 2.01 (0.38)	100 | 0.40 (0.13)
59 | 1.41 (1.12)	66 | 5.38 (1.40)	58 | 6.12 (1.42)	70 | 3.51 (1.06)	72 | 3.96 (0.69)	71 | 2.40 (0.48)	108 | 0.17 (0.10)
75 | 3.24 (0.70)	69 | 7.60 (1.33)	61 | 7.27 (1.37)	74 | 6.15 (1.10)	76 | 5.84 (0.80)	75 | 1.98 (0.36)	117 | 0.27 (0.09)
79 | 4.45 (1.16)	72 | 6.11 (1.32)	64 | 6.60 (1.29)	78 | 6.90 (0.95)	81 | 5.01 (0.71)	80 | 1.75 (0.36)	128 | 0.12 (0.06)
83 | 3.61 (0.90)	75 | 8.38 (1.34)	67 | 8.82 (1.46)	82 | 5.09 (0.87)	86 | 3.50 (0.50)	86 | 1.30 (0.28)	
87 | 4.40 (0.84)	79 | 6.57 (1.22)	70 | 6.90 (1.21)	87 | 4.85 (0.67)	91 | 3.07 (0.49)	92 | 1.32 (0.28)	
92 | 4.32 (0.85)	83 | 8.47 (1.24)	74 | 9.28 (1.28)	92 | 4.53 (0.69)	98 | 3.90 (0.60)	99 | 1.47 (0.26)	
97 | 4.62 (0.93)	87 | 6.57 (0.88)	77 | 8.50 (1.15)	97 | 4.17 (0.71)	105 | 2.98 (0.46)	107 | 1.44 (0.25)	
103 | 5.30 (0.80)	92 | 9.24 (1.20)	82 | 6.35 (0.82)	104 | 4.76 (0.65)			
109 | 4.20 (0.81)	97 | 9.48 (1.29)	86 | 4.70 (0.83)				
	103 | 9.00 (1.24)	91 | 4.00 (0.85)				
	109 | 5.92 (1.02)	97 | 5.28 (0.94)				

Table 188. Triton production cross sections for 400 MeV/u carbon on lead.

5	10	20	30	40	60	80
	24 | 10.97 (2.04)	22 | 5.70 (1.16)	24 | 5.26 (1.30)	24 | 5.96 (1.00)	26 | 3.64 (0.62)	33 | 1.68 (0.50)
	26 | 8.45 (1.43)	24 | 5.75 (1.08)	26 | 5.76 (1.09)	27 | 6.37 (0.95)	29 | 3.27 (0.62)	35 | 1.03 (0.35)
	29 | 8.05 (1.55)	27 | 8.04 (1.28)	29 | 6.32 (1.05)	30 | 5.93 (0.90)	32 | 2.12 (0.42)	39 | 0.69 (0.21)
	31 | 6.97 (1.38)	30 | 5.86 (1.07)	31 | 7.30 (1.19)	33 | 5.32 (0.80)	36 | 2.15 (0.43)	43 | 0.90 (0.24)
	34 | 6.09 (1.24)	32 | 6.99 (1.15)	34 | 3.52 (0.71)	37 | 2.06 (0.62)	40 | 1.80 (0.48)	47 | 0.36 (0.14)
	37 | 4.62 (1.00)	35 | 4.27 (0.91)	38 | 4.03 (0.76)	40 | 4.46 (0.74)	43 | 1.14 (0.34)	51 | 0.65 (0.20)
	40 | 5.18 (1.66)	39 | 5.17 (0.94)	42 | 3.76 (0.90)	44 | 4.52 (0.80)	46 | 1.70 (0.48)	55 | 0.30 (0.18)
	43 | 3.96 (0.95)	41 | 5.43 (0.97)	45 | 2.59 (0.74)	48 | 1.81 (0.36)	49 | 0.80 (0.37)	58 | 0.47 (0.23)
	46 | 3.13 (0.90)	45 | 3.93 (0.73)	48 | 3.50 (0.70)	51 | 2.70 (0.59)	51 | 0.73 (0.36)	61 | 0.40 (0.15)
	49 | 5.07 (1.03)	47 | 3.66 (1.08)	52 | 2.44 (0.73)	53 | 1.91 (0.47)	54 | 1.28 (0.38)	65 | 0.20 (0.12)
	52 | 3.99 (1.26)	49 | 4.56 (1.28)	54 | 3.57 (0.87)	56 | 1.99 (0.47)	57 | 0.92 (0.28)	69 | 0.23 (0.12)
	54 | 2.55 (0.86)	51 | 2.79 (0.80)	56 | 1.03 (0.37)	59 | 2.38 (0.51)	60 | 0.83 (0.27)	74 | 0.15 (0.11)
	56 | 3.47 (1.19)	54 | 3.78 (1.19)	59 | 2.02 (0.58)	62 | 1.61 (0.48)	64 | 0.62 (0.20)	79 | 0.02 (0.02)
	59 | 2.83 (0.87)	56 | 1.69 (0.63)	62 | 1.47 (0.59)	66 | 1.35 (0.31)	68 | 0.39 (0.14)	86 | 0.02 (0.02)
	61 | 3.61 (0.98)	59 | 2.85 (0.69)	65 | 1.95 (0.54)	70 | 1.82 (0.39)	72 | 0.18 (0.16)	
	64 | 2.55 (0.90)	62 | 3.11 (0.72)	68 | 1.14 (0.39)	74 | 0.42 (0.16)	77 | 0.30 (0.11)	
	67 | 4.23 (0.97)	65 | 1.43 (0.39)	72 | 1.28 (0.38)	78 | 0.26 (0.14)		
	70 | 1.82 (0.53)	68 | 2.16 (0.55)	76 | 1.58 (0.47)			
	73 | -0.28 (0.46)	72 | 1.58 (0.45)	80 | 0.78 (0.27)			
	77 | 3.57 (0.91)	76 | 2.11 (0.47)				
	81 | 0.21 (0.29)					

Table 189. ^{3}He production cross sections for 400 MeV/u carbon on lead.

5	10	20	30	40	60	80
	121 | 0.96 (0.40)	110 | 0.50 (0.31)	118 | 0.70 (0.19)	119 | 0.30 (0.13)		
	128 | 1.18 (0.39)	115 | 1.06 (0.33)	125 | 0.21 (0.36)	125 | 0.22 (0.10)		
	135 | 1.03 (0.35)	121 | 0.81 (0.21)	132 | 0.37 (0.18)	134 | 0.24 (0.13)		
	142 | 0.46 (0.35)	130 | 0.74 (0.24)	140 | 0.14 (0.19)	146 | 0.08 (0.09)		
	150 | 0.94 (0.35)	139 | 0.87 (0.25)	149 | 0.26 (0.17)	156 | 0.14 (0.08)		
	159 | 1.73 (0.39)	147 | 0.37 (0.19)	157 | 0.36 (0.16)	166 | 0.08 (0.05)		
	170 | 0.40 (0.18)	156 | 0.86 (0.23)	169 | 0.36 (0.13)	185 | 0.09 (0.04)		
	183 | 0.76 (0.23)	168 | 0.62 (0.20)		196 | 0.14 (0.10)		

Table 190. ^{4}He production cross sections for 400 MeV/u carbon on lead.

5	10	20	30	40	60	80
	99 | 0.73 (0.39)	90 | 0.51 (0.24)	95 | 0.55 (0.22)	95 | 0.16 (0.12)		
	104 | 0.16 (0.24)	94 | 0.70 (0.32)	99 | 0.38 (0.18)	100 | 0.22 (0.11)		
	109 | 0.80 (0.25)	99 | 0.23 (0.12)	105 | 0.17 (0.13)	106 | 0.16 (0.07)		
	115 | 0.34 (0.24)	104 | 0.30 (0.23)	111 | 0.19 (0.19)	112 | 0.14 (0.06)		
	121 | 0.26 (0.12)	110 | 0.13 (0.25)	117 | 0.30 (0.19)	120 | 0.03 (0.06)		
	128 | 0.03 (0.19)	124 | 0.26 (0.11)	125 | 0.42 (0.17)			
	136 | 0.42 (0.17)	132 | 0.33 (0.21)	133 | 0.09 (0.06)			
	145 | 0.75 (0.22)	141 | 0.32 (0.12)	142 | 0.12 (0.08)			
	156 | 0.01 (0.18)	152 | 0.05 (0.09)	153 | 0.11 (0.07)			

Table 191. Proton production cross sections for 600 MeV/u neon on aluminum.

5	10	20	30	40	60	80
61 | 1.94 (0.25)	60 | 4.48 (0.41)	59 | 3.80 (0.33)	61 | 3.76 (0.33)	63 | 4.08 (0.36)	73 | 3.10 (0.29)	117 | 1.25 (0.15)
66 | 1.84 (0.20)	64 | 3.99 (0.34)	63 | 4.39 (0.34)	65 | 3.83 (0.30)	68 | 4.03 (0.32)	78 | 2.63 (0.24)	122 | 1.31 (0.14)
71 | 2.11 (0.22)	68 | 5.23 (0.42)	68 | 4.34 (0.33)	70 | 4.24 (0.33)	74 | 3.78 (0.31)	85 | 2.60 (0.23)	130 | 1.12 (0.12)
77 | 1.69 (0.17)	73 | 4.63 (0.37)	74 | 4.23 (0.31)	75 | 4.18 (0.30)	82 | 3.47 (0.27)	94 | 2.32 (0.20)	142 | 0.80 (0.08)
83 | 2.10 (0.22)	79 | 5.13 (0.42)	79 | 4.17 (0.31)	81 | 4.26 (0.32)	89 | 3.17 (0.26)	104 | 2.03 (0.18)	157 | 0.57 (0.06)
89 | 2.25 (0.21)	84 | 4.74 (0.37)	85 | 4.41 (0.32)	86 | 4.18 (0.30)	97 | 3.15 (0.24)	115 | 1.85 (0.15)	176 | 0.47 (0.05)
95 | 1.82 (0.24)	90 | 4.54 (0.34)	92 | 4.15 (0.29)	93 | 4.00 (0.28)	105 | 3.06 (0.27)	125 | 1.80 (0.17)	196 | 0.31 (0.04)
99 | 1.05 (0.15)	95 | 4.19 (0.38)	98 | 3.89 (0.31)	99 | 3.67 (0.30)	111 | 2.77 (0.24)	134 | 1.47 (0.13)	214 | 0.37 (0.04)
103 | 0.94 (0.14)	99 | 4.78 (0.41)	103 | 4.15 (0.32)	104 | 3.88 (0.30)	117 | 2.69 (0.23)	144 | 1.58 (0.14)	237 | 0.26 (0.03)
108 | 1.22 (0.16)	103 | 4.45 (0.37)	108 | 3.97 (0.30)	109 | 3.55 (0.28)	125 | 2.50 (0.20)	156 | 1.18 (0.11)	268 | 0.17 (0.02)
113 | 1.53 (0.18)	108 | 4.17 (0.35)	114 | 4.22 (0.31)	115 | 3.55 (0.27)	133 | 2.44 (0.19)	170 | 1.42 (0.12)	309 | 0.11 (0.01)
119 | 1.17 (0.15)	113 | 4.34 (0.34)	121 | 4.28 (0.29)	121 | 3.61 (0.25)	143 | 2.15 (0.17)	187 | 0.42 (0.04)	367 | 0.04 (0.01)
	119 | 4.51 (0.34)	128 | 3.57 (0.24)	129 | 2.68 (0.19)	155 | 2.74 (0.21)		
	125 | 4.57 (0.32)	136 | 3.45 (0.25)	137 | 3.06 (0.22)	168 | 1.02 (0.10)		
	132 | 3.41 (0.24)	146 | 4.02 (0.27)	147 | 3.29 (0.23)			
	140 | 3.78 (0.28)	157 | 4.76 (0.31)	157 | 3.42 (0.24)			
	150 | 3.66 (0.27)					
	160 | 3.05 (0.23)					

Table 192. Deuteron production cross sections for 600 MeV/u neon on aluminum.

5	10	20	30	40	60	80
35 | 0.77 (0.20)	34 | 1.83 (0.28)	32 | 1.90 (0.25)	33 | 1.88 (0.23)	35 | 1.74 (0.22)	38 | 1.19 (0.17)	56 | 0.44 (0.10)
37 | 0.42 (0.13)	37 | 2.28 (0.30)	35 | 2.02 (0.24)	36 | 1.47 (0.19)	38 | 1.62 (0.18)	41 | 0.84 (0.13)	59 | 0.29 (0.07)
40 | 0.83 (0.17)	40 | 2.13 (0.25)	38 | 1.81 (0.20)	39 | 1.96 (0.20)	42 | 1.45 (0.19)	45 | 0.94 (0.13)	63 | 0.33 (0.07)
44 | 0.67 (0.17)	44 | 2.29 (0.28)	41 | 2.13 (0.22)	43 | 1.50 (0.18)	46 | 1.50 (0.17)	50 | 0.78 (0.11)	67 | 0.18 (0.04)
47 | 0.37 (0.11)	48 | 1.59 (0.20)	45 | 1.70 (0.18)	47 | 1.72 (0.17)	51 | 1.42 (0.16)	54 | 0.70 (0.10)	73 | 0.18 (0.04)
50 | 0.60 (0.16)	52 | 2.26 (0.23)	50 | 1.70 (0.17)	52 | 1.60 (0.16)	57 | 1.36 (0.16)	59 | 0.74 (0.10)	79 | 0.19 (0.03)
52 | 0.55 (0.20)	57 | 2.36 (0.27)	54 | 1.73 (0.18)	57 | 1.61 (0.17)	62 | 1.29 (0.15)	63 | 0.71 (0.12)	84 | 0.09 (0.03)
54 | 0.95 (0.25)	61 | 2.16 (0.24)	59 | 1.88 (0.18)	61 | 1.42 (0.15)	66 | 0.84 (0.14)	66 | 0.56 (0.10)	88 | 0.15 (0.04)
56 | 1.22 (0.28)	66 | 1.84 (0.21)	64 | 1.86 (0.17)	67 | 1.37 (0.14)	70 | 1.14 (0.16)	70 | 0.58 (0.10)	93 | 0.13 (0.03)
58 | 1.26 (0.27)	70 | 2.27 (0.29)	68 | 1.74 (0.20)	72 | 1.62 (0.18)	73 | 1.17 (0.15)	73 | 0.43 (0.08)	99 | 0.06 (0.02)
60 | 0.74 (0.17)	73 | 1.68 (0.23)	71 | 2.07 (0.22)	75 | 1.40 (0.16)	78 | 1.14 (0.15)	78 | 0.42 (0.07)	106 | 0.06 (0.02)
62 | 0.39 (0.16)	76 | 1.85 (0.24)	75 | 1.91 (0.20)	79 | 1.46 (0.16)	82 | 1.06 (0.13)	83 | 0.45 (0.07)	114 | 0.07 (0.02)
76 | 0.58 (0.12)	80 | 1.81 (0.24)	79 | 1.83 (0.19)	83 | 1.41 (0.16)	87 | 0.76 (0.10)	88 | 0.41 (0.07)	123 | 0.05 (0.02)
80 | 0.83 (0.14)	84 | 1.99 (0.23)	83 | 1.41 (0.14)	88 | 1.10 (0.12)	93 | 1.00 (0.12)	94 | 0.36 (0.06)	134 | 0.03 (0.01)
84 | 1.01 (0.16)	88 | 1.51 (0.17)	87 | 1.60 (0.16)	93 | 0.85 (0.11)	99 | 1.15 (0.12)	101 | 0.26 (0.04)	
88 | 0.99 (0.14)	93 | 1.79 (0.20)	93 | 1.53 (0.15)	99 | 1.02 (0.12)	106 | 0.67 (0.08)	110 | 0.33 (0.05)	
93 | 0.88 (0.14)	98 | 2.18 (0.23)	98 | 1.81 (0.17)	105 | 1.07 (0.11)			
98 | 1.16 (0.15)	104 | 2.22 (0.22)					
104 | 1.46 (0.17)	110 | 1.44 (0.16)					
110 | 1.11 (0.14)						
117 | 0.24 (0.06)						

Table 193. Triton production cross sections for 600 MeV/u neon on aluminum.

5	10	20	30	40	60	80
	25 | 1.13 (0.26)	23 | 0.76 (0.16)	25 | 0.62 (0.14)	27 | 0.64 (0.13)	27 | 0.25 (0.07)	36 | 0.09 (0.06)
	27 | 0.51 (0.16)	25 | 0.59 (0.13)	27 | 0.50 (0.13)	30 | 0.74 (0.14)	30 | 0.31 (0.08)	41 | 0.07 (0.04)
	29 | 0.65 (0.16)	28 | 0.68 (0.13)	30 | 0.76 (0.13)	33 | 0.50 (0.10)	33 | 0.23 (0.07)	44 | 0.04 (0.04)
	32 | 0.63 (0.17)	30 | 0.69 (0.13)	32 | 0.59 (0.12)	36 | 0.39 (0.08)	36 | 0.19 (0.06)	47 | 0.07 (0.04)
	35 | 0.48 (0.13)	33 | 0.65 (0.12)	35 | 0.56 (0.10)	40 | 0.34 (0.08)	39 | 0.26 (0.07)	51 | 0.01 (0.01)
	38 | 0.51 (0.13)	36 | 0.37 (0.08)	39 | 0.51 (0.09)	43 | 0.36 (0.08)	43 | 0.22 (0.06)	55 | 0.04 (0.02)
	41 | 0.38 (0.15)	39 | 0.50 (0.11)	42 | 0.46 (0.10)	45 | 0.27 (0.09)	46 | 0.18 (0.05)	60 | 0.02 (0.01)
	43 | 0.74 (0.16)	42 | 0.66 (0.12)	45 | 0.33 (0.07)	47 | 0.34 (0.11)	50 | 0.15 (0.05)	67 | 0.01 (0.01)
	46 | 0.64 (0.13)	45 | 0.34 (0.08)	49 | 0.34 (0.08)	50 | 0.37 (0.11)	52 | 0.21 (0.07)	75 | 0.01 (0.01)
	50 | 0.66 (0.15)	48 | 0.43 (0.12)	52 | 0.22 (0.08)	52 | 0.32 (0.10)	55 | 0.11 (0.05)	
	53 | 0.38 (0.12)	50 | 0.25 (0.08)	55 | 0.40 (0.10)	54 | 0.22 (0.07)	58 | 0.08 (0.04)	
	55 | 0.32 (0.11)	52 | 0.52 (0.12)	57 | 0.25 (0.08)	57 | 0.37 (0.09)	61 | 0.09 (0.04)	
	57 | 0.32 (0.13)	54 | 0.43 (0.10)	60 | 0.19 (0.06)	60 | 0.18 (0.06)	65 | 0.09 (0.02)	
	59 | 0.34 (0.11)	57 | 0.57 (0.12)	62 | 0.20 (0.06)	63 | 0.13 (0.04)	69 | 0.09 (0.03)	
	62 | 0.52 (0.15)	59 | 0.43 (0.09)	65 | 0.25 (0.07)	67 | 0.24 (0.07)	73 | 0.08 (0.03)	
	64 | 0.37 (0.11)	62 | 0.32 (0.08)	69 | 0.14 (0.05)	70 | 0.14 (0.05)	79 | 0.04 (0.02)	
	67 | 0.45 (0.13)	65 | 0.26 (0.06)	72 | 0.18 (0.05)	75 | 0.17 (0.06)	84 | 0.06 (0.02)	
	71 | 0.33 (0.10)	69 | 0.29 (0.07)	76 | 0.23 (0.06)			
	74 | 0.34 (0.10)	72 | 0.37 (0.08)	81 | 0.13 (0.04)			
	78 | 0.49 (0.13)	76 | 0.43 (0.08)				

Table 194. ^{3}He production cross sections for 600 MeV/u neon on aluminum.

5	10	20	30	40	60	80
	125 | 0.44 (0.08)	120 | 0.33 (0.06)	116 | 0.22 (0.05)	118 | 2.93 (0.26)		
	131 | 0.48 (0.08)	126 | 0.31 (0.05)	122 | 0.11 (0.05)	125 | 2.33 (0.21)		
	137 | 0.50 (0.08)	134 | 0.30 (0.05)	127 | 0.26 (0.05)	131 | 1.89 (0.17)		
	145 | 0.45 (0.07)	141 | 0.31 (0.05)	134 | 0.18 (0.04)	140 | 2.67 (0.22)		
	155 | 0.28 (0.05)	150 | 0.28 (0.04)	143 | 0.17 (0.03)	149 | 1.94 (0.17)		
	164 | 0.39 (0.06)	161 | 0.17 (0.03)	152 | 0.18 (0.03)	159 | 1.54 (0.13)		
	176 | 0.45 (0.06)	173 | 0.25 (0.03)	162 | 0.10 (0.02)	173 | 1.55 (0.13)		
	189 | 0.30 (0.05)		174 | 0.14 (0.03)	189 | 1.60 (0.13)		
			188 | 0.06 (0.01)	200 | 2.65 (0.35)		
			199 | 0.04 (0.03)			

Table 195. ^{4}He production cross sections for 600 MeV/u neon on aluminum.

5	10	20	30	40	60	80
	102 | 0.15 (0.05)	93 | 0.06 (0.03)	99 | 0.04 (0.02)	104 | 1.99 (0.19)		
	107 | 0.07 (0.04)	98 | 0.16 (0.05)	103 | 0.06 (0.03)	110 | 3.02 (0.26)		
	112 | 0.13 (0.05)	102 | 0.15 (0.04)	108 | 0.04 (0.03)	117 | 4.93 (0.37)		
	118 | 0.15 (0.05)	108 | 0.06 (0.02)	114 | 0.04 (0.02)	124 | 1.77 (0.16)		
	124 | 0.14 (0.04)	113 | 0.11 (0.03)	121 | 0.03 (0.02)	132 | 0.96 (0.10)		
	131 | 0.15 (0.05)	120 | 0.09 (0.03)	128 | 0.07 (0.02)	141 | 0.36 (0.05)		
	139 | 0.07 (0.03)	127 | 0.07 (0.02)	136 | 0.04 (0.02)			
	148 | 0.14 (0.04)	135 | 0.10 (0.02)	145 | 0.04 (0.01)			
	158 | 0.05 (0.02)	144 | 0.04 (0.02)				
		155 | 0.02 (0.01)				

Table 196. Proton production cross sections for 600 MeV/u neon on lithium.

5	10	20	30	40	60	80
59 | 0.08 (0.03)	58 | 0.24 (0.06)	59 | 0.71 (0.07)	57 | 0.69 (0.07)	61 | 0.61 (0.06)	68 | 0.55 (0.06)	106 | 0.14 (0.03)
63 | 0.06 (0.03)	62 | 0.29 (0.05)	65 | 0.78 (0.07)	62 | 0.64 (0.06)	67 | 0.67 (0.06)	74 | 0.57 (0.05)	111 | 0.10 (0.02)
69 | 0.11 (0.03)	67 | 0.19 (0.04)	71 | 0.74 (0.06)	67 | 0.65 (0.06)	75 | 0.55 (0.05)	81 | 0.52 (0.05)	120 | 0.10 (0.02)
75 | 0.10 (0.02)	73 | 0.26 (0.04)	79 | 0.78 (0.06)	72 | 0.73 (0.06)	85 | 0.58 (0.05)	90 | 0.46 (0.04)	131 | 0.09 (0.01)
81 | 0.10 (0.03)	79 | 0.39 (0.05)	87 | 0.74 (0.06)	78 | 0.66 (0.06)	98 | 0.55 (0.04)	101 | 0.44 (0.04)	146 | 0.07 (0.01)
88 | 0.15 (0.03)	85 | 0.36 (0.05)	94 | 0.81 (0.06)	84 | 0.70 (0.06)	113 | 0.51 (0.04)	113 | 0.37 (0.03)	165 | 0.04 (0.01)
93 | 0.13 (0.03)	91 | 0.28 (0.04)	102 | 0.82 (0.07)	91 | 0.66 (0.06)	128 | 0.44 (0.03)	128 | 0.31 (0.03)	184 | 0.03 (0.01)
97 | 0.10 (0.03)	97 | 0.32 (0.05)	107 | 0.76 (0.07)	98 | 0.63 (0.06)	143 | 0.40 (0.04)	144 | 0.30 (0.03)	201 | 0.02 (0.01)
101 | 0.08 (0.02)	102 | 0.32 (0.05)	113 | 0.79 (0.07)	102 | 0.58 (0.06)	155 | 0.53 (0.04)	156 | 0.22 (0.02)	222 | 0.02 (0.00)
106 | 0.06 (0.02)	106 | 0.23 (0.05)	120 | 0.77 (0.06)	108 | 0.62 (0.06)		171 | 0.27 (0.02)	250 | 0.02 (0.00)
112 | 0.06 (0.02)	112 | 0.23 (0.04)	127 | 0.71 (0.06)	114 | 0.56 (0.05)			286 | 0.01 (0.00)
118 | 0.05 (0.02)	118 | 0.29 (0.04)	136 | 0.71 (0.06)	120 | 0.60 (0.05)			
	124 | 0.22 (0.04)	145 | 0.79 (0.06)	128 | 0.57 (0.05)			
	132 | 0.25 (0.03)	157 | 0.85 (0.06)	137 | 0.57 (0.05)			
	140 | 0.24 (0.04)		146 | 0.59 (0.05)			
	149 | 0.26 (0.04)		157 | 0.62 (0.05)			
	160 | 0.13 (0.03)					

Table 197. Deuteron production cross sections for 600 MeV/u neon on lithium.

5	10	20	30	40	60	80
40 | 0.01 (0.03)	32 | 0.07 (0.04)	31 | 0.17 (0.05)	33 | 0.18 (0.05)	34 | 0.21 (0.04)	37 | 0.17 (0.03)	52 | 0.03 (0.02)
46 | 0.02 (0.03)	35 | 0.13 (0.04)	34 | 0.22 (0.05)	36 | 0.20 (0.04)	37 | 0.27 (0.04)	41 | 0.07 (0.02)	60 | 0.01 (0.02)
55 | 0.06 (0.04)	38 | 0.10 (0.03)	37 | 0.23 (0.04)	39 | 0.27 (0.04)	42 | 0.16 (0.03)	45 | 0.16 (0.03)	85 | 0.01 (0.01)
57 | 0.02 (0.05)	42 | 0.11 (0.04)	41 | 0.19 (0.04)	43 | 0.22 (0.04)	47 | 0.19 (0.03)	50 | 0.11 (0.02)	90 | 0.00 (0.01)
59 | 0.05 (0.03)	46 | 0.10 (0.03)	44 | 0.29 (0.04)	48 | 0.20 (0.03)	53 | 0.13 (0.02)	56 | 0.10 (0.02)	96 | 0.01 (0.00)
62 | 0.00 (0.03)	50 | 0.06 (0.03)	49 | 0.26 (0.04)	53 | 0.20 (0.03)	60 | 0.15 (0.02)	61 | 0.11 (0.02)	102 | 0.01 (0.00)
76 | 0.07 (0.02)	54 | 0.12 (0.03)	54 | 0.24 (0.04)	59 | 0.17 (0.03)	68 | 0.11 (0.02)	68 | 0.11 (0.02)	
80 | 0.08 (0.03)	58 | 0.08 (0.03)	58 | 0.22 (0.03)	64 | 0.11 (0.02)	76 | 0.11 (0.02)	74 | 0.06 (0.02)	
84 | 0.10 (0.03)	63 | 0.08 (0.03)	63 | 0.19 (0.03)	70 | 0.15 (0.02)	82 | 0.09 (0.02)	78 | 0.08 (0.02)	
88 | 0.08 (0.02)	67 | 0.07 (0.03)	68 | 0.26 (0.04)	75 | 0.18 (0.03)	88 | 0.06 (0.02)	83 | 0.05 (0.01)	
93 | 0.08 (0.02)	70 | 0.14 (0.04)	71 | 0.22 (0.04)	79 | 0.16 (0.03)	93 | 0.10 (0.02)	89 | 0.06 (0.01)	
98 | 0.06 (0.02)	73 | 0.06 (0.03)	75 | 0.21 (0.04)	83 | 0.16 (0.03)	100 | 0.10 (0.02)	95 | 0.03 (0.01)	
104 | 0.06 (0.02)	76 | 0.04 (0.03)	79 | 0.23 (0.04)	88 | 0.09 (0.02)	107 | 0.06 (0.01)	103 | 0.04 (0.01)	
110 | 0.05 (0.02)	80 | 0.04 (0.03)	83 | 0.19 (0.03)	93 | 0.10 (0.02)		111 | 0.04 (0.01)	
	84 | 0.08 (0.03)	88 | 0.15 (0.03)	99 | 0.15 (0.02)			
	88 | 0.08 (0.03)	93 | 0.24 (0.03)	105 | 0.15 (0.02)			
	93 | 0.10 (0.03)	99 | 0.21 (0.03)				
	98 | 0.14 (0.03)					
	104 | 0.11 (0.03)					
	110 | 0.08 (0.02)					

Table 198. Triton production cross sections for 600 MeV/u neon on lithium.

5	10	20	30	40	60	80
	25 | 0.01 (0.03) 29 | 0.04 (0.03) 32 | 0.02 (0.01) 36 | 0.01 (0.01) 40 | 0.02 (0.02) 44 | 0.04 (0.02) 58 | 0.01 (0.02) 63 | 0.01 (0.01) 69 | 0.00 (0.00) 74 | 0.02 (0.01) 82 | 0.01 (0.01)	24 | 0.05 (0.04) 27 | 0.04 (0.03) 30 | 0.17 (0.05) 33 | 0.07 (0.03) 37 | 0.01 (0.02) 41 | 0.03 (0.02) 45 | 0.03 (0.02) 49 | 0.05 (0.03) 53 | 0.03 (0.02) 57 | 0.07 (0.04) 60 | 0.01 (0.02) 62 | 0.05 (0.02) 66 | 0.02 (0.02) 69 | 0.02 (0.01) 73 | 0.01 (0.01) 77 | -0.01 (0.01) 81 | 0.00 (0.00)	24 | 0.05 (0.02) 27 | 0.09 (0.03) 30 | 0.05 (0.02) 33 | 0.03 (0.02) 36 | 0.02 (0.02) 40 | 0.03 (0.01) 44 | 0.02 (0.01) 47 | 0.02 (0.01) 51 | 0.04 (0.02) 55 | 0.00 (0.00) 57 | 0.01 (0.01) 60 | 0.01 (0.01) 63 | 0.02 (0.01) 66 | 0.01 (0.01) 69 | 0.01 (0.01) 73 | 0.01 (0.01) 77 | 0.02 (0.01) 81 | 0.01 (0.01)	26 | 0.06 (0.02) 29 | 0.06 (0.02) 33 | 0.04 (0.02) 36 | 0.05 (0.01) 41 | 0.03 (0.01) 46 | 0.03 (0.01) 51 | 0.01 (0.01) 57 | 0.03 (0.01) 60 | 0.00 (0.00) 63 | 0.00 (0.00) 71 | 0.01 (0.01) 80 | 0.00 (0.00)	27 | 0.06 (0.02) 30 | 0.03 (0.01) 35 | 0.04 (0.01) 42 | 0.01 (0.01) 48 | 0.02 (0.01) 63 | 0.01 (0.00) 77 | 0.00 (0.00) 86 | 0.00 (0.00)	34 | 0.07 (0.03) 41 | 0.04 (0.02) 69 | 0.01 (0.00)

Table 199. ^{3}He production cross sections for 600 MeV/u neon on lithium.

5	10	20	30	40	60	80
	109 | 0.01 (0.01) 115 | 0.03 (0.01) 122 | 0.01 (0.01) 130 | 0.00 (0.01) 138 | 0.01 (0.01) 147 | 0.01 (0.00) 158 | 0.01 (0.01)	104 | 0.02 (0.01) 110 | 0.02 (0.01) 117 | 0.01 (0.01) 125 | 0.03 (0.01) 134 | 0.04 (0.01) 143 | 0.01 (0.01) 155 | 0.03 (0.01) 168 | 0.03 (0.01) 182 | 0.01 (0.00)	99 | 0.01 (0.01) 105 | 0.01 (0.01) 118 | 0.02 (0.01) 125 | 0.01 (0.01) 144 | 0.01 (0.01) 155 | 0.00 (0.01) 168 | 0.01 (0.00)			

Table 200. ^{4}He production cross sections for 600 MeV/u neon on lithium.

5	10	20	30	40	60	80
		101 | 0.02 (0.01) 107 | 0.01 (0.01) 130 | 0.01 (0.01)	91 | 0.01 (0.01) 101 | 0.00 (0.01) 108 | 0.01 (0.01)			

Appendix B
Matlab® Codes

Appendix B contains all of the programs that were coded for the analysis of the experiment in this paper. The programs were coded using the Matlab® software. There were frequent changes to many portions of these programs depending on the analysis needs at the time. The codes listed here are a snapshot of the codes at the end of the analysis.

Some of the functions that aren't included in this appendix are those that aren't necessary for the analysis (such as those that write the data to text files).

B.1 Main Program

The following code is the main program that handles all other functions for use in the analysis.

```
% Main program linking all the things I want to do for my PhD research
% Create a save name "name=['Name of file']" before starting

% gammaTOF=[16.5 16.5 15 15 13.5 11.5 10]; %in ns
% solidangle=[0.494 0.494 0.608 0.608 0.767 0.989 1.35]; %in mSr
% solidangleerr=[0.0247 0.0247 0.034048 0.034048 0.047554 0.070219
% 0.11205];

while 1==1

    auto=0; % This triggers an automated process when the value becomes
1

    clc

    if auto==0

        disp('NOTE: Data does not clear.  Clear data manually')
        disp(' ')
        disp('Choose a command')
        disp(' ')
        disp('[1] Load Data')
        disp('[2] Save Data')
        disp('[3] Input new parameters (density, target thickness,
etc.)')
        disp('[4] Read in PAW output data and rebin it')
        disp('[5] Calculate counts, backgrounds, and errors')
        disp('[6] Time-of-flight measurements')
        disp('[7] Calculate cross sections and errors')
        disp('[8] Input additional parameters (To smooth out the
curves)')
        disp('[9] Plot something')
```

```
        disp('[10] Save an image of all plots')
        disp('[11] NEW: Import Neutron Data (temporary choice, do on
AUTO only)')
        disp('[12] NEW: Save images of p vs n plots (temp choice, AUTO
only)')
        disp('[13] NEW: Export all cross section data into text files
(temp, AUTO only)')
        disp('[14] NEW: Save images of plots: All angles and All
particles (soon)')
        disp('[0] BREAK')
        disp(' ')
        disp('[100] AUTOMATE A CHOICE FOR ALL DATA SETS (WILL CLEAR
VARIABLES)')
        disp(' ')
        n=input('>>  ');

    end

    if n==100
        clear all
        auto=1;
        save([pwd '\temp.txt'],'-ascii','auto')
        disp(' ')
        disp('Which choice do you want to automate (4-7 only (atm))?
')
        disp('You can also save figures for ALL PLOTS EVER! (10) ')
        n=input('>> ');
        if n~=4 && n~=5 && n~=6 && n~=7 && n~=8 && n~=10 && n~=11 &&
n~=12 ...
            && n~=13 && n~=14 && n~=20
            clc
            disp('No automated code for that choice')
            break
        end
    end

    if auto>0

        while 1==1

            names={...
                'PAW_Apr2000_290C_CTargets'
                'PAW_Apr2000_290C_CuTargets'
                'PAW_Apr2000_290C_PbTargets'
                'PAW_Apr2000_400Ne_CTargets'
                'PAW_Apr2000_400Ne_CuTargets'
                'PAW_Apr2000_400Ne_PbTargets'
                'PAW_Apr2000_600Ne_CTargets'
                'PAW_Apr2000_600Ne_CuTargets'
                'PAW_Apr2000_600Ne_PbTargets'
                'PAW_Apr2001_290C_CTargets'
                'PAW_Apr2001_290C_PbTargets'
                'PAW_Jan2002_400Kr_AlTargets'
                'PAW_Jan2002_400Kr_CTargets'
```

```
                'PAW_Jan2002_400Kr_CuTargets'
                'PAW_Jan2002_400Kr_LiTargets'
                'PAW_Jan2002_400Kr_PbTargets'
%                 'PAW_Jan2002_500Fe_AlTargets' %Skipped (channel
shift)
%                 'PAW_Jan2002_500Fe_LiTargets' %Skipped (channel
shift)
                'PAW_Jun2002_230He_AlTargets'
                'PAW_Jun2002_230He_CuTargets'
                'PAW_Jun2002_400N_CTargets'
                'PAW_Jun2002_400N_CuTargets'
                'PAW_Jun2002_400Xe_AlTargets'
                'PAW_Jun2002_400Xe_CTargets'  %%%% June Xe has weird
overlap correction issues
                'PAW_Jun2002_400Xe_CuTargets'
                'PAW_Jun2002_400Xe_LiTargets'
                'PAW_Jun2002_400Xe_PbTargets'
                'PAW_May2001_400Xe_AlTargets'
                'PAW_May2001_400Xe_LiTargets'
                'PAW_May2001_600Ne_AlTargets'
                'PAW_May2001_600Ne_LiTargets'
                'PAW_May2001_600Si_CTargets'
                'PAW_May2001_600Si_CuTargets'
                'PAW_May2001_600Si_PbTargets'
                'PAW_Nov2002_400C_AlTargets'
                'PAW_Nov2002_400C_CTargets'
                'PAW_Nov2002_400C_CuTargets'
                'PAW_Nov2002_400C_LiTargets'
                'PAW_Nov2002_400C_PbTargets'
                'PAW_Nov2002_600Ne_AlTargets'
                'PAW_Nov2002_600Ne_LiTargets'
                };

            auto=load([pwd '\temp.txt']);

            if auto>size(names,1)
                break
            end

            name=names{auto};

            names=n;    %Temporary due to loading overwrited n

            load([pwd '\Data\' name]);

            n=names;    %Fixes n!

            if n==4
                [binned rebinned]=Rebinning(runs, skip);
            elseif n==5
                [cpip pptofs pdtoverlaptofs]=...
```

```
Counts_Measurements(events,livetime,nruns,rebinned,skip,shbar,chans,gam
machans,ppoints,pdtoverlaps);
            elseif n==6
                [FIN
FIN2]=Time_of_Flight(FIN,FIN2,thtarget,density,targetname,cpip);
            elseif n==7

[xsec]=XSec_Measurements(density,mmass,thtarget,FIN2,cpip);
            elseif n==8
                [graphskips graphbins graphnorms graphables]=...

Graph_Setup(density,mmass,thtarget,cpip,xsec,FIN,FIN2,graphbins,graphsk
ips,graphnorms,graphables,pdtoverlaptofs,auto);
            elseif n==10
                [h]=Save_All_Plots(graphables,name);
                clear h
            elseif n==11
                [ndata ndataextrap
pdataextrap]=ImportNeutronData(beame,beamtype,targetname,graphables);
            elseif n==12

[h]=Save_All_Plots_2(graphables,name,ndata,ndataextrap);
                clear h
            elseif n==13
                ExportXSecs(ndataextrap,pdataextrap,graphables,name);
            elseif n==14
                [h]=Save_All_Plots_3(graphables,name);
                clear h
            elseif n==20 % This is the super secret setting, usually
only used ONE TIME!

            else
            end

            disp(['Completed ' num2str(auto) ' files.'])
            auto=auto+1;
            save([pwd '\temp.txt'],'-ascii','auto')
            clear auto
            clear temp
            clear names
            clear i
            clear j
            clear k
            clear A
            clear ans
            clear angle

            %%%%%%%%
            clear temp1
            clear temp2
            clear tempstring
            clear type
            clear PAW_Apr2000_290C_CTargets_13
```

```
            clear ndatatemp
            %%%%%%%%%%%%%%
            save([pwd '\Data\' name]);

        end
        disp('Paused until you are satisfied with the possible error
messages')
        pause()
        continue
    end

    clc


%%%%%%%%%%%%%%%%%%%%%%%%%%%%%%%%%%%%%%%%%%%%%%%%%%%%%%%%%%%%%%%%%%%%%%%%%%%%%%%
%%%%

    if n==1; %Load Data

        name=input('Which filename would you like to load?  ','s');
        load([pwd '\Data\' name]);
        n=1;

    end


%%%%%%%%%%%%%%%%%%%%%%%%%%%%%%%%%%%%%%%%%%%%%%%%%%%%%%%%%%%%%%%%%%%%%%%%%%%%%%%
%%%%

    if n==2; %Save Data

        temp=input('Are you sure you want save (y/n)?  ','s');
        if temp=='y'
            clc
            clear temp
            temp=input(['Do you want to overwrite the old file (' name
') (y/n)?  '],'s');
            if temp~='y'
                clc
                name=input('What filename do you want to save your data
in?  ','s');
            end

            clear auto
            clear temp
            clear i
            clear j
            clear ans
            save([pwd '\Data\' name]);
        end
    end
```

```
%%%%%%%%%%%%%%%%%%%%%%%%%%%%%%%%%%%%%%%%%%%%%%%%%%%%%%%%%%%%%%%%%%%%%%%
%%%%

    if n==3; %Input new parameters

        targetname=input('What is the target? (e.g., Aluminum)  ','s');
        clc
        density=input('What is the density of the target? (in g/cm^3)
');
        clc
        thtarget=input('What is the thickness of the target? (in
meters)  ');
        clc
        mmass=input('What is the molar mass of the target?  ');
        clc

        temp=input('Continue (y/n)?  ','s');
        clc
        if temp=='n'
            continue
        end

        nruns=input('Number of runs per target?  ');
        clc
        disp('Input the run run numbers in order of lowest shadowbar
position (N1, N2, etc.)')
        disp('to highest shadowbar position (N6, N7)')
        disp('etc.')
        disp(' ')
        runs=zeros(nruns,1);
        for i=1:nruns
            runs(i,:)=input(['Run number ' num2str(i) ':  ']);
        end

        clc
        events=zeros(1,nruns);
        livetime=zeros(1,nruns);
        disp('Input the number of events per run followed by the
livetime')
        disp(' ')
        for i=1:nruns
            events(1,i)=input(['Run ' num2str(runs(i)) '(events)    :
']);
            livetime(1,i)=input(['Run ' num2str(runs(i)) '(livetime) :
']);
        end

        clc
        temp=input('Continue? (y/n)  ','s');
        if temp=='n'
            continue
        end
```

```
        clc
        shbar=zeros(nruns,7);
        disp('Shadowbar configurations: 1 = Shadowbar is present (use
1x7 vector inputs)')
        disp(' ')
        for i=1:nruns
            shbar(i,:)=input(['Run ' num2str(runs(i)) ':  ']);
        end
        shbar=shbar';

        clc
        temp=input('Continue? (y/n)  ','s');
        if temp=='n'
            continue
        end

        chans=zeros(7,6);
        for j=1:7
            for i=1:6
                clc
                chans(j,i)=input(['What channel number does the
histogram start for Angle ' num2str(j) ' H-' num2str(i) '?  ']);
            end
        end

        gammachans=zeros(1,7);
        for i=1:7
            clc
            gammachans(1,i)=input(['What channel number contains the
gamma peak for Angle ' num2str(i) '?  ']);
        end

        ppoints=zeros(7,5);
        for j=1:7
            for i=1:5
                clc
                ppoints(j,i)=input(['What channel number contains the
punchthrough point for Angle ' num2str(j) ' H-' num2str(i) '?  ']);
            end
        end
        clc

        pdtoverlaps=zeros{7,5};
        for j=1:7
            for i=1:5
                clc
                disp(['What channel number contains the overlap point
[' num2str(i) '] for Angle ' num2str(j)])
                pdtoverlaps(j,i)=input(['([1]=pd, [2]=pt, [3]=dt)
>>']);
            end
        end
        clc
```

```
        beamtype=input('What is the beam type (e.g., Xenon)?  ','s');
        clc

        beame=input('What is the beam energy (in MeV/u)?  ');
        clc

        skip=Skip_Calc(gammachans, chans);

    end


%%%%%%%%%%%%%%%%%%%%%%%%%%%%%%%%%%%%%%%%%%%%%%%%%%%%%%%%%%%%%%%%%%%%%%%%%%%%%%%
%%%%

    if n==4; %Read in data and rebin it

            [binned rebinned]=Rebinning(runs, skip);

    end


%%%%%%%%%%%%%%%%%%%%%%%%%%%%%%%%%%%%%%%%%%%%%%%%%%%%%%%%%%%%%%%%%%%%%%%%%%%%%%%
%%%%

    if n==5; %Counts, background, and error measurements

        clc
        [cpip
pptofs]=Counts_Measurements(events,livetime,nruns,rebinned,skip,shbar,c
hans,gammachans,ppoints);

    end


%%%%%%%%%%%%%%%%%%%%%%%%%%%%%%%%%%%%%%%%%%%%%%%%%%%%%%%%%%%%%%%%%%%%%%%%%%%%%%%
%%%%

    if n==6; %TOF measurements

        clc
        [FIN FIN2]=Time_of_Flight(thtarget,density,targetname,cpip);

    end


%%%%%%%%%%%%%%%%%%%%%%%%%%%%%%%%%%%%%%%%%%%%%%%%%%%%%%%%%%%%%%%%%%%%%%%%%%%%%%%
%%%%

    if n==7 %Cross section and error measurements
```

```
        clc
        [xsec]=XSec_Measurements(density,mmass,thtarget,FIN2,cpip);

    end


%%%%%%%%%%%%%%%%%%%%%%%%%%%%%%%%%%%%%%%%%%%%%%%%%%%%%%%%%%%%%%%%%%%%%%%%%%%%%%
%%%%

    if n==8; %Additional parameters (curve smoothing parameters)

        if exist('graphskips','var')==0
            for i=1:7
                for j=1:6

                    graphskips{i,j}=zeros(1,size(cpip{i,j},1));

                end
            end
        end

        if exist('graphbins','var')==0
            for i=1:7
                for j=1:6

                    graphbins{i,j}=ones(1,size(cpip{i,j},1));

                end
            end
        end

        if exist('graphnorms','var')==0
            for i=1:7
                for j=1:6

                    graphnorms{i,j}=ones(1,size(cpip{i,j},1));

                end
            end
        end

        if exist('graphables','var')==0
            for i=1:7
                for j=1:6

                    graphables{i,j}=zeros(size(cpip{i,j},1),3);

                end
            end
        end

        [graphskips graphbins graphnorms graphables]=...
```

```
Graph_Setup(density,mmass,thtarget,cpip,xsec,FIN,FIN2,graphbins,graphsk
ips,graphnorms,graphables,pdtoverlaptofs,auto);

    end


%%%%%%%%%%%%%%%%%%%%%%%%%%%%%%%%%%%%%%%%%%%%%%%%%%%%%%%%%%%%%%%%%%%%%%%%
%%%%

    if n==9; %Plotting features

        clc
        Graph_Final(graphables);  % Unused

    end


%%%%%%%%%%%%%%%%%%%%%%%%%%%%%%%%%%%%%%%%%%%%%%%%%%%%%%%%%%%%%%%%%%%%%%%%
%%%%


%%%%%%%%%%%%%%%%%%%%%%%%%%%%%%%%%%%%%%%%%%%%%%%%%%%%%%%%%%%%%%%%%%%%%%%%
%%%%

    if n==10; %Plotting features

        clc
        Save_All_Plots(graphables,name);  % Unused

    end


%%%%%%%%%%%%%%%%%%%%%%%%%%%%%%%%%%%%%%%%%%%%%%%%%%%%%%%%%%%%%%%%%%%%%%%%
%%%%

    if n==0; %Break
        break
    end


%%%%%%%%%%%%%%%%%%%%%%%%%%%%%%%%%%%%%%%%%%%%%%%%%%%%%%%%%%%%%%%%%%%%%%%%
%%%%

    clear temp
    clear i
    clear j
    clear n

end
```

B.2 Experiment Data Import

The following code was used to import the experimental data into Matlab. The data was in the form of text files that contained a single column of data which corresponded to count rates in various TOF channels. These count rates were obtained using a separate program (PAW [25]) using the analysis described in section 3.2 Data Acquisition.

The file names are in the following format:

vrun<run number>det<detector number>h<particle number>.txt

Detector numbers correspond to detectors N1-N7 which are described in

Table 2. Particle number 1-5 corresponds to protons, deuterons, tritons, ^{3}He, and ^{4}He respectively. For example, the text file "vrun06det5h3.txt" contains the measured data for tritons at 40 degrees for run number 6.

The outputs of this function are vectors containing counts per channel number for every run in a particular system as well as a rebinned version of the counts, combining every 4 channels into one bin.

```
% Reads in the data you want and rebins it too.
function [A B]=Rebinning(runs, skip)

mfiles={' '};

runs=num2str(runs);
misses=0;

len=size(runs,1);

for i=1:len
    if runs(i,1)==' '
        runs(i,1)='0';
    end
end

for i=1:7
    for j=1:5
        A{i,j}=[];
        for k=1:len
            try
                A{i,j}(:,k)=dlmread([pwd '\Rebinning\' 'vrun' runs(k,:)
'det' num2str(i) 'h' num2str(j)]);
```

```
            catch

                A{i,j}(1,k)=0;
                misses=misses+1;
                mfile{misses,:}=['vrun' runs(k,:) 'det' num2str(i) 'h'
num2str(j)];
            end
        end
    end
    for k=1:len
        try
            A{i,6}(:,k)=dlmread([pwd '\Rebinning\' 'vrun' runs(k,:)
'det' num2str(i) 'hall']);
        catch
            A{i,6}(1,k)=0;
            misses=misses+1;
            mfile{misses,:}=['vrun' runs(k,:) 'det' num2str(i) 'hall'];
        end
    end
end

for i=1:7
    for j=1:6
        B{i,j}=[];
        for k=1:floor((size(A{i,j},1)-skip(i,j))/4)
            B{i,j}(k,:)=A{i,j}(4*k-3+skip(i,j),:)+A{i,j}(4*k-
2+skip(i,j),:)+A{i,j}(4*k-1+skip(i,j),:)+A{i,j}(4*k+skip(i,j),:);
        end
    end
end

if misses>0
    disp(mfile)
    disp(['Missed ' num2str(misses) ' files (Make sure this is
intentional before saving):'])
    disp('[Hit Enter to continue]')
    pause
end
```

B.3 Count Rate and Error Calculations

The following function takes the imported data from B.2 Experiment Data Import and combines them to find the total count rate per channel (taking into account background subtraction). The program also finds the error in the counts and propagates accordingly. This function also calculates the TOF of each bin by comparing it to the gamma channel number (described in section 3.3.4 TOF Calculations).

```
% This function combines all run measurements into total measurements
% (taking into account background subtractions).  Measurement errors
are
% calculated and propogated.

% Additional information such as pdt punchtrough TOF values are
calculated

function [cpip pptofs
pdtoverlaptofs]=Counts_Measurements(events,livetime,nruns,rebinned,skip
,shbar,chans,gammachans,ppoints,pdtoverlaps)

% Gamma peak TOF for angles 1-7
gammatof=[16.5 16.5 15 15 13.5 11.5 10];

pptofs=zeros(7,5);
pdtoverlaptofs=zeros(7,5);

% For the variable cpip:
%   Column 1 = TOF for a given channel number
%   Column 2 = counts for that TOF (normalized to amount of incoming
particles)
%   Column 3 = error
for i=1:7

    nbg=sum(shbar(i,:));

    for j=1:6

        cpip{i,j}=[];

        if size(rebinned{i,j},1)==0
            continue
        end
        cpip{i,j}(:,:)=zeros(size(rebinned{i,j},1),3);

        for k=1:size(cpip{i,j},1)

            %%% This part converts the channel numbers to TOF numbers
using the
```

```
            %%% starting point of the data (chans) and comparing to
gamma TOFs
            cpip{i,j}(k,1)=(gammachans(i)-(chans(i,j)+skip(i,j)+1+4*(k-
1)))*.25+gammatof(i);

        end

        for l=1:nruns

            if shbar(i,l)==1
                cpip{i,j}(:,2)=cpip{i,j}(:,2)-
rebinned{i,j}(:,l)/(events(l)*livetime(l)*nbg);

cpip{i,j}(:,3)=cpip{i,j}(:,3)+rebinned{i,j}(:,l)/((events(l)*livetime(l
)*nbg)^2);
            else

cpip{i,j}(:,2)=cpip{i,j}(:,2)+rebinned{i,j}(:,l)/(events(l)*livetime(l)
*(nruns-nbg));

cpip{i,j}(:,3)=cpip{i,j}(:,3)+rebinned{i,j}(:,l)/((nruns-
nbg)*events(l)*livetime(l))^2;
            end
        end
        cpip{i,j}(:,2)=cpip{i,j}(:,2);
        cpip{i,j}(:,3)=sqrt(cpip{i,j}(:,3));


        %%%This part is simple:  Just find the channel number where the
pdt
        %%%particles punchtrough the detector and convert to a TOF.
        %%%Does the same thing with pdt line overlap points.
        if j<6
            if ppoints(i,j)~=0
                pptofs(i,j)=(gammachans(i)-
ppoints(i,j))*.25+gammatof(i);
            end
            if pdtoverlaps(i,j)~=0
                pdtoverlaptofs(i,j)=(gammachans(i)-
pdtoverlaps(i,j))*.25+gammatof(i);
            end
        end
    end

end

end
```

B.4 TOF and Energy Calculations

The following code provides a multitude of calculations. The bulk of the program is designed to track a particle with a specific production energy and follow it along its path length until it either reaches a detector, or it is slowed to a complete stop. In doing so, it keeps track of flight time, energy loss, as well as probability of absorption (using another function described in B.5 Tripathi's Cross Section Model). Once this has been accomplished, the function repeats using another starting energy. By doing this iterative method, the TOF measurements provided by the experiment can be converted into a production energy value, a final energy value, and a "percentage of particles absorbed" value.

```
% The goal of this program is to find the Time of Flight of particles
from
% the point of creation in the target to the detectors that are placed
% several meters away.  The program begins by choosing arbitrary
initial
% energy values for the particles, then tracks them as they slow down
until
% they reach the detectors and the time of flight is recorded.  Since
the
% experiment tracks TOF data, this allows us to extrapolate what the
energy
% of the particles should be at the point of creation.

function [FIN
FIN2]=Time_of_Flight(FIN,FIN2,thtarget,density,targetname,cpip)

% Matrix contains data for stopping powers various targets
% The first column is for projectile protons
% and the rest are the various targets the protons will hit.
% Stopping powers are in units of MeV/cm
% [ KE - Air - Scintillator - Aluminum - Lead - Copper - Carbon -
Lithium ]

SP_Protons = dlmread('StoppingPowers_Protons.txt','\t');
SP_Alphas = dlmread('StoppingPowers_Alphas.txt','\t');

%Remember: 4=Aluminum, 5=lead, 6=copper, 7=carbon, 8=Lithium
if strcmp(targetname,'Aluminum')==1
    target=4;
    normdensity=2.7;
elseif strcmp(targetname,'Lead')==1
    target=5;
    normdensity=11.35;
elseif strcmp(targetname,'Copper')==1
    target=6;
    normdensity=8.96;
elseif strcmp(targetname,'Carbon')==1
    target=7;
```

```
    normdensity=1.784;
elseif strcmp(targetname,'Lithium')==1
    target=8;
    normdensity=.53;
else
    disp('Wrong target info (Hit enter to Continue)')
    pause
end

corr=density/normdensity;   %correction factor for adjusting SP to
various densities

%%%%%%%%%%This is here to prevent having to restart the program
multiple
%%%%%%%%%%times.  Delete when necessary.  (don't forget to change all
%%%%%%%%%%instances of jj (initial conditions and FIN2 (i think that's
it)
%%%%%%%%%%(same for kk)
for jj=1:7  %Ranges 1-7 (angle)
    disp(['   Angle: ' num2str(jj)])
for kk=1:5  %Ranges 1-5 (p d t He-3 He-4)
    disp(['      Ion:   ' num2str(kk)])
%%%%%%%%%%

% mass: rest mass of Hydrogen Deuteron and Triton
% ion: represents atomic mass of exiting projectile of interest; also
used
%   for determining other information
% target: 4=Aluminum, 5=lead, 6=copper, 7=carbon, 8=Lithium
% angle: represtents detector 1-7 in experimental setup
% dist: distance from target to detector for each angle
% thtarget: thickness of the target (units = m)
% disttarget: projectile assumed to start at center of target and
travel to
%   detector.  causes distance through target to change depending on
the
%   angle of travel.  (NOT the actual thickness of the target) (units =
m)
% sttime: numbers used for setting up the FIN variable below
%   (numbers can't start too high or else the program will not get
%   anywhere).
% stE: This is needed to allow the program to start somewhere.  If
mass=[938.779, 1876.1159, 2809.42, 2809.401, 3728.385];
Z=[1 1 1 2 2]; %Charge number
A=[1 2 3 3 4]; %Mass number
SPcorr=[1 1 1 4 4]; %Corrections for using different ions (tritons
instead of protons for example)
ion=kk;     %Remember: 1=Protons, 2=Deuterons, 3=Tritons 4=Helium-3
5=Alphas

if ion<4
    SP1=SP_Protons;
else
    SP1=SP_Alphas;
```

```
end


angle=jj;   %Remember: 1 is smallest angle, 7 is largest
i=0;
j=0;
k=0;
ii=0;

dist=[500 500 450 450 400 350 300];

% thtarget depends on the system in question
disttarget=thtarget./[1.99239 1.96962 1.87939 1.73205 1.53209 1
.347296];

% checks to see if there are counts for the particular angle/ion
if size(cpip{angle,ion},1)==0
    FIN{angle,ion}=[];
    FIN2{angle,ion}=[];
    continue
end
% sttime: Start time for the calculations
sttime=cpip{angle,ion}(1,1);

% This uses a "fine" setting for starting energies in order to find
% accurate energies for every half-nanosecond step. Alpha stopping
powers
% are adjusted to save computing time by eliminating unneeded energies.
if ion>4
    Ei=zeros(1,10*499+1);
    for i=0:length(Ei)
        Ei(i+1)=200+.1*i;
    end
else
    Ei=zeros(1,10*579+1);
    for i=0:length(Ei)
        Ei(i+1)=20+.1*i;
    end
end
Ef = zeros(size(Ei,2),1);
TOF = Ef;
reax = Ef;

% This is a matrix showing each half-ns TOF and the energy ranges that
lead
% to them (columns are: [TOF(ns)   Energy-i(MeV)  Energy-f (MeV)
error(%)]
FIN{jj,kk} = zeros(size(cpip{angle,ion},1)*2+1,5);
for i=1:size(FIN{jj,kk},1)
    FIN{jj,kk}(i,1)=sttime-.5*i+1;
end

% Initialize some variables
```

```
i=0;
ii=0;
j=0;


% These two will be used to determine the current position in FIN we
are
% interested in and the error between that TOF with the most recently
% calculated TOF
k=1;

for i=1:size(Ei,2)
    TOFc=0;   % current Time of Flight
    Ec=Ei(i); % current energy
    reaxc=1;  % current reaction cross section multiplier
    j=2;

    while 1==1
        if j==size(SP1,1)
            break
        end
        if Ec>= SP1(j,1)*(SPcorr(ion)/A(ion));
            j=j+1;
        else
            break
        end
    end

    th=disttarget(angle)/15;
    for ii=1:15     % Starting Target deposition
        j=2;
           while 1==1
               if j==size(SP1,1)
                   break
               end
               if Ec>= SP1(j,1)*(SPcorr(ion)/A(ion));
                   j=j+1;
               else
                   break
               end
           end
        SPc=(Ec-SP1(j-1,1))*(SP1(j,target)*corr-SP1(j-
1,target)*corr)/(SP1(j,1)-SP1(j-1,1))+SP1(j,target)*corr;
        TOFc=TOFc+th/(sqrt((300000000)^2-
((300000000)/(Ec/mass(ion)+1))^2));
        reaxc=XSec_Model(Ec,th,reaxc,ion,target);
        Ec=Ec-SPc*th*100;
        if Ec<=SP1(1,1)
            break
        end
    end

    % Starting Air Deposition (2 is air)
    % Change step and th values to vary distances through air
```

```
    % dist/#*th = total thickness (m)
    if Ec>=SP1(1,1)
    th=.1;
    for ii=1:dist(angle)/10
        j=2;
            while 1==1
                if j==size(SP1,1)
                    break
                end
                if Ec>= SP1(j,1)*(SPcorr(ion)/A(ion));
                 j=j+1;
                else
                    break
                end
            end
       SPc=(Ec-SP1(j-1,1))*(SP1(j,2)-SP1(j-1,2))/(SP1(j,1)-SP1(j-
1,1))+SP1(j,2);
       TOFc=TOFc+th/(sqrt((300000000)^2-
((300000000)/(Ec/mass(ion)+1))^2));
       reaxc=XSec_Model(Ec,th,reaxc,ion,100);
       Ec=Ec-SPc*th*100;
            if Ec<=SP1(1,1)
                break
            end
    end
    end

     % Starting Aluminum Deposition (4 is aluminum)
     % th = thickness (m)
     if Ec>=SP1(1,1)
     th=.00159;
             j=2;
            while 1==1
                if j==size(SP1,1)
                    break
                end
                if Ec>= SP1(j,1)*(SPcorr(ion)/A(ion));
                 j=j+1;
                else
                    break
                end
            end
     SPc=(Ec-SP1(j-1,1))*(SP1(j,4)-SP1(j-1,4))/(SP1(j,1)-SP1(j-
1,1))+SP1(j,4);
     TOFc=TOFc+th/(sqrt((300000000)^2-
((300000000)/(Ec/mass(ion)+1))^2));
     reaxc=XSec_Model(Ec,th,reaxc,ion,4);
     Ec=Ec-SPc*th*100;
     end

    % Starting Scintillator Deposition (3 is scintillator)
    % th = thickness (m)
    if Ec>=SP1(1,1)
            j=2;
```

```
            while 1==1
                if j==size(SP1,1)
                    break
                end
                if Ec>= SP1(j,1)*(SPcorr(ion)/A(ion));
                 j=j+1;
                else
                    break
                end
            end
    SPc=(Ec-SP1(j-1,1))*(SP1(j,3)-SP1(j-1,3))/(SP1(j,1)-SP1(j-
1,1))+SP1(j,3);
    th=.005;
    TOFc=TOFc+th/(sqrt((300000000)^2-
((300000000)/(Ec/mass(ion)+1))^2));
    Ec=Ec-SPc*th*100;
    end

    % Finalization
    Ef(i)=Ec;
    TOF(i)=TOFc;
    reax(i)=reaxc;
end

% This determines which particles were the closest to every half-
nanosecond
% TOF.  It calculates the relative error for each time and compares it
to
% the TOF in question (25.5 ns for example).  After finding which event
has
% the lowest error, it is recorded and the next half-nanosecond is
used.
error=zeros(length(Ef),1);
for k=1:size(FIN{jj,kk},1)
    error(1:length(Ef))=500;
    j=1;
    for i=1:length(error)
        error(i)=abs((TOF(i)*1e9-FIN{jj,kk}(k,1))/FIN{jj,kk}(k,1));
        if Ef(i)<=0
            error(i)=1000;
        end
    end
    for i=1:length(error)
        if error(i)<=error(j)
            j=i;
        end
    end
    FIN{jj,kk}(k,2)=Ei(j);
    FIN{jj,kk}(k,3)=Ef(j);
    FIN{jj,kk}(k,4)=error(j);
    FIN{jj,kk}(k,5)=reax(j);
end

% This portion creates a matrix with the following:
```

```
% [TOF+/-.5 (ns)  Energy-low (Mev)   Energy-mid (MeV)   Energy-high
(MeV)]
% (The energies are the initial energies at particle creation)
% The energies listed are those that provide the associated TOF.
% Energy-mid provides the listed TOF, Energy-low provides TOF-.5 and
% Energy-high provides TOF+.5
FIN2{jj,kk}=zeros(size(FIN{jj,kk},1)/2-.5,4);
for i=1:size(FIN2{jj,kk},1)
    FIN2{jj,kk}(i,1)=FIN{jj,kk}(2*i,1);
    FIN2{jj,kk}(i,2)=FIN{jj,kk}(2*i-1,2);
    FIN2{jj,kk}(i,3)=FIN{jj,kk}(2*i+0,2);
    FIN2{jj,kk}(i,4)=FIN{jj,kk}(2*i+1,2);
end


end
end
```

B.5 Tripathi's Cross Section Model

The following function is called at every iteration of the function described in B.4 TOF and Energy Calculations. The function is designed to calculate the percentage of particles that are lost during each transit step of a particle's flight path. The function is designed using Tripathi's cross section model [22, 23, 24].

```
% Calculates an energy dependent cross section based on target and
% projectile information.
function reaxc=XSec_Model(Ep,th,reaxc,projectile,target)
% clear all
% clc
%
% Erange=100; % Edit to change energy range
%
% Ep=zeros(1,Erange);
% Ep(1)=1;
% for i=2:Erange
%     Ep(i)=Ep(i-1)*1.1;
% end

stats1=[...
    'H-1   '    %1
    'H-2   '    %2
    'H-3   '    %3
    'He-3  '    %4
    'He-4  '    %5
    'Li-7  '    %6
    'C-12  '    %7
    'Al-27 '    %8
    'Cu-63 '    %9
    'Pb-207'    %10
    'N-14  '    %11
    'O-16  '];  %12
stats2=[...
%   A    Z     r0      N
    1,   1,   0.85,    1
    2,   1,   2.095,   1
    3,   1,   1.68,    1
    3,   2,   1.844    1
    4,   2,   1.696    1
    7,   3,   2.39,    .046
    12,  6,   2.472,   .0894
    27,  13,  3.06,    .0602
    63,  29,  3.876,   .0849
    207, 82,  5.513,   .033
    14,  7,   2.58,    .0000255    % air only
    16,  8,   2.73,    .0000255];  % air only

modif=1;
if target==4        % Aluminum
    target=8;
elseif target==5    % Lead
```

```
    target=10;
elseif target==6    % Copper
    target=9;
elseif target==7    % Carbon
    target=7;
elseif target==8    % Lithium
    target=6;
else
    target=[11 12];
    modif=[.78084 .209476];
end

%%%%%%%%%%%%%%

% These are the parameters dependent solely on projectile and target

for i=1:length(modif)

    At=stats2(target(i),1);
    Ap=stats2(projectile,1);
    Ac=12;
    Zt=stats2(target(i),2);
    Zp=stats2(projectile,2);
    N=stats2(target(i),4);

    %%%%%%%%%%
    %Define what Rc is depending on system
    Rc=1;
    if Ap==1 && Zp==1
        if At==2 && Zt==1       % p + d
            Rc = 13.5;
        elseif At==3 && Zt==2   % p + 3He
            Rc=21;
        elseif At==4 && Zt==2   % p + 4He
            Rc=27;
        elseif Zt==3            % p + Li
            Rc=2.2;
        elseif Zt==6            % p + C
            Rc=3.5;
        else
        end
    elseif Ap==2 && Zp==1
        if At==2 && Zt==1       % d + d
            Rc=13.5;
        elseif At==4 && Zt==2   % d + 4He
            Rc=13.5;
        elseif Zt==6            % d + C
            Rc=6;
        else
        end
    elseif Ap==4 && Zp==2
        if Zt==73               % 4He + Ta
            Rc=.6;
        elseif Zt==79           % 4He + Au
```

```
        Rc=.6;
    else
    end
else
end

%%%%%%%%%%%%%%%%%%

% T=stats2(projectile,5);

rtrms=stats2(target(i),3);
rprms=stats2(projectile,3);

rt=1.29*rtrms;
rp=1.29*rprms;
rc=1.29*2.472;

r0=1.1;

rhoAt=At/(4/3*pi*rt^3);
rhoAp=Ap/(4/3*pi*rp^3);
rhoAc=Ac/(4/3*pi*rc^3);

Ecm=Ep.*(At/(At+Ap));  % pretty sure At belongs in numerator

E=Ep./Ap;     % Energy is supposed to be in energy per nucleon

%%%%%%%%%%%%%%%%

% 1st set of equations

R=rp+rt+1.2*(Ap^(1/3)+At^(1/3))./Ecm.^(1/3);

B=1.44*Zp*Zt./R;

%%%%%%%%%%%%%%%%%%

% 2nd set of equations

%%%%%%%%%%%%%%%%%%%%%%%%%%%%%%

if Ap==1 && Zp==0           % n + X
    T=18;
    D=1.85+.16/(1+exp((500-E)/200));
elseif Ap==1 && Zp==1
    if At==4 && Zt==2       % p + 4He
        T=40;
        D=2.05;
    elseif At==3 && Zt==2   % p + 3He
        T=58;
        D=1.7;
    elseif At==6 && Zt==3   % p + 6Li
```

```
        T=40;
        D=2.05;
    elseif At==7 && Zt==3    % p + 7Li
        T=37;
        D=2.15;
    elseif At<=7             % p + light systems
        T=23;
        D=1.85+.16/(1+exp((500-E)/200));
    else                     % p + others
        T=40;
        D=2.05;
    end
elseif Ap==2 && Zp==1
    if At==4 && Zt==2        % d + 4He
        T=23;
        D=1.65+.22/(1+exp((500-E)/200));
    else                     % d + others
        T=23;
        D=1.65+.1/(1+exp((500-E)/200));
    end
elseif Ap==3 && Zp==2        % 3He + X
    T=40;
    D=1.55;
elseif At==3 && Zt==2        % X + 3He
    T=40;
    D=1.55;
elseif Ap==4 && Zp==2
    if At==4 && Zt==2        % 4He + 4He
        T=40;
        G=300;
    elseif Zt==4             % 4He + Be
        T=25;
        G=300;
    elseif Zt==7             % 4He + N
        T=40;
        G=500;
    elseif Zt==13            % 4He + Al
        T=25;
        G=300;
    elseif Zt==27            % 4He + Fe
        T=40;
        G=75;
    else                     % 4He + others
        T=40;
        G=75;
    end
    D=2.77-8e-3*At+1.8e-5*At^2-.8/(1+exp((250-E)/G));
elseif At==4 && Zt==2        % others + 4He
    T=40;
    G=75;
    D=2.77-8e-3*At+1.8e-5*At^2-.8/(1+exp((250-E)/G));
else                         % others
    T=40;
    D=1.75*(rhoAp+rhoAt)/(rhoAc+rhoAc);
end
```

```
    if Zp==3 || Zt==3
        D=D/3;
    end


    %%%%%%%%%%%%%%%%%%%%%%%%%%%%%

    CE=D.*(1-exp(-E/T))-.292.*exp(-E/792).*cos(.229*E.^.453);

    S=Ap^(1/3)*At^(1/3)/(Ap^(1/3)+At^(1/3));

    deltaE=1.85*S+0.16*S./Ecm.^(1/3)-CE+.91*(At-2*Zt)*Zp/(At*Ap);

    %%%%%%%%%%%%%%%%%

    if Ap==1 && Zp==0
        SL=1.2+1.6*(1-exp(-E/15));
        if At==4 && Zt==2
            X1=5.2;
        else
            X1=2.83-3.1e-2*At+1.7e-4*At^2;
        end
        Xm=1-X1*exp(-E./(X1.*SL));
    else
        Xm=1;
    end

    %%%%%%%%%%%%%%%%%

    % Final answer

    sigmaR=pi*r0^2*(Ap^(1/3)+At^(1/3)+deltaE).^2.*(1-Rc.*B./Ecm).*Xm;
    sigmaR=sigmaR*10;   % Convert from fm^2 to mb
    sigmaR=sigmaR/1000; % Convert from mb to b

    N=N*modif(i);    % Mostly used for air
    N=N*100;         % To convert from atoms/(barn*cm) to atoms/(barn*m)
    reaxc=reaxc*exp(-N*sigmaR*th);

end
```

B.6 Cross Section Calculations

The following function takes the count rates obtained from B.3 Count Rate and Error Calculations and the production energies obtained from B.4 TOF and Energy Calculations and uses them to calculate production cross sections.

```
% This function converts the measured counts into a cross section
% cross section in units of mb/(MeV*Sr)

function [xsec]=XSec_Measurements(density,mmass,thtarget,FIN2,cpip)

solidangle=[0.494 0.494 0.608 0.608 0.767 0.989 1.35]; %in mSr
solidangleerr=[0.0247 0.0247 0.034048 0.034048 0.047554 0.070219
0.11205];

xsec=cpip;  % Initializes xsec.  Will be the same size as cpip anyway.

for i=1:7
    for j=1:5
        if size(cpip{i,j},1)==0
            continue
        end

        xsec{i,j}(:,2)=((10^28*mmass)/(6.02e23*density*thtarget))...
            .*cpip{i,j}(:,2)./((FIN2{i,j}(:,4)-
FIN2{i,j}(:,2)).*solidangle(i));

        xsec{i,j}(:,3)=sqrt((cpip{i,j}(:,3)./solidangle(i)).^2+...

((cpip{i,j}(:,2).*solidangleerr(i))./solidangle(i)^2).^2)...
            .*((10^28*mmass)/(6.02e23*density*thtarget))./...
            (FIN2{i,j}(:,4)-FIN2{i,j}(:,2));

    end
end
```

B.7 Additional Rebinning and Corrections

The following function provides a multitude of corrections to the data. The corrections include pdt overlap corrections and absorption corrections, as well as skipping bad data points (such as those on the edges of cuts, or those that are in the pdt saturation areas). More information on these corrections can be seen in section 3.4 Cross Section Corrections.

```
% This function takes the calculated cross section data and puts it in
a
% graphable format.  Bad data points are able to be omitted (typically
% around graph cut edges), and bin averaging is possible (to smooth the
% curves).

% graphskips: some data points are bad (edge points, etc.) - this
vector
%   decides which cpip data points to keep
% graphbins: very low statistics - this vector combines bins of 1 into
bins
%   of sizes 1-4 (usually larger at lower energies and less farther
out)
% graphnorms: correction multiplies data points to account for overlaps
% graphrxns:  accounts for losses due to nuclear interaction losses -
%   vector points are ratios of particles that actually make it to
detector
%   - correction is the inverse of this ratio
% graphables: resulting product - hey, something needs to be plotted!

function [graphskips graphbins graphnorms
graphables]=Graph_Setup(density,mmass,thtarget,cpip,xsec,FIN,FIN2,graph
bins,graphskips,graphnorms,graphables,pdtoverlaptofs,auto)

solidangle=[0.494 0.494 0.608 0.608 0.767 0.989 1.35]; %in mSr
solidangleerr=[0.0247 0.0247 0.034048 0.034048 0.047554 0.070219
0.11205];

A=[1 2 3 3 4]; % Mass Number
Z=[1 1 1 4 4]; % Charge Number

particle=1;
angle=1;

while 1==1

    if auto==0
        clc

        disp('Choose a command')
        disp(' ')
        disp('[1] Choose a particle type and angle')
        disp('[2] Skip some values')
```

```
        disp('[3] Unskip some values')
        disp('[4] Rebin some values')
        disp('[5] Test results in graph')
        disp('[6] Normalize some values (mainly for pdt overlaps)')
        disp('[10] APPLY ALL CHANGES')
        disp('[111] Reset skips and bins')
        disp(' ')
        disp('[0] Exit')
        disp(' ')
        n=input('>>  ');
    else
        n=10;
    end


%%%%%%%%%%%%%%%%%%%%%%%%%%%%%%%%%%%%%%%%%%%%%%%%%%%%%%%%%%%%%%%%%%%%%%%%%%%%%%%

    if n==0
        break
    end


%%%%%%%%%%%%%%%%%%%%%%%%%%%%%%%%%%%%%%%%%%%%%%%%%%%%%%%%%%%%%%%%%%%%%%%%%%%%%%%

    if n==1

        clc
        angle=input('Choose an angle (1-7)): ');
        particle=input('Choose a particle type (1, 2, 3, 4, 5 or
6(all)): ');

    end


%%%%%%%%%%%%%%%%%%%%%%%%%%%%%%%%%%%%%%%%%%%%%%%%%%%%%%%%%%%%%%%%%%%%%%%%%%%%%%%

    if n==2;

        clc
        disp('Choose the values to skip, or type 0 to end')
        disp(['Max value is: '
num2str(length(graphskips{angle,particle}))])
        disp(' ')

        while 1==1

            nn=input('>> ');
            if nn>length(graphskips{angle,particle})
                disp('too high')
                continue
            end
```

```
            if nn==0
                break
            end

            graphskips{angle,particle}(1,nn)=1;

        end

        graphbins{angle,particle}=ones(1,size(cpip{angle,particle},1)-
sum(graphskips{angle,particle}));

    end


%%%%%%%%%%%%%%%%%%%%%%%%%%%%%%%%%%%%%%%%%%%%%%%%%%%%%%%%%%%%%%%%%%%%%%%%%%%%

    if n==3;

        clc
        disp('Choose the values to unskip, or type 0 to end')
        disp(['Max value is: '
num2str(length(graphskips{angle,particle}))])
        disp(' ')

        while 1==1

            nn=input('>> ');
            if nn>length(graphskips{angle,particle})
                disp('too high')
                continue
            end

            if nn==0
                break
            end

            graphskips{angle,particle}(1,nn)=0;

        end

    end


%%%%%%%%%%%%%%%%%%%%%%%%%%%%%%%%%%%%%%%%%%%%%%%%%%%%%%%%%%%%%%%%%%%%%%%%%%%%

    if n==4;

        clc
        disp('Choose the number of values to be placed in each bin
(sizes can vary)')
```

```
        disp(['All values must add up to: '
num2str(length(graphskips{angle,particle})-
sum(graphskips{angle,particle}))])
        disp('Input values in a horizontal vector format')
        disp(' ')

        while 1==1

            nn=input('>> ');
            if sum(nn)==length(graphskips{angle,particle})-
sum(graphskips{angle,particle})
                break
            end
            disp(['Adds up to ' num2str(sum(nn)) '. Try again'])

        end

        graphbins{angle,particle}=nn;

    end


%%%%%%%%%%%%%%%%%%%%%%%%%%%%%%%%%%%%%%%%%%%%%%%%%%%%%%%%%%%%%%%%%%%%%%%%%%%%%%%

    if n==5 && isempty(graphables{angle,particle})==0;

        temp=zeros(4,length(graphskips{angle,particle})-
sum(graphskips{angle,particle}));

        k=0;

        for i=1:length(graphskips{angle,particle})
            if graphskips{angle,particle}(i)==0
                temp(1:4,i-
k)=[cpip{angle,particle}(i,2).*graphnorms{angle,particle}(i)./FIN{angle
,particle}(i,5)

cpip{angle,particle}(i,3).*graphnorms{angle,particle}(i)./FIN{angle,par
ticle}(i,5)
                    FIN2{angle,particle}(i,4)-FIN2{angle,particle}(i,2)
                    FIN2{angle,particle}(i,3)];
            else
                k=k+1;
            end
        end

        k=1;

        tempcpip=zeros(1,length(graphbins{angle,particle}));
        tempcerror=zeros(1,length(graphbins{angle,particle}));
        tempespread=zeros(1,length(graphbins{angle,particle}));
        tempeavg=zeros(1,length(graphbins{angle,particle}));
```

```
        for i=1:length(graphbins{angle,particle})

            binsize=graphbins{angle,particle}(i);

            tempcpip(i)=sum(temp(1,k:k+binsize-1));              %total
binned counts
            tempcerror(i)=sqrt(sum((temp(2,k:k+binsize-1).^2))); %error
in counts
            tempespread(i)=sum(temp(3,k:k+binsize-1));
%Energy spread over bin
            tempeavg(i)=(temp(4,k+binsize-1)+temp(4,k))/2;
%Average energy over bin

            k=k+binsize;

        end


graphables{angle,particle}=zeros(length(graphbins{angle,particle}),3);

        graphables{angle,particle}(:,1)=tempeavg/A(particle);


graphables{angle,particle}(:,2)=((10^28*mmass)/(6.02e23*density*thtarge
t))...
            .*tempcpip./(tempespread.*solidangle(angle)/A(particle));


graphables{angle,particle}(:,3)=sqrt((tempcerror./solidangle(angle)).^2
+...

((tempcpip.*solidangleerr(angle))./solidangle(angle)^2).^2)...

.*((10^28*mmass)/(6.02e23*density*thtarget))./(tempespread)*A(particle)
;

        clf
        hold on


plot(FIN2{angle,particle}(:,3)./A(particle),xsec{angle,particle}(:,2)./
A(particle),'-ob','MarkerSize',3)


plot(graphables{angle,particle}(:,1),graphables{angle,particle}(:,2),'-
sr','MarkerSize',3)

    elseif n==5 && isempty(graphables{angle,particle})==1

        clc
        disp('No data for this particle angle and particle')
```

```
        disp('Hit ENTER to continue')
        pause

    end


%%%%%%%%%%%%%%%%%%%%%%%%%%%%%%%%%%%%%%%%%%%%%%%%%%%%%%%%%%%%%%%%%%%%%%%%%%%%%%%%

    if n==6

        while 1==1

            clc
            clf

            hold on
            try

plot(cpip{angle,particle}(:,1),cpip{angle,particle}(:,2),'bo-
','Markersize',3)

plot(cpip{angle,particle}(:,1),cpip{angle,particle}(:,2).*graphnorms{an
gle,particle}','sr-','Markersize',3)
            catch
                disp('No data for this particle angle and particle')
                disp('Hit ENTER to continue')
                pause
            end
            if particle==1 || particle==2
                if pdtoverlaptofs(angle,1)~=0

plot([round(pdtoverlaptofs(angle,1)),round(pdtoverlaptofs(angle,1))]...

,[min(cpip{angle,particle}(:,2)),max(cpip{angle,particle}(:,2))],'r-.')
                end

            end
            if particle==1 || particle==3

                if pdtoverlaptofs(angle,2)~=0

plot([round(pdtoverlaptofs(angle,2)),round(pdtoverlaptofs(angle,2))]...

,[min(cpip{angle,particle}(:,2)),max(cpip{angle,particle}(:,2))],'m--')
                end

            end
            if particle==2 || particle==3

                if pdtoverlaptofs(angle,3)~=0

plot([round(pdtoverlaptofs(angle,3)),round(pdtoverlaptofs(angle,3))]...
```

```
,[min(cpip{angle,particle}(:,2)),max(cpip{angle,particle}(:,2))],'g:')
                end

            end

            disp(num2str(pdtoverlaptofs)) % Overlap channels
            disp('')
            disp('[1] Change angle to view')
            disp('[2] Choose particle to view')
            disp('[3] Create overlap normalization factors')
            disp('[4] Create nuclear reaction corrections')
            disp('[10] Reset factors to 1')
            disp('[0] Back')
            disp('')
            m=input('>>  ');

            %%%%%%%%%%%%%%%%%%%%%%
            if m==0
                break
            end
            %%%%%%%%%%%%%%%%%%%%%%
            if m==1

                clc
                disp('Choose an angle (1-7): ')
                angle=input('>> ');

            end
            %%%%%%%%%%%%%%%%%%%%%%
            if m==2

                clc
                disp('Choose a particle: ')
                particle=input('>> ');

            end
            %%%%%%%%%%%%%%%%%%%%%%
            if m==3

                clc
                disp('Choose the values to normalize, or type 0 to
end')
                disp(['Max value is: '
num2str(length(graphnorms{angle,particle}))])
                disp(' ')

                while 1==1

                    nn=input('>> ');
                    if nn>length(graphnorms{angle,particle})
                        disp('too high')
                        continue
```

```
                    end

                    break

                end

                if nn==0
                    break
                end

                clc
                disp('Choose a normalization factor')
                disp(' ')
                graphnorms{angle,particle}(1,nn)=input('>> ');

            end
            %%%%%%%%%%%%%%%%%%%%%%%
            if m==4

                clc
                disp('This is an automated process using Tripathis
formula')



            end
            %%%%%%%%%%%%%%%%%%%%%%%
            if m==10

                graphnorms{angle,particle}(:)=1;
                graphrxns{angle,particle}(:)=1;

            end
            %%%%%%%%%%%%%%%%%%%%%%%

        end

    end


%%%%%%%%%%%%%%%%%%%%%%%%%%%%%%%%%%%%%%%%%%%%%%%%%%%%%%%%%%%%%%%%%%%%%%%%%%%%%%%

    if n==10

        for angle=1:7
            for particle=1:5

                if isempty(graphables{angle,particle})==0;

                    temp=zeros(4,length(graphskips{angle,particle})-
sum(graphskips{angle,particle}));
```

```
                    k=0;


                    % This sets up a temporary matrix that will contain
a
                    % running all the information for the final
                    % product - This is required due to the nature of
the
                    % skips.  When there is a skip, k++, which prevents
0s
                    % from appearing in the final matrix (essentially,
                    % skips make the temp matrix smaller than cpip
lengths)
                    for i=1:length(graphskips{angle,particle})
                        if graphskips{angle,particle}(i)==0
                            temp(1:4,i-
k)=[cpip{angle,particle}(i,2).*graphnorms{angle,particle}(i)./FIN{angle
,particle}(i,5)

cpip{angle,particle}(i,3).*graphnorms{angle,particle}(i)./FIN{angle,par
ticle}(i,5)    % FIN contains rxn corrections
                                FIN2{angle,particle}(i,4)-
FIN2{angle,particle}(i,2)
                                FIN2{angle,particle}(i,3)];
                        else
                            k=k+1;
                        end
                    end

                    k=1;

                    % These variables will be used instead of a matrix
                    % (easier to manage that way).  Will be even
smaller
                    % than temp matrix - these variables contained
combined
                    % bins

tempcpip=zeros(1,length(graphbins{angle,particle}));

tempcerror=zeros(1,length(graphbins{angle,particle}));

tempespread=zeros(1,length(graphbins{angle,particle}));

tempeavg=zeros(1,length(graphbins{angle,particle}));

                    for i=1:length(graphbins{angle,particle})

                        binsize=graphbins{angle,particle}(i);

                        tempcpip(i)=sum(temp(1,k:k+binsize-1));
%total binned counts
```

```
                        tempcerror(i)=sqrt(sum((temp(2,k:k+binsize-
1).^2))); %error in counts
                        tempespread(i)=sum(temp(3,k:k+binsize-1));
%Energy spread over bin
                        tempeavg(i)=(temp(4,k+binsize-1)+temp(4,k))/2;
%Average energy over bin

                        k=k+binsize;

                    end

                    % After all is said and done, final product can be
made


graphables{angle,particle}=zeros(length(graphbins{angle,particle}),3);


graphables{angle,particle}(:,1)=tempeavg/A(particle); % Energy in MeV/u


graphables{angle,particle}(:,2)=((10^28*mmass)/(6.02e23*density*thtarge
t))...

.*tempcpip./(tempespread.*solidangle(angle)/A(particle)); % Cross
section in mb/(MeV/u)/Sr


graphables{angle,particle}(:,3)=sqrt((tempcerror./solidangle(angle)).^2
+...

((tempcpip.*solidangleerr(angle))./solidangle(angle)^2).^2)...

.*((10^28*mmass)/(6.02e23*density*thtarget))./(tempespread)*A(particle)
; % Cross section error

                else
                end
            end
        end

        if auto>0
            return
        end

    end


%%%%%%%%%%%%%%%%%%%%%%%%%%%%%%%%%%%%%%%%%%%%%%%%%%%%%%%%%%%%%%%%%%%%%%%%

    if n==111
```

```
        for i=1:7
            for j=1:4

                graphskips{i,j}=zeros(1,size(cpip{i,j},1));
                graphbins{i,j}=ones(1,size(cpip{i,j},1));

            end
        end

    end


%%%%%%%%%%%%%%%%%%%%%%%%%%%%%%%%%%%%%%%%%%%%%%%%%%%%%%%%%%%%%%%%%%%%%%%%%

end
```

B.8 Main Coalescence Radii Program

The following function was used as a starting point for calculation coalescence radii. The required inputs are text files containing double differential cross section data for neutrons, protons, and the light ion in question. This particular version requires data for deuterons, tritons, ^{3}He and ^{4}He. The contents of the text files are an arbitrary amount of description text (in this case 6 rows) and 4 columns of data. The first column contains the energies at which the double differential cross sections were measured, and the second , third, and fourth columns contain the neutron, proton, and light ion production cross section respectively.

The file name for the text files are in the following format:

<system name>_<detector number><particle number>.txt

The system names can all be seen in the first few lines of the code that follows. Detector number ranges from 1-7 and their descriptions can be seen in Table 2.

```
% Main program for calculating coalescence radius for my dissertation
% Main output = coalradius, coalradiusE, coalradiusEA
%       1st column: Energy per nucleon at which radii were calculated
%       1st column: Calculated with proton cross sections in mind
%       2nd column: Calculated with neutron cross sections in mind
%
%
% coalradius:  radii calculated at every energy/angle for a particle
% coalradiusE: fitted radii over all energies for a specific
particle/angle
% coalradiusEA:fitted radii over all energies and angles for a particle

clear all
clc

%c=2.99792458e8;     %speed of light (m/s)
c=1;
massn=939.57;           %Neutron mass (MeV/c^2)
massp=938.27;           %Proton mass  (MeV/c^2)

names={...
    'PAW_Apr2000_290C_CTargets'
    'PAW_Apr2000_290C_CuTargets'
    'PAW_Apr2000_290C_PbTargets'
    'PAW_Apr2000_400Ne_CTargets'
    'PAW_Apr2000_400Ne_CuTargets'
    'PAW_Apr2000_400Ne_PbTargets'
    'PAW_Apr2000_600Ne_CTargets'
    'PAW_Apr2000_600Ne_CuTargets'
    'PAW_Apr2000_600Ne_PbTargets'
```

```
    'PAW_Apr2001_290C_CTargets'
    'PAW_Apr2001_290C_PbTargets'
    'PAW_Jan2002_400Kr_AlTargets'
    'PAW_Jan2002_400Kr_CTargets'
    'PAW_Jan2002_400Kr_CuTargets'
    'PAW_Jan2002_400Kr_LiTargets'
    'PAW_Jan2002_400Kr_PbTargets'
%     'PAW_Jan2002_500Fe_AlTargets' %Skipped (channel shift)
%     'PAW_Jan2002_500Fe_LiTargets' %Skipped (channel shift)
    'PAW_Jun2002_230He_AlTargets'
    'PAW_Jun2002_230He_CuTargets'
    'PAW_Jun2002_400N_CTargets'
    'PAW_Jun2002_400N_CuTargets'
    'PAW_Jun2002_400Xe_AlTargets'
    'PAW_Jun2002_400Xe_CTargets'  %%%% June Xe has weird overlap
correction issues
    'PAW_Jun2002_400Xe_CuTargets'
    'PAW_Jun2002_400Xe_LiTargets'
    'PAW_Jun2002_400Xe_PbTargets'
    'PAW_May2001_400Xe_AlTargets'
    'PAW_May2001_400Xe_LiTargets'
    'PAW_May2001_600Ne_AlTargets'
    'PAW_May2001_600Ne_LiTargets'
    'PAW_May2001_600Si_CTargets'
    'PAW_May2001_600Si_CuTargets'
    'PAW_May2001_600Si_PbTargets'
    'PAW_Nov2002_400C_AlTargets'
    'PAW_Nov2002_400C_CTargets'
    'PAW_Nov2002_400C_CuTargets'
    'PAW_Nov2002_400C_LiTargets'
    'PAW_Nov2002_400C_PbTargets'
    'PAW_Nov2002_600Ne_AlTargets'
    'PAW_Nov2002_600Ne_LiTargets'
    };

beame=[...
    290
    290
    290
    400
    400
    400
    600
    600
    600
    290
    290
    400
    400
    400
    400
    400
%     500  % Skipped systems
%     500  % Skipped systems
    230
```

```
    230
    400
    400
    400
    400
    400
    400
    400
    400
    400
    600
    600
    600
    600
    600
    400
    400
    400
    400
    400
    600
    600
    ];
beamtype={...
    'C'
    'C'
    'C'
    'Ne'
    'Ne'
    'Ne'
    'Ne'
    'Ne'
    'Ne'
    'C'
    'C'
    'Kr'
    'Kr'
    'Kr'
    'Kr'
    'Kr'
%     'Fe'    % Skipped systems
%     'Fe'    % Skipped systems
    'He'
    'He'
    'N'
    'N'
    'Xe'
    'Xe'
    'Xe'
    'Xe'
    'Xe'
    'Xe'
    'Xe'
    'Ne'
    'Ne'
```

```
    'Si'
    'Si'
    'Si'
    'C'
    'C'
    'C'
    'C'
    'C'
    'Ne'
    'Ne'
    };

targetname={...
    'C'
    'Cu'
    'Pb'
    'C'
    'Cu'
    'Pb'
    'C'
    'Cu'
    'Pb'
    'C'
    'Pb'
    'Al'
    'C'
    'Cu'
    'Li'
    'Pb'
%     'Al'    % Skipped systems
%     'Li'    % Skipped systems
    'Al'
    'Cu'
    'C'
    'Cu'
    'Al'
    'C'
    'Cu'
    'Li'
    'Pb'
    'Al'
    'Li'
    'Al'
    'Li'
    'C'
    'Cu'
    'Pb'
    'Al'
    'C'
    'Cu'
    'Li'
    'Pb'
    'Al'
    'Li'
    };
```

```
coalradius{:,2}=[];
coalradiusE{:,2}=[];
coalradiusEA{:,2}=[];

for i=1:size(names,1)

    if strcmp(beamtype{i},'Xe')==1
        projectile=15;
    elseif strcmp(beamtype{i},'Ne')==1
        projectile=9;
    elseif strcmp(beamtype{i},'Si')==1
        projectile=11;
    elseif strcmp(beamtype{i},'C')==1
        projectile=6;
    elseif strcmp(beamtype{i},'Fe')==1
        projectile=12;
    elseif strcmp(beamtype{i},'Kr')==1
        projectile=14;
    elseif strcmp(beamtype{i},'N')==1
        projectile=7;
    elseif strcmp(beamtype{i},'He')==1
        projectile=4;
    else
        disp(['No beamtype "' beamtype{i} '" in List'])
        return
    end

    if strcmp(targetname{i},'Pb')==1
        target=16;
    elseif strcmp(targetname{i},'Cu')==1
        target=13;
    elseif strcmp(targetname{i},'Li')==1
        target=5;
    elseif strcmp(targetname{i},'C')==1
        target=6;
    elseif strcmp(targetname{i},'Al')==1
        target=10;
    else
        disp(['No targetname "' targetname{i} '" in List'])
        return
    end

    stats2=[...
        %   A    Z     r0        Rc     T      N
        1,   1,   0.85,     1,     23     1
        2,   1,   2.095,    1,     23     1
        3,   1,   1.68,     1,     23     1
        4,   2,   1.696,    1,     40     .0
        7,   3,   2.39,     1,     40     .046
        12,  6,   2.472,    1,     40     .0894
        14,  7,   2.58,     1,     40     .0
        16,  8,   2.730,    1,     40     .0
        20,  10,  3.040,    1,     40     .0
```

```
        27,  13,  3.06,     1,     40     .0602
        28,  14,  3.106,    1,     40     .0
        56,  26,  3.729,    1,     40     .0
        63,  29,  3.876,    1,     40     .0849
        84,  36,  4.15,     1,     40     .0   % Guessed r0
        131, 54,  4.84,     1,     40     .0   % Guessed r0
        207, 82,  5.513,    1,     40     .033
        14,  7,   2.58,     1,     40     .0000255    % air only
        16,  8,   2.73,     1,     40     .0000255];  % air only

    %%%%%%%%%%%%%%%%%%%%

    % These are the parameters dependent solely on projectile and
target

    At=stats2(target,1);
    Ap=stats2(projectile,1);
    Zt=stats2(target,2);
    Zp=stats2(projectile,2);

    Nt=At-Zt;
    Np=Ap-Zp;

    coalradius{i,1}=names{i};   % Coalescence radii calculated for each
point
    coalradiusE{i,1}=names{i};  % Best fit over entire energy range
    coalradiusEA{i,1}=names{i}; % Best fit over entire system

    %%%%%%%%%%%%%%%%%%%%
    sigmaR=Tripathi(beame(i),beamtype{i},targetname{i});
    if sigmaR<0
        sigmaR=1500;  % Xe falls below 0 with all targets, Kr does w/
Pb target
        disp(names{i})
    end
    coalradius{i,2}{7,5}=[];
    coalradiusE{i,2}{7,5}=[];
    coalradiusEA{i,2}{1,5}=[];
    for part=2:5
        Gp=0;
        Gn=0;
        TopEAp=0;
        TopEAn=0;
        BotEAp=0;
        BotEAn=0;
        TopEApERR=0;
        TopEAnERR=0;
        BotEApERR=0;
        BotEAnERR=0;
        coalradiusEA{i,2}{1,part}=[0 0 0 0 0];
        for angle=1:7
            Gp=0;
            Gn=0;
            TopEp=0;
```

```
            TopEn=0;
            BotEp=0;
            BotEn=0;
            TopEpERR=0;
            TopEnERR=0;
            BotEpERR=0;
            BotEnERR=0;
            coalradiusE{i,2}{angle,part}=[0 0 0 0 0];

            try xsec=dlmread([pwd '\Exported Cross Sections\' names{i}
'_' num2str(angle) num2str(part) '.txt'],...
                    '\t',6,0);
            catch
                continue
            end

            if part==1
                A=1;
                Z=1;
                N=0;
            elseif part==2
                A=2;
                Z=1;
                N=1;
            elseif part==3
                A=3;
                Z=1;
                N=2;
            elseif part==4
                A=3;
                Z=2;
                N=1;
            elseif part==5
                A=4;
                Z=2;
                N=2;
            end
            % To convert from mb/AMeV/Sr to mb/MeV/Sr
            try
                xsec(:,6)=xsec(:,6)/A;
                xsec(:,7)=xsec(:,7)/A;
            catch
                continue   % In case file exists but is empty
            end

            for j=1:size(xsec,1)

                % Begin defining constants
                Ep=xsec(j,1);
                gammap=Ep/(massp*c^2)+1;
                momentump=sqrt((massp*c+Ep/c)^2-(massp*c)^2);

                En=Ep;
                gamman=En/(massn*c^2)+1;
```

```
                momentumn=sqrt((massn*c+En/c)^2-(massn*c)^2);

                coalradius{i,2}{angle,part}(j,1)=Ep;

                NZratio=(Np+Nt)/(Zp+Zt);
                ZNratio=1/NZratio;
                factratio=factorial(N)*factorial(Z);
                constp=(4*pi*gammap)/(3*sigmaR*(Ep+massp)*momentump);
                constn=(4*pi*gamman)/(3*sigmaR*(En+massn)*momentumn);
                % combines all the constants into a manageable variable
                bigconstp=A^2/factratio*NZratio^N*constp^(A-1);
                bigconstn=A^2/factratio*ZNratio^Z*constn^(A-1);

                Zpxsecratio=xsec(j,6)/(xsec(j,4))^A;
                Znxsecratio=xsec(j,6)/(xsec(j,2))^A;

                % Test for negative ratios
                if Zpxsecratio<0
                    Zpxsecratio=0;
                end
                if Znxsecratio<0
                    Znxsecratio=0;
                end

                % Coalescence radius using proton cross sections
                try
                    coalradius{i,2}{angle,part}(j,2)=...
                        nthroot(Zpxsecratio/bigconstp,3*(A-1));
                    coalradius{i,2}{angle,part}(j,3)=...
                        (1/(3*(A-1))*(1/bigconstp)^(1/(3*A-
1)))*sqrt(...
                        (1/xsec(j,4)^A*Zpxsecratio^(1/(3*(A-1))-
1))^2*xsec(j,7)^2+...

(A*xsec(j,6)/(xsec(j,4)^(A+1))*Zpxsecratio^(1/(3*(A-1))-
1))^2*xsec(j,5)^2);
                catch
                    coalradius{i,2}{angle,part}(j,2)=0;
                    coalradius{i,2}{angle,part}(j,3)=0;
                end

                % Coalescence radius using neutron cross sections
                try
                    coalradius{i,2}{angle,part}(j,4)=...
                        nthroot(Znxsecratio/bigconstn,3*(A-1));
                    coalradius{i,2}{angle,part}(j,5)=...
                        (1/(3*(A-1))*(1/bigconstn)^(1/(3*A-
1)))*sqrt(...
                        (1/xsec(j,2)^A*Znxsecratio^(1/(3*(A-1))-
1))^2*xsec(j,7)^2+...

(A*xsec(j,6)/(xsec(j,2)^(A+1))*Znxsecratio^(1/(3*(A-1))-
1))^2*xsec(j,3)^2);
                catch
```

```
                    coalradius{i,2}{angle,part}(j,4)=0;
                    coalradius{i,2}{angle,part}(j,5)=0;
                end

                %  Begin LS fitting. Test first to see if cross
sections are
                %  real numbers>0, then begin calculations.
                if isinf(xsec(j,6))~=1 && xsec(j,6)>0 &&
isnan(xsec(j,6))~=1 && ...
                        isinf(xsec(j,7))~=1 && xsec(j,7)>0 &&
isnan(xsec(j,7))~=1
                    if xsec(j,4)>0 && isinf(xsec(j,4))~=1 &&
isnan(xsec(j,4))~=1 && ...
                            isinf(xsec(j,5))~=1 && xsec(j,5)>0 &&
isnan(xsec(j,5))~=1
                        TopEp=bigconstp*xsec(j,4)^A*xsec(j,6)+TopEp;

TopEpERR=sqrt((bigconstp*xsec(j,6)*(A*xsec(j,4)^(A-1))*xsec(j,5))^2+...

(bigconstp*xsec(j,4)^A*xsec(j,7))^2+TopEpERR^2);
                        BotEp=(bigconstp*xsec(j,4)^A)^2+BotEp;

BotEpERR=sqrt((2*bigconstp^2*xsec(j,4)^A*A*xsec(j,4)^(A-
1)*xsec(j,5))^2+BotEpERR^2);
                        TopEAp=bigconstp*xsec(j,4)^A*xsec(j,6)+TopEAp;

TopEApERR=sqrt((bigconstp*xsec(j,6)*(A*xsec(j,4)^(A-
1))*xsec(j,5))^2+...

(bigconstp*xsec(j,4)^A*xsec(j,7))^2+TopEApERR^2);
                        BotEAp=(bigconstp*xsec(j,4)^A)^2+BotEAp;

BotEApERR=sqrt((2*bigconstp^2*xsec(j,4)^A*A*xsec(j,4)^(A-
1)*xsec(j,5))^2+BotEApERR^2);
                    end
                    if xsec(j,2)>0 && isinf(xsec(j,2))~=1 &&
isnan(xsec(j,2))~=1 && ...
                            isinf(xsec(j,3))~=1 && xsec(j,3)>0 &&
isnan(xsec(j,3))~=1
                        TopEn=bigconstn*xsec(j,2)^A*xsec(j,6)+TopEn;

TopEnERR=sqrt((bigconstn*xsec(j,6)*(A*xsec(j,2)^(A-1))*xsec(j,3))^2+...

(bigconstn*xsec(j,2)^A*xsec(j,7))^2+TopEnERR^2);
                        BotEn=(bigconstn*xsec(j,2)^A)^2+BotEn;

BotEnERR=sqrt((2*bigconstn^2*xsec(j,2)^A*A*xsec(j,2)^(A-
1)*xsec(j,3))^2+BotEnERR^2);
                        TopEAn=bigconstn*xsec(j,2)^A*xsec(j,6)+TopEAn;

TopEAnERR=sqrt((bigconstn*xsec(j,6)*(A*xsec(j,2)^(A-
1))*xsec(j,3))^2+...

(bigconstn*xsec(j,2)^A*xsec(j,7))^2+TopEAnERR^2);
                        BotEAn=(bigconstn*xsec(j,2)^A)^2+BotEAn;
```

```
BotEAnERR=sqrt((2*bigconstn^2*xsec(j,2)^A*A*xsec(j,2)^(A-
1)*xsec(j,3))^2+BotEAnERR^2);
                    end
                end

            end
            coalradiusE{1,2}{angle,part}(1,1)=0;
            if TopEp>0
            coalradiusE{i,2}{angle,part}(1,2)=nthroot(TopEp/BotEp,3*(A-
1));
            tempERR=1/BotEp*sqrt(TopEpERR^2+(TopEp/BotEp*BotEpERR)^2);
            coalradiusE{i,2}{angle,part}(1,3)=...
                1/(3*(A-1))*(TopEp/BotEp)^(1/(3*(A-1))-1)*tempERR;
            end
            if TopEn>0
            coalradiusE{i,2}{angle,part}(1,4)=nthroot(TopEn/BotEn,3*(A-
1));
            tempERR=1/BotEn*sqrt(TopEnERR^2+(TopEn/BotEn*BotEnERR)^2);
            coalradiusE{i,2}{angle,part}(1,5)=...
                1/(3*(A-1))*(TopEn/BotEn)^(1/(3*(A-1))-1)*tempERR;
            end
        end
        coalradiusEA{1,2}{1,part}(1,1)=0;
        if TopEAp>0
        coalradiusEA{i,2}{1,part}(1,2)=nthroot(TopEAp/BotEAp,3*(A-1));
        tempERR=1/BotEAp*sqrt(TopEApERR^2+(TopEAp/BotEAp*BotEApERR)^2);
        coalradiusEA{i,2}{1,part}(1,3)=...
            1/(3*(A-1))*(TopEAp/BotEAp)^(1/(3*(A-1))-1)*tempERR;
        end
        if TopEAn>0
        coalradiusEA{i,2}{1,part}(1,4)=nthroot(TopEAn/BotEAn,3*(A-1));
        tempERR=1/BotEAn*sqrt(TopEAnERR^2+(TopEAn/BotEAn*BotEAnERR)^2);
        coalradiusEA{i,2}{1,part}(1,5)=...
            1/(3*(A-1))*(TopEAn/BotEAn)^(1/(3*(A-1))-1)*tempERR;
        end
    end
    disp(['Completed ' num2str(i) ' systems.'])
end
disp('    Done    ')

%
Export_Radii(coalradius,coalradiusE,coalradiusEA,beame,beamtype,targetn
ame,names)
```

B.9 Tripathi's Cross Section Model – 2

The following function also uses Tripathis's cross section model [22, 23, 24]. The coalescence model requires the use of the projectile/target system's total reaction cross section, which this function provides.

```
% Calculates total reaction cross section given the following
parameters:
%   Beam Energy
%   Beam Type
%   Target

function [sigmaR]=Tripathi(Ep,beamtype,targetname)

if strcmp(beamtype,'Xe')==1
    projectile=15;
elseif strcmp(beamtype,'Ne')==1
    projectile=9;
elseif strcmp(beamtype,'Si')==1
    projectile=11;
elseif strcmp(beamtype,'C')==1
    projectile=6;
elseif strcmp(beamtype,'Fe')==1
    projectile=12;
elseif strcmp(beamtype,'Kr')==1
    projectile=14;
elseif strcmp(beamtype,'N')==1
    projectile=7;
elseif strcmp(beamtype,'He')==1
    projectile=4;
else
    disp(['No beamtype "' beamtype '" in List'])
    return
end

if strcmp(targetname,'Pb')==1
    target=16;
elseif strcmp(targetname,'Cu')==1
    target=13;
elseif strcmp(targetname,'Li')==1
    target=5;
elseif strcmp(targetname,'C')==1
    target=6;
elseif strcmp(targetname,'Al')==1
    target=10;
else
    disp(['No targetname "' targetname '" in List'])
    return
end

% stats1=[...
%     'H-1   '    %1
```

```
%      'H-2   '    %2
%      'H-3   '    %3
%      'He-4  '    %4
%      'Li-7  '    %5
%      'C-12  '    %6
%      'N-14  '    %7
%      'O-16  '    %8
%      'Ne-20 '    %9
%      'Al-27 '    %10
%      'Si-28 '    %11
%      'Fe-56 '    %12
%      'Cu-63 '    %13
%      'Kr-84 '    %14
%      'Xe-131'    %15
%      'Pb-207'    %16
%      ];

stats2=[...
%   A    Z     r0       Rc     T      N
    1,   1,   0.85,     1,     23     1          % protons
    2,   1,   2.095,    1,     23     1          % deuterons
    3,   1,   1.68,     1,     23     1          % tritons
    4,   2,   1.696,    1,     40     .0         % He-4
    7,   3,   2.39,     1,     40     .046       % Li
    12,  6,   2.472,    1,     40     .0894      % C
    14,  7,   2.58,     1,     40     .0         % N
    16,  8,   2.730,    1,     40     .0         % O
    20,  10,  3.040,    1,     40     .0         % Ne
    27,  13,  3.06,     1,     40     .0602      % Al
    28,  14,  3.106,    1,     40     .0         % Si
    56,  26,  3.729,    1,     40     .0         % Fe
    63,  29,  3.876,    1,     40     .0849      % Cu
    84,  36,  4.15,     1,     40     .0         % Kr-Guessed on r0
    131, 54,  4.84,     1,     40     .0         % Xe-Guessed on r0
    207, 82,  5.513,    1,     40     .033       % Pb
    14,  7,   2.58,     1,     40     .0000255   % air only
    16,  8,   2.73,     1,     40     .0000255];% air only

%%%%%%%%%%%%%%
modif=1;   % Here in case you have an alloy: In that case a vector of %
comps will be placed here
%%%%%%%%%%%%%%

% These are the parameters dependent solely on projectile and target
for i=1:length(modif)

    At=stats2(target(i),1);
    Ap=stats2(projectile,1);
    Ac=12;
    Zt=stats2(target(i),2);
    Zp=stats2(projectile,2);
    %N=stats2(target(i),6);

    %%%%%%%%%%
```

```
%Define what Rc is depending on system
Rc=1;
if Ap==1 && Zp==1
    if At==2 && Zt==1       % p + d
        Rc = 13.5;
    elseif At==3 && Zt==2   % p + 3He
        Rc=21;
    elseif At==4 && Zt==2   % p + 4He
        Rc=27;
    elseif Zt==3            % p + Li
        Rc=2.2;
    elseif Zt==6            % p + C
        Rc=3.5;
    else
    end
elseif Ap==2 && Zp==1
    if At==2 && Zt==1       % d + d
        Rc=13.5;
    elseif At==4 && Zt==2   % d + 4He
        Rc=13.5;
    elseif Zt==6            % d + C
        Rc=6;
    else
    end
elseif Ap==4 && Zp==2
    if Zt==73               % 4He + Ta
        Rc=.6;
    elseif Zt==79           % 4He + Au
        Rc=.6;
    else
    end
else
end

%%%%%%%%%%%%%%%%%%

% T=stats2(projectile,5);

rtrms=stats2(target(i),3);
rprms=stats2(projectile,3);

rt=1.29*rtrms;
rp=1.29*rprms;
rc=1.29*2.472;

r0=1.1;

rhoAt=At/(4/3*pi*rt^3);
rhoAp=Ap/(4/3*pi*rp^3);
rhoAc=Ac/(4/3*pi*rc^3);

Ecm=Ep.*(At/(At+Ap));  % pretty sure At belongs in numerator
```

```
E=Ep./Ap;     % Energy is supposed to be in energy per nucleon

%%%%%%%%%%%%%%%

% 1st set of equations

R=rp+rt+1.2*(Ap^(1/3)+At^(1/3))./Ecm.^(1/3);

B=1.44*Zp*Zt./R;

%%%%%%%%%%%%%%%%%

% 2nd set of equations

%%%%%%%%%%%%%%%%%%%%%%%%%%%%

if Ap==1 && Zp==0           % n + X
    T=18;
    D=1.85+.16/(1+exp((500-E)/200));
elseif Ap==1 && Zp==1
    if At==4 && Zt==2       % p + 4He
        T=40;
        D=2.05;
    elseif At==3 && Zt==2   % p + 3He
        T=58;
        D=1.7;
    elseif At==6 && Zt==3   % p + 6Li
        T=40;
        D=2.05;
    elseif At==7 && Zt==3   % p + 7Li
        T=37;
        D=2.15;
    elseif At<=7            % p + light systems
        T=23;
        D=1.85+.16/(1+exp((500-E)/200));
    else                    % p + others
        T=40;
        D=2.05;
    end
elseif Ap==2 && Zp==1
    if At==4 && Zt==2       % d + 4He
        T=23;
        D=1.65+.22/(1+exp((500-E)/200));
    else                    % d + others
        T=23;
        D=1.65+.1/(1+exp((500-E)/200));
    end
elseif Ap==3 && Zp==2       % 3He + X
    T=40;
    D=1.55;
elseif At==3 && Zt==2       % X + 3He
    T=40;
    D=1.55;
```

```
elseif Ap==4 && Zp==2
    if At==4 && Zt==2       % 4He + 4He
        T=40;
        G=300;
    elseif Zt==4            % 4He + Be
        T=25;
        G=300;
    elseif Zt==7            % 4He + N
        T=40;
        G=500;
    elseif Zt==13           % 4He + Al
        T=25;
        G=300;
    elseif Zt==27           % 4He + Fe
        T=40;
        G=75;
    else                    % 4He + others
        T=40;
        G=75;
    end
    D=2.77-8e-3*At+1.8e-5*At^2-.8/(1+exp((250-E)/G));
elseif At==4 && Zt==2       % others + 4He
    T=40;
    G=75;
    D=2.77-8e-3*At+1.8e-5*At^2-.8/(1+exp((250-E)/G));
else                        % others
    T=40;
    D=1.75*(rhoAp+rhoAt)/(rhoAc+rhoAc);
end
if Zp==3 || Zt==3
    D=D/3;
end


%%%%%%%%%%%%%%%%%%%%%%%%%%%%%%

CE=D.*(1-exp(-E/T))-.292.*exp(-E/792).*cos(.229*E.^.453);

S=Ap^(1/3)*At^(1/3)/(Ap^(1/3)+At^(1/3));

deltaE=1.85*S+0.16*S./Ecm.^(1/3)-CE+.91*(At-2*Zt)*Zp/(At*Ap);

%%%%%%%%%%%%%%%%%

if Ap==1 && Zp==0
    SL=1.2+1.6*(1-exp(-E/15));
    if At==4 && Zt==2
        X1=5.2;
    else
        X1=2.83-3.1e-2*At+1.7e-4*At^2;
    end
    Xm=1-X1*exp(-E./(X1.*SL));
else
```

```
        Xm=1;
    end

    %%%%%%%%%%%%%%%%

    % Final answer

    sigmaR=pi*r0^2*(Ap^(1/3)+At^(1/3)+deltaE).^2.*(1-Rc.*B./Ecm).*Xm;
    sigmaR=sigmaR*10;   % Convert from fm^2 to mb
%     sigmaR=sigmaR/1000; % Convert from mb to b

end
```

VITA

Matthew Beach was born on February 7, 1986 in Greeneville, TN. He graduated Cherokee High School in 2004 and went to the University of Tennessee for his B.S. in Nuclear Engineering. After getting his degree in 2008, he remained at the University of Tennessee to pursue a PhD in Nuclear Engineering. He received his M.S. in 2012. He was co-author for two conference papers, both of which were submitted to the IEEE Aerospace Conference; one in March 2011 and the other in March 2013. The first paper was titled “Light-Ion Production from Intermediate-Energy Heavy-Ion Interactions and the second was similarly titled “Light-Ion Production for Medium-Energy Heavy-Ion Interactions. After completion of his doctoral degree requirements and gaining more experience in the field, he is planning on eventually having a career in academics.